SYNTHESIS AND CHARACTERIZATION OF FLUORINATED CELLULOSE DERIVATIVES

by

Charles Edward Frazier

Dissertation submitted to the Faculty of the

Virginia Polytechnic Institute and Sate University

in partial fulfillment of the requirements for the degree of

DOCTOR OF PHILOSOPHY

in

Wood Science and Forest Products

APPROVED:

Wolfgang G. Glasser, Chairman

Thomas C. Ward

James E. McGrath

Harry W. Gibson

Larry T. Taylor

September, 1992
Blacksburg, Virginia

SYNTHESIS AND CHARACTERIZATION OF FLUORINATED CELLULOSE DERIVATIVES

by

Charles Edward Frazier
Committee Chairman: Wolfgang G. Glasser
Wood Science and Forest Products

(ABSTRACT)

The synthesis of fluorinated cellulose derivatives was pursued for the purpose of investigating the effects of fluorine on the interfacial properties of cellulose derivatives, in multiphase materials. Synthetic approaches included: 1) the replacement of hydroxyl groups on cellulose with fluorine using fluoride displacement chemistry, or direct, one step fluorination 2) the replacement of hydroxyl groups on hydroxypropyl cellulose, HPC, with direct one step fluorinating agents, or 3) the conventional derivatization of cellulose with prefluorinated agents. Fluoride displacement of cellulose sulfonate esters was plagued low yields, and was therefore ineffective. Direct cellulose fluorination with aminofluorosulfur, and aminofluorocarbon reagents was effective for the surface fluorination of cellulose. However, the bulk, homogeneous fluorination of cellulose was complicated by side reactions that often precluded fluorination. Cellulose dissolved in DMAC/LiCl underwent simultaneous chlorination, and branching reactions when treated with dialkylaminosulfur trifluoride, DAST. Branching resulted from an anhydrous HF catalyzed trans-glycosidation reaction, which produced mainly β-1,6 branching. Serendipitously, this discovery allows for the first known synthesis of long chain branched cellulose derivatives, with increased molar mass, and increased polydispersity.

Treatment of HPC with DAST and FAR gave good levels of fluorination; however, the HF catalyzed gelation was always a complicating factor. The lower reactivity of FAR allowed for partial control of gelation with the use of nonnucleophilic bases.

The easiest way to introduce fluorine was to perform conventional derivatization using prefluorinated reagents such as for the synthesis of fluorobenzyl cellulose. Mixed benzyl ethers of controlled fluorine content were made by altering the ratio of p-fluorobenzyl chloride to benzyl chloride during reaction. 2-Dimensional NMR techniques were used to identify most proton and carbon resonances of cellulose and amylose fluorobenzyl ethers. Thermal analysis, solution analysis, and ^{13}C spin-lattice relaxation experiments were used to compare the rod-like and coil-like behavior of the fluorobenzyl cellulose and amylose.

Polycaprolactone, PCL, was blended with tri-O-benzylated cellulose with different degrees of fluorination. PCL was found to be immiscible with all derivatives, of fluorine contents from 0% to as high as 11.7%. PCL did display some degree of mechanical compatibility with all derivatives. The greatest compatibility was found with benzylated cellulose having fluorine contents slightly below the maximum. It was found that no specific interactions were occurring between PCL and fluorobenzyl cellulose. The enhanced compatibility of the mixed fluorobenzyl/benzyl cellulose ethers was postulated to arise from intramolecular interactions, which served to enhance the mixing of the copolymeric mixed benzyl ethers with PCL.

ACKNOWLEDGEMENT

I would like to thank my committee members, Drs. Tom Ward, Jim McGrath, Larry Taylor, Harry Gibson, and Wolfgang Glasser for their respective contributions to my education and graduation process. I have interacted with each of these gentleman to varying degrees, sometimes great and sometimes small. Regardless of the extent of interaction these individuals have all contributed significantly to my education because each has participated in building a fine polymer program at Virginia Tech. I have benefitted from all of their activities.

I must give special thanks to my major professor Wolfgang Glasser. It is very awesome when one considers the potential result of a chance meeting between two individuals. No one can predict the outcome. In my own case, I can only say that I was very fortunate to have stumbled upon the educational philosophy developed by Wolfgang Glasser. He has contributed profoundly to my personal, scientific, and professional development. I hope that I may repay him by affecting another young scientist in a similar fashion.

I would also like to thank the many colleagues with whom I worked during my graduate education, graduate students and Post-Docs alike. Klaus Hofmann, Willer de Oliveira, Vipul Dave, and Gil Garnier are special members of the original nucleus in the Wood Chemistry group. I thank these men, particularly and heartily. I would also like to thank Tom Piccariello, Gamini Samaranayake, Rajesh Jain, and Will Kaar for their patience, support, and friendship during the fun and pain. The record should show that Tom Piccariello made a special and enormous contribution to my education and personal development. I must also thank Jim Sealey, Bob Wright, Jody Jervis, Paul Vail, Nancy Rauschenberg, Sven van Winkle, and Akio Takemura for their friendship and support.

I reserve the last words for two women that gave selflessly for my benefit during my graduate education. I was fortunate to receive the support and love of Janet Cleary. She raised the quality of my life. And she helped carry my hardships when I was weak. I owe her an immense debt that I shall attempt to repay slowly for many years to come.

While all of my family members played a crucial role in my education, I must single out the love provided to me by my mother. She gave of herself, without question. I dedicate this work to my mother, Linda B. Frazier, whom I love deeply.

LIST OF FIGURES

LIST OF FIGURES continued

CHAPTER FIVE:

PART ONE:

PART TWO:

LIST OF FIGURES continued

LIST OF TABLES

GLOSSARY OF TERMS

PVF_2	polyvinylidenefluoride
PMMA	polymethylmethacrylate
HPC	hydroxypropyl cellulose
PCL	polycaprolactone
DS	degree of substitution
TBAF	tetrabutylammonium fluoride
CTC	cellulose tricarbanilate
DMAC	dimethylacetamide
TMS	trimethylsilyl
THF	tetrahydrofuran
DAST	dialkylaminosulfur trifluorde
DMSO	dimethylsulfoxide
FAR	fluoroalkylamino reagent
DQCOSY	double quantum filtered correlation spectroscopy
DEPT	distortionless enhancement polarization transfer
TOCSY	total correlation spectroscopy
HETCOR	heteronuclear correlation spectroscopy
PROTON SPONGE	bis-1,8-(dimethylamino)naphthalene
FTIR	fourier transform infrared (spectrometer)
NMR	nuclear magnetic resonance
GPC	gel permeation chromatography
DSC	differential scanning calorimetry
DMTA	dynamic mechanical thermal analysis
TEM	transmission electron miscroscopy
SEM	scanning electron microscopy
BDSD	bis(diethylamino)sulfur difluoride
DSF	degree of substitution of fluorine

TABLE OF CONTENTS

SYNTHESIS AND CHARACTERIZATION OF FLUORINATED CELLULOSE DERIVATIVES

TABLE OF CONTENTS (continued)

TABLE OF CONTENTS (continued)

TABLE OF CONTENTS (continued)

SYNTHESIS AND CHARACTERIZATION OF FLUORINATED CELLULOSE DERIVATIVES

PREFACE

Worldwide, the rising concern for the preservation of natural resources has changed the focus of many in the polymer community. A search has begun for the replacement of materials that have no mechanism for reentering the carbon cycle. Such materials, among other things, are contributing to the anxiety over the possible damage to the environment. New materials are being sought that are neutral in their impact upon the Earth. This new climate, the so called "Green Movement", has risen from the citizens and legislators of the industrialized nations. For better, or worse, this new attitude could offer a significant financial payoff. Businesses are recognizing the market value of products that are perceived by the consumer as being "environmentally safe". Consequently, global interests from governments, citizens, and businesses are weighing upon the activities of polymer scientists. The number of technical papers devoted to the manufacture and evaluation of environmentally neutral plastics is steadily rising. Environmentally neutral is often referred to as the property of being biodegradable, or even "bio-friendly". Caution must be exercised when using such terms, because no clear definitions are available. Within this context, a biodegradable, or bio-friendly material is something that has some propensity to reenter the carbon cycle, without being combusted.

The biological origin of cellulose gives cellulosic materials an intrinsic potential for biodegradation. Therefore, there is growing interest in increasing the use of cellulosics in modern materials. While cellulosic materials are appreciated for qualities such as high modulus, and good film formation, cellulosics fall short in many material applications. Such voids may be filled by combining cellulosics with other polymers that meet our needs. This combination, be it in the form of blends, or composite materials, may satisfy our need to manufacture products of utility, and environmental neutrality.

The remarkable bioactivity of fluorodeoxy sugars[1] suggests that fluorodeoxycellulose may be biodegradable. The size and electron density of aliphatic fluorine is very similar to that of the hydroxyl group[1]. Therefore, the electronic and steric interactions between an enzyme and the hydroxyl group may be mimicked by aliphatic fluorine. If possible, this mimicry would enhance the biodegradation of fluorodeoxycellulose and its derivatives. Keep in mind that not all fluorinated cellulosics have the same potential for biodegradation; not all will have such a striking similarity to cellulose.

However, all fluorinated cellulosics may have good potential in material uses. Contemporary organo-fluorine polymers are valuable materials because of the extreme electronegativity of fluorine. Fluorine is known to have a strong effect upon polymer properties, such as dielectric constant, surface free energy, and the potential for secondary interactions with other polymers. Of these, the potential for polymer-polymer interactions is particularly important in the science of multicomponent, polymeric materials. Specific interactions in systems such as polymer blends, composites, and adhesives are generally considered to enhance the performance of these materials. It has been shown that some fluorinated polymers possess local dipoles that serve to promote good mixing with other polar polymers. A classic example is the miscibility of polyvinylidenefluoride(PVF_2)withpolymethylmethacrylate(PMMA)[2].Thesetwopolymers

are completely miscible in all proportions. The large negative enthalpy of mixing is thought to arise from specific dipole-dipole interactions between the carbon-fluorine bonds, and the carbonyl groups of the respective polymers[2]. The promotion of these types of specific interactions between cellulosics and other materials would be of great interest, and value, for the use of cellulose derivatives. Furthermore, the incorporation of waste paper fiber into thermoplastic materials is rapidly growing as a research topic around the world. The technical challenge lies in the development of polymer-polymer interactions at the fiber interface. Consequently, the heterogeneous treatment, or the surface treatment of cellulose with fluorine also has pertinence in the field of cellulose utilization.

OBJECTIVES

Above all, the objective of this research is to enhance the compatibility of cellulose with thermoplastic materials. For the reasons mentioned above, the incorporation of fluorine has been selected as the means to this end. Consequently, the immediate objective is to explore the synthetic methods for incorporating fluorine into the cellulose molecule. The course of the work has been dictated by three variables: 1) the chemistry of fluorination, 2) the feasibility of applying it to cellulose, or a derivative of cellulose, and 3) the selection of homogeneous or heterogeneous reaction conditions. These three variables are interdependent. For example, the appropriateness of a particular chemistry often depends upon practical restrictions, such as the solvent system. Selection of a solvent system is directly dependent upon the properties of cellulose, or a derivative of cellulose. This in turn will allow for homogeneous, or heterogeneous reaction conditions. The interdependency of these types of considerations has directed the research down the path of least resistance. An appreciation for this interdependency necessarily requires a brief definition of the three variables.

1. The chemistry of fluorination: The existing synthetic alternatives are classified here as 1) fluoride displacement techniques, and 2) direct fluorination

techniques. Displacement techniques require the prior modification of cellulose with a good leaving group, followed by treatment of the activated cellulose with a source of free fluoride. This is typically a two step process that often requires isolation of a reactive intermediate. On the other hand, direct techniques employ reagents that fluorinate the substrate in one step. Mechanistically, the two approaches are the same. A reactive intermediate is formed, and is then acted upon by free fluoride. However, during direct fluorination, the reactive intermediate is, in most cases, impossible to isolate. These reactions are called one step reactions, and they take place in one pot. While displacement techniques go through two distinct steps, often occurring in two pots.

2. The choice between cellulose or a cellulose derivative: Sometimes a cellulose derivative is used as a reactive intermediate. This intermediate may be isolated, and subsequently dissolved in a second reaction medium. In such a case, cellulose is considered the substrate. The intermediate cellulose derivative is not considered as such, because it is destroyed in the process. Hydroxypropyl cellulose, HPC, is the only derivative that was used as a substrate for fluorination in this work. In this case, HPC is considered to be the substrate, because the intrinsic nature of HPC is maintained during fluorination.

3. Homogeneous versus heterogeneous chemistry: Homogeneous reaction conditions imply that cellulose, or a derivative of cellulose, is completely dissolved in solution. Therefore only one liquid phase exists. Under special conditions, this can occur with pure, underivatized cellulose. Or, this may occur with cellulose derivatives, and/or reactive intermediates, dissolved in common organic solvents. Heterogeneous conditions are employed with pure cellulose, in which case the cellulose is a solid suspended in an organic solvent.

CHAPTER ONE

FLUORINATION BY HOMOGENEOUS FLUORIDE DISPLACEMENT

I. FLUORINATION BY HOMOGENEOUS FLUORIDE DISPLACEMENT

INTRODUCTION

Over the years, there has been a moderate degree of interest in the synthesis of fluorodeoxycellulose. The synthetic approaches used may be classified into two groups. These are fluoride displacement techniques, and direct fluorination techniques (Figure 1). Displacement chemistry requires the prior activation of cellulose with an appropriate leaving group. This activated cellulose is then treated with a source of anhydrous fluoride. Alkyl and aryl sulfonate esters of cellulose are the most commonly used precursors in this procedure[3,4,5]. For example, cellulose sulfonate esters have been treated with potassium fluoride[6], and tetrabutylammonium fluoride[5]. In these cases, fluorine incorporation has always been relatively low, less than 1% fluorine. However, there is one report that 3.3% fluorine(DS=0.28) was obtained with KF[6,7]. (DS, or degree of substitution refers to the number of hydroxyls per cellulose anhdroglucose unit which have been reacted. The DS may range from 0-3)

Little has changed in the selection of leaving groups; the alkyl and aryl sulfonate esters remain the first choice. New developments in displacement chemistry lie in the selection of the fluoride source. Historically, alkali metal salts of fluoride have been used[8]. However, organic fluoride salts such as tetrabutylammonium fluoride(TBAF), and variations of this form, are available and very popular[9]. Regardless of the source of fluoride used in displacement reactions, it is absolutely necessary to maintain anhydrous conditions[9]. Hydrated fluoride is relatively unreactive, whereas the naked fluoride anion has remarkable basicity and nucleophilicity[9].

Previous reports of the synthesis of fluorodeoxycellulose using displacement

chemistry are deficient in the description of experimental details. For example, there are reports of the synthesis of fluorodeoxycellulose with relatively low degrees of fluorine substitution[4,5]. However, these papers either do not report experimental methods, or completely fail to describe analytical methods, experimental methods, and specific results. The most successful report of the synthesis of fluorodeoxycellulose was from a Russian scientist, unfortunately, the translation was not obtained[6]. Therefore, this work began with an attempt at reproducing the classic approach to cellulose fluorination.

Consequently, the objective of this section is to evaluate fluoride displacement chemistry for the synthesis of fluorodeoxycellulose. This evaluation must necessarily begin with the repetition of "classic" techniques that have been reported previously, but were reported with little detail. Afterwards, a novel method will be described. The evaluation of the chemistry rests upon the ability to incorporate fluorine at high levels, that is, with degrees of substitution from 0.5 to 1.0. In order to study the effects of fluorine content on blend properties, we must first be able to make cellulose derivatives with a reasonably wide range of fluorine content. Therefore, the initial goal is to maximize fluorine incorporation, with hopes of controlling subsequent reactions to provide lower fluorinations. So the immediate task is to determine if fluoride displacement techniques will provide high degrees of fluorination.

EXPERIMENTAL

MATERIALS:

All solvents were freshly distilled with the appropriate desiccants prior to use. For example, THF was distilled over potassium metal unedr dry nitrogen atmosphere. Unless otherwise stated, all reagents were purchased from Aldrich Chemical company, and used as received. All liquid transfers were strictly anhydrous, using syringe and cannula techniques.

Whatman cellulose, type CF-11, was used as starting material in all cellulose reactions. Number average degree of polymerization was determined as approximately 200; polydispersity was 1.67. Molecular weight information for the cellulose starting material was obtained by synthesizing the triphenylcarbamate derivative[10]. This derivative is often referred to as cellulose tricarbanilate, or CTC. CTC is organic soluble, and is therefore amenable to gel permeation chromatography in organic phase, as a means of obtaining molecular weight information of the parent cellulose[10].

METHODS:

Molecular Weight Analysis:

Gel permeation chromatography was used, where tetrahydrofuran was pumped by a Waters 510 into a series of 3 Waters Ultrastyragel columns, with pore sizes of 10^3, 10^4, and 10^6 angstroms. Detection was with a Waters 410 refractometer, in series with a Viskotek differential viscometer, model 100. The columns were heated to 40°C in an Eldex column heater, and both detectors were also heated to 40°C. Tetrahydrofuran was freshly degassed, and always stored under a helium atmosphere during use. Narrow polydispersity, polystyrene standards from Polymer Laboratories were used to establish a universal calibration.

Nuclear Magnetic Resonance Spectroscopy:

A Varian, Unity-400, nuclear magnetic resonance spectrometer was used to collect ^1H, ^{19}F, and ^{13}C NMR spectra at 400, 376, and 100 Mhz, respectively. Samples were prepared by dissolving the analyzed material in the appropriate deuterated solvents, using 5 millimeter, or 10 millimeter Wilmad glass tubes. Where appropriate, the percent fluorine present in a sample was determined with ^{19}F NMR using an internal standard analysis. Precisely weighed amounts of sample and fluorine internal standard were placed into a 25 ml round bottom flask. The mixture was dissolved in $CDCl_3$, and then run on the NMR. Percentages of fluorine would be calculated based upon the ^{19}F integrations,

and the known masses of sample and standard. The internal standard was 3-trifluoromethyl acetophenone(chemical shift=-64.26 ppm, relative to trifluoroacetic acid at -77.05 ppm).

Elemental Analysis:

Elemental analyses were performed by Galbraith Laboratories, 2323 Sycamore Dr., Knoxville, TN, 37921-1750.

Cellulose Activation:

Whatman CF-11 cellulose was dried thoroughly under high vacuum, at a temperature of 105° C, for a period of at least 24 hours. The method of cellulose activation described by McCormick and Calais[11]includes a water soaking of the cellulose. In order to maintain anhydrous conditions, an alternative cellulose activation was developed, where the cellulose was simply soaked in anhydrous DMAC until swelling was complete. Completeness was judged by visual inspection, and this normally required 3-5 days. The activated cellulose was then filtered in a Buchner funnel under a nitrogen atmosphere. Finally, the swollen polymer was sealed in a container for later use. Three samples were extracted for solids analysis, via vacuum drying. This method generally produced an activated cellulose of 30-50% solids.

Cellulose Mesylation:

Mesylations were performed in the LiCl/dimethylacetamide (DMAC) solvent system, with the procedure adapted from McCormick and Calais[11]. An amount of activated cellulose equal to 1 gram of dry material(1.9 mmole OH), was suspended in a 50 ml solution of 9% LiCl(wt/vol) in DMAC. All materials where placed in a dry, 200 ml, three neck flask, attached with: dry nitrogen inlet, drying tube outlet, addition funnel, and mechanical stirrer. The mixture was allowed to stir at room temperature until dissolution was complete, 2-8 hours. The reaction flask was immersed in an ice water

bath for the duration of the reaction. Pyridine and mesyl chloride, 8 ml (9.9 mmole) and 7.3 ml (9.4 mmole) respectively, were placed in the addition funnel. The mesyl chloride/pyridine solution was added slowly over a period of about 30 minutes, with constant stirring. Afterwards, the solution stirred at 0°C for 12 hours. The solution was precipitated into a 300 ml volume of ice water. The white fibrous material was then washed exhaustively with ice cold methanol. The material was dried at ambient temperature under approximately 20 mm Hg vacuum for 24 hours. This procedure yielded 1.62 grams of white, fibrous powder, soluble in DMSO and DMAC, insoluble in $CHCl_3$ and THF.

Treatment of Cellulose Mesylate with KF:

Mesyl cellulose, 0.835 grams, was dissolved in 25 ml of anhydrous DMAC in a freshly flamed 100 ml triple neck flask. The flask was fitted with condenser, nitrogen inlet and outlet, thermometer, and magnetic stirrer. Dry 18-crown-6 ether, 1 gram ,(3.8 mmoles), was quickly transferred into the reaction flask. Then dried KF, 1.02 grams, (17.6 mmoles), was added to the reaction flask. The solution was heated to 100° C, and held there for 3 hours. Subsequently, the solution was cooled to room temperature, and then poured into 200 ml of hot water. The light brown material was washed with methanol, and dried under high vacuum at 40° C over night. Approximately, 0.4 grams of a light brown, flaky material was recovered. Elemental analysis revealed 38.74% Carbon, 5.6% Hydrogen, and 0.49% Fluorine.

Synthesis of Cellulose Trimethylsilyl Ether:

The method of Stein and Klemm[12]was adapted for the synthesis of cellulose trimethylsilyl ether, (TMS cellulose). Whatman CF-11 cellulose was dried at 104°C for at least 24 hours. Chlorotrimethylsilane (TMS chloride) tetrahydrofuran (THF) and pyridine were freshly distilled prior to use. 1 g of dried cellulose,(18.5 mmoles OH) was placed in a freshly flamed 3 neck round bottom flask. The flask was equipped with dry

nitrogen inlet and outlet, condenser, addition funnel, and magnetic stir bar. Anhydrous pyridine, 100 ml, was added to the flask and the suspension was refluxed for about 1 hour. After cooling to room temperature, 300 ml of THF was added via cannula. TMS chloride, 65.2 grams,(600 mmole), dissolved in 100 ml THF was added to the addition funnel. This solution was added slowly to the reaction flask over a period of 45 minutes. The reaction was allowed to stir for a period of about 12 hours. The solution was collected and centrifuged, and then precipitated into about 500 ml of anhydrous methanol. The white, sticky mass was washed with about 500 ml more of anhydrous methanol. The product was quickly transferred to a vacuum oven where it was dried under 20 mm Hg vacuum at 50°C for 24 hours. About 2 grams of white, soft polymer was recovered.

Fluorination of Cellulose TMS Ether:

For the fluorination of cellulose TMS ether, an ether DS of 2.5 was assumed for the calculation of reagent stoichiometry. Dried cellulose TMS ether, 500 milligrams, was placed into a freshly flamed 200 ml round bottom flask. The flask was fitted with dry nitrogen inlet and outlet, rubber septum, condenser, and magnetic stir bar. In a separate 100 ml, flamed, round bottom flask, 2.54 (9.7 mmoles) grams of tetrabutylammonium fluoride hydrate, was heated to 40°C, under high vacuum for a period of at least 24 hours. During this time, the fluoride salt changes from a crystalline solid to a viscous syrup, indicating a very high degree of dehydration. Anhydrous THF, 50 ml, was added to the tetrabutylammonium fluoride. Approximately one half of this solution was added to the reaction flask by cannula, at room temperature. Upon addition of the fluoride salt, the cellulose derivative precipitated from solution. The reaction flask was cooled to -65°C in a dry ice/acetone bath. Triflic anhydride, 419 milligrams (5.3 mmoles) was added to the reaction flask using a syringe. At this time, some of the precipitated polymer went back into the THF solution. The flask was then allowed to warm to room temperature, when the rest of the tetrabutylammonium fluoride solution was added. The reaction was

refluxed for 3 hours, where it was noticed that the solution was heterogeneous during most of this time. Finally, the flask was cooled to room temperature, and poured into water. The solid was washed with water, and methanol thoroughly, and then vacuum dried at 50°C for 24 hours. Approximately 300 milligrams of light brown solid was recovered. Elemental analysis revealed 45.34% Carbon, 6.68% Hydrogen, and 0.44% Fluorine.

Treatment of Cellulose Mesylate with DAST:

Cellulose mesylate, 300 milligrams, was dissolved in 30 ml of anhydrous DMAC in a freshly flamed 100 ml round bottom flask, equipped with magnetic stirrer, and rubber septum. The flask was maintained under positive dry nitrogen gas pressure at all times. The flask was then cooled to -15° in a dry ice/acetone bath. Dimethylaminosulfur trifluoride, methyl-DAST 1 ml (10.2 mmoles), was added slowly to the solution with a syringe. With constant stirring, the flask was removed from the cooling bath, and heated to 65° over a period of 35 minutes. Afterwards, the solution was cooled to room temperature, and poured into a mixture of 100 ml of 2% $NaHCO_3$, and about 100 grams ice. This suspension was stirred until CO_2 evolution ceased. The mixture was centrifuged, and the pellet was resuspended in methanol and recentrifuged. This procedure was repeated three more times. Then the pellet was resuspended in acetone, and centrifuged again. The pellet was dried under 20 mm Hg vacuum at 40° overnight. 152 milligrams of a brown material was recovered.

Treatment of Cellulose Mesylate/DAST Reaction Product with Phenylisocyanate:

The product of the DAST, cellulose mesylate displacement reaction, 152 milligrams, was placed in a dry 200 ml 2 neck round bottom flask. The flask was fitted with a rubber septum, dry nitrogen, and magnetic stir bar. Anhydrous pyridine, 10 ml, (123.6 mmoles), and 5 ml of phenylisocyanate,(46 mmoles) was added to the reaction flask using a syringe. The suspension was heated to 80°C, where after 1 hour the

polymer was completely dissolved. The solution was maintained at 80°C for a total of two hours, and then stirring was maintained at room temperature over night. The solution was then precipitated into 100 ml methanol/water, 50/50. An emulsion was formed, so NaCl was added slowly until a good precipitant fell out. The material was washed extensively with water, followed by methanol. Drying was conducted at high vacuum, over night, at 40°C. 150 milligrams of brown material was recovered, which was insoluble in $CHCl_3$ and CH_3N, and soluble in DMSO.

RESULTS AND DISCUSSION

Table 1 lists the results of the fluoride displacement reactions, in percent fluorine present in the product. This data was collected by elemental analysis for methods 1 and 2, and by ^{19}F NMR for method 3. The 3 displacement schemes are shown in Figure 2. In all cases, the cellulose was first derivatized as the sulfonate ester using mesyl chloride or triflic anhydride. Method 1 involved the treatment of mesyl cellulose with KF, and 18-crown-6 ether[13]. Method 2 started with the synthesis of the trimethylsilyl, TMS, ether of cellulose. The cellulose TMS ether was then converted to cellulose triflate, and subsequently treated with TBAF. Method 3 started with the same cellulose mesylate used in method 1. However, the mesylate was reacted with dimethylaminosulfur trifluoride, or methyl-DAST.

A common term used to describe the extent of cellulose reaction is the degree of substitution, or DS. Because cellulose has 3 hydroxyl groups per anhydroglucose unit, the possible range of cellulose DS is from 0 to 3.0. Cellulose mesylate used in methods 1 and 3 had a mesylate DS of approximately 1.0, as estimated from the ^1H NMR.

The techniques used in method 1 served as a reproduction of the methods used in previous papers[3,4,5]. The product was insoluble in DMSO, DMAC, and THF. Elemental analysis showed a 0.49% fluorine content. This corresponds to an approximate

DS of 0.04. This compares favorably with two previous reports[4,5]. However, this is much lower than the 3.3% fluorine (DS=0.28) incorporation reported by Sletkina and Rogovin[3,6].

Method 2 gave essentially the same result as method 1, fluorine content of 0.44%. The experimental procedures used in methods 1 and 2 are considerably different, a direct comparison may be misleading. But it is still surprising to find no difference between the use of methanesulfonate, and the trifluoromethanesulfonate leaving groups. Trifluoromethanesulfonate is roughly 5000 times more effective as a leaving group than methanesulfonate[14]. In any event, fluorine incorporation is disappointingly low. Method 1, using KF displacement of a sulfonate ester, is historically one of the most common techniques of fluorinating an alcohol[8]. Yields with simple alcohols are typically much higher, i.e. at least 50% conversion of primary hydroxyls[8]. The low yields for this cellulose fluorination may be an indication of the difference in chemical reactivity of functional groups on polymers, as opposed to those on small molecule homologs[15,16,17,18]. For example, it is known that the "microenvironment" created by a solvated polymer chain, may be very different from the conditions in the bulk solvent[16,17]. This could cause a large deviation in the reactivity of a polymer, when compared to the reactivity of a homologous small molecule. This argument may explain the poor conversion of cellulose primary hydroxyls in fluoride displacement reactions.

Method 3 was unique from the previous methods because it involved the use of DAST as a fluoride displacement reagent. DAST is typically used as a direct fluorinating agent[19]. ^{19}F NMR of the product from method 3 revealed no fluorine incorporation. (The product from method 3 was reacted with phenylisocyante to give a soluble sample suitable for NMR analysis.) Cellulose mesylate (DS of mesylate = 1.0) was treated with 6 equivalents of DAST per anhydroglucose unit. No displacement reactions occurred at C6, and surprisingly, no direct fluorination occurred at the free secondary hydroxyls.

These results are interesting in that they shed light on the nature and reactivity of DAST. It has been stated that DAST alone is a source of free fluoride[19], and should function in a displacement reaction. To the extent that there was no fluorine incorporation, we may conclude that under strictly anhydrous conditions, DAST is not a source of free fluoride in DMAC. DAST requires water, or reactive alcohols to produce free fluoride. Furthermore, under these circumstances, DAST is unreactive towards free secondary hydroxyls of cellulose. This observation is in agreement with those of Kasuya et al.[7]. After treating a cellulose acetate homogeneously with DAST, they found no fluorination at free secondary hydroxyls. They did find that all free primary hydroxyls had been converted to alkyl fluoride. This would suggest that the cellulose mesylate starting material had a mesylate DS of at least 1.0. A mesylate DS of less than 1.0 would insure the presence of primary hydroxyls, which should be easily converted to fluoride[7].

As mentioned above, no detailed information is available about the methods and results of previous reports concerning the preparation of fluorodeoxycellulose using displacement chemistry. Therefore, comparisons and conclusions are difficult to make here. It may be safe to conclude that fluorine incorporations on the order of 1% are normal. While fluorine incorporations of 3% may be exceptional, using displacement chemistry. Based upon the results here and in the literature, the fluorination of cellulose by fluoride displacement chemistry appears to be very difficult. The methods used so far hold very little promise. However, these methods do not include all of the possible displacement techniques. Consequently, there is still room for exploration. For present purposes, this chemistry is not suitable for the synthesis of variously fluorinated cellulose derivatives. Fluorine incorporations are very low, and therefore do not provide any means of control.

CONCLUSIONS

1. Fluorination of cellulose with fluoride displacement techniques gave low

fluorination yields. Yields produced here were all less than previous reports. The conversion of primary cellulose sulfonate esters to alkyl fluoride, occurs with yields far lower than for small molecule homologs. These low yields make this technique unsuitable for the synthesis of cellulose derivatives with variable fluorine contents.

2. There was no difference between the use of mesylate and triflate leaving groups. Though direct comparison of these reagents may not be valid in this case, this is surprising considering the extreme potency of the triflate leaving group.

3. DAST did not serve as a source of free fluoride for the displacement of sulfonate esters. Furthermore, DAST did not directly fluorinate free secondary hydroxyls, which is in agreement with an earlier report.

LITERATURE CITATIONS

1. Kent, P.W., *Fluorinated Carbohydrates, Chemical and Biochemical Aspects*, ACS Sym. Ser., N.F. Talor;editor, 374, 1, 1988.

2. Paul, D.R., J.W. Barlow, R.E. Bernstein, and D.C. Wahrmund, Poly. Eng. Sci., 18, 16, 1225, 1978.

3. Krylova, R.G., Russian Chemical Reviews, 56, 1, 1987.

4. Pascu, E., and R.F. Schwenker, Jr., Text. Res. Journal, 27, 173, 1957.

5. Titcombe, L.A., J.B. Bremner, M.I. Burgar, M.J. Ridd, J. French, and K.N. Maddern, Appita, 42, 282, 1989.

6. Sletkina, L.S., and Z.A. Rogovin, Vysokomol. Soyed., B9, 37, 1967(Not translated in Polymer Sci., USSR).

7. Kasuya, N., K. IIyama, and A. Ishizu, Appita, 6th Internat. Sym. Wood, Pulping Chem., vol. 2, 415, 1991.

8. Hudlicky, M., *Chemistry of Organic Fluorine Compounds*, 2nd Revised Edition, Ellis Horwood Lmtd. Pub., 1976.

9. Clark, J., Chem. Rev., 80, 429, 1980.

10. Evans, R., and A.F.A. Wallis, 4th. Int. Symp. Wood and Pulping Chem., Paris, 1, 201, 1987.

11. McCormick C.L., and P.A. Calais, Polymer, 28, 2317, 1987.

12. Stein, A., and D. Klemm, Makromol. Chem., Rapid Commun., 9, 569, 1988.

13. Liotta, C.L., and E.E. Grisdale, Tet. Letters, 48, 4205, 1975.

14. Carey, F., and R.J. Sundberg, *Advanced Organic Chemistry, Part A: Structure and Mechanisms*, Plenum Press, p.271, 1984.

15. Lenz, R.W., *Organic Chemistry of Synthetic High Polymers*, Chapter 17, Interscience Pub., 1967.

16. Morawetz, H., Pure Appl. Chem., 51, 2307, 1979.

17. Morawetz, H., J. Macromol. Sci., Chem., A13, 3, 311, 1979.

18. Morawetz, H., J. Polymer Sci., Polym. Symp., 62, 271, 1978.

19. Hudlicky, M., Organic Reactions, Vol. 35, 513, 1988.

Table 1.Weight percent fluorine contents of products of fluoride displacement reactions.

METHOD	% FLUORINE
1. KF/18-CROWN-6 ETHER	0.49
2. TRIFLIC ANHYDRIDE/TBAF	0.44
3. MESYLATE/DAST	0.00

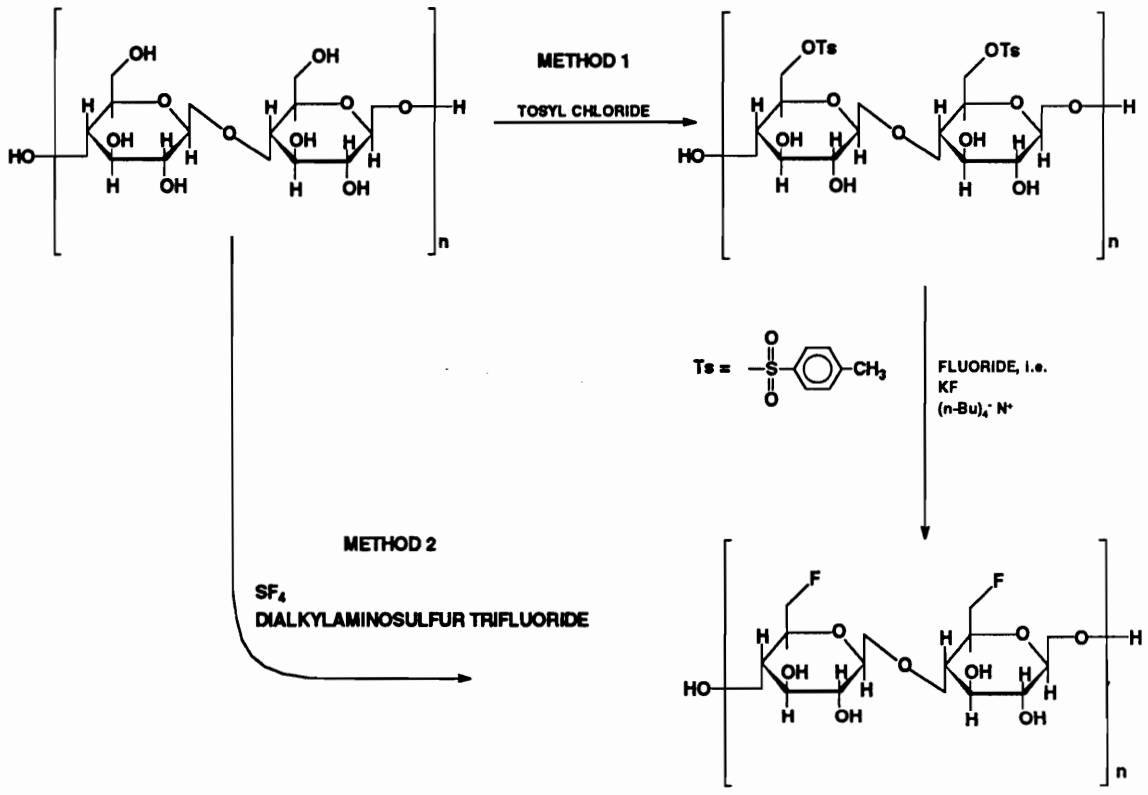

Figure 1. Synthetic approaches previously applied to the formation of fluorodeoxycellulose.

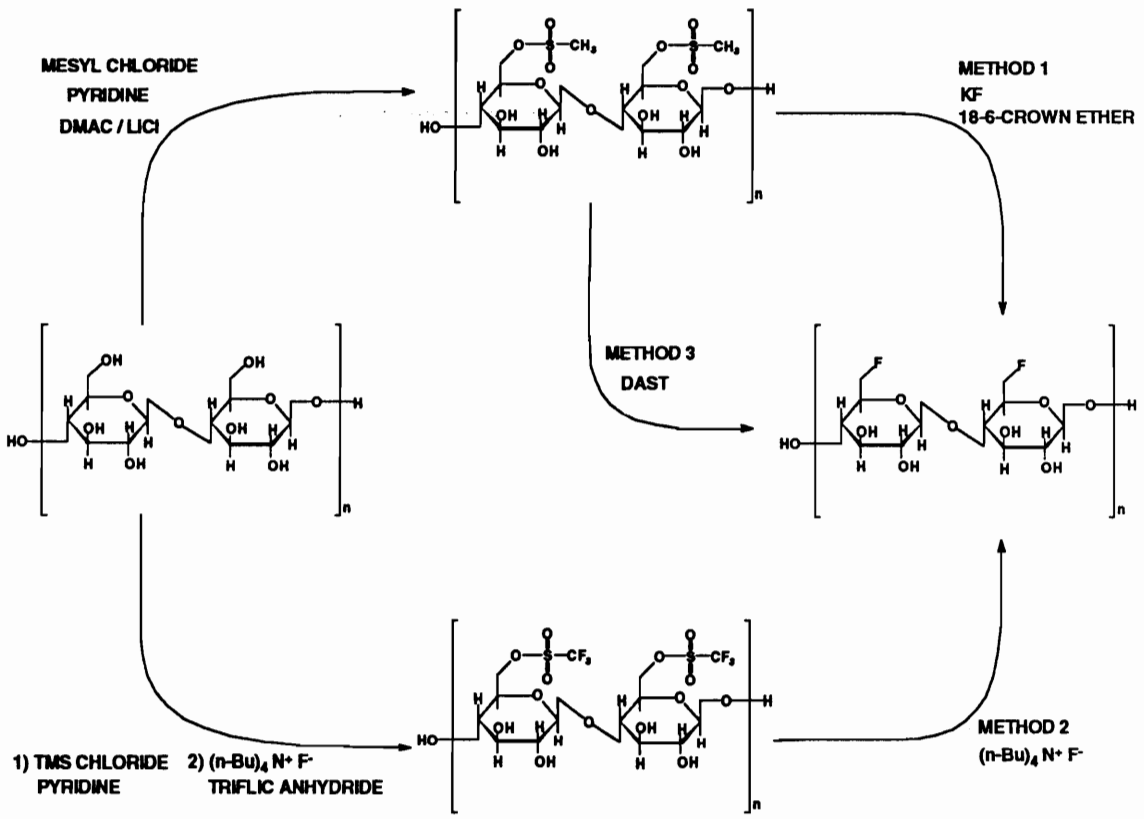

Figure 2. Synthesis of fluorodeoxycellulose using three different fluoride displacement techniques.

CHAPTER TWO

CELLULOSE FLUORINATION USING DIRECT FLUORINATION REAGENTS

PART ONE. HETEROGENEOUS, DIRECT FLUORINATION OF CELLULOSE

PART TWO. HOMOGENEOUS, DIRECT FLUORINATION OF CELLULOSE AND CELLULOSE DERIVATIVES

- **Model Reactions Between DAST and Trimethylsilyl Derivatives**
- **Evaluation of DAST in the DMAC/LiCl Solvent System**

II. CELLULOSE FLUORINATION USING DIRECT FLUORINATION REAGENTS

INTRODUCTION

The second technique previously employed for the synthesis of fluorodeoxycellulose has been the direct fluorination using two varieties of fluorosulfur reagents, Figure 1, previous section[1,2,3]. These methods have given the best results, but each has its own limitations. For example, Gorbunov et al. used sulffur tetrafluoride, in an autoclave at elevated temperatures to obtain a fluorodeoxycellulose with a DS as high as 1.5, or 17.3% fluorine[1]. However, it has been reported that severe degradation occurred under these conditions[1,3]. The extreme reactivity, and difficulty in handling, is an additional complication in the use of sulffur tetrafluoride[4]. Middleton developed an improved form of sulffur tetrafluoride that is still highly reactive but simpler to use[2]. The liquid, dialkyaminosulfur trifluoride, or DAST, is the adduct of SF_4 and trimethylsilyl dialkylamine, where the most commonly used form is the diethylamino sulfur compound[5]. Middleton reacted DAST with a cellulose extraction thimble and reportedly produced a drastic reduction of the surface free energy of the thimble[2]. Fluorine incorporation of the bulk material was low (0.69%) due to heterogeneous reaction conditions. Kasuya et al. overcame the limitations of heterogeneous chemistry by reacting DAST with a preformed cellulose acetate, homogeneously in dioxane or diglyme[3]. The cellulose acetates were only partially acetylated, with an acetate DS at C6 as low as 0.4. The free hydroxyls at the primary position were completely converted to deoxyfluoro groups. No reaction was reported to occur at free secondary hydroxyls.

From the literature, it appears that fluorosulfur compounds are the best fluorinating reagents for cellulose. However, little detail has been given to the issues of sulfur incorporation, or the effect on molecular weight and molecular weight distribution.

Gorbunov et al. report that sulfur was not detected by elemental analysis, however brown discoloration of the products is clearly stated[1]. Furthermore, extreme molecular weight loss is alluded to, and is probably unavoidable under the harsh conditions used with SF_4[1,3]. Molecular weight loss is not a problem with the heterogeneous conditions used by Middleton. However, no account of sulfur incorporation, as judged by product color, is given in this report[2]. The results of Kasuya et al. appear to be the most promising. The reaction of DAST with an organic soluble cellulose derivative gives significant fluorine incorporation, in addition to the relative ease of the procedure. In this case, the authors report a small molecular weight loss, and show a broadening of the size distribution[3]. No mention is made as to the exact nature of the increase in dispersity, whether it occurs by simple acid hydrolysis, or by branching under the effects of anhydrous HF. The potential for anhydrous HF catalyzed branching of cellulose has been known for some time[6,7,8]. However, the conditions for these branching reactions are heterogeneous, with large excesses of HF. Extensive depolymerization accompanies branching. As in previous cases, Kasuya et al. give no indication of sulfur content, or degree of discoloration of their fluorodeoxycellulose acetate.

DAST and DAST derivatives are actually a subgroup within a larger class of one step, direct fluorination reagents[4,9]. These reagents come in two varieties, and each shares a common structure and reaction mechanism (Figure 1). Both classes of reagents are activated by the lone pair of electrons from an attached dialkylamino group. The nucleus connected to the amino group also has two or three fluorine atoms attached to make this the active center of the reagent. The reactivity of the direct fluorinating reagents depends upon the nature of the active nucleus, X, shown in Figure 1. If X= Sulfur, the reagents are the highly reactive aminofluorosulfuranes, such as DAST[4]. If X= Carbon, then we have the less reactive fluoroalkylamino reagents (FAR). As with the fluoride displacement techniques, the direct fluorinating agents also require strictly anhydrous conditions.

DAST, FAR, and their respective derivatives react with alcohols rapidly, and in one step. Reactions are cleanest when the substrate is a primary alcohol, whereas eliminations and rearrangements are more common with secondary and tertiary alcohols[4,5,9]. DAST-type reagents are more reactive than the FAR-type reagents. This is because the sulfur-fluorine bond is much more labile than the fluorine-carbon bond. For example, in addition to the normal reaction with alcohols to give alkyl fluorides, DAST reacts with ketones and aldehydes to give geminal difluorides[4]. While aminocarbon fluorinating agents such as Ishikawa's reagent (hexafluoropropyldiethylamine) react with alcohols, and not with ketones and aldehydes[9].

The most significant drawback of the direct fluorinating agents is that they all produce HF as a by-product. This could cause a significant depolymerization of the cellulose chain, and give rise to the so called "reversion" oligomers[6,7,8]. These oligomers arise from the reaction of glycosyl fluoride with a free hydroxyl of any other carbohydrate, usually a monosaccharide[6]. The published work on the reaction between cellulose and anhydrous HF has, so far, been under heterogeneous conditions, and with very large excesses of HF[6,7,8]. These large amounts of HF are much greater than the amounts produced during the fluorination of cellulose. Consequently, it may be possible to avoid extreme depolymerization during cellulose fluorination with these reagents.

PART ONE

HETEROGENEOUS, DIRECT FLUORINATION OF CELLULOSE[a]

INTRODUCTION

Certainly, under heterogeneous reaction conditions, the low amount of HF produced during the fluorination of cellulose does not pose a problem. Middleton made no report of degradation during the surface fluorination of a cellulose extraction thimble[2]. We can safely conclude that low amounts of HF are not able to penetrate solid cellulose to cause any significant depolymerization. Therefore, and as Middleton reports, the direct fluorinating agents should offer a convenient method for the surface fluorination of solid cellulose.

Various surface treatments of cellulose have been successfully applied to the growing research of cellulose fiber/thermoplastic composites[10,11,12]. The objective has been to reduce the polarity of the cellulose surface in order to enhance compatibility with thermoplastics. Most research has concentrated upon dispersive interactions between treated cellulose and the thermoplastic matrix[10,11,12]. The surface fluorination of cellulose is of interest because of the potential for specific interactions with polar thermoplastics.

The work reported by Middleton is a convenient method for the surface fluorination of cellulose[2]. However, there is no mention of the surface character of this cellulose preparation; only a bulk fluorine content of 0.69% is reported[2]. The sulfur

[a] **This work was a collaboration with Gil Garnier, who performed all surface analysis. All synthetic work was performed by myself.**

content of Middleton's fluorinated cellulose is also not mentioned. With this specific interest in surface phenomena, the surface fluorination of solid cellulose was sought after.

The aim of this work was to prepare surface treated, or surface fluorinated cellulose. Two direct fluorinating reagents have been compared by their ability to effectively fluorinate the cellulose surface, with a minimum of extraneous surface contamination. The resulting surfaces have been characterized by X-ray Photoelectron Spectroscopy, XPS.

EXPERIMENTAL

MATERIALS:

All solvents were freshly distilled with the appropriate desiccants, prior to use. Unless otherwise stated, all reagents were purchased from Aldrich Chemical company, and used as received. All liquid transfers were strictly anhydrous, using syringe and cannula techniques. Whatman cellulose, type CF-11, was used as starting material in all cellulose reactions. Number average degree of polymerization was determined as approximately 200; polydispersity was 1.67.

METHODS:

X-Ray Photoelectron Spectroscopy:

X-ray Photoelectron Spectroscopy, XPS, was performed using a Perkin-Elmer 5400 instrument. The X-ray source was a magnesium ray of 1253.6 eV, operating at 400 watts, 15 kV. Analyses were run with a vacuum of approximately 1 x 10^{-7} torr, using a hemispherical analyzer, and fixed analyzer ratio. System controls were handled by an Appollo 3500 computer system.

Wide Angle X-Ray Scattering:

Wide angle X-ray scattering experiments were performed using a Phillips, PW

1720 X-ray generator, operating at 40 Kv, and 20 milli-amps. Detection was with Warhus cameras.

Prepararion of Cellulose Beads:

The procedure for cellulose dissolution in DMAC/LiCl was adapted, and modified from the literature[13,14]. Cellulose was activated by prolonged soaking in DMAC, 3-5 days. Afterwards, the suspension was filtered down to a DMAC drenched mass. Gravimetric analysis of samples from this mass was used to determine the solids content of the activated cellulose. With this known solids content, a 1% solution of cellulose in 8% LiCl (wt/vol)/DMAC was prepared. The initial suspension was stirred at room temperature until complete dissolution, normally 8-12 hours. This viscous cellulose solution was then regenerated drop by drop into a isopropanol/water, 50/50, nonsolvent. Dropwise regeneration causes the formation of highly spherical cellulose beads. Immediately following regeneration, the beads are opaque, and gelatinous, but with good mechanical integrity. These beads were subsequently solvent exchanged by soaking in distilled water. The aqueous solution was decanted off the top, and fresh water was replaced. This procedure was repeated several times. At this point all DMAC and LiCl was removed. Finally, the beads were dried thoroughly under 20 mm Hg vacuum and moderate temperature, to a final form of a 100-200 micron diameter bead.

Synthesis of Hexafluoropropyl Diethylamine:

Hexafluoropropyl diethylamine was synthesized using the procedure of Takaoka et al[9]. Two techniques are described, where method 2, the "Reaction at Atmospheric Pressure", was used in this work.

Heterogeneous Treatment of Cellulose Beads with DAST:

Dry cellulose beads, 25 grams, were quickly transferred into a flamed 100 ml round bottom flask under dry nitrogen flow. The flask was fitted with rubber septum,

and magnetic stir bar. Anhydrous THF, 30 ml, was transferred to the flask with a cannula, and slow stirring was started. The flask was cooled to -70°C in a dry ice/acetone bath. Methyl-DAST, 3 ml (30.7 mmoles), was added to the flask using a syringe. Afterwards, the flask was removed from the cooling bath and allowed to warm slowly to room temperature. The reaction proceeded at room temperature for 15 hours, when it was noticed that a dark brown color was developing. The reaction was ended by pouring the suspension over a mixture of ice and excess $NaHCO_3$. After thorough stirring, the mixture was filtered in a scintered glass Buchner funnel. The brown colored beads were then washed with about 2 liters of distilled water, followed by 1 liter of methanol, and 500 ml of dimethylformamide. In order to remove the discoloration, the beads were refluxed in THF for 15 minutes, then filtered and washed with water, methanol, and acetone. However, this treatment removed little if any color. Therefore, the beads were subsequently sohxlet extracted in: acetone for 24 hours, dioxane for 24 hours, and methanol for 48 hours. The methanol extraction did remove a significant amount of color. The beads were thoroughly dried under high vacuum, yielding a heterogeneously light brown colored bead product.

Heterogeneous Treatment of Cellulose Beads with FAR:

The experimental procedure was the same as above, aside from the following exceptions. Using a syringe, 8.8 ml of Ishikawa's reagent was added to the THF/cellulose bead suspension at room temperature. The reagent was a 1.6:1.0 mixture of the active, and inactive fluorinating agents respectively (see text). At a density of 1.262 g/cc, this means that approximately 31 mmoles of the active fluorinating agent were added. The reaction was allowed to stir at room temperature for 46 hours under dry nitrogen. After ending the reaction with ice and $NaHCO_3$, the beads were filtered and washed with: 2 liters of distilled water, 1 liter of methanol, and 500 ml of acetone. Finally, the beads were sohxlet extracted with methanol for 24 hours. The beads were dried under 20 mm Hg vacuum and moderate temperature to give the final product.

RESULTS AND DISCUSSION

The regenerated cellulose beads had an average diameter of 100-200 microns, and they were highly spherical. The density of the beads was measured at 1.35 g/cc, which is below the density of microcrystalline cellulose at 1.50-1.60 g/cc[15]. This difference in density suggested that the regenerated beads were highly amorphous. X-ray analysis confirmed the complete absence of crystallinity in these beads, Figure 2. While the cellulose beads were completely amorphous, there was no indication of swelling during fluorination with either DAST or FAR. Therefore, any fluorination that occurred is believed to have been only on the surface of the beads.

X-ray photoelectron spectroscopy, XPS, of the bead surfaces revealed that the DAST reacted beads had a surface fluorine content of 4.7%. This translates to a surface DS of approximately 0.4 to 0.5. XPS also showed that the DAST reacted beads had about 1% sulfur present on the surface. The second batch of beads was reacted with FAR, or Ishikawa's reagent. These beads had approximately 1.0% surface fluorine, or a surface DS of about 0.1.

The DAST reacted beads were treated with a 0.2 mass ratio of DAST to cellulose, in THF at room temperature for 15 hours. The FAR reacted beads were treated initially with a mass ratio of 0.27, FAR to cellulose, in THF at room temperature for 46 hours. In contrast, Middleton fluorinated a cellulose thimble in methylene chloride using a 0.9 mass ratio of DAST/cellulose for 24 hours at room temperature. In contrast to Middleton's reaction, this DAST reaction was only allowed to run for 15 hours, because the reaction medium was becoming very dark in color. This is normally indicative of severe discoloration of the cellulose product. Based upon this experience, it is safe to predict that Middleton's fluorinated cellulose thimble was probably, severely discolored. After prolonged extraction, the resulting beads were heterogeneously discolored brown. That is, some of the beads appeared white, while others where lightly to darkly brown

colored. XPS of the bead surface showed a 4.7% fluorine content, and an approximate sulfur content of 1%(Figure 3). No nitrogen was detected on the bead surface. It is very probable that the discoloration of the beads was the result of sulfur compounds that were either adsorbed or covalently bound to the cellulose surface. Based on the absolute fluorine content, and the elemental ratios, both determined by XPS, the surface fluorine DS of the beads was between 0.4 and 0.5. Roughly speaking, every other anhydroglucose unit on the bead surface was fluorinated.

In contrast, the FAR reacted beads had a lower surface fluorination, but without discoloration from sulfur contamination. XPS showed only slight fluorination, at approximately 1%(Figure 4). The stoichiometry of the Ishikawa reaction is not well controlled. As synthesized, the Ishikawa reagent is a mixture of an active saturated compound, and an inactive unsaturated compound[9] (Figure 5). HF generated in the fluorination of an alcohol is free to combine with the inactive molecule, giving rise to another mole of active fluorinating agent. Consequently, while the initial charge of active fluorinating agent is known, the total charge in this reaction is unknown. The Ishikawa reaction was allowed more time than the DAST reaction for two reasons. The first is that Ishikawa's reagent is less reactive than DAST. The second reason is that no discoloration of the cellulose was occurring, and therefore no threat of surface contamination was perceived. These beads were purified with much less effort than the DAST reacted beads; they were perfectly white, with no visual evidence of contamination. The surface DS of the FAR reacted beads was approximately 0.1, 1.0% fluorine. Or, on average, 1 hydroxyl fluorinated out of every 10 anhydroglucose units.

From these results we may conclude that both fluorinating agents provide an easy method for the surface fluorination of solid cellulose. Under the present circumstances, DAST appears to be much more effective than Ishikawa's reagent. However, DAST visibly contaminates the cellulose surface, probably due to the incorporation of sulfur.

Ishikawa's reagent causes no surface contamination, but it is not commercially available. Gratefully, it is easily synthesized, and has a reasonably good shelf life[9]. On the other hand DAST is commercially available in various forms, and is more reactive. It is likely that the drawbacks of both reagents could be controlled effectively. For example, the surface fluorination gained from Ishikawa's reagent could no doubt be enhanced with greater reaction time and temperature. Furthermore, sulfur contamination by DAST may be controlled using longer reaction times at reduced temperature. While there is no literature record, experience in this laboratory has shown that discoloration from DAST may be reduced by using lower reaction temperatures.

CONCLUSIONS

1. DAST and FAR are both convenient and effective reagents for the surface fluorination of cellulose.
2. DAST is more effective than FAR, but at a cost of sulfur contamination, and discoloration of the surface. FAR causes no contamination or discoloration of the cellulose surface.
3. It is very likely that the discoloration caused by DAST could be reduced by extended reaction times at much lower temperatures. Likewise, the effectiveness of FAR could probably be improved by extended reaction times, at higher temperatures.

LITERATURE CITATIONS

1. Gorbunov, B.N., A.A. Nazarov, P.A. Protopopov, and A.P. Khardin, Vysokomol. Soyed., A14, 12, 2527, 1972.

2. Middleton, W.J., U.S. Patent, 3 976 691, August, 1976.

3. Kasuya, N., K. Iiyama, and A. Ishizu, Appita, 6th Internat. Sym. Wood, Pulping Chem., vol. 2, 415, 1991.

4. Hudlicky, M., Organic Reactions, Vol. 35, 513, 1988.

5. Middleton, W.J., J. Organic Chem., 40, 5, 1975.

6. Franz, R., W. Fritsche-Lang, H.-M. Deger, R. Erckel, and Schlingmann, J. Applied Poly. Sci., 33, 1291, 1987.

7. Hardt, H., and D.T.A. Lamport, Phytochemistry, 21, 9, 2301, 1982.

8. Defaye, J., and A. Gadelle, Carbohydrate Res., 110, 217, 1982.

9. Takaoka, A., H. Iwakiri, and N. Ishikawa, Bull. Chem. Soc. Japan, 52, 11, 3377, 1979.

10. Felix, J.M., and P. Gatenholm, J. Applied Polymer Sci., 42, 609, 1991.

11. Kishi, H., M. Yoshioka, A. Yamanoi, and N. Shiraishi, Mokuzai Gakkaishi, 34, 2, 133, 1988.

12. Maldas, D. B.V. Kokta, and C. Daneault, J. Applied Polymer Sci., 37, 751, 1989.

13. McCormick C.L., and P.A. Calais, Polymer, 28, 2317, 1987.

14. McCormick, C.L., U.S. Patent No. 4 278 790, July, 1981.

15. Brandrup, J., and E.H. Immergut, Polymer Handbook, 3rd Edition, Wiley Interscience, New York, 1989.

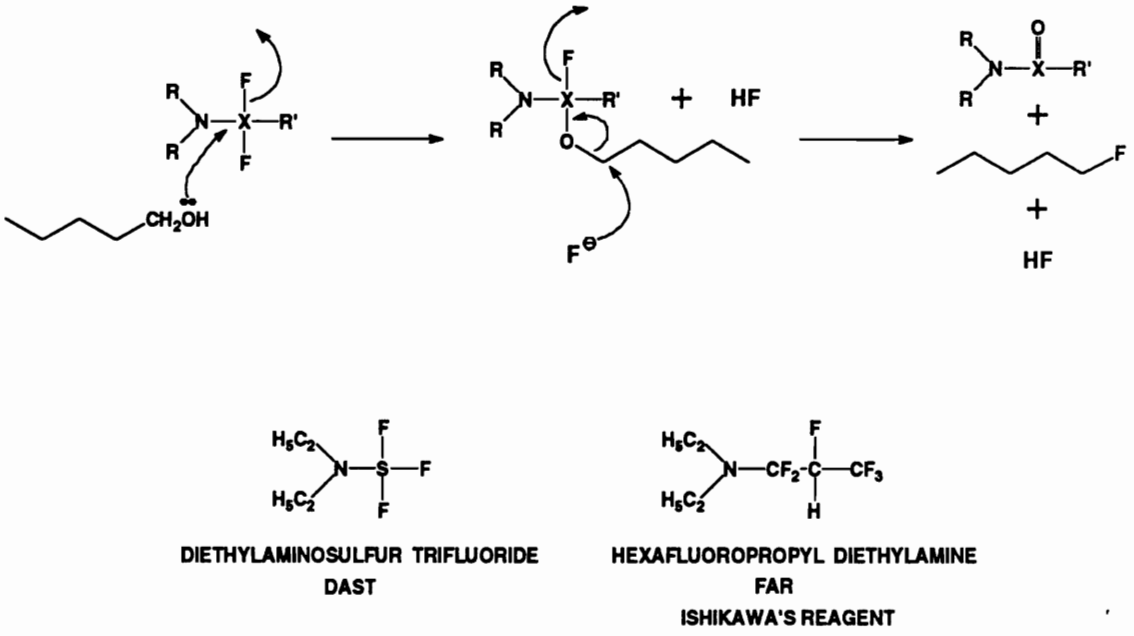

DIETHYLAMINOSULFUR TRIFLUORIDE
DAST

HEXAFLUOROPROPYL DIETHYLAMINE
FAR
ISHIKAWA'S REAGENT

Figure 1. Structure and reaction mechanism of one step fluorinating agents.

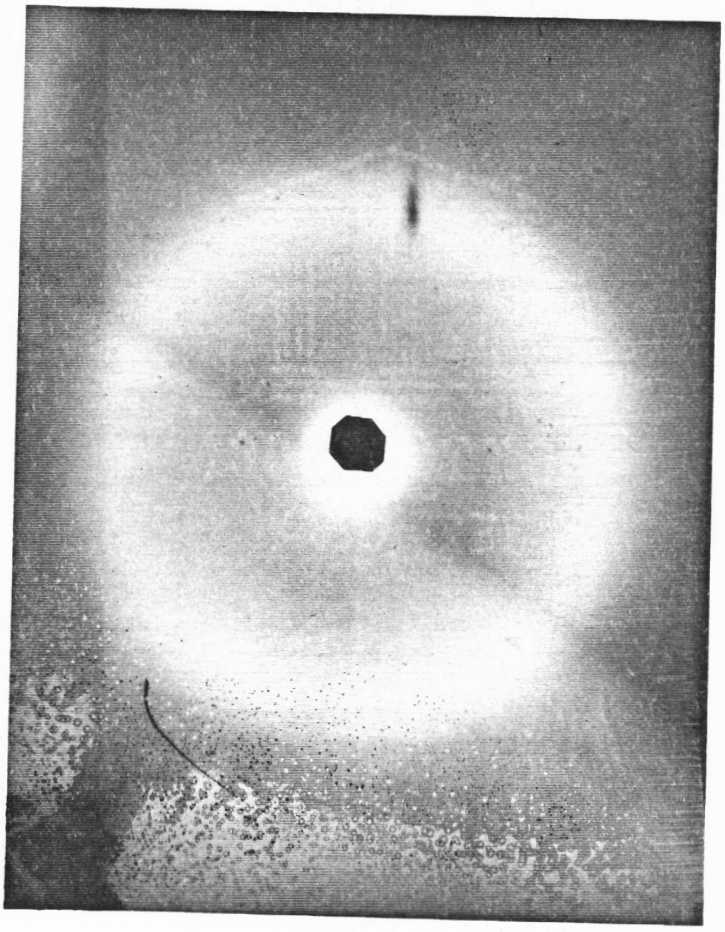

Figure 2. Wide angle X-ray of cellulose beads regenerated from DMAC/LiCl. The diffuse halo, and the lack of sharp reflections, indicate that there is no crystallinity present in this sample.

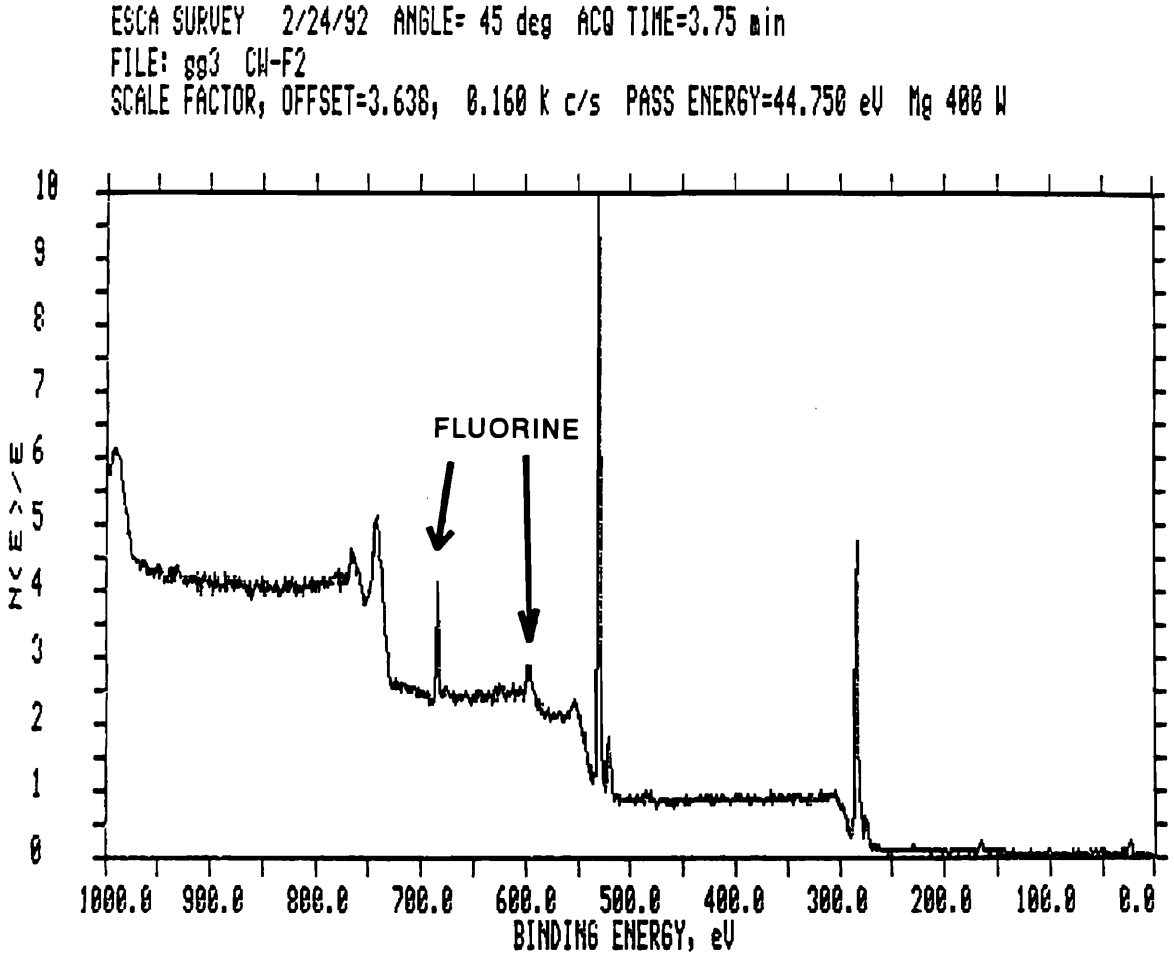

Figure 3. XPS of DAST reacted beads. The two signals from fluorine are indicated. The signal for sulfur is outside of the range shown here.

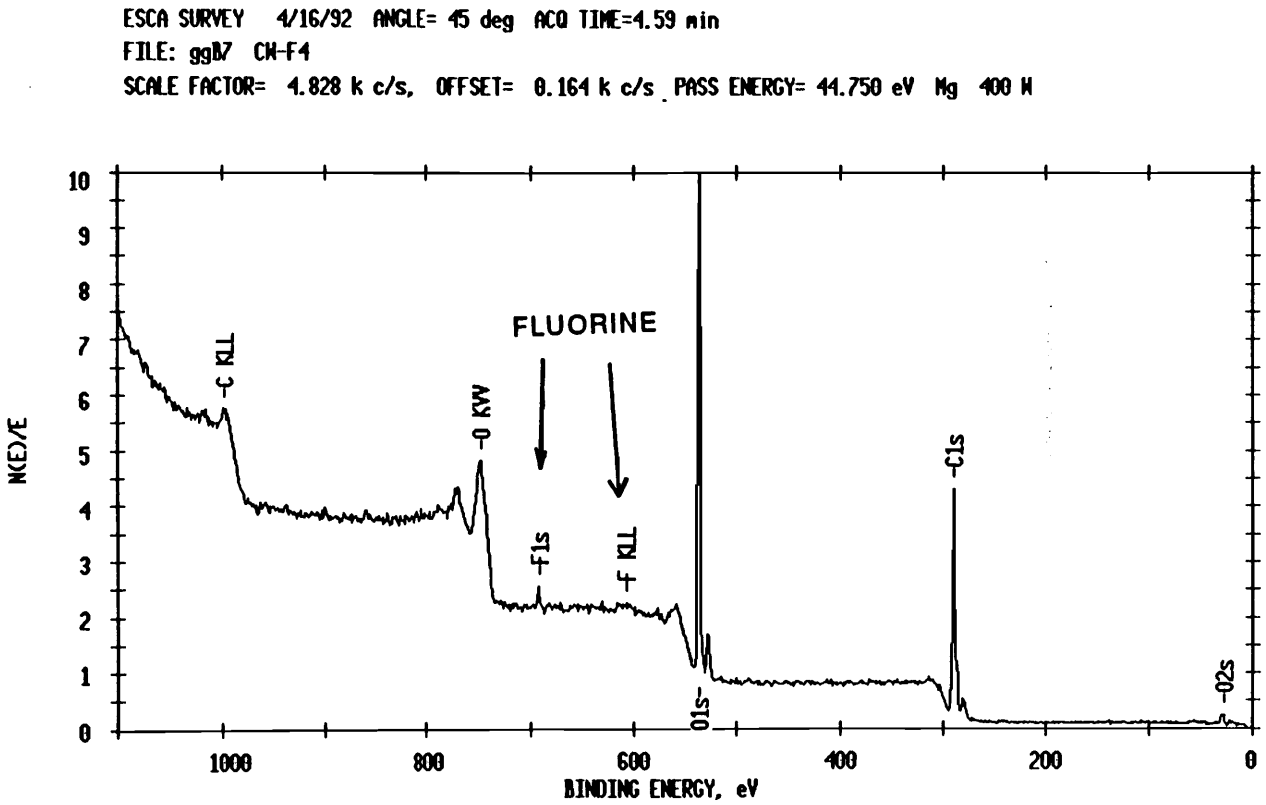

Figure 4. XPS of cellulose beads reacted with FAR, or Ishikawa's reagent. The presence of fluorine is indicated.

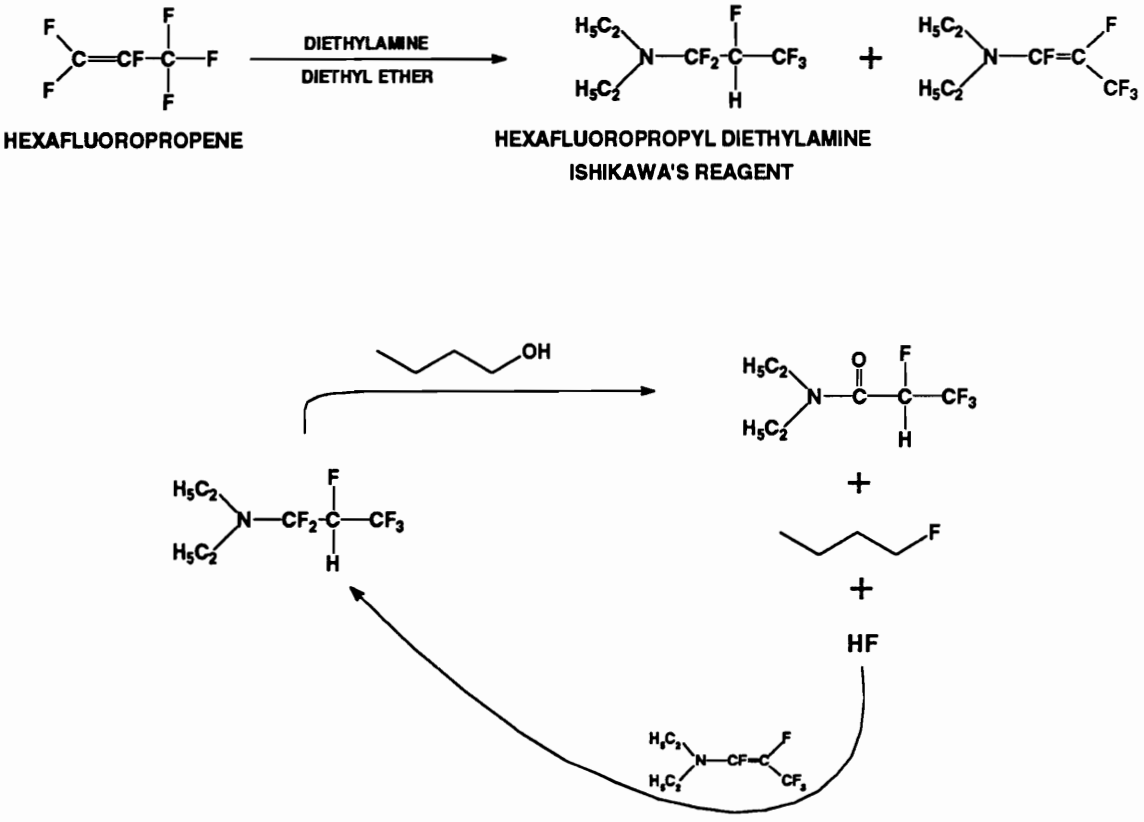

Figure 5. Synthesis of Ishikawa's reagent. The action of this reagent upon an alcohol generates a mole of HF. This HF combines with the unsaturated product to produce another mole of active fluorinating agent, as shown.

PART TWO

HOMOGENEOUS, DIRECT FLUORINATION OF CELLULOSE AND CELLULOSE DERIVATIVES

INTRODUCTION

Heterogeneous treatments of cellulose with reagents like DAST and FAR are effective for surface treatment. However, bulk fluorination of cellulose will require free access to all hydroxyls. Dissolution of cellulose is the obvious way of achieving this goal, but normally requires exotic, and highly polar solvent systems. Fluorinating agents such as DAST and FAR may be incompatible with these solvent systems. For example, DAST is used in solvents such as tetrahydrofuran, and methylene chloride. These common solvents can only dissolve cellulose derivatives, and not pure cellulose. Consequently, the homogeneous reaction of cellulose with one step fluorinating agents requires at least one of the following: 1) a soluble cellulose derivative that possesses reactivity with DAST, and/or FAR, or, 2) a solvent system that solubilizes cellulose without reacting with DAST or FAR. Curiously, DAST has the potential to fulfill both of these requirements.

DAST reacts with the trimethylsilyl ether of some alcohols in much the same way as with the parent alcohol[1,2]. Furthermore, DAST is also known to be unreactive towards acid derivatives such as esters[3] and amides. This suggests that dimethylacetamide, with LiCl may be compatible with DAST. With this in mind, the purpose of this work was to determine if DAST could fluorinate cellulose in a homogeneous solution. Two routes were taken toward this goal. One tested the compatibility of DAST with a cellulose solvent system, and the other was a search for a cellulose derivative, in

which the substituent was reactive with DAST directly.

PART TWO. SECTION A

MODEL REACTIONS BETWEEN DAST AND TRIMETHYLSILYL ETHERS

INTRODUCTION

The electronic character of TMS ethers is very similar to that of the parent alcohol. Like the proton, the silicon nucleus is an electropositive center that is susceptible to attack from fluoride. In fact, silicon has a remarkable affinity for fluoride, which is exploited in the numerous methods for the deprotection of silyl ethers. Silicon's affinity for fluoride makes TMS ethers of alcohols good candidates for reactions with reagents like DAST. To date, there are two reports of the successful fluorination of the TMS ethers of alcohols[1,2]. In both cases, however, the fluorinated nucleus was attached to a strongly electron withdrawing substituent. As such, these two cases are not appropriate models for the reaction between DAST and the TMS ether of cellulose.

Consequently, two model reactions were performed to test the feasibility of the reaction between DAST and the TMS ether of cellulose. The first model reaction was that between DAST and 4-phenyl-2-butanol-TMS ether, and secondly, the reaction between DAST and the TMS ether of cellobiose. The first model reaction tested the general reactivity of DAST with TMS ethers of aliphatic alcohols. The second model reaction was to determine if the above reaction was compatible with polysaccharides.

EXPERIMENTAL

MATERIALS:

All solvents were freshly distilled with the appropriate desiccants, prior to use. Unless otherwise stated, all reagents were purchased from Aldrich Chemical company, and used as received. All liquid transfers were strictly anhydrous, using syringe and cannula techniques.Whatman cellulose, type CF-11, was used as starting material in all cellulose reactions. Number average degree of polymerization was determined as approximately 200; polydispersity was 1.67.

METHODS:

Nuclear Magnetic Resonance:

A Varian, Unity-400 nuclear magnetic resonance spectrometer was used to collect ^{1}H spectra at 400 Mhz. Samples were prepared by dissolving the analyzed material in the appropriate deuterated solvents, using 5 mm Wilmad glass tubes.

Elemental Analysis:

Elemental analyses were performed by Galbraith Laboratories, 2323 Sycamore Dr., Knoxville, TN, 37921-1750.

Reaction of DAST with 4-Phenyl-2-Butanol TMS Ether:

4-phenyl-2-butanol, 2 ml (12.9 mmole), was dissolved into 25 ml of anhydrous THF, using a 50 ml triple neck round bottom flask. The flask was fitted with dry nitrogen atmosphere, rubber septum, and magnetic stir bar. Using a syringe, 2.08 ml (14.2 mmole) of trimethylsilyl imidazole was added to the reaction flask, at room temperature. Silylation was monitored by thin layer chromatography, TLC, using silica plates and petroleum ether:ethyl ether, 3:1. After completion of silylation, as judged by TLC, the reaction flask was cooled to -40°C in a dry ice/acetone bath. Then, methyl-DAST, 2.52 ml (25.8 mmole), was added to the flask with a syringe.

Again, the reaction was monitored by TLC using silica plates, and 100% petroleum ether. After 3.5 hours at -40°C, the reaction had only progressed partially. Subsequently, the flask was slowly warmed to 0°C over a 2 hour period. By this time the reaction was complete, by TLC. The solution was poured into a 250 ml separatory funnel which contained ice, excess $NaHC0_3$, and 50 ml ethyl ether. After thorough mixing, the organic layer was isolated and set aside. The aqueous layer was extracted with 25 ml ethyl ether, 4 times. All organic layers were combined, and washed with excess distilled water. The organic phase was dried with anhydrous $NaS0_4$, filtered, and concentrated to a yellow oil. This oil was run over a silica flash column using 100% petroleum ether as eluent. Two fractions were collected; one was 767 mg, and the other was 192 mg.

Synthesis of the TMS Ether of Cellobiose:

Silylation of cellobiose was performed using the methods adapted from Stein and Klemm[6]. All under dry nitrogen, 500 mg of dry cellobiose (11.7 mmole OH) was suspended in 50 ml of anhydrous THF using a flamed 100 ml round bottom flask fitted with rubber septum, and magnetic stir bar. Dry pyridine, 92 mg (1.16 mmole) was added with a syringe. At room temperature, 2.2 ml of TMS chloride,(17.3 mmoles) was added with a syringe. The flask was thoroughly flushed with dry nitrogen, and the rubber septum was sealed tightly with wire and parafilm. The flask was then placed in the refrigerator over night. The following morning, the flask was removed from the refrigerator, when it was noticed that the cellobiose was completely dissolved, and thin, long crystals of pyridine hydrochloride had formed. The crystals were quickly filtered from the THF solution using a Buchner funnel and Whatman filter paper. The THF solution was then concentrated on the rotational evaporator for a period of at least 3 hours. This left approximately 1 g of a viscous, light yellow oil, 74% yield.

Treatment of the TMS Ether of Cellobiose with DAST:

The silylated cellobiose oil was dried by storage under reduced pressure in the presence of phosphorous pentoxide for a period of 48 hours. The treatment of the oil with DAST proceeded with the flame drying of a 100 ml round bottom flask. The flask had a magnetic stir bar, and was sealed under dry nitrogen with a rubber septum. Silylated cellobiose (450 mg) was dissolved in 25 ml anhydrous THF, and then transferred to the reaction flask with a cannula. The reaction flask was cooled to -70°C with a dry ice/acetone bath, while positive dry nitrogen pressure was maintained. Ethyl-DAST, 1 ml (7.6 mmoles), was added slowly to the solution using a syringe. The flask was maintained at -70°C for about 2 hours, and then the flask was allowed to warm to room temperature over a period of 2 hours. At this time the solution was a light brown color, and appeared to be heterogeneous. The solution was poured into a 200 ml volume of ice water, containing an excess of $NaHCO_3$. After thorough stirring, the product was filtered and washed exhaustively with distilled water, and methanol. The solid material was dried under a 20 mm Hg vacuum, and at temperature of 40°C for 24 hours. Approximately, 200 mg of an orange-brown material was isolated. This material was insoluble in THF, $CHCl_3$, methanol, and water. Elemental analysis revealed 40.97% Carbon, 6.21% Hydrogen, and 3.11% Fluorine.

RESULTS AND DISCUSSION

The model reaction between DAST and the TMS-ether of 4-phenyl-2-butanol produced 1-phenyl-3-fluorobutane as the major product. ^1H NMR of the major fraction, 1-phenyl-3-fluorobutane, shows a multiplet centered at about 4.65 ppm, which results from the proton attached to the fluorinated carbon(Figure 1). This signal should be a multiplet with about 32 lines. The fluorinated methine and attached methyl group give rise to 8 lines, while the methylene attached to the fluorinated carbon has two inequivalent protons which split the signal into a mutiplet of 32 lines.

Indeed the expansion of this region shows about 28 resolved signals. The absolute chemical shift, and the extreme multiplicity of this signal, confirm the presence of fluorine in the sample. A minor fraction, a mixture of olefinic isomers, resulted from elimination, as indicated by the signals between 5 and 6 ppm(Figure 2). The incidence of elimination is common with DAST, and often varies with conditions[4]. The yields of the fluoride, and elimination products, was only 38 and 9% of the total, respectively. The reason for the great loss is not clear, and must be attributed to loss during work up. Regardless, this suggests that the fluorination of aliphatic TMS ethers is possible with DAST. Absolute proof requires the elimination of imidazole. It is possible that imidazole could initiate the deprotection of the TMS ether, which would subsequently react with DAST in the normal fashion. Therefore, it is necessary to isolate the TMS ether, and then react it with DAST. With this in mind, the model reaction between DAST and the TMS ether of cellobiose was performed.

The TMS ether of cellobiose was formed and isolated from imidazole. Fluorination did occur, but the dominant reaction appears to have been cross-linking. Elemental analysis showed a good degree of fluorination, 3.1%. However, the insolubility of the product precluded any other type of analysis. The product was insoluble in all solvents, including water, acetone, THF, and methanol. This fluorinated material did swell in DMSO. The exact cause of cellobiose cross-linking was not determined in this case. In reference to the literature, the conditions employed here suggest that anhydrous HF could catalyze cross-linking through the formation of glycosyl fluoride[7,8,9](Figure 3). HF readily attacks glycosidic linkages, and under anhydrous conditions, α-glycosyl fluoride is formed. The small nuclear diameter of fluorine allows for good orbital overlap between fluorine and the lone pair of electrons of the ring oxygen. Consequently, carbon 1 of α-glycosyl fluoride enjoys a substantial contribution from the oxonium resonance structure(Figure 3). As a result, carbon 1 is extremely vulnerable to nucleophilic attack. Glucose effectively

becomes a highly functional, and polymerizable monomer[7,8,9]. Given the degree of fluorination, the reaction between DAST and the TMS ether of cellobiose does appear to work. Complications seem to arise, possibly, due to the action of anhydrous HF on the glycosidic linkage. Silylation of all alcohols should prevent the production of free HF. Instead of HF, a TMS ether will form fluorotrimethylsilane. Therefore, if this cross-linking was HF catalyzed, then silylation was incomplete, and /or, there was sufficient moisture present to form HF. Another possible mechanism could have been a DAST mediated etherification between individual alcohols[4,10]. However, this mechanism also requires free alcohol, in which case HF will form. Under these circumstances, and given the hydrolytic instability of TMS ethers, it seems likely that cellobiose was incompletely silylated. Furthermore, the proposed HF cleavage of the glycosidic bond is catalytic in HF, provided there are free hydroxyls to react with glycosyl fluoride. There are no reports of the direct cleavage of glycosidic bonds by DAST, in the absence of HF.

Although this was only a model reaction, it appears that the direct fluorination of cellulose derivatives may be compromised by cross-linking. Kasuya et al. report no such complications during the reaction between DAST and a lightly derivatized cellulose acetate[3]. DAST was mixed with cellulose acetates which had an overall DS of 1.7, and 2.2. Reportedly, as much as 50% of the primary positions were free, and unacetylated. After the DAST treatment, all of the free hydroxyls were converted to alkyl fluorides. Kasuya et al. show GPC elution profiles of the products, where there appears to be an increase in a low molecular weight component. But there is no mention of branching or gelation. If a sufficient quantity of hydroxyls is capped as acetates, then the gelation reaction may be inhibited. In such a case, all HF would be titrated during the formation of glycosyl fluoride. Consequently, all glycosyl fluorides will be hydrolysed during work up. The effect would be a molecular weight loss, without branching. The capping of hydroxyls by partial acetylation, may explain why

Kasuya observes molecular weight loss, without branching.

CONCLUSIONS

1. DAST successfully converts the TMS ether of simple aliphatic alcohols to the corresponding alkyl fluoride.
2. When DAST is reacted with the TMS ether of cellobiose, fluorination occurs, but in competition with an apparent cross-linking reaction.
3. This cross-linking appears to be HF catalyzed.

LITERATURE CITATION

1. Markovskii, L.N., L.S. Bobkova, and V.E. Pashinnik, Zhg. Org. Khim., 17, 1903, 1981.

2. LeTourneau, M.E., and J.R. McCarthy, Tetrahedron Letters, 25, 5227, 1984.

3. Kasuya, N., K. IIyama, and A. Ishizu, Appita, 6th Internat. Sym. Wood, Pulping Chem., vol. 2, 415, 1991.

4. Hudlicky, M., Organic Reactions, Vol. 35, 513, 1988.

5. Middleton, W.J., E.M. Bingham, and D.H. Smith, J. Fluorine Chem., 23, 557, 1983.

6. Stein, A., and D. Klemm, Makromol. Chem., Rapid Commun., 9, 569, 1988.

7. Franz, R., W. Fritsche-Lang, H.-M. Deger, R. Erckel, and Schlingmann, J. Applied Poly. Sci., 33, 1291, 1987.

8. Hardt, H., and D.T.A. Lamport, Phytochemistry, 21, 9, 2301, 1982.

9. Defaye, J., and A. Gadelle, Carbohydrate Res., 110, 217, 1982.

10. Johnson, A.L., J. Organic Chem., 47, 5220, 1982.

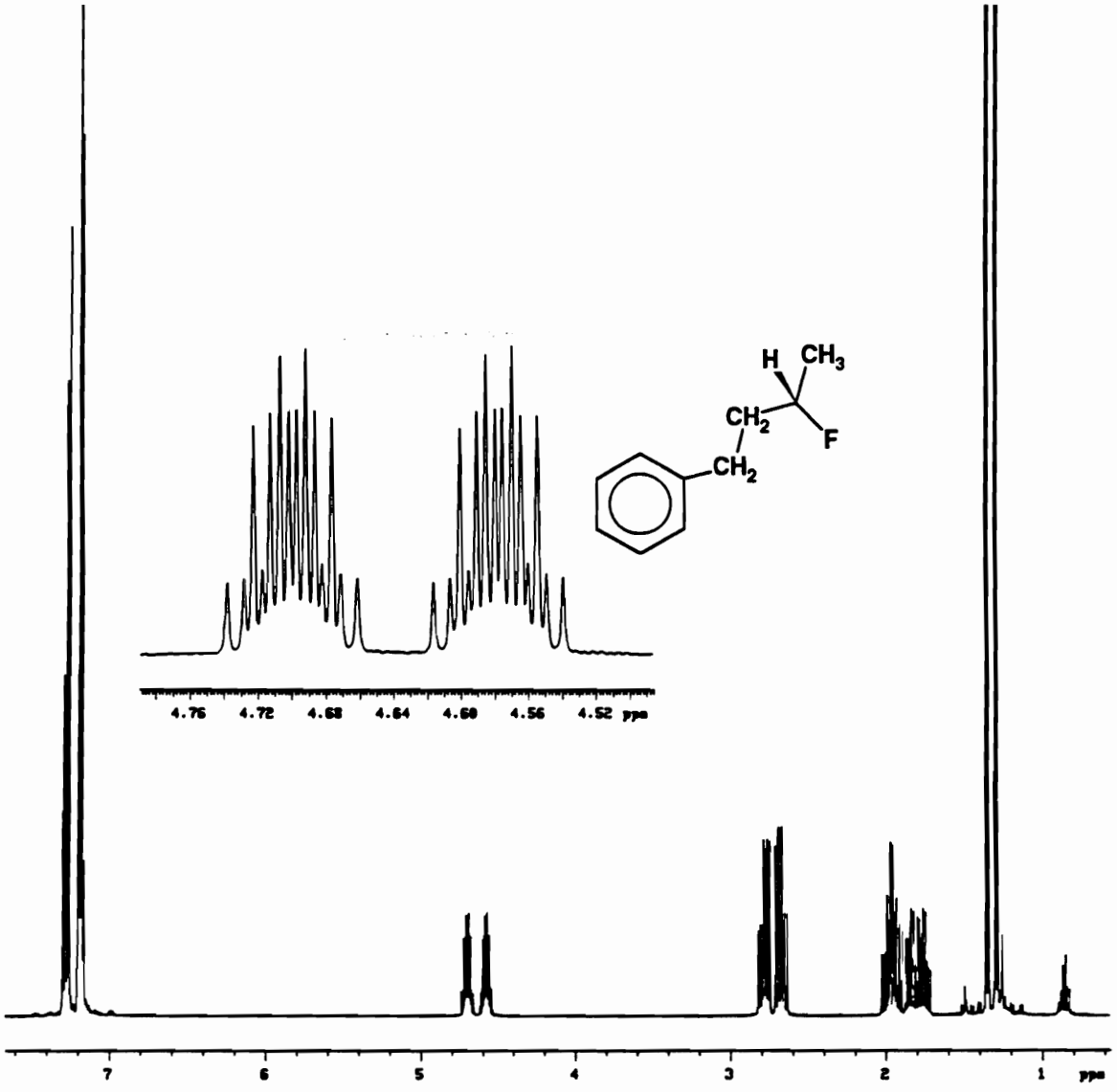

Figure 1. ^{1}H NMR spectrum of 1-phenyl-3-fluorobutane, one product of the model reaction of DAST with 4-phenyl-2-butanol-TMS ether. The inset shows the extreme mutiplicity of the proton which is attached to the fluorinated carbon.

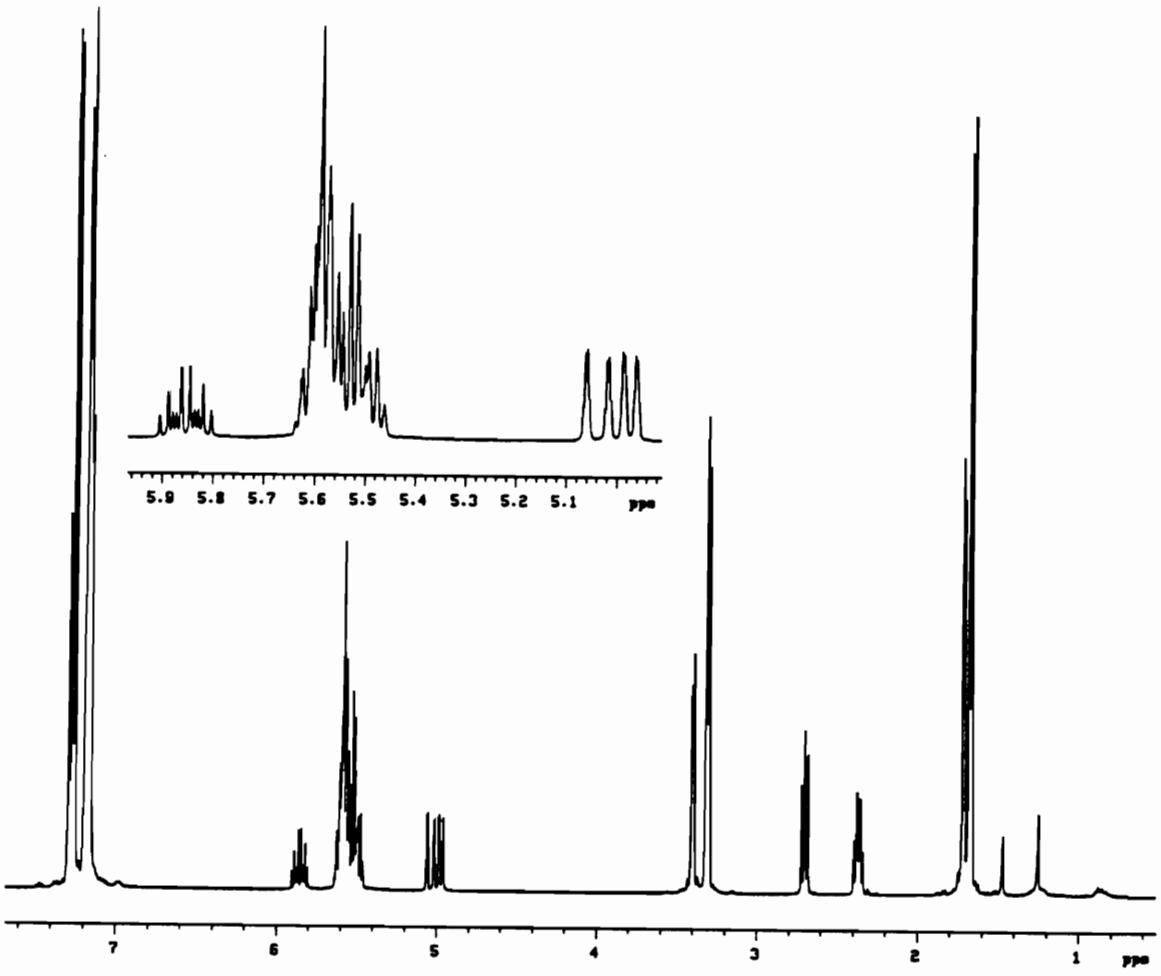

Figure 2. ^{1}H NMR spectrum of phenylbutene isomers resulting from model reaction of DAST with 4-phenyl-2-butanol-TMS ether. The inset shows signals in the olefin range, which indicate that this is the product of elimination.

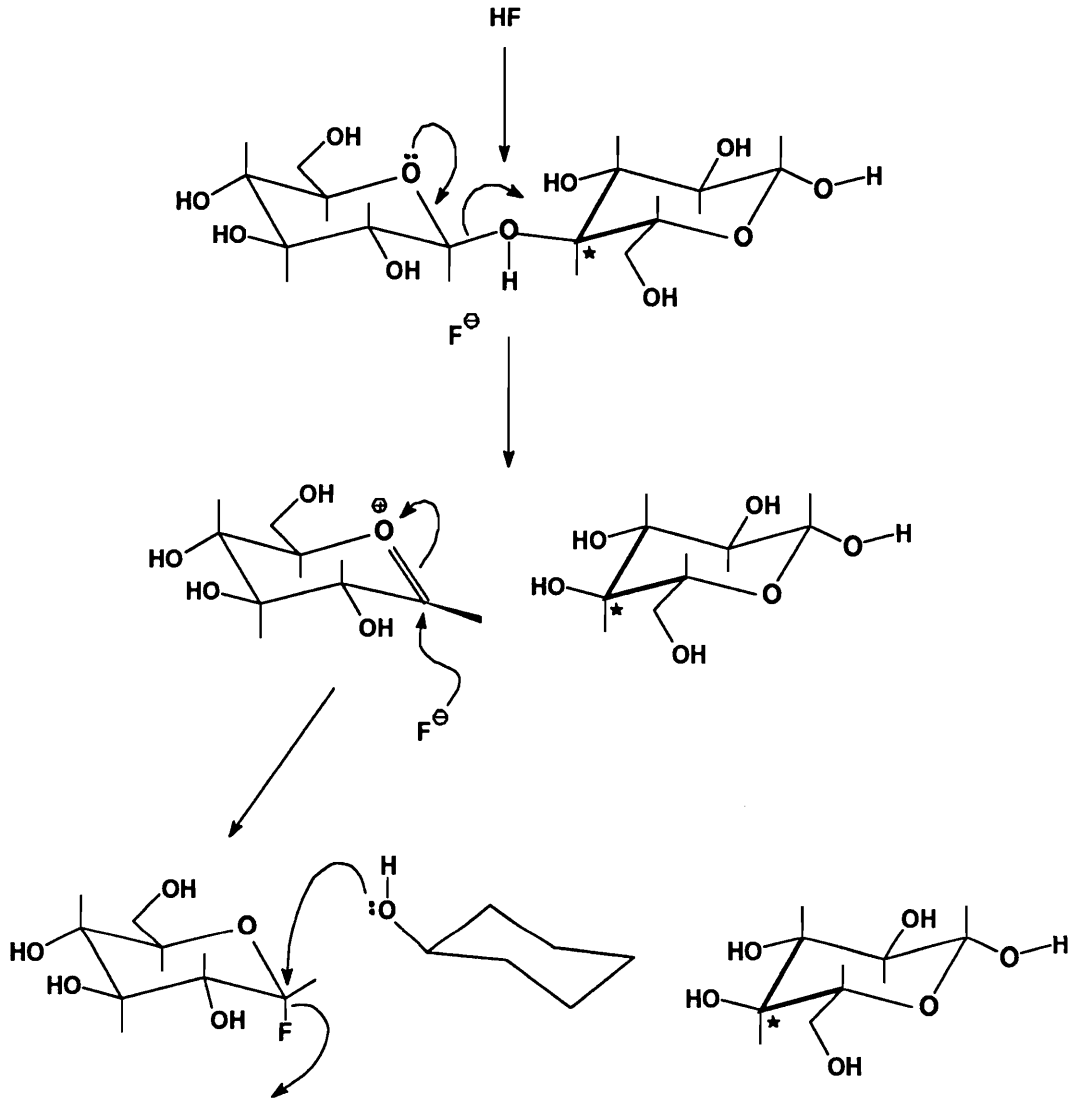

Figure 3. Mechanism showing the HF catalyzed crosslinking of β-glycosides. Note, that any nucleophile may attack the glycosyl fluoride intermediate. The cyclohexanol shown here represents any nucleophile, besides the exiting endgroup.

PART TWO. SECTION B

EVALUATION OF DAST IN THE DMAC/LiCl SOLVENT SYSTEM

INTRODUCTION

DAST reportedly does not react with amides, which is surprising when considering the mechanism, and extreme reactivity of DAST[1,2]. There has been only one report of inert DAST and amide mixtures[2]. In this report, Middleton shows that DAST is unreactive towards the amide functionality of hydroxy diazepam. Diazepam is a relatively complex, cyclic amide that bears very little resemblance to dimethylacetamide. Therefore, the first task was to show that DAST/DMAC mixtures were stable. Afterwards, ternary mixtures of DAST/DMAC/LiCl were similarly observed. These tests were performed by observing changes in the ^{1}H NMR of DAST mixtures, as a function of time, and temperature. With the completion of these experiments, this ternary mixture had to be tested for its activity in model reactions. Lastly, it was necessary to observe the effects of DAST on DMAC/LiCl/cellulose solutions, directly.

EXPERIMENTAL

MATERIALS:

All solvents were freshly distilled with the appropriate desiccants, prior to use. Unless otherwise stated, all reagents were purchased from Aldrich Chemical company, and used as received. All liquid transfers were strictly anhydrous, using syringe and cannula techniques. Whatman cellulose, type CF-11, was used as starting material in all cellulose reactions. Number average degree of polymerization was determined as approximately 200; polydispersity was 1.67.

METHODS:

Nuclear Magnetic Resonance:

A Varian, Unity-400 nuclear magnetic resonance spectrometer was used to collect ^1H NMR spectra at 400 MHz. Samples were prepared by dissolving the analyzed material in the appropriate dueterated solvents, using 5 millimeter Wilmad glass tubes.

Mass Spectroscopy:

Mass spectral analyses were performed usinga model 7070 E-HF, magnetic sector, double focusing, mass spectrometer, maufactured by VG Analytical, of Manchester, UK. Samples were analyzed using a direct probe.

Elemental Analysis:

Elemental analyses were performed by Galbraith Laboratories, 2323 Sycamore Dr., Knoxville, TN, 37921-1750.

^1H NMR Study of DAST/DMAC Mixtures:

Anhydrous, DMAC was mixed with methyl-DAST (2:1 molar ratio), at room temperature in a 25 ml round bottom flask, which was fitted with magnetic stir bar, rubber septum, and dry nitrogen atmosphere. This mixture was allowed to stir for 4 hours before sampling. Using a syringe an aliquot of approximately 0.1 ml was transferred to a 5 mm NMR tube which was sealed with a rubber septum. The NMR tube was then filled to a height of 55 millimeters with deuterated $CHCl_3$, and after replacing the septum with the NMR tube cap, it was thoroughly shaken. After 24 hours, another aliquot was taken from the DAST/DMAC mixture, and a similar NMR sample was prepared. Finally, after 48 hours, another sample was taken, and then the original DAST/DMAC mixture was heated to 80°C over a 45 minute period. Three samples were taken during this 45 minute period of heating, one each at 40° , 50° , and 80°. Each time the DAST/DMAC mixture was sampled for NMR analysis, a small portion of the

mixture was added to water as a gross indication of its reactivity.

^{1}H NMR Study of DAST/DMAC/LiCl Mixtures:

The same procedure was used here, as was mentioned above. Initially, however, an amount of LiCl was weighed into a 25 ml round bottom flask that would give a 7%, wt/vol, solution in DMAC. Under dry nitrogen flow, the LiCl was thoroughly dried by prolonged flaming of the round bottom flask, with simultaneous rapid stirring. Aliqouts were taken immediately after, and 48 hours after, making the solution. NMR samples were prepared as mentioned above. Similarly, as above, the solution was tested for water reactivity each time an aliquot was removed.

Treatment of 4-Phenyl-2-Butanol with DAST/DMAC/LiCl Solution:

LiCl, 2 g, was placed into a clean 100 ml round bottom flask. The flask was fitted with magnetic stir bar, rubber septum, and dry nitrogen. Under a steady flow of dry nitrogen, and rapid spinning of the stir bar, the flask was flamed thoroughly to ensure the dryness of the LiCl. After the flask cooled to room temperature, 25 ml of anhydrous DMAC was added with a syringe. After complete dissolution of the LiCl, 245 mg (1.63 mmoles), of 4-phenyl-2-butanol was added to the flask with a syringe. The solution was cooled to 0°C, and the mixture was completely homogeneous under constant stirring. Methyl-DAST, 435 mg (3.27 mmoles), was added slowly to the reaction flask using a syringe. Afterwards, the solution was allowed to warm to room temperature, and subsequently stirred for 1 hour. Then the solution was poured into a separatory funnel containing 25 ml of diethyl ether, and 100 ml of ice water with excess $NaHCO_3$. After thorough shaking, the ether layer was set aside, and the aqueous layer was extracted 5 times with 50 ml of ethyl ether. The combined ether layers were washed with distilled water. The organic phase was then dried with anhydrous $NaSO_4$, and concentrated to a light yellow/orange oil. The yield of this crude fraction was 291.3 mg, 106% of theoretical.

DAST Treatment of Cellulose Dissolved in DMAC/LiCl; Part 1:

LiCl, 8 g, was quickly transferred to a clean 250 ml triple neck flask. The flask was fitted with a dry nitrogen atmosphere, a 50 ml addition funnel, and a magnetic stir bar. With rapid spinning of the stir bar, the flask was flamed thoroughly in order to completely dry the LiCl. After the flask cooled to room temperature, 100 ml of anhydrous DMAC was added, followed by heating to 80°C to facilitate dissolution of LiCl. Upon complete dissolution of LiCl, heating was stopped and 2.9 gm of DMAC activated cellulose (1 g dry cellulose, 18.5 mmoles OH) was quickly transferred to the DMAC/LiCl solution. Cellulose dissolution was complete after approximately 6 hours. When the cellulose was totally dissolved, preparations were made for the addition of DAST. Using a dry cannula, 25 ml of anhydrous DMAC was transferred to the addition funnel. Then, methyl-DAST, 1.81 ml (18.5 mmoles), was added to the addition funnel with a syringe. The DAST solution was added slowly to the cellulose solution at room temperature over a period of about 90 minutes. Approximately 30 minutes into the addition of DAST, the cellulose solution gelled completely. The gel was transparent and jelly-like; stirring was inhibited. At this point, more of the DAST solution was added, and the flask was shaken manually to assist in breaking the gel. Finally, the gel did break, and unassisted magnetic stirring was resumed. The rest of the DAST solution was added, and the flask was allowed to stir at room temperature for 20 hours. Subsequently, the contents of the flask were poured into a 500 ml volume of ice water with excess $NaHCO_3$. The cellulose precipitated in a gelatinous form. The product was washed with distilled water and methanol, dried, and then sohxlet extracted in methanol for 48 hours. The product was then dried under a 20 mm Hg vacuum, at 50°C. 2.723 g of a light yellow powder was recovered. This material was then acetylated to provide an organic soluble sample for NMR, and molecular weight analysis.

Acetylation of DAST/DMAC/LiCl/Cellulose Reaction Product:

The dried product of the above reaction was placed in a dry 100 ml double neck

flask, which was fitted with condenser, dry nitrogen, rubber septum, and magnetic stir bar. Anhydrous pyridine and acetic anhydride, 15 ml of each were added to the flask. The mixture was heated to 60°C. After approximately 4 hours, the solution became too viscous to stir, and an additional 15 ml each, of pyridine and acetic anhydride was added. The solution stirred at 60°C for 24 hours, and then the temperature was raised to 100°C for 4 more hours. The flask was cooled to room temperature, and the contents were poured into 200 ml of methanol. The light brown precipitate was sohxlet extracted with ethanol for 24 hours, and then with methanol for 4 hours. The product was dried and dissolved in $CHCl_3$. The cloudy solution was centrifuged, and the supernatant was poured into methanol. The precipitate was dried under high vacuum at 40°C. 1.162 g of a brown colored material was recovered. This material was soluble in $CHCl_3$ and THF. Elemental analysis revealed 10.03% Chlorine.

DAST Treatment of Cellulose Dissolved in DMAC/LiCl; Part 2:

The DAST reaction on cellulose dissolved in DMAC/LiCl was repeated twice more under the same conditions as stated above, besides the following exceptions.

Duplicate Reaction # 1:

After precipitation of the product into ice water and excess $NaHCO_3$, the product was sohxlet extracted in: methanol for 6 hours, water for 5 hours, acetone for 19 hours, and finally THF for 15 hours. Then the product was dried and 2.1262 g of a dirty-yellow material was recovered. This material (250 mg) was subjected to reaction with phenylisocyanate, in pyridine at 80°C for 3 days using the method of Evans and Wallace[3]. The product of this reaction was dried, dissolved in DMSO, and reprecipitated in water. After vacuum drying, 98 mg of a black material was recovered.

Duplicate Reaction # 2:

Duplicate DAST reaction # 2 was performed exactly as duplicate reaction number

1, except for the following. Before the addition of the DAST solution, a solution of 1.947 g (9.1 mmoles), of bis-1,8(dimethylamino)naphthalene, or Proton Sponge, was dissolved in 15 ml of anhydrous DMAC, and added to the cellulose solution via the addition funnel. During, and after the addition of the Proton Sponge solution, no precipitation of the cellulose solution occurred. Furthermore, during and after the addition of the DAST solution, no gelation of the reaction medium occurred. The product of this reaction was also treated with phenylisocyanate, in pyridine, as in duplicate reaction # 1. The product from this phenylisocyanate reaction was dissolved in THF, and centrifuged. The supernatant was poured into methanol, and the precipitate was vacuum dried at 40°C. A yellow powder (391 mg) was recovered.

RESULTS AND DISCUSSION

The ^{1}H NMR spectra of pure methyl-DAST, pure DMAC, and the mixture of methyl-DAST and DMAC indicate that mixtures of DAST and DMAC are inert. A small broadening of the signals occurs upon mixing, and the methyl signal of DAST has shifted from 3.18 ppm for the pure sample to 2.99 ppm in the mixture(Figure 1). The three signals of DMAC are also shifted, but only very slightly. Because there are no major changes in the positions of the signals, it is reasonable to conclude that the shifts result from solvent effects, and not from chemical reaction. This mixture reacts explosively with water, which also demonstrates that DAST remains active when mixed with DMAC. Likewise, the DAST/DMAC mixture remains stable over time. There are no changes in the ^{1}H NMR spectra 24 hours after sample preparation(Figure 2). After 48 hours at room temperature, the mixture was slowly heated to 80°C over a period of 45 minutes. Considerable siganl broadening occurs with heating(Figure 3). However, the signals do not shift drastically, and the samples react violently with water after heat treatment. These results clearly support the previous report that mixtures of DAST and N,N-disubstituted amides are inert.

Ternary mixtures of DAST/DMAC/LiCl have ^{1}H NMR spectra similar to the above binary mixture, with 3 notable exceptions: 1) a slight field shift, probably due to the presence of LiCl, 2) signal broadening in the sample containing LiCl, and most notably, 3) a small additional signal downfield from the other signals at about 3.12 ppm(Figure 4). The additional signal at 3.12 ppm suggests that some reaction is occurring, but it does not seem to go to completion. This particular signal does not grow in intensity after 48 hours at room temperature(Figure 5). All signals remain at the same intensity; however, there is about a 0.1 ppm downfield shift with time. As above, this ternary mixture reacted violently with water. The ^{1}H NMR indicates that LiCl does alter the DAST/DMAC mixture. However, one may argue that the changes are minor, and the mixture does appear stable over time. The explosive reactivity of this mixture with water certainly proves that DAST retains activity in the presence of LiCl. These results suggest that DAST is stable in the DMAC/LiCl solvent system. As such, it may be possible to directly fluorinate cellulose, homogeneously, in DMAC/LiCl solution.

However, the abundance of chloride ion in the DAST/DMAC, and 7% LiCl, mixture, could cause chlorination, and not fluorination of an alcohol. Consequently, this complex mixture was tested for its ability to fluorinate and/or chlorinate 4-phenyl-2-butanol. 4-Phenyl-2-butanol was treated with DAST in the DMAC/LiCl solvent system, using conditions employed for normal DAST reactions.

The ^{1}H NMR of 4-phenyl-2-butanol and the model reaction product are very similar(Figure 6). This reaction has eliminated the hydroxyl, and has also caused a downfield shift of all proton signals in the product, relative to 4-phenyl-2-butanol. This signal shift indicates that an elctronegative element has replaced the hydroxyl. However, the methyl signal at 1.99 ppm is a doublet, and not a quartet as it would be if the sample was fluorinated. The ^{1}H NMR suggests that the alcohol has been chlorinated, and it indicates that the crude product mixture is over 90% pure.

Double Quantum filtered COSY, DQCOSY, and Distortionless Enhancement Polarization Transfer, DEPT, NMR experiments proved that no rearrangements of the butane backbone occurred as a result of the action of DAST/LiCl. The DQCOSY experiment demostrated that all protons in the product retained the same connectivity as in the starting material(Figure 7). Like wise, the DEPT experiment showed that the product, like the starting material, contained one methine, two methylenes, and one methyl carbon in the butane backbone(Figure 8). As expected, the ^{19}F NMR showed no sign of fluorine in the product. Therefore it appears that the DAST/DMAC/LiCl mixture is a good chlorination reagent, but is not suitable for fluorination.

In fact, the mass spectrum of the crude reaction product demonstrates that this mixture is extremely potent for chlorination(Figure 9). Computer analysis of the isotope cluster abundance shows that the sample was chlorinated in two positions. The atomic formula for the sample is $C_{10}H_{12}C_2$. Based upon the mass and NMR spectral evidence, the product of this reaction is 1-(p-chlorophenyl)-3-chlorobutane(Figure 9). The molecular ion for this sample would then be 202 with an M+2 ion aproximately 65% of the parent ion intensity, as is the case. Furthermore, common fragment losses are as follows:

FRAGMENT LOST		ION GENERATED
-63	C_2H_4Cl	139
-50	CH_3Cl	152
-71	HCl_2	131
-77	C_3H_6Cl	125
-126	$C_4H_8Cl_2$	76

These common fragment losses support the assignment of the proposed structure. The proton splitting pattern in the aromatic region suggests that chlorine substitution occurred

para to the alkyl substituent(Figure 6). The aromatic substitution by chlorine is most probably a para directed electrophilic attack of the sulfur nucleus of DAST, as shown in Figure 10. These results suggest that DAST does retain its activity in the DMAC/LiCl solvent system. However, the mass action of the extreme excess of chloride causes chlorination exclusively, and potently.

Indeed, cellulose became highly chlorinated when treated with DAST in DMAC/LiCl. The chlorinated cellulose product was acetylated to facilitate analysis. The peracetylated material had a chlorine content of about 10.03%, by elemental analysis. Assuming a 6-chlorordeoxy-2,3-diacetate structure, this chlorine content corresponds to a chlorine DS of about 0.8. Curiously, during molecular weight and NMR analysis, there was evidence for a very peculiar side reaction that appears to have caused branching of the cellulose backbone. Indeed, the reaction medium gelled during the addition of DAST. The gel broke with time and vigorous stirring. Based upon previous experience with the cross-linking of cellobiose, HF was immediately suspected as the culprit. Therefore, this reaction was repeated twice more, under slightly different conditions. The repeated reactions differed from the first reaction in that they were not acetylated after DAST treatment. Instead, the products were reacted with phenylisocyante to give an organic soluble carbanilate (phenyl carbamate) derivative. This was necessary in order to provide direct comparison to cellulose tricarbanilate, CTC. CTC is simply the derivatized cellulose starting material that is used as the molecular weight standard in this study. The second duplicate reaction had one additional modification, bis-1,8(dimethylamino)naphthalene, or Proton Sponge, was added to the solution before DAST. Proton Sponge is a non-nucleophilic base that is effective in complexing free protons, without reacting with electropositive nuclei. For example, Proton Sponge "absorbs" HF while not attacking the sulfur nucleus of DAST. The second duplicate reaction was run with approximately 1 equivalent of Proton Sponge per anhydroglucose unit.

For the sake of convenience, the following nomenclature will be used when describing these reactions:

DAST-acetate: Cellulose dissolved in DMAC/LiCl and reacted with DAST, then subsequently peracetylated.

DAST/urethane-1: Cellulose dissolved in DMAC/LiCl and reacted with DAST, then subsequently carbanilated.

DAST/urethane-2: Cellulose dissolved in DMAC/LiCl and reacted with DAST in the presence of Proton Sponge, and then subsequently carbanilated.

Cellulose dissolved in DMAC/LiCl incurs an increase in molecular weight by the action of DAST, whereas DAST with Proton Sponge causes a loss in DP relative to the starting cellulose(Figure 11). The molecular weight of the starting cellulose is represented as the phenyl carbamate, or cellulose tricarbanilate, CTC. CTC is THF soluble and thus allows for direct molecular weight comparison using gel permeation chromatoghraphy (Figure 11). Notice that the polydispersity of the starting cellulose is 1.79, while the polydispesities of DAST/acetate, and DAST/urethane-2 are 19.6 and 15.0, respectively. DAST/urethane-1 was insoluble in THF, and therefore no molecular weight information could be obtained. This data suggests that some type of branching reaction has occurred which has resulted in molecular weight gain for DAST/acetate. The fact that DAST/urethane-2 shows a loss in molecular weight suggests that the branching may be an HF catalyzed reaction. Apparently, Proton Sponge complexed with free HF and inhibited molecular weight gain. Additionally, the reaction medium did not gel, as was the case for the DAST-acetate reaction. Also note that the polydispersity of DAST/urethane-2 greatly increased, this sample has a very high molecular weight component. Therefore, it appears that branching occurred, but on average, hydrolysis was predominant.

The DEPT carbon spectrum of DAST/acetate provides more evidence that branching has occurred(Figure 12). There are at least 3 different C1 carbon signals in the 100 ppm range. HF catalyzed branching reactions of cellulose are well documented[4,5,6]. The mechanism involves the formation of a glycosyl fluoride endgroup. Subsequent branching occurs when a nucleophile attacks C1 to displace the fluoride anion, Figure 3, Part 2, section A. Under this scenario, multiple C1 signals are expected. The increased molar mass, and multiple C1 signals provide strong evidence for cellulose branching at the one position. Make note that multiple C1 signals may also be caused by chlorination. Other work has indicated that the C6 hydroxyl is the most likely candidate for the attacking nucleophile[6]. This would give rise to ß-1,6-linked branches. If this is the case then we should expect to see multiple signals for C1 **and** C6. In fact, there are 4 different methylene carbons present in DAST/acetate(Figure 12). One of these methylenes occurs at about 62.4 ppm. Three additional methylenes appear in the area around 43 ppm. Of course, methylene signals correspond to carbon 6; all other carbons in cellulose are methines. Consequently, at first glance, this carbon NMR is consistent with the predicted branch structure of a cellulose derivative. Multiple C1 and C6 signals suggest 1,6 branching, which is consistent with the postulated mechanism in the literature.

However, detailed inspection of this carbon spectrum raises a few questions. For most cellulose derivatives, i.e., esters and ethers, the C6 carbon signal is normally between 60 and 70 ppm. For example the C6 carbon of cellulose triacetate occurs at about 61.9 ppm[7]. Indeed, one of the methylenes of DAST/acetate occurs at 62.4 ppm. Oddly, the remaining methylene signals occur upfield near 43 ppm. This is far from the normal region of C6 carbons in common cellulose derivatives. It may be that the 1,6 configuration shields C6 so significantly that these signals occur near 43 ppm. Chlorination could cause an upfield shift, realtive to an acetylated cellulose carbon. However, it is unlikely that a 19 ppm shift would occur from chlorination. For example,

the methine signal at 61.5 ppm may arise from C2 or C3 chlorination; this signal exhibits no more than a 13 ppm shift from the methine region. These ambiguities probably result from the combination of chlorination and branching. Based upon this hypothesis, we would predict that DAST/acetate is a branched chlorodeoxy-cellulose-acetate derivative with predominantly 1,6-branching.

A comparison of the ^{1}H NMR of DAST/urethane-1, DAST/urethane-2, and the linear CTC suggests that DAST/urethane-2 has a character intermediate between the other two samples(Figure 13). Obviously, chlorination will alter the proton spectrum from the appearance of linear cellulose triphenylcarbamate. Given that, it is still reasonable to conclude that DAST/urethane-2 is more similar to the linear derivative. Of course, the difference between the DAST/urethane reactions was the absence, or presence, of a strong organic base during DAST treatment. This difference must have affected the concentration of free HF; DAST/urethane-2 experienced less free HF than DAST/urethane-1. As mentioned above, DAST reactions run without Proton Sponge gelled, while gelation was avoided when this base was present. This observation suggests that the differences observed in the ^{1}H NMR arise from the relative occurrence of HF catalyzed branching. DAST/urethane-1 gelled during synthesis, and is soluble in only highly polar solvents such as DMSO. DAST/urethane-2 did not gel during synthesis, and its solubility, and ^{1}H NMR, more closely resemble that of the linear CTC.

The findings from these few experiments do not further our efforts in the fluorination of cellulose. However, serendipitously, we have discovered a method for the synthesis of branched cellulose derivatives. This is the first report of the synthesis of a cellulose derivative with long chain branches. There is a previous report of the synthesis of a highly branched cellulose[8]. However, this cellulose preparation has branches that are one sugar unit long. Interestingly, the mechanism of synthesis is quite similar. A cellulose derivative is reacted with a glucosyl halide, which adds to the cellulose

backbone in a manner analogous to that shown in Figure 3, Part 2, section A. The critical difference here is that the reactive species is a polymeric glycosyl halide. Consequently, the product has a long chain branched structure. All of this is the result of the unique combination of anhydrous HF, with a homogeneously dissolved cellulose. Previous researchers have discussed the action of anhydrous HF on cellulose[4,5,6]. However, these reports have all been under heterogeneous conditions, where high concentrations of HF are required to dissolve cellulose. Branched cellulose has been formed under these conditions also, but the products are oligomeric. The combination of dissolved cellulose in DMAC/LiCl, and a relatively low concentration of HF, provides control over branching, and molecular weight gain. This method may also be exploited to synthesize branched cellulose based copolymers. By adding a hydroxyl containing polymer to a DMAC/LiCl/cellulose solution, anhydrous HF might catalyze the combination of the two polymers via a glycosidic linkage at C1 of cellulose.

CONCLUSIONS

1. DAST does not react with DMAC, not even at elevated temperatures.
2. While the ^{1}H NMR spectrum of DAST changes in mixtures of DMAC with 7% LiCl, DAST retains its reactivity.
3. The mixture of DAST in DMAC/LiCl is a powerful chlorinating agent. Very little elimination occurs during chlorination of alcohols. Fluorination of alcohols is precluded by the mass action of excess chloride.
4. When cellulose, dissolved in DMAC/LiCl is treated with DAST, extensive chlorination and chain branching occurs.
5. This is the first report of the synthesis of a branched cellulose with long chain branches. The branching is believed to occur by an HF catalyzed trans-glycosidation.

LITERATURE CITATIONS

1. Hudlicky, M., Organic Reactions, Vol. 35, 513, 1988.

2. Middleton, W.J., E.M. Bingham, and D.H. Smith, J. Fluorine Chem., 23, 557, 1983.

3. Evans, R., and A.F.A. Wallis, 4th. Int. Symp. Wood and Pulping Chem., Paris, 1, 201, 1987.

4. Franz, R., W. Fritsche-Lang, H.-M. Deger, R. Erckel, and Schlingmann, J. Applied Poly. Sci., 33, 1291, 1987.

5. Hardt, H., and D.T.A. Lamport, Phytochemistry, 21, 9, 2301, 1982.

6. Defaye, J., and A. Gadelle, Carbohydrate Res., 110, 217, 1982.

7. Buchanan, C.M., J.A. Hyatt, and D.W. Lowman, Macromolecules, 20, 2750, 1987.

8. Nakamura, S., Y. Saegusa, K. Watanabe, and H. Suzuki, *Cellulose, Structural and Functional Aspects*, editors: J.F. Kenedy, G.O. Phillips, and P.A. Williams, Ellis Horwood Ltd. Pub., Chichester, 21, 181, 1989.

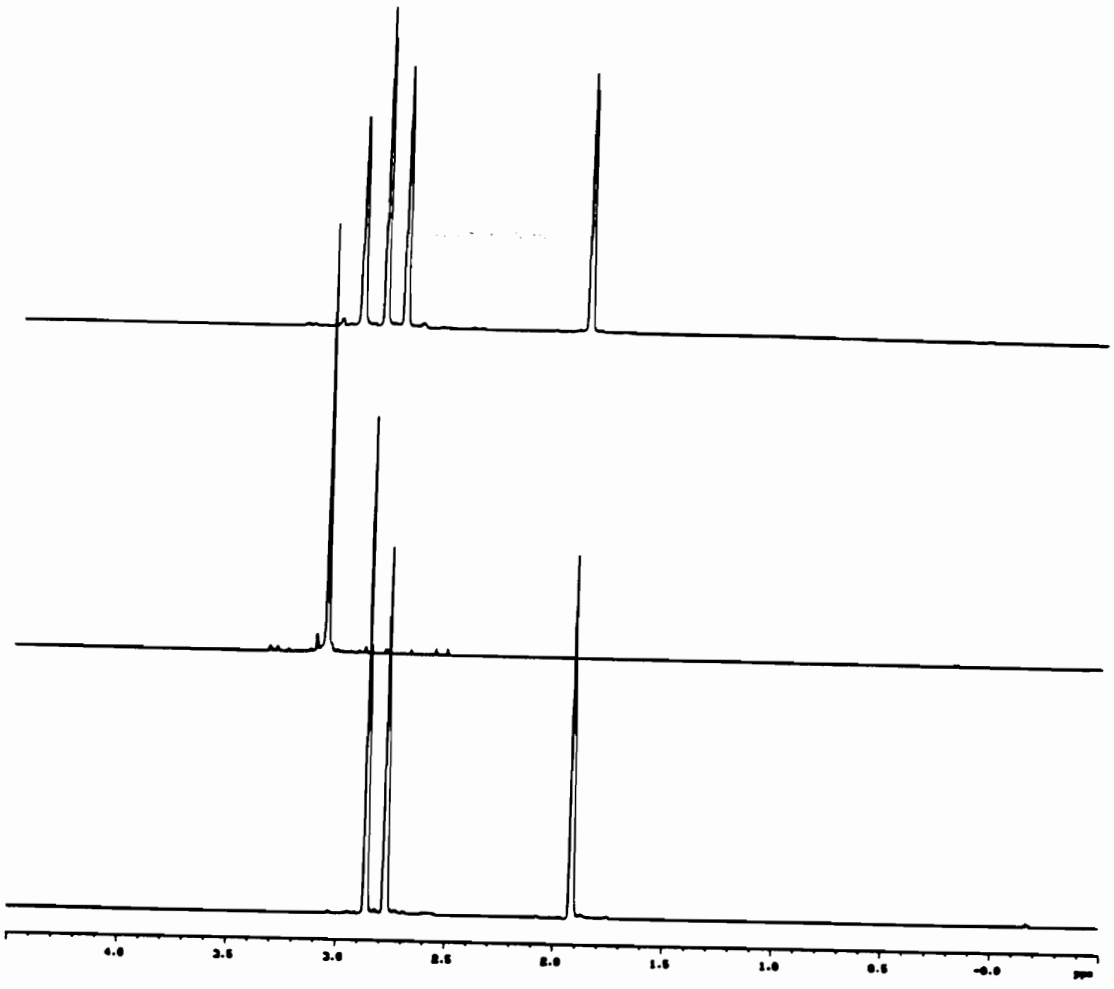

Figure 1. ^{1}H NMR spectra of the mixture of methyl-DAST and DMAC (TOP) with pure methyl-DAST (MIDDLE) and pure DMAC (BOTTOM). The spectrum of the mixture demonstrates that no reaction occurs between DAST and DMAC.

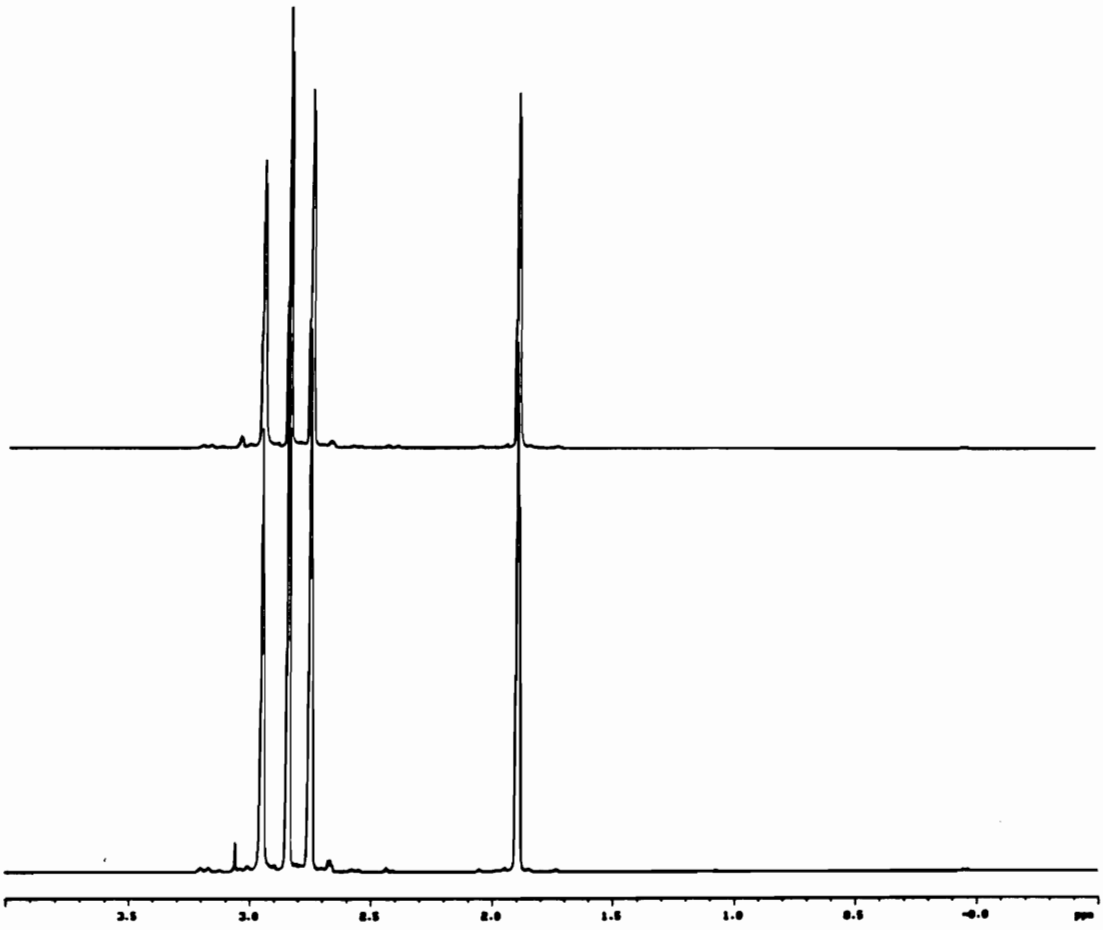

Figure 2. ^{1}H NMR spectra of mixture of methyl-DAST and DMAC, 4 hours,(TOP), and 24 hours, after preparation of mixture, at room temeperature.

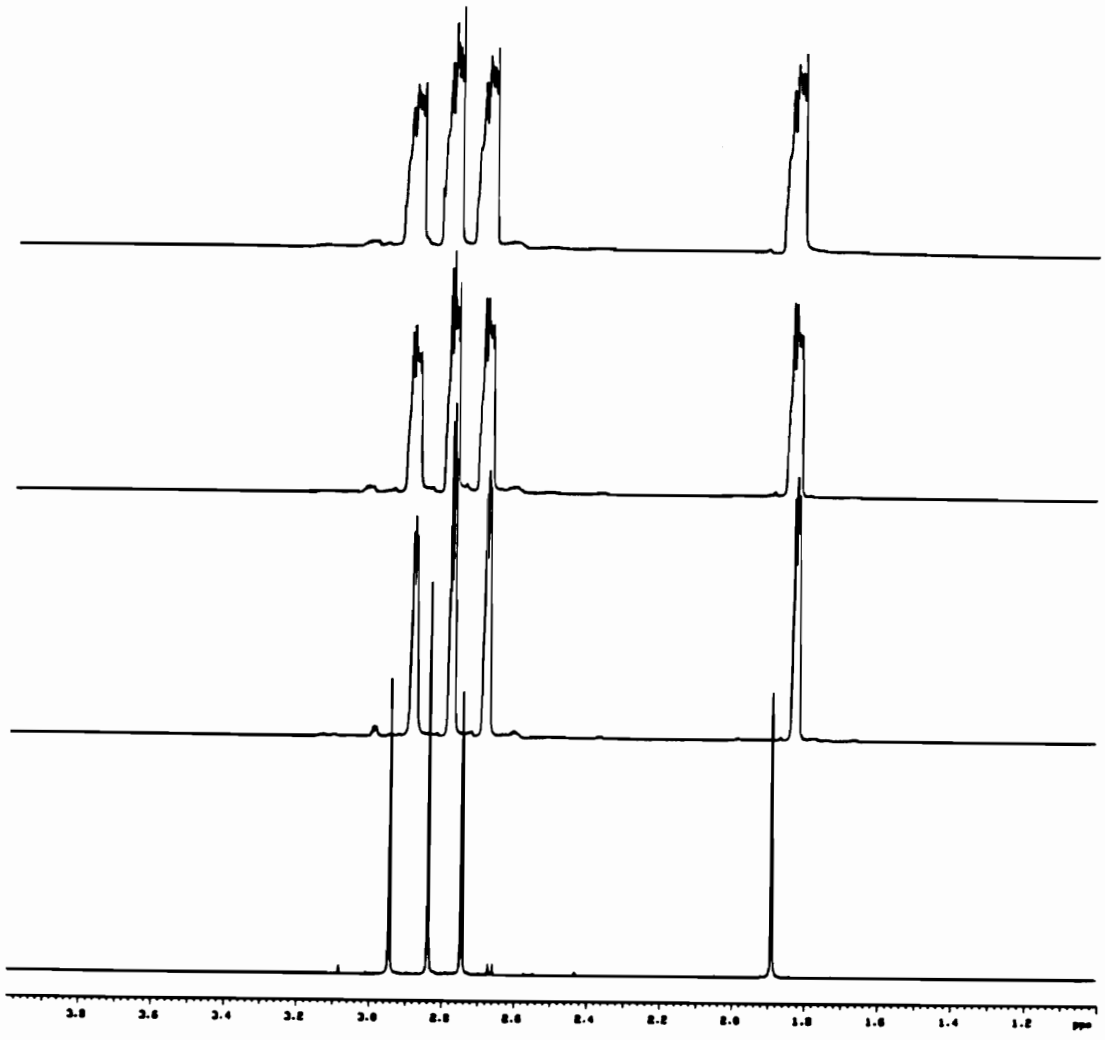

Figure 3. ^{1}H NMR spectra of me-DAST and DMAC mix. From bottom to top: after 48 hours, room temperature; after heating to 40°C, over 30 minutes; after heating to 50°C, over 30 minutes; after heating to 80°C, over 45 minutes. These spectra indicate that the DAST/DMAC mixture is stable at elevated temperatures.

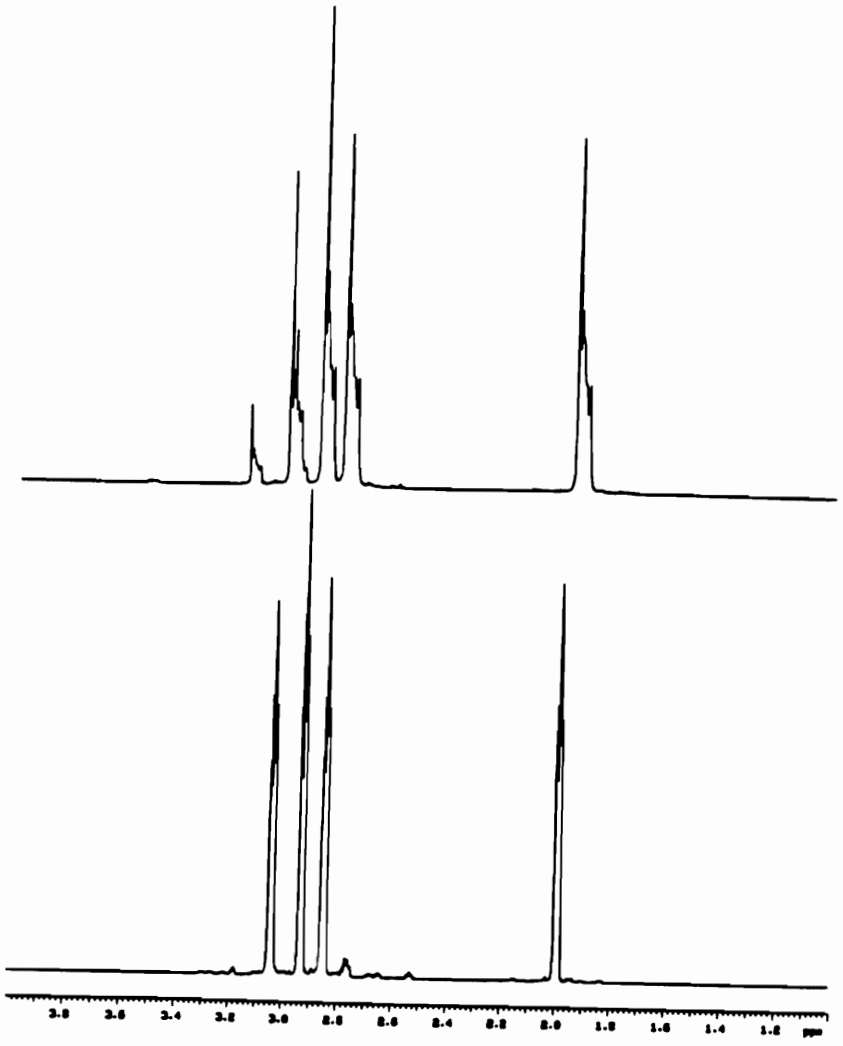

Figure 4. ^{1}H NMR spectra comparing the mixture of DMAC/DAST (Bottom) to the mixture of DMAC/DAST/LiCl (TOP).

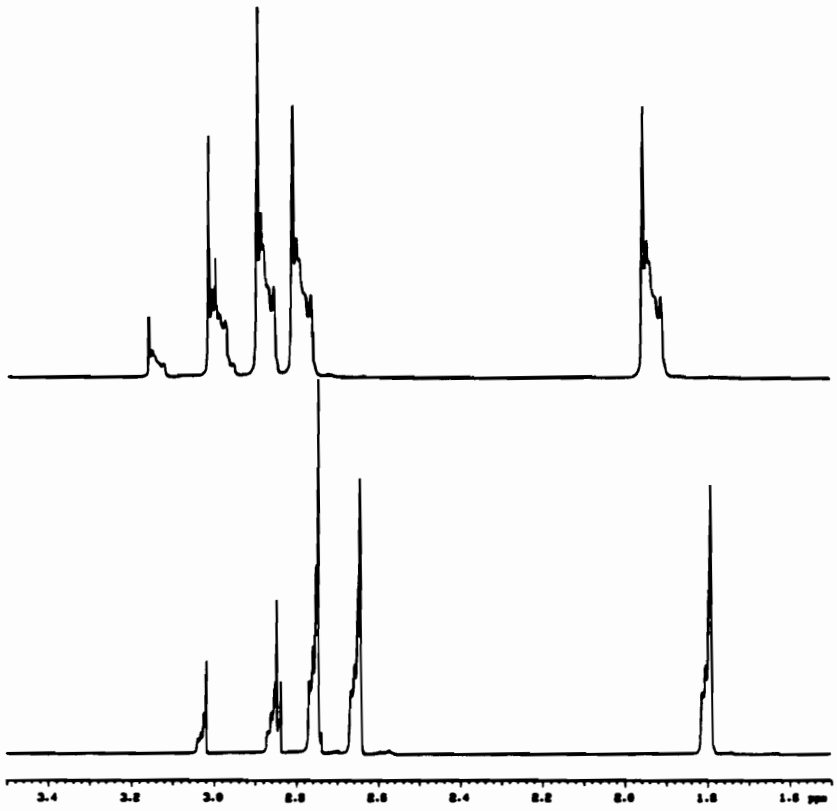

Figure 5. ^{1}H NMR spectra of the mixture of methyl-DAST/DMAC/LiCl, 1 hour (TOP) and 48 hours after preparation, indicating the stability of this mixture over time.

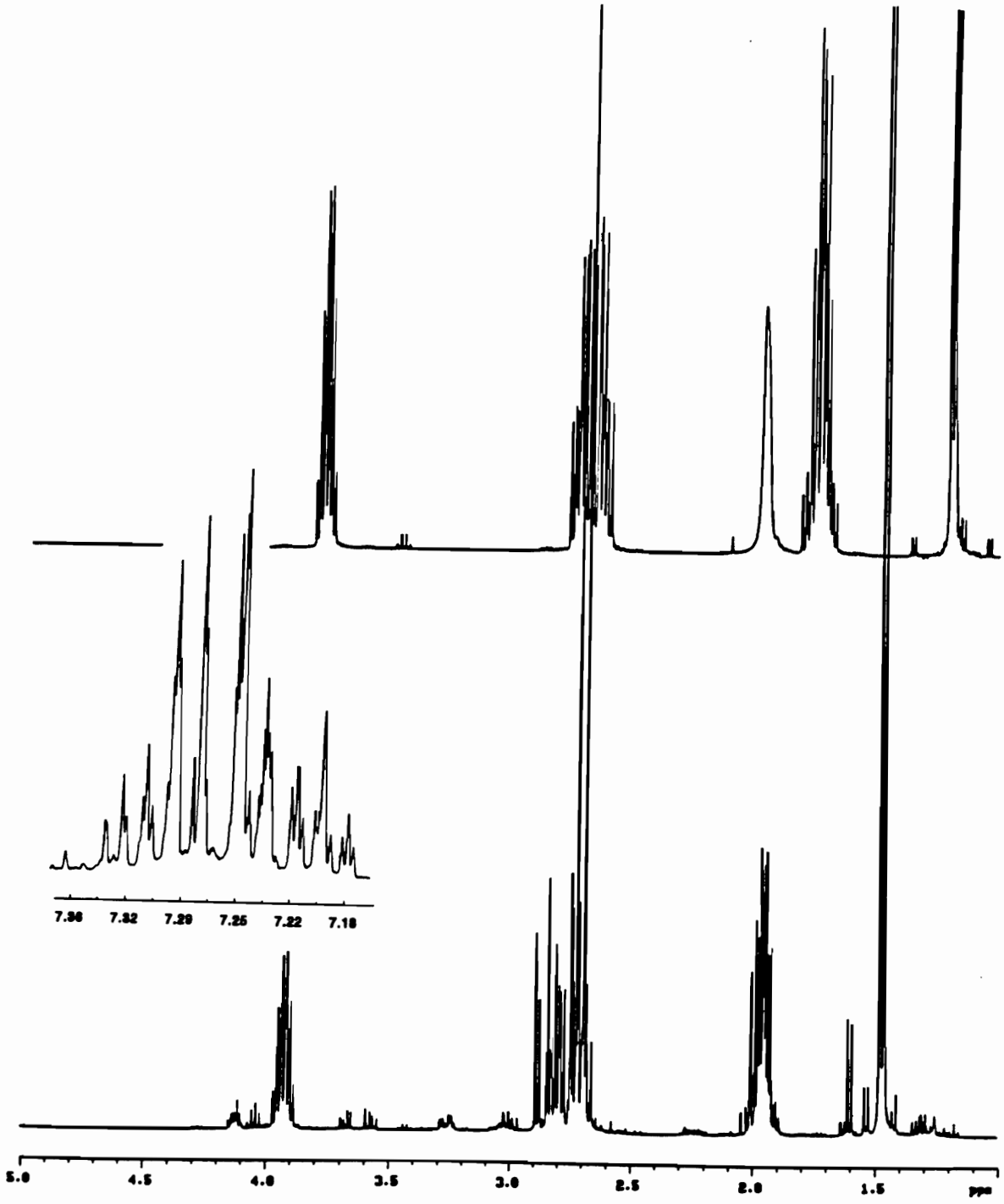

Figure 6. ^{1}H NMR spectra of crude product mixture of reaction of 4-phenyl-2-butanol with DAST in DMAC/LiCl. Inset shows aromatic region of product, which indicates para substitution of chlorine. Top spectrum shows starting material.

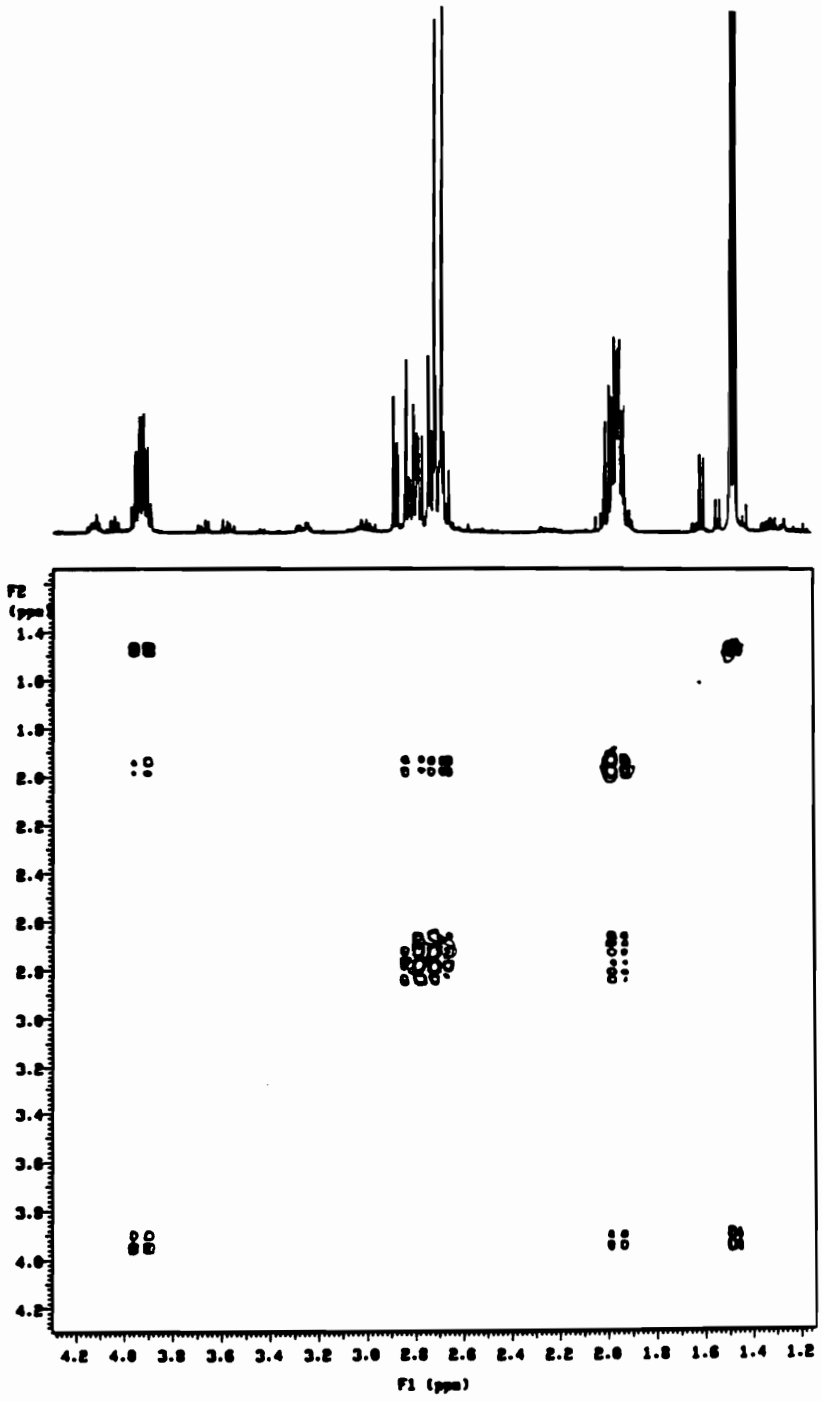

Figure 7. DQCOSY spectrum of crude product mixture from reaction of 4-phenyl-2-butanol with DAST in DMAC/LiCl, demonstrating the same carbon connectivity that exists in the starting material.

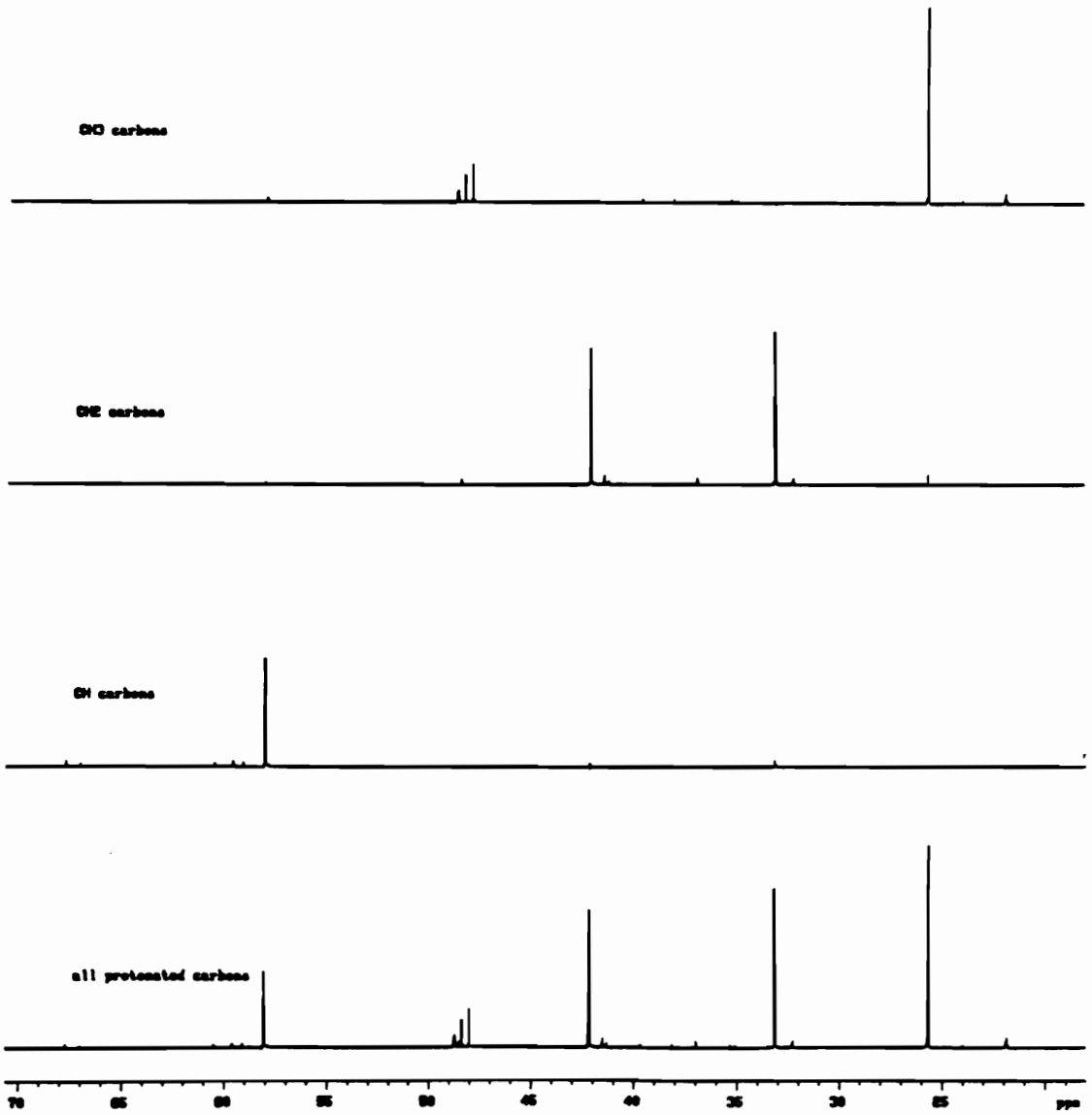

Figure 8. DEPT spectrum of crude product mixture of reaction of 4-phenyl-2-butanol with DAST in DMAC/LiCl. As with the DQCOSY, this spectra indicates that no skeletal rearrangements have taken place during this reaction.

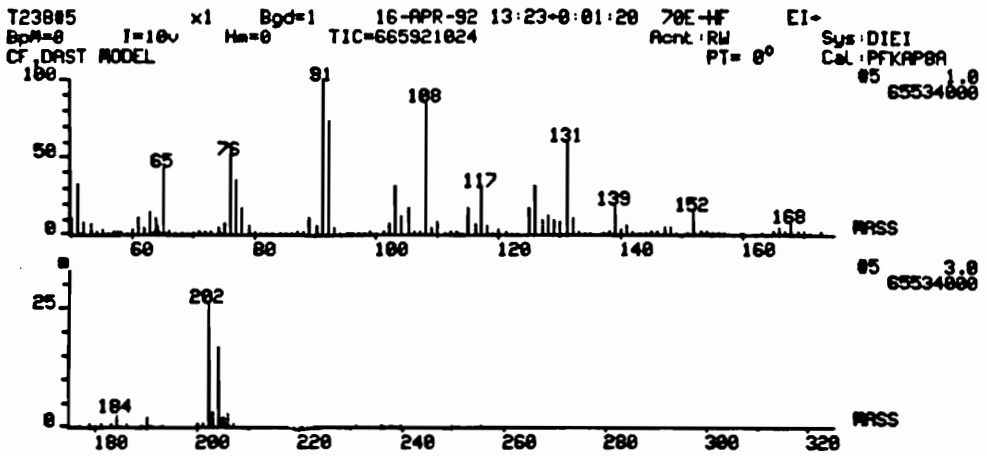

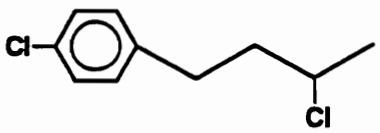

MW= 202

Figure 9. Mass spectrum of crude product mixture of reaction of 4-phenyl-2-butanol with DAST in DMAC/LiCl. The structure of the sample is also shown.

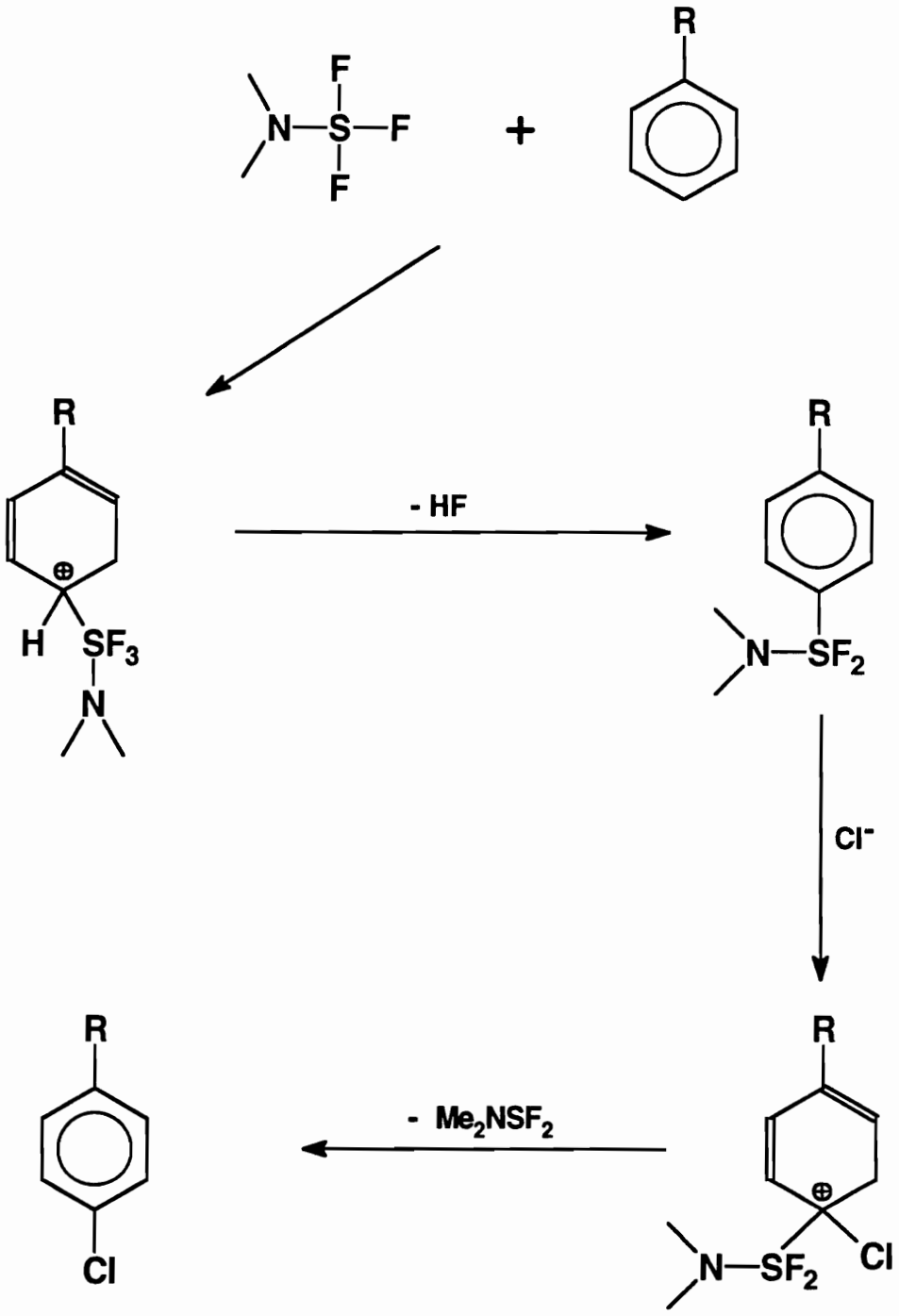

Figure 10. Proposed mechanism for the aromatic chlorination of 4-phenyl-2-butnanol by DAST in combination with LiCl, showing a para directed electrophilic attack of the aromatic ring by the sulfur nucleus, followed by chloride displacement.

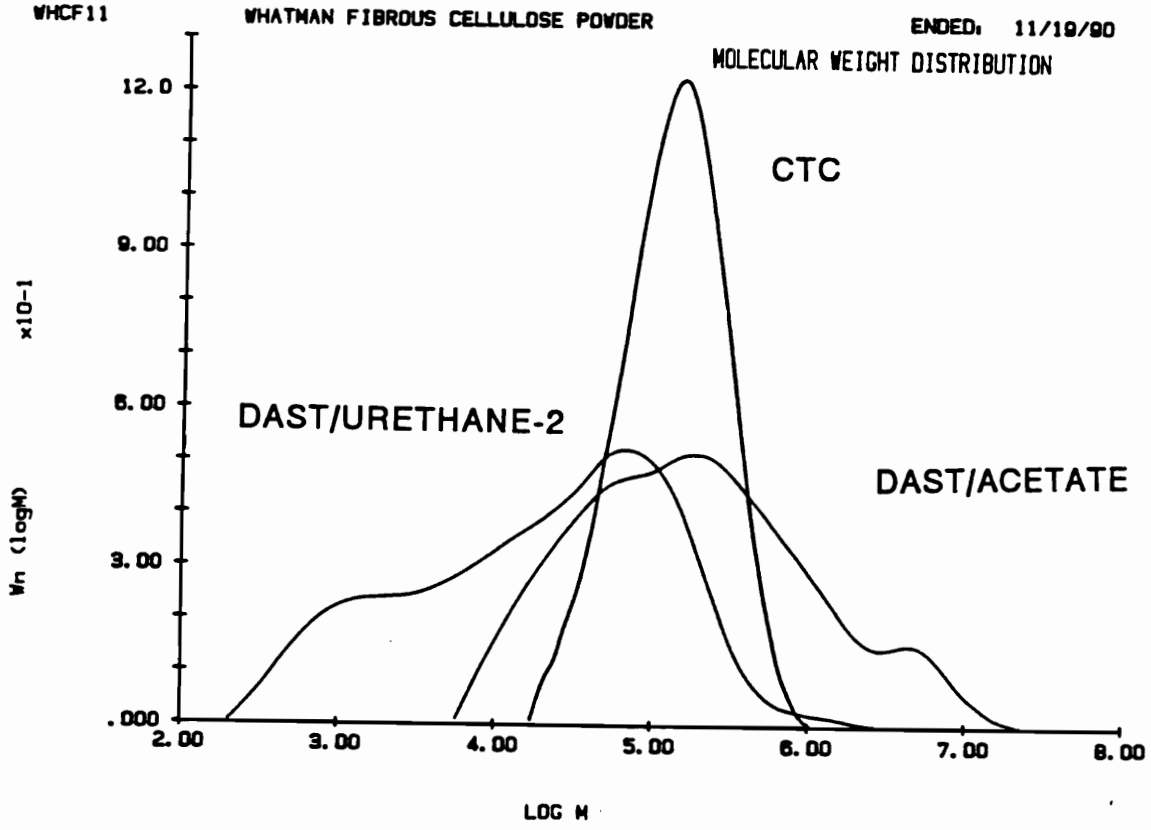

Figure 11. Molecular weight distributions of DAST/ACETATE, DAST/URETHANE-2, and linear cellulose triphenylcarbamate. DAST/URETHANE-2 was treated with Proton Sponge while DAST/ACETATE was not.

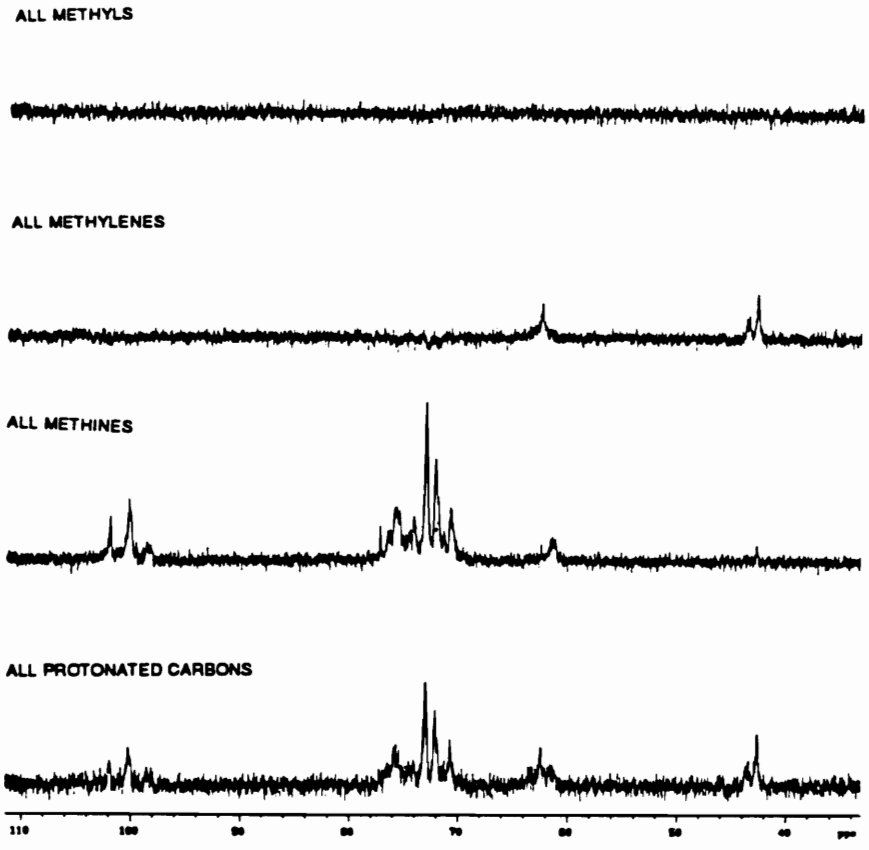

Figure 12. DEPT spectrum of DAST/ACETATE.Multiple C1 signals near 100 ppm provides evidence of branching in this sample, see text.

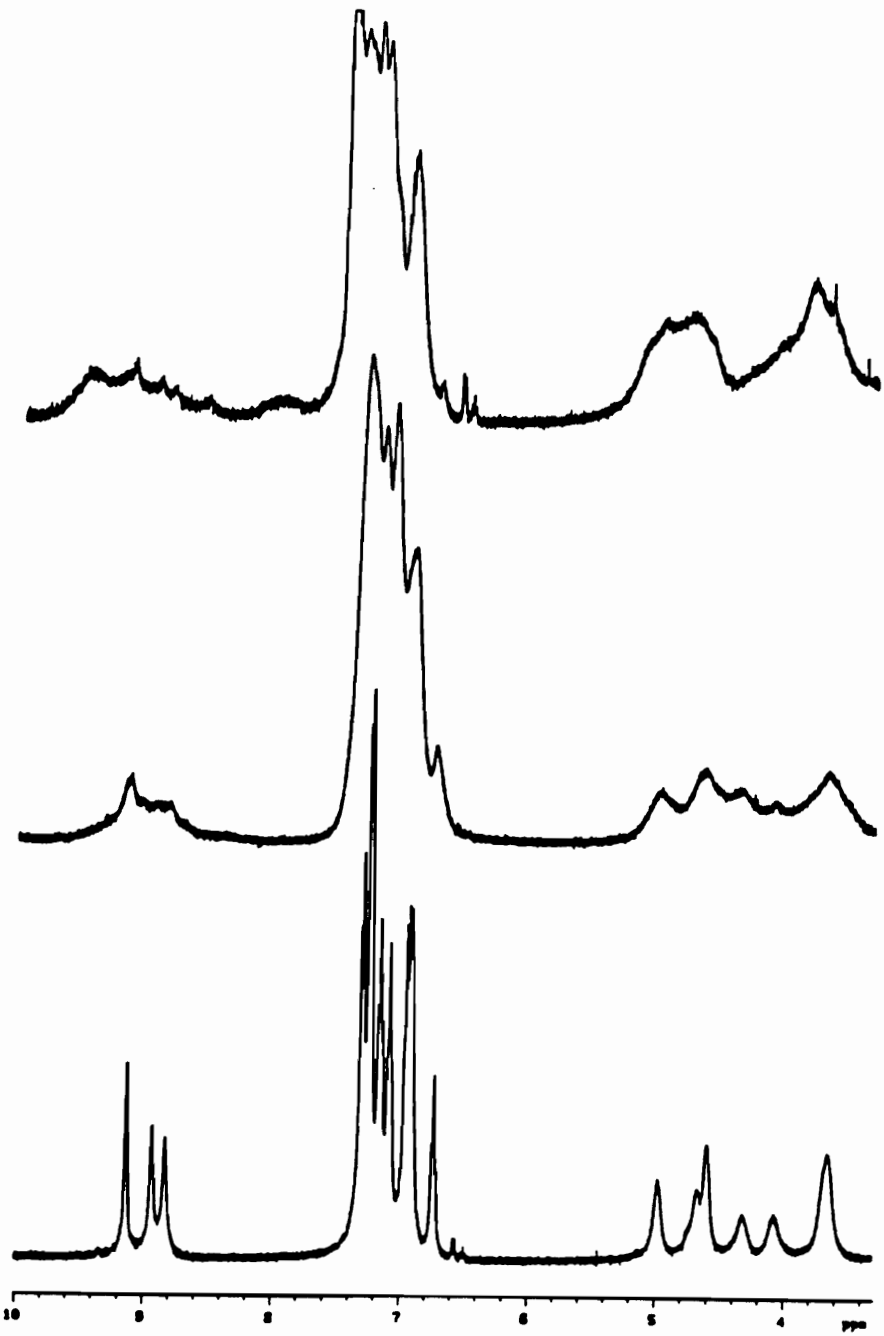

Figure 13. ^{1}H NMR spectra of DAST/urethane-1 (TOP) DAST/urethane-2 (MIDDLE) and linear cellulose triphenylcarbamate. These spectra demonstrate the intermediate character of DAST/urethane-2, which experienced less HF catalyzed branching due to the presence of Proton Sponge.

CHAPTER THREE

PSEUDO-HOMOGENEOUS REACTION OF DAST WITH CELLULOSE

III. PSEUDO-HOMOGENEOUS REACTION OF DAST WITH CELLULOSE BEADS

INTRODUCTION

From the previous section it became obvious that cellulose fluorination was impossible in the DMAC/LiCl solvent system. While DAST retained its reactivity in DMAC/LiCl, the shear mass action of excess chloride caused the exclusive chlorination of alcohols. In hopes of avoiding the effect of chloride, a novel heterogeneous reaction between cellulose and DAST was devised. Interestingly enough, this novel method still involved the use of the DMAC/LiCl solvent system. It has been shown that cellulose regenerated from DMAC/LiCl solution is both highly amorphous, and highly porous[1]. Regeneration of this cellulose solution normally involves precipitation into aqueous alcohol. The aqueous nonsolvent allows for complete extraction of DMAC and LiCl. And the resulting cellulose remains porous as long as the hydrogel is never dried to a critical solids content. Given this information, it should be possible to exchange the aqueous nonsolvent with a miscible organic phase that is compatible with direct fluorinating agents such as DAST. In this way, the cellulose preparation should retain its gel-like state, and therefore, also its high porosity.

The goal of this series of experiments was then to determine if the cellulose gel can be maintained by exchanging a miscible organic solvent into the network. Subsequently, the porosity of the organic gel was tested by diffusing fluorinating reagents into the interior of the cellulose gel. It was hoped that this would serve as a compromise between strictly hetergeneous, unreactive systems, and homogeneous, highly reactive solutions of cellulose.

EXPERIMENTAL

MATERIALS:

All solvents were freshly distilled with the appropriate desiccants, prior to use. Unless otherwise stated, all reagents were purchased from Aldrich Chemical company, and used as received. All liquid transfers were strictly anhydrous, using syringe and cannula techniques. Whatman cellulose, type CF-11, was used as starting material in all cellulose reactions. Number average degree of polymerization was determined as approximately 200; polydispersity was 1.67.

METHODS:

Infrared Spectroscopy:

Infrared spectra were collected on a Nicolet, 5SXC, Fourier Transform InfraRed spectrometer, FTIR. Samples were prepared by grinding in KBr, followed by high pressure formation of the sample pellet. Samples were scanned at a resolution of two cm^{-1}, with at least 32 repetitions.

Elemental Analysis:

Elemental analyses were performed by Galbraith Laboratories, 2323 Sycamore Dr., Knoxville, TN, 37921-1750.

Preparation of Anhydrous, THF Swollen, Cellulose Beads:

A solution of 4% Whatman CF-11 cellulose dissolved in DMAC/LiCl (8% LiCl) was obtained, and 25 ml (2 g cellulose) of the solution was withdrawn using a 60 ml disposable syringe. The cellulose solution was regenerated drop-by-drop into an isopropanol/water 50:50, solution, producing beads with a 3-4 millimeter diameter. These beads were allowed to stir slowly, while the aqueous solution was decanted from the top of the vessel. The decanted liquid was replaced with distilled water, and slow stirring continued. This process of repeated dilutions was continued for a period of 7 hours, in order to assure that all DMAC and LiCl had

been removed. Water was filtered from the beads in a scintered glass Buchner funnel. The beads were then immersed in THF and allowed to exchange with the water inside the beads. The THF was filtered away, and then replaced with a fresh batch. The beads were then placed into a sohxlet extraction apparatus, which was fitted with a dry nitrogen atmosphere. In the pot, THF was refluxed over freshly cut potassium metal. A tablespoon of benzophenone was added as a colormetric indicator of dryness. The beads were dried in this fashion for a period of 12 hours.

Reaction of the Anhydrous Beads with DAST:

The dry, THF swollen beads were quickly transferred to a dry 250 ml round bottom flask. This flask was fitted with rubber septum, dry nitrogen atmosphere, and magnetic stir bar. Anhydrous THF, 20 ml, was added to the beads, just enough to cover them. The flask was cooled to -70°C in a dry ice/acetone bath. Methyl-DAST, 4.5 ml (46.1 mmoles), was added slowly to the flask. While slowly stirring, the beads warmed from -70° to 0°C over a period of 5 hours. Subsequently, the beads were maintained between -20 and 0°C for a period of 3.5 hours. The flask was then removed from the cooling bath, and allowed to warm to room temperature. Quickly, the beads were poured into 200 ml of ice water, containing excess $NaHCO_3$. At this time, the beads were still transparent, and completely spherical. They were slightly discolored orange. The beads were allowed to sit in the bicarbonate solution over night. The following morning, the beads were exchanged with large amounts of distilled water. After filtration, 150 ml of dimethylformamide, DMF, was added to the beads. The DMF was filtered away, and another 150 ml was added. This solvent exchange was repeated twice more. The beads were filtered again, and 150 ml of anhydrous DMF was added. At this point, the beads were held under flowing dry nitrogen. Again the beads were filtered, and then quickly transferred to a dry, triple neck flask for acetylation.

Acetylation of the DAST Treated Beads:

The DAST reacted beads were then acetylated using a procedure adapted from Shimizu and Hayashi[2]. The triple neck flask was fitted with a 50 ml addition funnel, dry nitrogen atmosphere, thermometer, and magnetic stir bar. Anhydrous DMF, 30 ml, was added to the beads with a cannula. Then acetic acid, 4.24 ml (74.1 mmoles), was added to the beads with a syringe. At this point, 14.13 g (74.1 mmoles) of tosyl chloride was dissolved in 30 ml of anhydrous DMF in a dry 100 ml round bottom flask. This tosyl chloride solution was transferred to the addition funnel using a cannula. The tosyl chloride solution was added slowly to the beads over a period of 1 hour. Afterwards, the flask was heated to 50°C, and the beads were allowed to stir for 19.5 hours. The flask was then allowed to cool, and the suspension was poured into 500 ml of distilled water while stirring. A small amount of precipitation occurred at this point. The beads were washed with large volumes of distilled water and methanol. Finally, the beads were dried under 20 mm Hg vacuum at 50°C for 2 days. Elemental analysis revealed 2.85% Fluorine.

RESULTS AND DISCUSSION

After exchanging water for anhydrous THF, the beads had shrunken to about 80% of their original diameter, and they were completely transparent. It appeared that complete porosity was maintained. For instance, when the aqueous beads first contacted THF, one could visibly observe the water streaming from within the bead, out into the orgnanic phase. Previous experience with similar cellulose beads suggests that the beads were completely amorphous, Figure 2, Chapter 2, Part 1. Therefore, the shrinkage of these beads must result from growth of the glassy domains thought to serve as mechanical cross-links in these beads, or possibly from densification of these domains.

After treatment with DAST, the beads were peracetylated in hopes of

providing a soluble sample, amenable to NMR and molecular weight analysis. However, this was not the case. In their final state, the dried, peracetylated beads had shrunken to approximately one tenth of their swollen diameter. These dried beads were insoluble and nonswelling in THF, $CHCl_3$, acetone, and methanol. When heated in DMSO, the beads swelled back to their original diameter, but did not dissolve. In this swollen state, they were completely transparent, and seemed to be viscoelastic when dropped against a hard surface. According to infrared analysis, the beads head been very highly acetylated(Figure 1). Cellulose acetate, and cellulose triacetate are both quite soluble in DMSO. Given this information, we must conclude that the DMSO insolubility is caused by network formation in the beads. This network must result from an HF catalyzed trans-glycosidation under the action of DAST. During both the fluorination and acetylation steps, the cellulose beads retained complete transparency and apparent porosity. There was never an indication of bead collapse or morphology change. Elemental analysis of the peracetylated beads revealed a 2.85% fluorine content. Assuming a 2,3-diacetyl-6-fluorodeoxy structure, this corresponds to a fluorine DS of about 0.4.

Interestingly, the THF swollen beads reacted similarly to a homogeneous solution of cellulose in DMAC/LiCl. A network was formed, as was the case in homogemeous solution. As in homogeneous solution, the chains were sufficiently accessible to allow cross-linking. However, because there was no LiCl present, fluorination did occur, and to a relatively high degree. Nonetheless, this is far from a complete conversion of primary hydroxyls. This leads one to speculate that competition for free primary hydroxyls must arise from the cross-linking reaction, or from the hydrogen bonded morphology of the network. In any event, this particular cellulose preparation deserves the label of being pseudo-homogeneous. No doubt, this cellulose preparation will allow others to perform previously excluded, and novel chemistries on cellulose.

It appears, that under any circumstances, fluorination of cellulose is doomed to be a low yield reaction. At best, we probably only hope to achieve a maximum fluorine DS of 1.0. This is a theoretical maximum based upon the assumption that only the primary hydroxyl of cellulose is reactive to fluorination. In this work, the maximum obtainable fluorine DS has been from 0.4 to 0.5. Displacement chemistry appears to achieve only 1% fluorine incorporations. Fluorination using direct regents such as DAST give much higher yields. In fact the heterogenous, surface fluorination of cellulose with DAST is very successful. On the other hand, homogeneous fluorination of cellulose is complicated by competitive reactions. In DMAC/LiCl, chlorination, and gelation completely exclude fluorination. Under pseudo-homogeneous conditions, fluorination does occur. But again, the yield is much below the theoretical maximum.

On the brighter side, the discovery of the action of anhydrous HF on homogeneous or pseudo-homogeneous cellulose may lead to new materials. The synthesis of novel branched cellulose derivatives and copolymers in homogeneous solution has been mentioned. The findings from chemistry on pseudo-homogeneous cellulose may provide a new way to make cross-linked cellulose membranes.

CONCLUSIONS

1. Cellulose can be regenerated from homogeneous solution to provide a highly organic swollen gel. This gel allows complete diffusion of reagents into the solid, and therefore acts as a pseudo-homogeneous cellulose solution.
2. This type of cellulose gel can be fluorinated successfully. However, there appears to be a strong competition with HF catalyzed trans-glycosidation.
3. This cellulose preparation must be considered a pseudo-homogeneous solution. As such, this development will allow previously unattainable chemistries for cellulose.

LITERATURE CITATIONS

1. de Oliveira, Willer, Personal Communication.

2. Y. Shimizu, and J. Hayashi, Cellulose Chem. Tech., 23, 667, 1989.

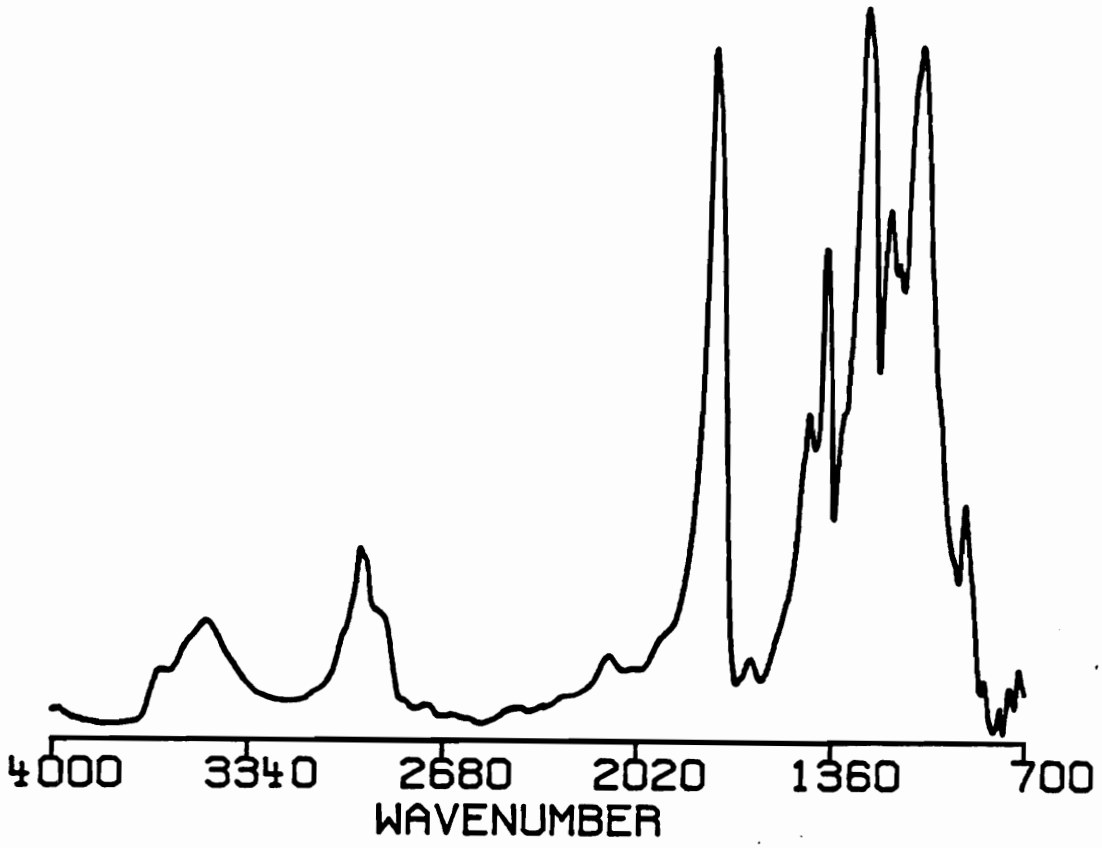

Figure 1. FTIR spectrum of DAST/acetate beads, where the hydroxyl signal is very weak, demonstrating the high degree of acetylation of the sample.

CHAPTER FOUR

THE FLUORINATION OF HYDROXYPROPYL CELLULOSE

IV.THE FLUORINATION OF HYDROXYPROPYL CELLULOSE

INTRODUCTION

One of the main obstacles to cellulose fluorination is the low reactivity of the secondary hydroxyls. These hydroxyls are endocyclic, and therefore resist the inversion that normally occurs in fluorination of carbohydrates[1]. This means that cellulose will scarcely reach a fluorine DS greater than 1.0. Hydroxypropyl cellulose, HPC, on the other hand, has secondary hydroxyls that enjoy free rotation, as attached to the propylene oxide substituents. Furthermore, HPC has good solubility in a wide range of solvents, many of which, for example THF and $CHCl_3$, are compatible with the highly reactive direct fluorinating reagents. This combination theoretically makes HPC more reactive to fluorination than cellulose.

Of course, HPC is still susceptible to HF catalyzed trans-glycosidation. Consequently, the aim of these experiments has been to take advanatge of the convenience of HPC, while trying to avoid complications, such as gelation. The course to this end has involved the testing of DAST derivatives, and modifications of DAST and FAR reactions. All of this has been for the purpose of maximaizing fluorination, while minimizing side reactions.

EXPERIMENTAL

MATERIALS:

Klucel HPC with a molar substitution of 3.27 was obtained from the Hercules Corporation. A small batch of Klucel HPC was dried under 20 mm Hg vacuum, at a temperature of no greater than 40°C for a period of 48 hours. All glassware was thoroughly dried in an oven and/or by flaming prior to use. All solvents were freshly distilled with the appropriate desiccant. Unless otherwise stated, all reagents were purchased from Aldrich Chemical company, and used as received. All liquid transfers

were strictly anhydrous, using syringe and cannula techniques.

METHODS:

Molecular Weight Analysis:

Gel permeation chromatography was used where tetrahydrofuran was pumped by a Waters 510 into a series of 3 Waters Ultrastyragel columns, with pore sizes of 10^3, 10^4, and 10^6 angstroms. Detection was with a Waters 410 refractometer in series with a Viskotek differential viscometer, model 100. The columns were heated to 40°C in an Eldex column heater, and both detectors were also heated to 40°C. Tetrahydrofuran was freshly degassed, and always stored under a helium atmosphere during use. Narrow polydispersity, polystyrene standards from Polymer Laboratories were used to establish a universal calibration.

Nuclear Magnetic Resonance:

A Varian Unity-400 nuclear magnetic resonance spectrometer was used to collect ^1H, ^{19}F, and ^{13}C NMR spectra at 400, 376, and 100 Mhz, respectively. Samples were prepared by dissolving the analyzed material in the appropriate deuterated solvents, using 5 millimeter, or 10 millimeter Wilmad glass tubes. Where appropriate, the percent fluorine present in a sample was determined with ^{19}F NMR using an internal standard analysis. Precisely weighed amounts of sample and fluorine internal standard were placed into a 25 ml round bottom flask. The mixture was dissolved in $CDCl_3$, and then run on the NMR. Percentages of fluorine would be calculated based upon the ^{19}F integrations, and the known masses of sample and standard. The internal standard was 3-trifluoromethylacetophenone (chemical shift=-64.26 ppm, relative to trifluoroacetic acid at -77.05 ppm).

Elemental Analysis:

Elemental analyses were performed by Galbraith Laboratories, 2323 Sycamore Dr., Knoxville, TN, 37921-1750.

Reaction of HPC with Bis(Diethylamino)Sulfur Difluoride, (BDSD), D1:

HPC, 1 g (8.5 mmoles OH), was dissolved in 50 ml of anhydrous $CHCl_3$, in a 100 ml double neck flask, which was fitted with septum, dry nitrogen gas, and magnetic stir bar. This mixture was given about 1 hour to completely dissolve. Meanwhile, a separate 100 ml triple neck flask was equipped with a 100 ml addition funnel, dry nitrogen atmosphere, septum, and magnetic stir bar. Then, anhydrous $CHCl_3$, 10 ml, was transferred to this flask, followed by, 2.4 ml (18.2 mmoles), ethyl-DAST. The reaction flask was cooled to -60°C in a dry ice/acetone bath. Trimethylsilyldiethylamine, 3.55 ml (18.7 mmoles), was slowly added to the DAST solution with a syringe, in order to form bis(diethylamino)sulfur difluoride, BDSD. This solution was allowed to warm, slowly, to room temperature. The homogeneous HPC solution was transferred to the addition funnel with a wide bore cannula. Once again, the reaction flask was cooled to -40°C. The HPC solution was dripped slowly into the BDSD solution, over a period of 45 minutes. A precipitate formed immediately, followed by the formation of a gel on the surface of the solution. The reaction was allowed to stir while slowly warming to room temperature during a period of 3.5 hours. At this time the contents of the reaction flask were poured into 200 ml of ice water, with excess $NaHCO_3$. After CO_2 evolution was complete, the emulsion was concentrated in a rotational evaporator. The resulting aqueous layer was centrifuged, and the solid product was recovered, and briefly vacuum dried. This brown solid was then stirred in dioxane over night. The resulting solution was precipitated in water, and the solid was recovered and placed in an acetone, sohxlet extractor over night. The solid was then vacuum dried at 60°C for 24 hours. Approximately, 600 mg of a brown, rubbery material was recovered. After extraction and drying, the sample was no

longer soluble in dioxane. In fact, this sample was insoluble in THF, acetone, DMF, and DMSO. Elemental analysis revealed 52.2% Carbon, 7.99% Hydrogen, and 4.5% Fluorine.

Reaction of HPC with BDSD in the Presence of Excess Base, D2:

Dried HPC, 2 g (17.0 mmoles OH), was placed in a 250 ml triple neck flask. The flask was fitted with a 25 ml addition funnel, dry nitrogen atmosphere, rubber septum, and a magnetic stir bar. The HPC was dissolved in 100 ml of anhydrous THF. Separately, in a dry 50 ml round bottom flask, 4.76 ml (36 mmoles) of ethyl-DAST was dissolved in 20 ml of anhydrous THF. This flask was cooled to -78°C in a dry ice/acetone bath. Then, trimethylsilyl diethylamine, 6.82 ml (36.0 mmoles), was added to the cold DAST solution. This mixture was allowed to slowly cool to room temperature. Afterwards, this solution of BDSD was added to the addition funnel with a cannula. The HPC solution was cooled to -40°C. At this point, 6.3 ml (36.2 mmoles), of n,n-diisopropylethylamine was added to the HPC solution. After complete mixing of this hindered base with the HPC solution, the contents of the addition funnel were added to the HPC over a period of 15 minutes. This mixture was allowed to warm to room temperature with constant stirring for 2 hours. Then the reaction flask was poured into 200 ml of ice water, with excess $NaHCO_3$. The precipitate was filtered, and washed thoroughly with distilled, followed by methanol. The solid was vacuum dried over night at 40°C. This dried product, 2.23 g, was placed in 90 ml of THF, and stirred for 2 days. This mixture was then centrifuged, and the supernatant was collected and poured into water. The precipitate was washed with methanol, and dried over night in the vacuum oven at ambient temperature. The THF insoluble portion was sohxlet extracted in THF over night, while the THF soluble portion was extracted in ethyl ether. 874 mg of the reprecipitated material was recovered. 988 mg of the THF insoluble material was recovered. Elemental analysis revealed 7.24% Fluorine.

Reaction of HPC with DAST in the Presence of Proton Sponge, D3:

This method was the same as the previous reaction, except for the following. BDSD was not used. Methyl-DAST, 2.5 ml (25.6 mmoles), was dissolved in 10 ml of anhydrous THF, and added as is to the HPC solution with an addition funnel. Bis-1,8-dimethylaminonaphthalene, or Proton Sponge, 3.7 g (17.1 mmoles) was dissolved in 20 ml anhydrous THF, and added to the HPC solution as before. This reaction started at -40°C, and warmed to room temperature over a period of 1.5 hours. The reaction was ended as before. The solid product was washed with large quantities of water, methanol, isopropanol, and finally, water again. The product was dried under 20 mm Hg vacuum at 40°C for 2 days. 2.15 g of a yellow/white material was recovered. Elemental analysis revealed 3.58% Fluorine.

Synthesis of FAR, Hexafluoropropyl Diethylamine:

Hexafluoropropyl diethylamine was synthesized using the procedure of Takaoka et al[2]. Two techniques are described, where method 2, the "Reaction at Atmospheric Pressure", was used in this work.

Reaction of HPC with FAR, F1:

Dried HPC, 1 g (8.5 mmoles OH) was dissolved in 75 ml of anhydrous THF, in a 250 ml triple neck flask. The flask was fitted with a 25 ml addition funnel, dry nitrogen atmosphere, and a magnetic stir bar. At this point, 10 ml of anhydrous THF, and 4.0 ml (13.9 mmoles), of FAR, or Ishikawa's reagent, were transferred directly to the addition funnel with cannula, and syringe respectively. The reaction flask was cooled to 0°C in an ice water bath. The FAR solution was slowly added to the HPC over a period of 30 minutes. After the complete addition of the FAR solution, the reaction flask was removed from the ice bath, and allowed to stir for 24 hours under dry nitrogen. Some precipitation was noticed during the reaction. The reaction was ended by pouring the contents of the flask into 200 ml of ice water which contained excess $NaHCO_3$. An

emulsion was formed, so the entire mixture was concentrated on the rotational evaporator until all THF was gone. When the THF was removed, the product precipitated from the aqueous solution. The product was filtered, and washed with distilled water. The off-white product was sohxlet extracted with hexane over night. After vacuum drying, about 700 mg of material was recovered.

Reaction of HPC with FAR, in the Presence of Proton Sponge, F2:

Dried HPC, 1 g (8.5 mmoles OH) was dissolved in 75 ml of anhydrous THF, in a 250 ml triple neck flask. The flask was fitted with a 25 ml addition funnel, dry nitrogen atmosphere, and magnetic stir bar. After complete dissolution of the HPC, 2.647 g (12.4 mmoles) of bis-1,8-dimethylaminonaphthalene, or Proton Sponge, was dissolved in 10 ml of anhydrous THF, in a separate 100 ml round bottom flask. This Proton Sponge solution was directly transferred to the HPC solution with a cannula. 5 additional ml of anhydrous THF was used to rinse any residual Proton Sponge from the round bottom flask into the reaction flask, via cannula. At this point, 10 ml of anhydrous THF, and 4.0 ml (13.9 mmoles), of Ishikawa's reagent were transferred directly to the addition funnel with cannula, and syringe respectively. The reaction flask was cooled to 0°C in an ice water bath. The FAR solution was slowly added to the HPC over a period of 30 minutes. After the complete addition of the FAR solution, the reaction flask was removed from the ice bath, and allowed to stir for 24 hours under dry nitrogen. The reaction was ended by pouring the contents of the flask into 200 ml of ice water which contained excess $NaHCO_3$. An emulsion was formed, so the entire mixture was concentrated on the rotational evaporator until all THF was gone. When the THF was removed, the product precipitated from the aqueous solution. The product was filtered, and washed with distilled water. The off-white product was sohxlet extracted with hexane over night. The solid was dried, dissolved in THF and centrifuged. The supernatant was poured into hexane, and the precipitate was collected. The product was again reprecipitated from THF into hexane. Finally, the product was dried under 20 mm Hg

vacuum, at 40°C for 24 hours. 481 mg of an off-white material was recovered.

Reaction of HPC with FAR, in the Presence of Proton Sponge, F3:

This reaction was repeated in the same fashion as in method 1, except that after the addition of the FAR solution, the flask was heated to 40°C, for 24 hours. The reaction was ended by pouring the contents of the reaction flask into 200 ml of ice water, with excess $NaHCO_3$. This time a precipitate formed on the surface of the aqueous solution. The precipitate was skimmed from the top, and predried under high vacuum, at ambient temperature for 2 hours. The yellowish product was placed in a sohxlet apparatus, and extracted with hexane for 24 hours. Then the product was dissolved in THF, and all insolubles were centrifuged out of the solution. The supernatant was precipitated into hexane. This reprecipitation was repeated again. Finally, the product was dried under high vacuum, at 40°C for 24 hours. 662 mg of a light brown material was recovered.

Reaction of HPC with FAR, in the Presence of Proton Sponge, F4:

Method 3 was performed in the same way as method 2, except the that the reaction was run at a temperature of 50°C for 24 hours. 833 mg of a yellowish material was recovered after extraction, and reprecipitation.

Reaction of HPC with FAR, in the Presence of Proton Sponge, F5:

Method 4 was performed the same way as method 3, except the reaction flask was fitted with a condenser, and the solution was refluxed for 24 hours. The sample was purified, and dried as above. 72.4 mg of an orange/yellow solid was recovered. The sample was dissolved in THF during the purification. Elemental analysis revealed 15.22% Fluorine.

RESULTS AND DISCUSSION

HPC fluorinations using DAST derivatives, and modified DAST and FAR reactions gave products with varying degrees of fluorination, and branching, or cross-linking(Table 1). For convenience, the reactions that involved the use of DAST, or a derivative of DAST, will be labeled as D1, D2, or D3. Similarly, reactions that used FAR, will be labeled as reactions F1, F2, F3, F4, and F5. Percentages of fluorine were determined by elemental analysis when samples were insoluble, or when they were soluble, by ^{19}F NMR using internal standard analysis.

Because of the previous problems encountered with gelation, a modification was sought that might reduce the amount of free HF during DAST reactions. Three separate reactions, D1-D3, were performed, in which a different modification was introduced for each. Reaction D1 was run with a DAST derivative, bis(diethylamino)sulfur difluoride, or BDSD. BDSD is the adduct between DAST and trimethylsilyldialkylamine[1](Figure 1). BDSD has one additional dialkyamino functionality that helps complex free HF. Otherwise, BDSD has about the same reactivity towards alcohols as DAST. Reaction D1 was run with a BDSD/OH ratio of approximately 2.1.

Reaction D2 was run with a combination of BDSD and a hindered amine base, diisopropylethyl amine. Any base used with DAST, or derivatives of DAST, must be sterically hindered so as to avoid consuming the fluorinating agent. Diisopropylethyl amine was used to help soak up free HF, while not reacting with DAST. The ratio of BDSD/OH/AMINE was 2.1/1.0/2.1.

Reaction D3 was run with a different hindered base, bis-1,8-dimethylamino naphthalene, or Proton Sponge, but this time methyl-DAST was used and not BDSD. The ratio of DAST/OH/AMINE was 2.1/1.0/1.0.

A visible precipitation and/or gelation occurred with each of reactions D1-D3. While the products did become fluorinated, gelation appeared to dominate the reaction. For example, the product of reaction D1 experienced a very high conversion of hydroxyls, as judged by FTIR(Figure 2). But with only 4.5% fluorine, or a fluorine DS of approximately 0.8, most of the remaining hydroxyls must have been converted during gelation. Product D1 was completely insoluble in organic solvents, and was not wetted by water.

Reaction D2 was similar to D1, except for the addition of n,n-diisopropylethylamine, which is a hindered base that should complex with HF, without reacting with DAST. This additional base did not stop the immediate precipitation that occurs when the BDSD was added to the HPC solution. However, the extent of gelation seemed to be inhibited. After the initial isolation, roughly half of the material was soluble in THF, whereas, the product of reaction D1 was in no way soluble. Curiously however, after extensive purification and drying, this once THF soluble fraction would only swell in THF, and was only partially soluble in DMSO. As above, water did not swell or wet this sample. This partially soluble sample must represent a highly branched sol fraction. It was sufficiently soluble in DMSO to allow NMR analysis(Figure 3). (This sample did not form a homogeneous solution in the NMR tube. It resembled more of a suspension of small, swollen, gel particles.) Apparently, the addition of hindered base precluded extensive gelation, because this sample had a 7.2% fluorine content, as determined by elemental analysis(Figure 4). This is about a 60% increase over reaction D1, which was run without hindered amine. ^{1}H NMR showed that product D2 was altered significantly from the structure of pure HPC(Figure 3). The most notable differences in the proton NMR occur near 1.2 ppm. HPC has one broad singlet in this range, which arises from the methyl groups of the propylene oxide substituents. Whereas, product D2, has three signals in this area. There are also significant differences in the range between 3 and 6 ppm. These differences must arise from a combination of fluorination and cross-linking.

These differences are also evident when comparing the ^{13}C NMR of the product and starting material(Figure 5). In HPC, the 3 signals between 16 and 20 ppm arise from methyl carbons of the polypropylene oxide substituents. For this discussion, we will only concentrate on the 2 strong peaks in this region. The low field methyl carbon, at 19.9 ppm, is assigned as the methyl terminus of the polypropylene oxide, PPO, substituents[2]. Whereas, the high field methyl signal, at 16.5 ppm, comes from methyl carbons internal to the PPO substituents[3]. Similarly, the strong signal at 64.9 ppm comes from methine carbons of the PPO substituent terminus, while the weaker signal at 76.1 ppm is from the internal methine carbons[3]. Notice that the terminal methyl signal at 19.9 ppm, and the terminal methine signal at 64.9 ppm, are both greatly reduced in the fluorination product, D2. The signal near 115 ppm corresponds to an olefinic carbon. Signs of olefin formation were also seen in the ^{1}H NMR(Figure 3). Therefore some of the changes seen in the carbon spectrum may be the result of elimination during fluorination. The identity of the fluorine bearing carbon in Figure 5 is not clear. There are two doublets appearing between 86 and 90 ppm. A doublet is expected from the fluorinated methine of HPC. However, it seems very unlikely that two separate doublets would appear. Especially when we know that all terminal methine carbons of HPC appear as one signal, regardless of the position on the anhydroglucose ring. Therefore the two carbon doublets near 98 ppm may have some other origin, such as from branching. The fluorine bearing carbon is probably hidden from clear view among the cellulose backbone carbons, between 68 and 82 ppm. Even in light of the ambiguity of this carbon spectra, the ^{1}H and ^{13}C NMR clearly show a drastic change in HPC as a result of treatment with BDSD. Furthermore, the ^{19}F NMR shows a relatively broad fluorine signal, which is consistent with a fluorinated polymer(Figure 4). This signal occurs at -45.8 ppm. (The ^{19}F chemical shifts are reported here upfield from $FCCl_3$.) Based upon published ^{19}F shifts of monofluoroalkanes, the shift of this fluorine signal is far from its expected position[4]. For example, the chemical shift of 2-fluoropropane is reported as -164 ppm. We would expect that a fluorinated HPC should have fluorine signals in this range. The ^{19}F

chemical shift of BDSD is -9.7 ppm[1]. We can see that the exact nature of the fluorine present in this sample is unclear. However, comfort is found when we consider the inherent unpredictability of ^{19}F NMR[5]. The extreme range of ^{19}F NMR, (> 1000 ppm), often contributes to a failure in shift correlations[5].

The treatment of HPC with DAST in the presence of Proton Sponge, reaction D3, gave an insoluble product that would swell in THF and DMSO. This product was essentially identical to the product of reaction D1.

Judging from these results, it appears that fluorosulfur reagents such as DAST, and BDSD, fluorinate HPC , but always with simultaneous gelation. The attempts at complexing free HF by using BDSD, and amine bases did not eliminate gelation. DAST and DAST derivatives seem to be too reactive to use with HPC. Furthermore, the yields of fluorination are still relatively low. Fluorine DS approaches 1.3. This is much higher than what was obtained with pure cellulose, but it seems low when considering the enhanced reactivity of HPC.

In yet another attempt at reducing the effects of free HF, HPC was treated with the much less reactive fluorinating agent, FAR, specifically hexafluoropropyl diethylamine. HPC was first reacted with a FAR/OH ratio of 1.64. Four subsequent reactions were performed with the addition of 1.5 equivalents of Proton Sponge per hydroxyl. These last four reactions were run at four different temperatures: room temperature, 40°C, 50°C, and at reflux temperature in THF.

The first FAR reaction, F1, also produced an insoluble material that appeared to be cross-linked. The product swelled in organic solvents, but would not dissolve. As before, the product appeared to be significantly fluorinated, as judged by its hydrophobic nature. Reaction F1 also gelled during the reaction, but by qualitative observation, not

as severely as with DAST and BDSD. The subsequent FAR reactions were more successful. FAR reactions 2-4 did not gel during preparation. Product F2, F3, and F4, were THF soluble after treatment with FAR and Proton Sponge. Notice however, that reaction F2 did not fluorinate HPC(Table 1). Apparently, Proton Sponge inhibited fluorination. The following reaction, F3, was run at 40°C, and produced a soluble product with 1.8% fluorine incorporation. FAR reaction F4 was run at 50°C, and the fluorine incorporation rose to 4.4%. Finally, reaction F5 was run at reflux in THF, about 65°C, and had a fluorine content of 15.2%, a DS of roughly 2.5! However, the product of this reaction would only swell, and not dissolve, in organic solvents. Appparently, in the presence of Proton Sponge, both fluorination, and gelation are enhanced as temperature rises.

It appears that the lower reactivity of FAR, in combination with a hindered amine base, does allow the fluorination of HPC, without extensive gelation. The progression of fluorination of products F3, and F4 is evident in the ^{1}H NMR as compared to HPC (Figure 6). As fluorination increases from F3 to F4, a peak at about 1.62 ppm grows in intensity. Recall a similar peak in product D2(Figure 3). There is also a peak at 5.5 ppm which also grows in intensity as fluorination increases. This signal may be from an olefinic proton that would result from elimination. Notice that the ^{1}H NMR of the FAR treated materials is vastly different from that of the BDSD reaction shown in Figure 3.

As with product D2, Product F4 displays significant differences from HPC in the ^{13}C NMR(Figure 7). The FAR reacted sample does not show the drastic changes that the BDSD reaction product shows in Figure 5. For example, the signals at 19.9 and 64.7 ppm are not significantly different from HPC. Recall that these signals correspond to the terminal methyl and methine carbons of the PPO substituents, respectively. These signals were drastically reduced in the product of the BDSD reaction, D2. Judging from proton and carbon NMR, it appears that the FAR reacted material has retained more of the HPC

character than the BDSD products. This is reasonable when considering that branching and gelation did not significantly affect the FAR reacted material, with the exception of F5. Table 2 lists the molecular weight information for HPC, and the FAR products F2-F4. There is a gradual reduction in molecular weight as fluorination increases, but there is no indication of extensive branching. The polydispersity and the Mark-Houwink-Sakurada exponent stay relatively constant. When the temperature of the FAR reaction is raised to 65°C, reaction F5, then branching does become significant. Therefore, we can conclude that HPC can be fluorinated using FAR, with successful control of branching. Furthermore, the changes effected by FAR are much less extensive than those resulting from DAST or BDSD. FAR, in the presence of Proton Sponge, primarily fluorinates HPC, with little change in the architecture of the chains. DAST and DAST derivatives fluorinate and drastically alter chain architecture, probably through branching.

The differences in the effects of the two reagent types is also evident in the ^{19}F NMR. The ^{19}F NMR of the F4 product shows the fluorine signal at -75.8 ppm (Figure 8). Recall that the fluorine signal from the BDSD reaction, Figure 5, occurs at -45.8 ppm. It is evident that the fluorine atoms in these two samples reside in significantly different environments. The chemical shifts differ by 30 ppm. This difference in chemical environment may arise from differences in chain architecture, as a function of the presence or absence of branching.

This work shows that the fluorination of HPC with direct fluorinating agents is wrought with difficulties. Fluorination is not difficult. However, fluorination without extensive branching or gelation is quite challenging. The fluorosulfur reagents, such as DAST, are too reactive for the fluorination of HPC. While the addition of excess amine base reduces the extent of gelation in DAST reactions, it does not eliminate it. This, in turn, always results in a cross-linked mass that resists analysis, and precludes characterization for potential uses. On the other hand, the FAR reagent, hexafluoropropyl

diethylamine, does offer a method of fluorinating HPC. Here too, the complications of free HF are a significant problem. But, the reduced reactivity of FAR, at least allows the inhibition of branching by amine base.

CONCLUSIONS

1. DAST and DAST derivatives fluorinate HPC, but always with simultaneous branching and gelation. The addition of hindered amine bases inhibits gelation, but does not eliminate it.
2. FAR, hexafluoropropyl diethylamine, fluorinates HPC, also with simultaneous gelation. However, addition of the hindered amine, bis-1,8-dimethylaminonaphthalene can prevent branching and gelation. The reduced reactivity of FAR allows for the control of free HF. Therefore, a fluorinated HPC can be successfully synthesized.
3. Products from both fluorosulfur and fluorocarbon reagents show evidence of elimination in the NMR spectra.
4. By any means, the fluorination of cellulose and cellulose derivatives is frustratingly difficult. Displacement chemistry gives very low yields. Direct fluorinating reagents fluorinate satisfactorily, but the concomitant production of HF catalyzes a trans-glycosidation that causes extensive branching, which can lead to gelation.

LITERATURE CITATIONS

1. Hudlicky, M., Organic Reactions, Vol. 35, 513, 1988.

2. Takaoka, A., H. Iwakiri, and N. Ishikawa, Bull. Chem. Soc. Japan, 52, 11, 3377, 1979.

3. K. Kimura, T. Shigemura, M. Kubo, and Y. Maru, Makromol. Chem., 186, 61, 1985.

4. Dungan, C.H. and J.R. Van Wazer, *Compilation of Reported F^{19} NMR Chemical Shifts*, Wiley and Sons Pub., New York, 1970.

5. Mooney, E.F., *An Introduction To ^{19}F NMR Spectroscopy*, Heyden & son LTD. Pub.,Philadelphia, Pa., 1970.

TABLE 1. Weight percent fluorine contents of products of DAST and FAR reactions on HPC. Product solubilities, which provide an indication of cross-linking, are also provided.

REACTION	REAGENT SYSTEM	WT % F	ORGANIC SOLUBLE ?
D1	BDSD	4.5	NO
D2	BDSD, DIPEA	7.2	PARTIALLY
D3	me-DAST, H-SPONGE	3.6	NO
F1	FAR, RT	-	NO
F2	FAR, H-SPONGE, RT	0	YES
F3	FAR, H-SPONGE, 40°C	1.8	YES
F4	FAR, H-SPONGE, 50°C	4.4	YES
F5	" REFLUX	15.2	NO

BDSD; Bis(diethylamino)sulfur difluoride
DIPEA; Diisopropylethyl amine
FAR; Ishikawa's reagent
H-Sponge; Proton Sponge

TABLE 2. Molecular weights of products of FAR/HPC reaction.

SAMPLE	M_n (10^{-3})	M_w(10^{-3})	M_z(10^{-3})	M_w/M_n	α
HPC	63	167	777	2.65	0.87
F2	50	155	771	3.08	0.74
F3	49.4	164	690	3.32	0.70
F4	47. 7	133	360	2.78	0.73

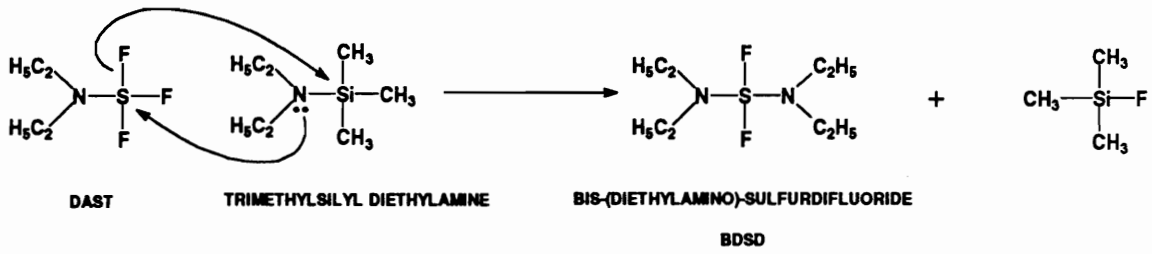

Figure 1. Synthesis of bis-(dialkylamino)sulfur difluoride, BDSD.

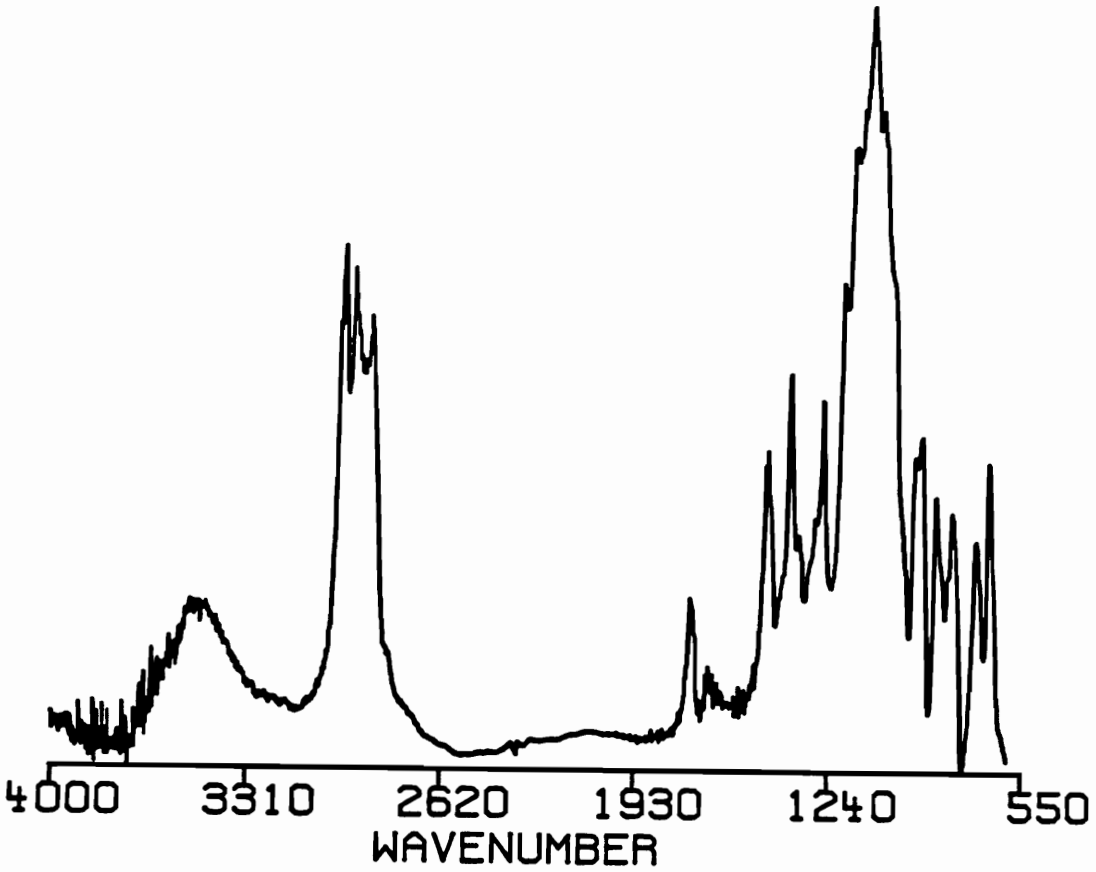

Figure 2. FTIR spectrum of BDSD/HPC reaction product, reaction D1. The very weak hydroxyl signal indicates a very high degree of hydroxyl conversion in the BDSD/HPC reaction. Where fluorination, and cross-linking are thought to be responsible.

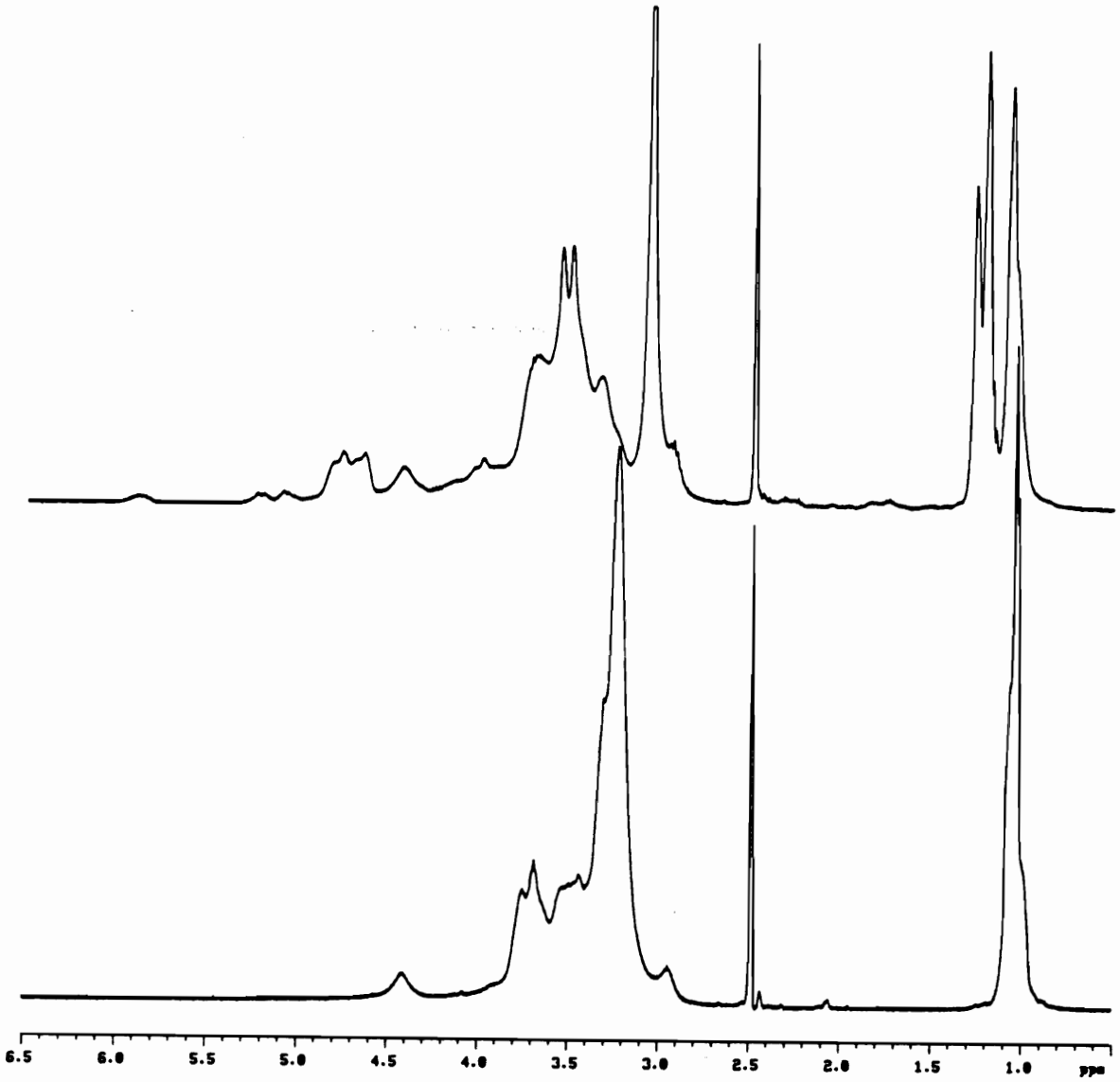

Figure 3. ^{1}H NMR spectra of BDSD/HPC/AMINE reaction product (TOP) reaction D2, compared to HPC.

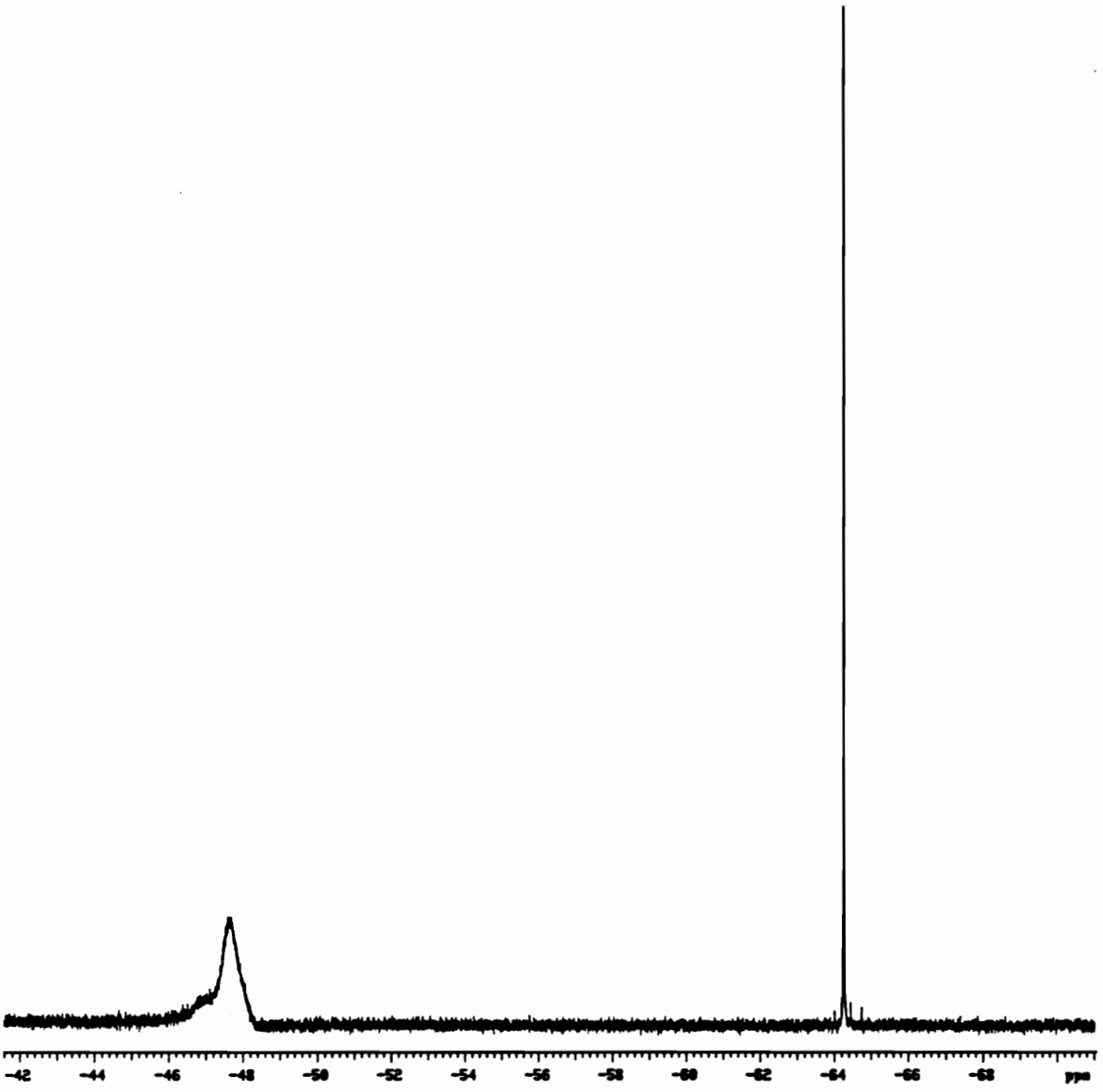

Figure 4. ^{19}F NMR spectrum of BDSD/HPC/AMINE product, reaction D2. Fluorine chemical shifts are shown upfield from $CFCCl_3$. The fluorine standard is trifluoromethyl acetophenone, at -64.26ppm.

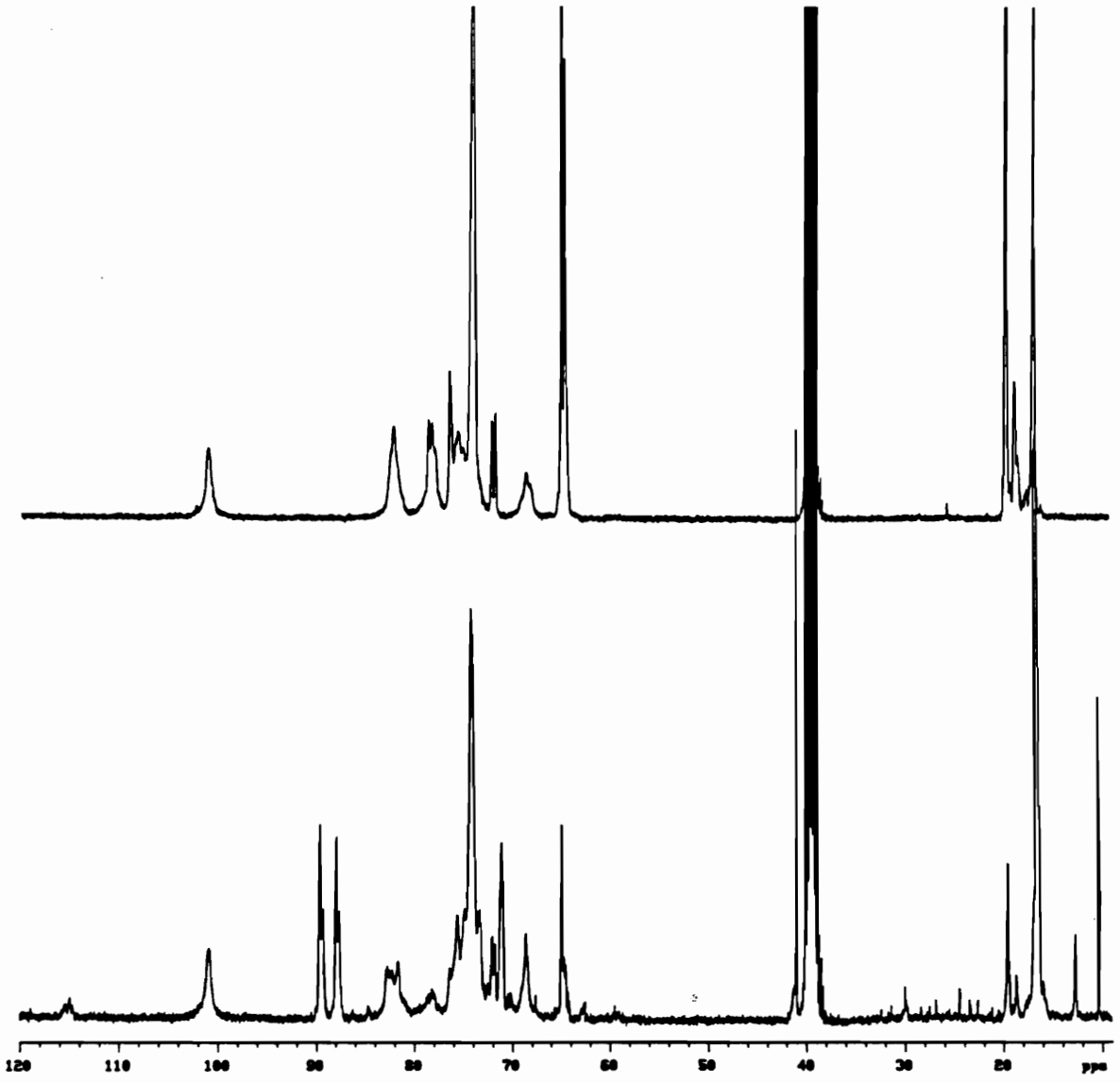

Figure 5. ^{13}C NMR spectrum of BDSD/HPC/AMINE product, reaction D2, compared to HPC, solvent DMSO-d_6, at 80°C.

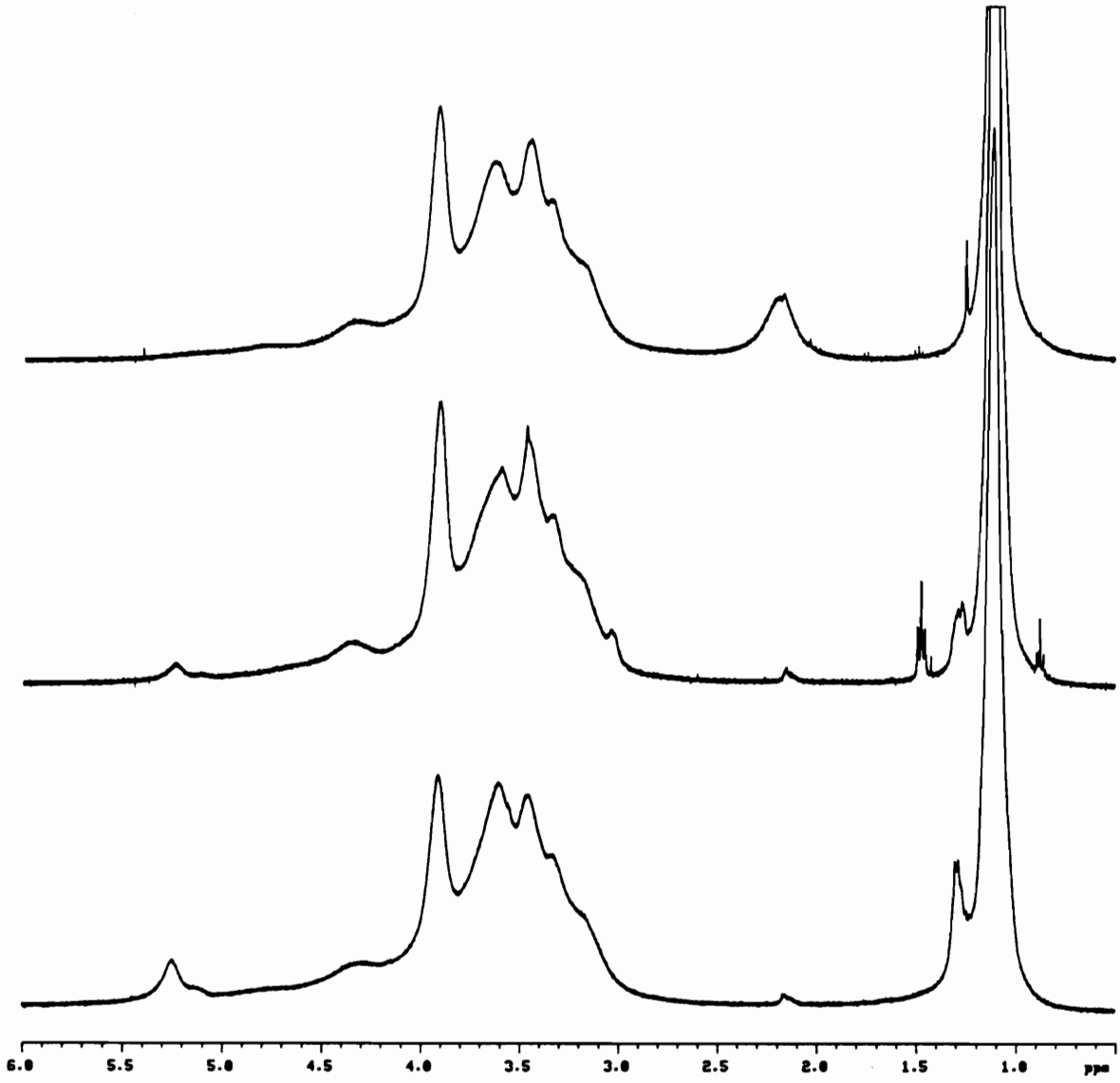

Figure 6. ^{1}H NMR spectra comparing HPC (TOP) with FAR reaction products F3, and F4 (BOTTOM). Solvent $CDCl_3$ at room temperature.

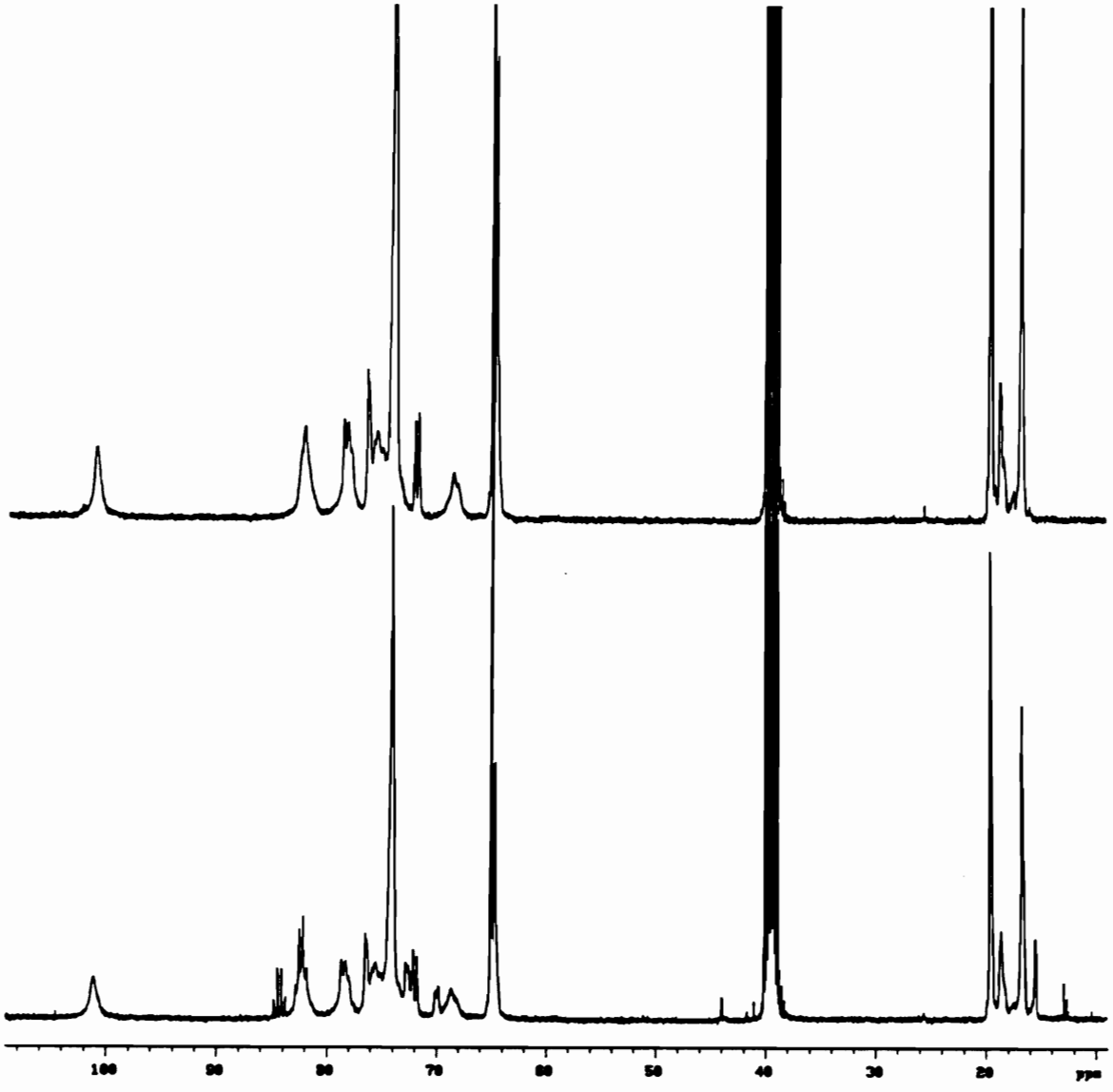

Figure 7. ^{13}C NMR spectra comparing HPC (TOP) to the FAR reaction product, F3. Sample was scanned in DMSO-d6, at 80°C.

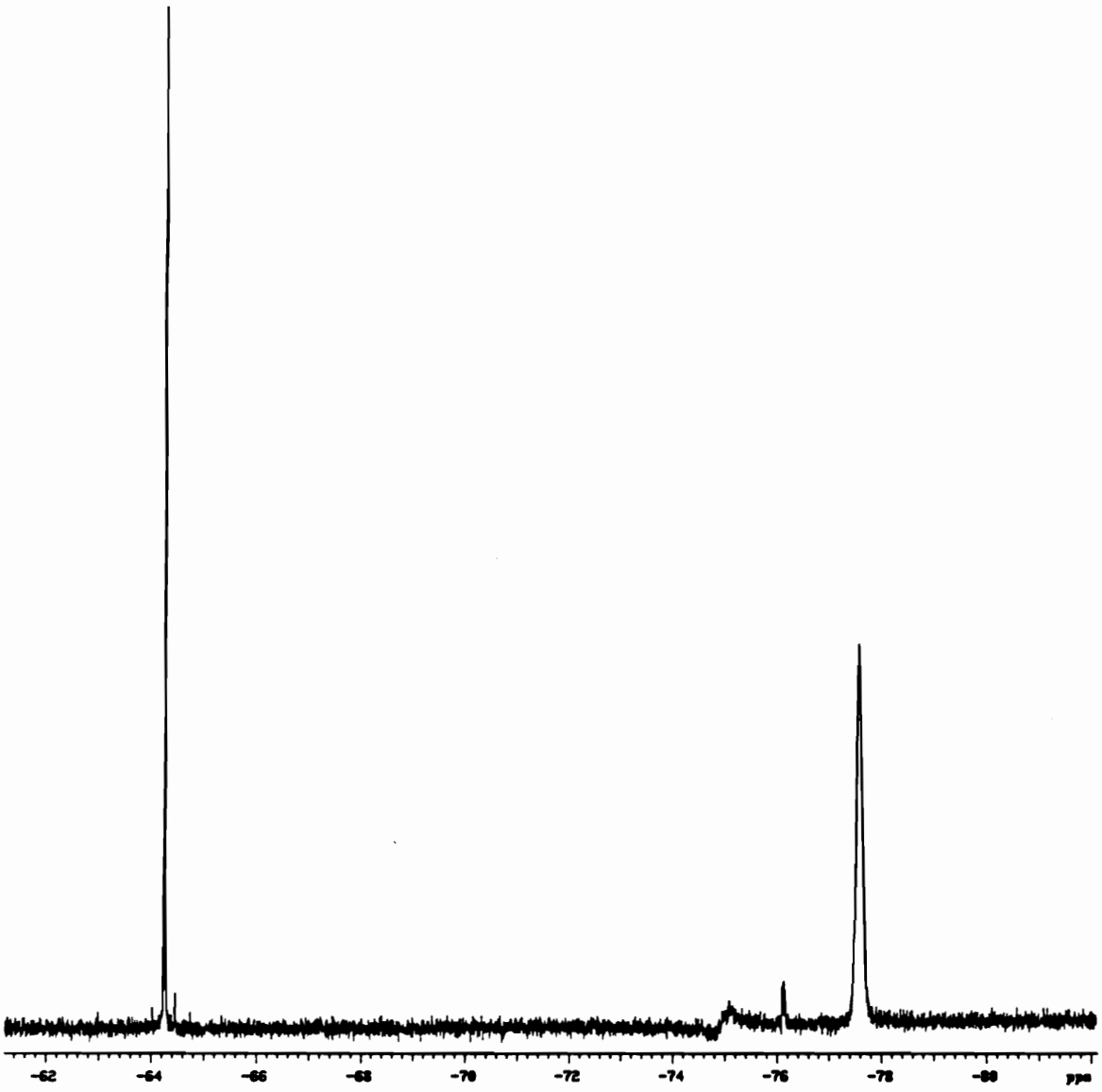

Figure 8. ^{19}F NMR of FAR reaction product, F4. Fluorine chemical shifts are shown upfield from $CFCCl_3$.

CHAPTER FIVE

CONVENTIONAL DERIVATIZATION OF CELLULOSE WITH PREFLUORINATED REAGENTS

PART ONE. SYNTHESIS AND CHARACTERIAZTION OF BENZYLATED, p-FLUOROBENZYLATED, AND MIXED BENZYL POLYSACCHARIDE ETHERS

PART TWO. THE EFFECT OF FLUORINE CONTENT ON THE BLENDING PROPERTIES OF BENZYLATED CELLULOSE

V. CONVENTIONAL DERIVATIZATION OF CELLULOSE WITH PREFLUORINATED REAGENTS

INTRODUCTION

Previous attempts at the fluorination of cellulose were wrought with difficulties. For example, fluorination using displacement chemistry gave poor yields, and appeared fruitless for the controlled synthesis of fluorodeoxycellulose. Whereas, fluorination of cellulose, and hydroxypropyl cellulose, with DAST and FAR type reagents was always complicated by HF catalyzed side reactions. These problems made it virtually impossible to control the fluorine content of these derivatives. Certainly, no study of the effects of fluorine content on polymer properties could occur without synthetic control over the degree of fluorination. Therefore, these methods were abandoned, and a search began for a technique with simplicity and control of fluorination.

It became immediately obvious that reacting cellulose with a prefluorinated reagent would be the easiest route, where the difficulties of fluorination would be avoided. This naturally lead to the use of existing chemistry for the synthesis of either fluorinated cellulose esters or fluorinated cellulose ethers.

Recently, the synthesis tri-O-benzyl cellulose has been reported by Isogai et al.[1]. This particular method was of interest because it was the first report of a single pot, high yield reaction that provided the trisubstituted benzyl ether. Other methods have failed to give high degrees of benzylation in high yield[2,3]. This method had the added attraction of using the nonaqueous cellulose solvent system dimethyl sulfoxide (DMSO), diethylamine (DEA), and sulfur dioxide (SO_2). Such homogeneous cellulose solutions have recently been recognized for potential synthetic advances in cellulose chemistry[1,4]. As such, the novelty of this particular solvent system made tri-O-benzyl cellulose an

attractive choice for the study of fluorinated cellulose derivatives. Furthermore, the fluorine content of these ethers could be controlled by simply using a mixture of fluorinated, and nonfluorinated benzylating reagent. Under this synthetic scheme, all derivatives are fully substituted, but the relative degree of fluorination varies, as these are mixed cellulose benzyl ethers.

PART ONE

SYNTHESIS AND CHARACTERIZATION OF BENZYLATED, p-FLUOROBENZYLATED, AND MIXED BENZYL POLYSACCHARIDE ETHERS

INTRODUCTION

Historically, the complexity of cellulose derivative NMR spectra has made signal assignments very difficult. Before the refinement of two-dimensional NMR techniques, and polarization transfer experiments, spectral assignments of cellulose derivatives were based upon chemical techniques, and by analogy to the corresponding monosaccharides[5,6,7,8,9]. Recently however, cellulose esters have been thoroughly characterized by NMR techniques alone[10,11,12,13]. On the other hand, cellulose ether characterization is still largely dependent upon comparison to monomeric glucosides, and the corresponding tri-O-substituted monosaccharides[14,15,16,17]. The polymers synthesized here have had all backbone, proton and carbon, resonances assigned using only NMR experiments. The aim of this study was to test the validity of using NMR resonances of monosaccharide analogs, to assign resonances of the corresponding polymers.

Therefore, fluorobenzylated polysaccharides were subjected to acid catalyzed methanolysis. The resulting α- and ß-2,3,6-tri-O-fluorobenzyl methyl glucosides were isolated and characterized using the same NMR techniques applied to the polymers. Because, the methanolysis provides both the α- and ß- methyl glucosides, it was appropriate to expand the study to include benzylated amylose derivatives. Of course, amylose is a α-1,4-anhydroglucan, the stereoisomer of ß-linked cellulose. This allowed the comparison of carbon and proton NMR signals of the anomers, to the

stereochemically analogous polymer.

With the addition of amylose to this study, the goals of this work grew to include a fundamental comparison of chain flexibility between isomeric polymer chains. Differences in chain flexibility were probed with calorimetric studies, carbon spin-lattice relaxation measurements, and differential viscometry.

Lastly, the mixed cellulose benzyl ethers were studied with respect to their spectral and thermal characteristics.

EXPERIMENTAL

MATERIALS:

All solvents were freshly distilled with the appropriate desiccants, prior to use. Unless otherwise stated, all reagents were purchased from Aldrich Chemical company, and used as received. All liquid transfers were strictly anhydrous, using syringe and cannula techniques.

Whatman cellulose, type CF-11, was used as starting material in all cellulose reactions. Number average degree of polymerization was determined as approximately 200; polydispersity was 1.67. Potato amylose, type III, was obtained from Sigma Chemical Company. This amylose had a number average degree of polymerization of about 477, and a polydispersity of 3.5. Molecular weight information for the cellulose, and amylose, starting material was obtained by synthesizing the triphenylcarbamate derivative[18]. This derivative is often referred to as cellulose tricarbanilate, or CTC, or ATC, for amylose tricarbanilate. CTC, and ATC, are organic solvent soluble, and are therefore amenable to gel permeation chromatography in organic phase, as a means of obtaining molecular weight information of the parent carbohydrate[18].

METHODS:

Molecular Weight Analysis:

Gel permeation chromatography was used, where tetrahydrofuran was pumped by a Waters 510 into a series of 3 Waters Ultrastyragel columns, with pore sizes of 10^3, 10^4, and 10^6 angstroms. Detection was with a Waters 410 refractometer, in series with a Viskotek differential viscometer model 100. The columns were heated to 40°C in an Eldex column heater, and both detectors were also heated to 40°C. Tetrahydrofuran was freshly degassed, and always stored under a helium atmosphere during use. Narrow polydispersity, polystyrene standards from Polymer Laboratories were used to establish a universal calibration.

Nuclear Magnetic Resonance Spectroscopy:

A Varian Unity-400 nuclear magnetic resonance spectrometer was used to collect ^1H, ^{19}F, and ^{13}C NMR spectra at 400, 376, and 100 Mhz, respectively. Samples were prepared by dissolving the analyzed material in the appropriate deuterated solvents, using 5 millimeter, or 10 millimeter Wilmad glass tubes. Where appropriate, the percent fluorine present in a sample was determined with ^{19}F NMR using an internal standard analysis. Precisely weighed amounts of sample and fluorine internal standard were placed into a 25 ml round bottom flask. The mixture was dissolved in $CDCl_3$, and then run on the NMR. Percentages of fluorine would be calculated based upon the ^{19}F integrations, and the known masses of sample and standard. The internal standard was 3-trifluoromethyl acetophenone(chemical shift=-64.26 ppm, relative to trifluoroacetic acid at -77.05 ppm).

Samples for carbon T_1 measurements were prepared in 10 mm NMR tubes using approximately 290 milligrams of sample in 2.8 ml of deuterated chloroform. These samples were degassed by the freeze-pump-thaw technique, where each sample was treated to at least seven cycles. Carbon T_1 experiments were performed using the

standard, 180-τ-90, inversion recovery method. Carbon T_1's were determined using the Varian exponential fit software routine.

The following standard pulse sequences were used: Double Quantum filtered COSY(DQCOSY), Heteronuclear Correlation spectroscopy(HETCOR), Total Correlation Spectroscopy(TOCSY), and Distortionless Enhancement by Polarization Transfer(DEPT). For the TOCSY sequence, mixing times of 60 and 55 milliseconds were used for fluorobenzyl cellulose and fluorobenzyl amylose respectively.

Infrared Spectroscopy:

Infrared spectra were collected on a Nicolet 5SXC Fourier Transform InfraRed spectrometer, FTIR. Samples were prepared by grinding in KBr, followed by high pressure formation of the sample pellet. Otherwise, thin films were deposited from solution, dried, and analyzed directly in the spectrometer. Samples were scanned at a resolution of two cm^{-1}, with at least 32 repetitions.

Mass Spectroscopy:

Mass spectral analyses were performed using a model 7070 E-HF, magnetic sector, double focusing, mass spectrometer, manufactured by VG Analytical, of Manchester, UK.

Thermal Analysis:

Thermal transitions of polymers were observed using a differential scanning calorimeter, DSC. A Perkin Elmer, DSC-4, equipped with the Thermal Analysis Data System, TADS, was used with the Perkin Elmer Intracooler. This cooling system allows scanning from as low as -55°C. The DSC was calibrated in the usual fashion, with high purity indium.

Synthesis of Tri-O-p-Fluorobenzyl Cellulose:

Tri-O-p-fluorobenzyl cellulose was synthesized using 4-fluorobenzyl chloride, and 10 grams of cellulose, according to the method described by Isogai et al[1], with the following exceptions. All reactions were carried out under nitrogen atmosphere. During the initial addition of benzylating reagent, the reaction was cooled in a water bath so as to counter the exotherm which occurs during mixing. After the first addition of benzylating reagent, the flask was warmed to 70°C. After reaching 70°C, there were 3 more additions of benzylating agent as per the method of Isogai[1], except these were at 1, 2 and 18 hours after reaching the 70°C temperature. After the last addition of benzylating reagent, the reaction was heated to 85°C for 2 hours. Then the flask was allowed to cool to room temperature, and the solution was poured into 4 liters of distilled water. The polymer formed a stable emulsion which settled nicely to the bottom of the beaker. The liquid layer was decanted off, and more distilled water was added with vigorous stirring. This procedure was repeated until the liquid layer was colorless. Then the water was decanted off again, and 3 liters of methanol was added to cause precipitation of the polymer. The product was filtered and extracted with methanol in a soxhlet for at least 24 hours. The polymer was dried, dissolved in tetrahydrofuran, and centrifuged to remove any insoluble material. The supernatant was concentrated and then precipitated into methanol. The polymer was finally dried under high vacuum for 24 hours. Yields were typically 70 to 80% of theoretical. The product was soluble in tetrahydrofuran, chloroform, dioxane, etc. The material is insoluble in methanol, ethanol, and the like.

Synthesis of Tri-O-Benzyl Cellulose:

The same method as listed above was used.

Synthesis of Mixed p-Fluorobenzyl/Benzyl Cellulose:

A series of 5 different mixed benzyl ethers were synthesized using the same method that was described for the synthesis of tri-O-p-fluorobenzyl cellulose. Mixed ethers were synthesized using different mole ratios of p-fluorobenzyl chloride and benzyl chloride. The following 5 mole ratios were used, fluorobenzyl/benzyl chloride: 75/25, 50/50, 40/60, 25/75, and 15/85. p-Fluorobenzyl chloride and benzyl chloride **WERE NOT** mixed, and then added to the reaction flask. Instead, they were added sequentially to the reaction flask, according to the procedures listed above. p-Fluorobenzyl chloride was always added before benzyl chloride. For example, in the synthesis using a mole ratio of 75/25, fluorobenzyl chloride to benzyl chloride the first 3 additions of benzylating agent were fluorobenzyl chloride. When all of the fluorobenzyl chloride was used, only then, was the benzyl chloride added.

Synthesis of Tri-O-p-Fluorobenzyl Amylose, I:

The first synthesis of tri-O-p-fluorobenzyl amylose was performed the same way as mentioned above for the benzylation of cellulose, using the DMSO/DEA/SO_2 solvent system.

Synthesis of Tri-O-p-Fluorobenzyl Amylose, II:

The second method was the same as used by BeMiller and Wing[19]. This method only uses DMSO as the solvent.

Synthesis of α, and ß-2,3,6-Tri-O-p-Fluorobenzyl Methyl Glucoside:

2 grams of tri-O-p-fluorobenzyl amylose were placed in a dry 250 ml 3-neck flask, with condenser, drying tube, and rubber septum. Using syringe techniques, 75 ml of anhydrous methanol, and 150 ml of 4 molar anhydrous HCl in dioxane (Sure Seal, Aldrich Chemical) was added sequentially. The flask was warmed to reflux and monitored by thin layer chromatography (TLC) on silica plates using petroleum

ether/acetone, in a 4:1 ratio. The reaction was complete within 48 hours. The solution was partitioned between ethyl ether and dilute aqueous alkali, and then concentrated. A preparative isolation of the mixture of α- and ß- anomers was performed by running the oil over a silica column using petroleum ether/acetone, 4:1. The α- and ß- anomers were obtained in pure form by preparative TLC using 3:1 petroleum ether/acetone. Structures were confirmed by proton NMR, carbon NMR, and GC-mass spectroscopy.

RESULTS AND DISCUSSION

A: SPECTRAL CHARACTERIZATION OF AMYLOSE AND CELLULOSE DERIVATIVES, AND ANALOGOUS MONOSACCHARIDES

The ^{1}H and ^{13}C NMR spectra of tri-O-p-fluorobenzyl cellulose, tri-O-p-fluorobenzyl amylose are provided for the reader to observe the spectral differences between isomeric polysaccharide derivatives(Figures 1-4). Likewise, compare the ^{1}H and ^{13}C NMR of the α and ß-2,3,6-tri-O-p-fluorobenzyl methyl glucosides to the analogous or stereochemically similar polysaccharide(Figures 5-8).

Upon inspection of these spectra, one can immediately appreciate that the proton NMR spectra of the α- and β- monosaccharides bear little resemblance to the analogous polysaccharides. While, not surprisingly, there appears to be a superficial resemblance between corresponding mono- and polysaccharides, in the carbon NMR. Table 1 lists the assignments for the proton resonances of tri-O-p-fluorobenzyl cellulose, and tri-O-p-fluorobenzyl amylose. Table 1 also includes proton assignments for the α and ß anomers of 2,3,6-tri-O-p-fluorobenzyl methyl glucoside. Table 2, lists the assignments of carbon resonances for the same polymers and monomers.

These resonances were assigned through the use of a combination of two-

dimensional NMR experiments. For example, the analysis of tri-O-p-fluorobenzyl amylose started with the **D**ouble **Q**uantum filtered **CO**rrelation Spectroscop**Y** experiment, DQCOSY(Figure 9). The DQCOSY experiment reveals the proximity of protons, based upon the strong couplings that occurs between geminal, and vicinal protons. The diagonal of Figure 9 shows the ^{1}H resonances of a normal 1-D NMR spectra. The off-diagonal signals represent couplings of nearest neighbor protons. An off-diagonal signal that is equidistant from two signals lying on the diagonal, represents a coupling between proton resonances. Schematically, this gives rise to a perfect right angle. Because, there is an off-diagonal signal on both sides of the diagonal, this coupling may be represented as a perfect square, as shown in bold(Figure 9). These lines depict the coupling between protons located at positions 1 and 2 of the anydroglucose ring, at $\delta = 5.60$ and 3.46 ppm, respectively. These are protons H1 and H2 of the amylose derivative. The identity of the signal at 5.60 ppm is determined from heteronuclear correlation to carbon 1 of the derivative, as will be discussed shortly. The identification of H1, through heteronuclear correlation, allows for the sequential identification of the remaining protons. This is accomplished by simply following the correlations as shown, Figure 9.

The carbon resonances for tri-O-p-fluorobenzyl amylose were assigned by combining the information from the DQCOSY, with the **HET**eronuclear **COR**relation spectroscopy, HETCOR, experiment(Figure 10). In this case, the ^{1}H signals are shown on the top, and ^{13}C signals on the left side of the figure. A signal in the interior of Figure 10 will align with one proton, and one carbon signal. This alignment is a schematic representation of the coupling that exists between attached proton and carbon nuclei. For example, in Figure 10, the proton assigned to position 1 of the amylose derivative, 5.6 ppm, correlates with the carbon signal at 96.2 ppm. This is the most deshielded carbon in the spectrum, and therefore means that this is carbon 1 of the anhydroglucose ring, as has been well established[1,13,20,21,22,23,24]. Notice, that the carbon at 68.6 ppm shows no correlation to a proton, while carbons 1-5 do show correlations, Figure 10. Figure 11

shows an enhanced view of the HETCOR of Figure 10. Here we can now see two protons that correlate with the carbon at 68.6 ppm. As suspected, this is good evidence for a methylene carbon, or C6 of the amylose derivative. Definitive proof is found in the **D**istortionless **E**nhancement **P**olarization **T**ransfer, DEPT, experiment(Figure 4). This experiment enables one to distinguish between methyl, methylene, and methine carbons. The DEPT experiment confirms that the carbon at 68.6 ppm is a methylene, and therefore we may now confidently assign this signal to carbon 6 of tri-O-p-fluorobenzyl amylose. This DEPT spectra also shows how the signal for carbon 4 is hidden by the methylene signals of the benzyl carbons(Figure 4). This is a good example of how the DEPT experiment helps to clear up any confusion that exists from considering only the DQCOSY and the HETCOR.

The process just described for tri-O-p-fluorobenzyl amylose was also used for the assignment of proton and carbon resonances for tri-O-p-fluorobenzyl cellulose, and the α and ß anomers of 2,3,6-tri-O-p-fluorobenzyl methyl glucoside. From the above discussion, it is clear that no one NMR experiment can provide all assignments for complex spectra. However, the combination of a few well selected experiments often solves the puzzle of NMR assignments. The extreme multiplicity of the monomer ^{1}H spectra made the assignments much more difficult than for the polymers. Therefore monomer proton assignments were based upon the 2-D and polarization transfer techniques mentioned above, in addition to a thorough examination of coupling patterns and signal intensities.

The benzyl carbons for the amylose and cellulose derivatives were assigned with the **TO**tal **C**orrelation **S**pectrosco**Y**, TOCSY, experiment. TOCSY is similar to DQCOSY, in that proton-proton couplings are revealed. The difference is that TOCSY shows long range, as well as short range proton-proton couplings. The TOCSY experiment was used to establish the connectivity of benzyl substituents, across oxygen,

to either of positions 2,3, or 6. The information from the TOCSY was combined with that from DQCOSY and HETCOR for the assignment of the benzyl carbons. Frankly however, the TOCSY experiments gave results that were difficult to interpret. Nonetheless, assignments were made, and they were subsequently supported by carbon relaxation experiments that will be mentioned later. It is interesting to note that benzyl carbons of secondary positions, 2 and 3, are similar in their ^{13}C chemical shifts. While, on the other hand, the benzyl carbon of position 6, the primary position, has a distinct chemical shift in both the cellulose and amylose derivatives(Figures 2,4 and Table 2). The benzyl carbons of the methyl glucosides were not assigned using the TOCSY experiment. Instead they were assigned based upon analogy to the respective polymers.

Assigning the monomer benzyl carbon signals by analogy to the polymers is a valid approach. Because, Table 2 shows that the α monomer and the α polymer show very good agreement in the chemical shift of the corresponding carbons. The same is true of the ß methyl glucoside, and the cellulose derivative. In short, analogous carbohydrate polymers and monomers have very similar ^{13}C chemical shifts. Within this context, analogous qualifies as similarity in derivatization at positions 2,3, and 6, and also similarity in the anomeric configuration at carbon 1. Therefore, we may conclude that previous researchers were justified in assigning carbon signals of cellulose derivatives by analogy to the appropriate monomeric model.

However, as was alluded to earlier, monomeric models are not appropriate for the assignment of proton signals, in analogous polysaccharide derivatives(Table 1). Chemical shifts of corresponding protons on analogous monomer/polymer pairs are as great as 0.95 ppm. The narrow range of proton spectra makes this a significant difference. Furthermore, the complex multiplicity of the proton spectra of the methyl glucosides makes analogy to polymers inherently troublesome.

B: ANALYSIS OF MIXED BENZYL CELLULOSE ETHERS, SYNTHETIC CONSIDERATIONS

Cellulose benzylations in DMSO/DEA/SO_2 provided a simple method for synthesizing cellulose benzyl ethers, with variable degrees of fluorination. The general synthetic scheme for the formation of tri-O-benzylcellulose is shown in figure 12. Intermediate degrees of fluorination were obtained by using various ratios of p-fluorobenzyl chloride, to benzyl chloride. In this way, all derivatives were completely substituted, but as mixed ethers, variable in the ratio of benzyl, to p-fluorobenzyl substitution. With this in mind, a new nomenclature will be introduced to aid in the discussion of these mixed ethers. The degree of substitution of fluorine, or DSF, can vary between 0.0 and 3.0. If for example, a sample has a DSF of 2.0, then, on average, 2 of 3 positions are fluorobenzylated, while the remaining position is a nonfluorinated benzyl group(Figure 13). A DSF of 0.0 refers to tri-O-benzyl cellulose, while a DSF of 3.0 refers to tri-O-p-fluorobenzyl cellulose. DSF values were obtained by integration of carbon signals in the quantitative, or gate decoupled, ^{13}C NMR of each of the mixed benzyl ethers. The relative degrees of p-fluorobenzyl and benzyl substitution were verified through elemental analysis. Fluorine, carbon, and hydrogen ratios from elemental analysis were in good agreement with the DSF obtained from quantitative ^{13}C NMR. The mole ratios of p-fluorobenzyl chloride to benzyl chloride gave the indicated DSF(Table 3).

Keep in mind that p-fluorobenzyl chloride, and then benzyl chloride were added sequentially to the reaction mixture, in that order. Furthermore, there was a total of 4 additions of benzylating reagent, where 85 mole% of the total was charged initially, with three subsequent additions of 5% each. P-fluorobenzyl chloride was added first because of its lower reactivity, relative to benzyl chloride. The relative degree of fluorination can be observed in the ^{19}F NMR(Figure 14). The 3 samples labeled as DSF 3.0, 2.9, and 2.8 appear to have about the same fluorine content in the ^{19}F NMR. Fine differences between

these mixed benzyl ethers are more apparent in the ^{13}C NMR(Figure 15). Signals centered at 127.5 and 138.5 ppm arise from nonfluorinated benzyl substituents. As the DSF increases, these two signals decrease(Figure 15). Notice that the sample with a DSF of 2.9 still has a very weak signal from the nonfluorinated benzyl substituents. Therefore, this sample, with DSF of 2.9, is truly a mixed fluorobenzyl/benzyl cellulose ether.

The ^{19}F and ^{13}C NMR provide no indication of the substitution pattern for the mixed benzyl ethers. For example, the DEPT carbon spectrum for DSF 2.0, clearly indicates the copolymeric nature of this sample(Figure 16). There are approximately 6 benzyl carbon signals, 71-75 ppm. These signals no doubt represent weighted averages of the 8 monomer residues that are theoretically possible. However, it is impossible to determine the relative predominance of any one repeat unit from the NMR. The chemical shifts of the mixed ether backbone carbons are essentially the same as for tri-O-p-fluorobenzyl cellulose. There are very slight field shifts, and signal broadenings (Figure 16). The copolymeric nature of DSF 2.0 is more evident in the ^{1}H NMR, as signal broadenings are more severe than in the ^{13}C spectra(Figure 17). At any rate, the proton and carbon assignments from DSF 3.0 generally apply to all of the mixed benzyl ethers.

One could imagine that the microstructure of these derivatives may be significantly altered by simple manipulations. For example, if benzyl chloride was added prior to p-fluorobenzyl chloride, a different substitution pattern would likely be the result. The relative reactivity of the 3 hydroxyls would not change, but the differential reactivity of these benzylating agents could give rise to different substitution patterns based upon the order of addition. Indeed, the combination of relative hydroxyl reactivity, and the differential reactivity of benzyl and fluorobenzyl chloride, probably does result in the preponderance of a particular repeat unit.

C: MOLECULAR CHARACTERISTICS-MOLECULAR WEIGHT, THERMAL PROPERTIES, AND CARBON SPIN-LATTICE RELAXATION

While this chemistry successfully gave cellulose derivatives with variable fluorine content, this reaction was found to be extremely degradative to the cellulose chain (Table 4). Molecular weight data of cellulose tricarbanilate, CTC, and, amylose tricarbanilate, ATC, are included for comparison. Carbanilates are the phenylurethane derivatives of the starting carbohydrates. They represent the molecular weights of the starting materials used in this study. On average, the cellulose derivatives lost about 73% of the weight average degree of polymerization, DP_w. Isogai et al. report an average loss of 45% of the starting viscosity average DP[1].The greater molecular weight loss seen in this work is due to the longer reaction times used, a total of 6 hours longer than described by Isogai, et al. It was claimed that molecular weight loss was due to the presence of atmospheric air, in combination with sodium hydroxide[1]. However, all benzylations in this study were conducted under a dry nitrogen atmosphere. Extreme DP loss in this reaction results from the highly oxidative nature of the solvent system, DMSO/DEA/SO_2. In particular, SO_2 was found to be the prime cause of degradation. DMSO soluble amylose was benzylated with and without the SO_2/amine component of the solvent system. Amylose benzylated in the DMSO/DEA/SO_2 solvent system suffered an 87% loss in DP_w. However, the benzylation in pure DMSO resulted in a 55% loss in DP_w(Table 4). It appears that the combination of DMSO with sodium hydroxide is very degradative to polysaccharides. But the addition of SO_2 causes a far more serious depolymerization.

Differential scanning calorimetry, DSC, shows no clear melting transition in any of these derivatives. Instead, they showed a strong exotherm, just prior to degradation, at temperatures between 150 and 250°C(Figure 18). (Fluorinated cellulose benzyl ethers appeared to be more stable than benzyl cellulose.) This is in contrast to tri-O-benzyl

cellulose made by Isogai et al[1]. These authors show a clear melting transition at about 255°C, and they do mention that decomposition occurs soon after melting[1]. Furthermore, incompletely substituted cellulose benzyl ethers were shown to decompose before melting[1]. In fact, the thermograms of these incompletely substituted cellulose derivatives look very similar to the thermograms in this work(Figure 18). However, all of the benzyl derivatives in this study are trisubstituted, as indicated by infrared analysis(Figure 19, for example). In the infrared spectra, the region between 3200 and 3600 cm^{-1} is completely flat, and therefore indicates that cellulose is trisubstituted. Consequently, the lack of a clear melting transition in these derivatives is not due to incomplete substitution. The only notable difference is that these benzyl derivatives have a significantly lower molecular weight than those analyzed by Isogai et al.

Glass transition temperatures, T_g, of all of these cellulose benzyl ethers lie within a range of 40-60°C. There is no apparent effect of fluorine content on the value of the T_g. The T_g of these derivatives is very subtle, and requires repetition of fast heating followed by slow cooling, for clear observation of the transition(Figure 20). This is in remarkable contrast to the thermal behavior of tri-O-p-fluorobenzyl amylose, which is also shown for comparison. The amylose derivative shows a very strong T_g. Furthermore, in contrast to the cellulose derivative, p-fluorobenzyl amylose displays crystallization, melting, and thermal stability above the melt(not shown in Figure 20). The α-linkage of the amylose backbone imparts a much more coil-like configuration to the chain. Whereas, the ß-linkage of the cellulose chain is stiffening. The different configurations of these polymeric stereoisomers result in drastically different thermal behavior.

These differences are also apparent when measuring the ^{13}C spin-lattice relaxation times, T_1, of the two polymers. 10% solutions, (w/v), of tri-O-p-fluorobenzyl cellulose, and tri-O-p-fluorobenzyl amylose (sample 10 in Table 4) were made in deuterated

chloroform. T_1 measurements were made at 8 temperatures, ranging from -30° to 54°C, using a standard inversion recovery pulse sequence. T_1 values of the backbone, and benzyl carbons, are listed in Tables 5 and 6, for the cellulose and amylose derivatives respectively. The backbone carbons of the cellulose derivative all displayed the same relaxation behavior. That is, T_1 relaxation was independent of position in the cellulose backbone. The same was true for tri-O-p-fluorobenzyl amylose. However, there was stark contrast between the polymers(Figure 21). The cellulose derivative spin-lattice relaxations were insensitive to the experimental temperature range, in $CDCl_3$. Whereas, tri-O-p-fluorobenzyl amylose displayed a steady decrease in T_1 relaxation as the temperature rose(Figure 21).

We may confidently state that the relaxation mechanism in these polymers is strictly dipolar[25,26]. As such, a much simplified relationship between temperature and T_1 arises. The dipolar relaxation of carbon nuclei depends upon fluctuating local magnetic fields that arise from the motion of the carbon-hydrogen dipole. Of course, the motion of a C-H dipole is a direct function of the mobility of the carbon center itself. When motions are very fast, as in small molecules, dipolar relaxation is inefficient, and carbon T_1's are very long. When carbon mobilities decline, as for the interior carbons of hydrocarbon chains, relaxation becomes more favorable, and T_1's begin to fall. In very large polymeric chains, mobility is too slow to support efficient relaxation, and T_1 times rise again. This relationship is shown in diagram form(Figure 22). Figure 22 shows T_1 plotted versus τ_c, the correlation time. τ_c is a function of the frequency of C-H bond motion that contributes to carbon relaxation. Higher τ_c means slower molecular motion. At the center of the correlation function, relaxation is insensitive to changes in mobility, or changes in temperature. This is the case for tri-O-p-fluorobenzyl cellulose, as shown in Figure 21. We can also see that tri-O-p-fluorobenzyl amylose is experiencing a decline in T_1 as temperature rises. This suggests that the amylose derivative is positioned near the right hand side of the minima in Figure 22. Actually, it is more appropriate to say

that p-fluorobenzylated amylose and cellulose, each, have distinctly different correlation functions. Figure 23 shows a hypothetical diagram of how these two correlation functions may compare. The shaded region represents the experimental temperature range. The cellulose derivative correlation function is centered upon the experimental temperature range. Therefore, no change in T_1 results from the change in temperature. On the other hand, the amylose derivative correlation function is shifted to the left of the experimental temperature range. In this range, we would expect a drop in T_1 relaxation as temperature rises. In other words, the data suggests that the correlation function of the amylose derivatives is shifted to lower values than for the cellulose derivative(Figure 23). As we would expect, this means that tri-O-p-fluorobenzyl amylose has a higher segmental mobility than tri-O-p-fluorobenzyl cellulose. This is in agreement with the thermal behavior we saw above. The more flexible amylose chain has a more energetic glass transition than the stiff cellulose chain.

The relaxation behavior of the pendant benzyl carbons also reveal fundamental differences between these derivatives(Figures 24 and 25). There is no great difference between benzyl carbons at primary and secondary positions in fluorobenzyl amylose (Figure 24). (Unfortunately, only 2 of 3 amylose benzyl carbons could be measured for fluorobenzyl amylose, because of signal overlap.) The C6 benzyl T_1's are slightly higher than those of the secondary, C2 benzyl. This reasonably suggests that the primary benzyl carbon has a little more motional freedom than secondary benzyl carbons in fluorobenzyl amylose. But, the slopes of the curves are similar, so the mode of relaxation must also be similar.

This is not the case for tri-O-p-fluorobenzyl cellulose(Figure 25). The primary, C6 benzyl, in the cellulose derivative, has a very different behavior from the secondary benzyl carbons(Figure 25). The C6 benzyl is more sensitive to temperature change than the C2 and C3 benzyls. This implies that the energy barrier to relaxation is higher for

the primary benzyl carbon. Whereas, benzyl carbons at positions 2 and 3 have restricted mobility relative to the primary benzyl carbon[a].

This is an indication of the anisotropic nature of the cellulose derivative. The cellulose chain is stiffer, and more rod-like. Consequently, the C6 benzyl sticks out in free space, with relative freedom in motion. The coiled nature of the amylose derivative serves to average out the differences between primary and secondary positions, probably by crowding the mobility of the primary substituent. Again, these observations are consistent with the general knowledge of cellulose and amylose chains. A reminder is found in Table 4, where a contrast in solution behavior is seen. As we would expect, the Mark-Houwink-Sakurada exponent is higher for the stiffer cellulose derivative.

CONCLUSIONS

1. The ^{13}C NMR shifts of α and ß-2,3,6-tri-O-p-fluorobenzyl methyl glucosides were very similar to the corresponding shifts of tri-O-p-fluorobenzylated amylose and cellulose. Therefore basing ^{13}C NMR assignments of benzylated polysaccharides on the known ^{13}C shifts of benzylated monosaccharides is justified. This does, however, require the anomerically similar monosaccharide.
2. ^{1}H NMR shifts of polysaccharide derivatives should not be assigned by analogy to the corresponding monosaccharide.
3. The DMSO/DEA/SO_2 solvent system allows for the easy synthesis of mixed p-fluorobenzyl/benzyl cellulose ethers. This procedure allows for control of the fluorine content of these polymers.
4. The mixed benzyl ethers can be considered as copolymeric in nature. Differential

---

[a] Note that this relaxation behavior confirms the positional assignment of the 6 position benzyl carbon according to TOCSY. Further evidence is seen in the fact that the secondary position benzyl carbons have more similar ^{13}C NMR shifts, while the primary benzyl carbons have distinct chemical shifts(Figures 2 and 4).

hydroxyl and benzylating reagent reactivity probably give rise to a nonrandom microstructure. But there is no hard proof of this in the ^{1}H or ^{13}C NMR.

5. The fluorine content of these mixed benzyl ethers does not significantly alter the ^{1}H or ^{13}C NMR signals, or the value of the glass transition temperature.
6. Benzylation in the DMSO/DEA/SO_2 solvent system is highly degradative to amylose and cellulose. Depolymerization of these chains does not require the presence of air. The SO_2 component of the solvent system causes most of the degradation during benzylation.
7. As expected, tri-O-p-fluorobenzylated cellulose and amylose have very different thermal properties. The differences are due to the rod-like and coil-like behavior of the respective polymers.
8. As expected, ^{13}C spin-lattice relaxation measurements, of the amylose and cellulose derivative backbone carbons, indicate that the cellulose chain has restricted mobility relative to the amylose chain. Furthermore, the relaxation behavior of the benzyl carbons indicates that the local environment of the cellulose substituents is anisotropic, relative to the benzyl groups of amylose. This also arises from the rod-like and coil-like nature of these polymers.

LITERATURE CITATIONS

1. Isogai, A., A. Ishizu, and J. Nakano, J. Applied Polym. Sci., 29, 2097, 1984.

2. Day, W.H., and J.D. Caldwell, J. Polym. Sci., Polym. Lett. Ed., 17, 55, 1979.

3. Keilich, G., N. Frank, and E. Husemann, Makromol. Chem., 176, 3269, 1975.

4. McCormick, C.L. and P.A. Calais, Polymer, 28, 2317, 1987.

5. Friebolin, H., G. Keilich, and E. Siefert, Angew. Chem., Int. Ed. Engl., 8, 10, 766, 1969.

6. Goodlett, V.W., J.T. Dougherty, and H.W. Patton, J. Polymer Sci.:Part A-1, 9, 155, 1971.

7. Kamide, K., and K. Okajima, Polymer J., 13, 2, 127, 1981.

8. Miyamoto, T., Y. Sato, T. Shibata, H. Inagaki, and M. Tanahashi, J. Polymer Sci., 22, 2363, 1984.

9. Miyamoto, T., Y. Sato, T. Shibata, M. Tanahashi, and H. Inagaki, J. Polymer Sci., 23, 1373, 1985.

10. Buchanan, C.M., J.A. Hyatt, and D.L. Lowman,Macromolecules, 20, 2750, 1987.

11. Buchanan, C.M, J.A. Hyatt, and D.W. Lowman, Carbohydrate Research, 177, 228, 1988.

12. Buchanan, C.M., J.A. Hyatt, and D.W. Lowman, J. Am. Chem. Soc., 111, 7312, 1989.

13. Buchanan, C.M., J.A. Hyatt, S.S. Kelley, and J.L. Little, Macromolecules, 23, 3747, 1990.

14. Parfondry, A.,and A.S. Perlin, Carbohydrate Res., 57, 39, 1977.

15. Lee, Dae-Sil, and A.S. Perlin, Carbohydrate Res., 106, 1, 1982.

16. DeMember, J.R., L.D. Taylor, S. Trummer, L.E. Rubin, and C.K. Chikliss, J. Applied Polymer Sci., 21, 621, 1977.

17. Lee, Dae-Sil, and A.S. Perlin, Carbohydrate Res., 124, 172, 1983.

18. Evans, R., and A.F.A. Wallace, Fourth International Symp. Wood and Pulping Chemistry, vol. 1, 201, 1987.

19. BeMiller, J.N., and R.E. Wing, Carbohydrate Res., 6, 197, 1968.

20. Friebolin, H., G. Keilich, N. Frank, and U. Dabrowski, Organic Mag. Res., 12, 4, 216, 1979.

21. Gagnaire, D., and M. Vincendon, Organic Mag. Res., 11, 7, 344, 1978.

22. Tezuka, Y., K. Imai, M. Oshima, and T. Chiba, Carbohydrate Res., 196, 1, 1990.

23. Hjertberg, T., P. Zadorecki, and M. Arwidsson, Makromol. Chem., 187, 899, 1986.

24. Kimura, K., T. Shigemura, M. Kubo, and Y. Maru. Makromol. Chem., 186, 61, 1985.

25. Heatly, F., Prog. NMR Spectroscopy, 13, 47, 1979.

26. Lyerla, J.R., and G.C. Levy, *Topics in NMR Spectroscopy*, Wiley Pubs., New York, 1, 79, 1974.

TABLE 1. ^{13}C NMR resonances for tri-O-p-fluorobenzyl polymers and monomers. The numbering scheme is defined below.

	C1	C2	C3	C4	C5	C6	BENZYL CARBONS		
							B2	B3	B6
tri-O-p-fluoro benzyl cellulose	102.7	81.9	83.4	76.8	75.2	68.1	74.7	74.4	72.3
tri-O-p-fluoro benzyl amylose	96.2	79.4	81.5	72.4	70.8	68.6	72.9	72.8	72.3
α-2,3,6-tri-O-p-fluoro benzyl methyl glucoside	98.0	79.6	81.2	70.9	69.8	69.5	74.6	72.9	72.3
ß-2,3,6-tri-O-p-fluoro benzyl methyl glucoside	104.7	81.5	83.8	71.8	73.9	70.3	74.5	73.9	73.0

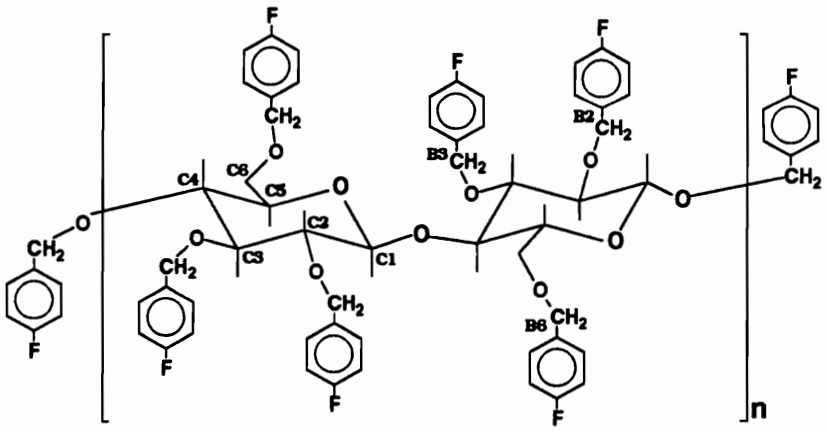

TABLE 2. ^{1}H NMR resonances fot tri-O-p-fluorobenzyl poymers and monomers. Proton numberings are defined below.

	H1	H2	H3	H4	H5	H6	H6'
tri-O-p-fluoro benzyl cellulose	4.33	3.20	3.30	3.87	3.09	3.60	-
tri-O-p-fluoro benzyl amylose	5.60	3.46	3.93	4.03	3.80	3.67	3.40
α-2,3,6-tri-p-fluoro-benzyl methyl glucoside	4.65 J_{12}-4Hz	3.50 J_{23}-12Hz	3.75 J_{34}-8Hz	3.61 J_{45}-8Hz	3.68 J_{56}-8Hz	AB-3.68 δv=0	-
ß-2,3,6-tri-p-fluoro-benzyl methyl glucoside	4.31 J_{12}-8Hz	3.37 J_{23}-12Hz	3.42 J_{34}-8Hz	3.59 J_{45}-8Hz	3.44 J_{56}-4Hz	AB-3.73 δv=10.6	-

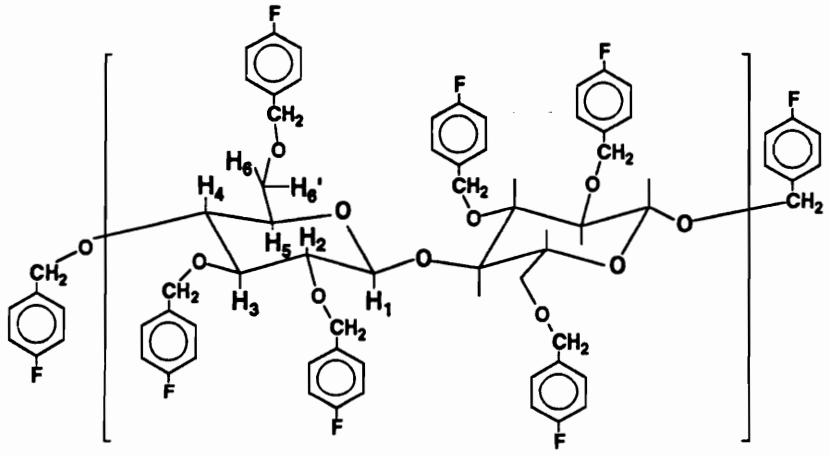

TABLE3. Mole ratios of p-fluorobenzyl chloride (F) and benzyl chloride (H) used to obtain mixed benzyl ethers with specified Degree of Substitution of Fluorobenzyl chloride, DSF.

DSF	3.0	2.9	2.8	2.0	1.3	0.65	0.0
F/H	100/0	75/25	50/50	40/60	25/75	15/85	0/100

TABLE 4. Molecular weight information for cellulose benzyl, and mixed benzyl ethers, amylose benzyl ethers ,and cellulose and amylose tricarbanilates

	DP_n	DP_w	α
Cellulose triphenyl carbamate	167	300	0.85
Fluorobenzyl cellulose, DSF 3.0	29	54	1.19
Mixed Benzyl Ether, DSF 2.9	56	119	0.96
Mixed Benzyl Ether, DSF 2.8	32	74	0.98
Mixed Benzyl Ether, DSF 2.0	40	87	1.0
Mixed Benzyl Ether, DSF 1.3	27	61	1.0
Mixed Benzyl Ether, DSF 0.65	30	68	1.0
Benzyl cellulose, DSF 0.0	31	95	.67
Amylose triphenyl carbamate	477	1668	0.74
Fluorobenzyl amylose DMSO/SO_2/DEA	89	225	0.62
Fluorobenzyl amylose DMSO, no SO_2	363	758	0.84

TABLE 5. ^{13}C spin-lattice relaxation times in milliseconds, for backbone and benzyl carbons of tri-O-p-fluorobenzyl cellulose in $CDCl_3$. B2, B3, and B6 refers to benzyl carbons in positions 2,3, and 6 respective;y, as shown below with all carbon numberings..

°C	C1	C2	C3	C4	C5	C6	B2	B3	B6
54	260	270	260	310	250	140	330	370	510
45	260	240	270	290	270	160	320	370	490
30	270	280	260	300	240	140	320	320	390
22	270	250	260	-	260	150	310	330	360
10	300	310	260	260	280	150	270	300	300
0	350	300	290	320	270	230	270	280	280
-10	290	270	260	390	270	150	260	290	240
-30	-	-	-	-	-	-	270	250	190

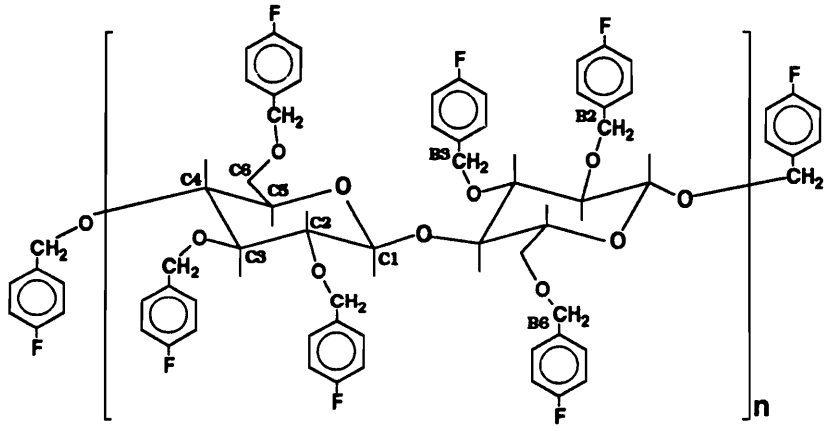

TABLE 6. ^{13}C spin-lattice relaxation times in milliseconds, for backbone and benzyl carbons of tri-O-p-fluorobenzyl amylose in $CDCl_3$. B2, B3, and B6 refers to benzyl carbons in positions 2,3, and 6 respective;y, as shown below with all carbon numberings.

°C	C1	C2	C3	C5	C6	B3	B6
54	260	290	260	260	140	340	360
45	250	290	280	280	170	280	320
30	310	320	330	300	160	270	300
22	290	340	320	310	150	260	300
10	350	340	370	380	150	230	290
0	350	460	390	420	170	250	270
-10	510	630	470	510	300	230	250
-30	-	-	-	-	-	230	230

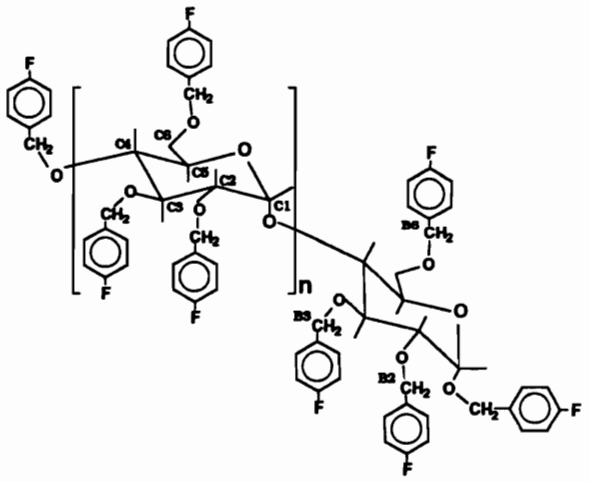

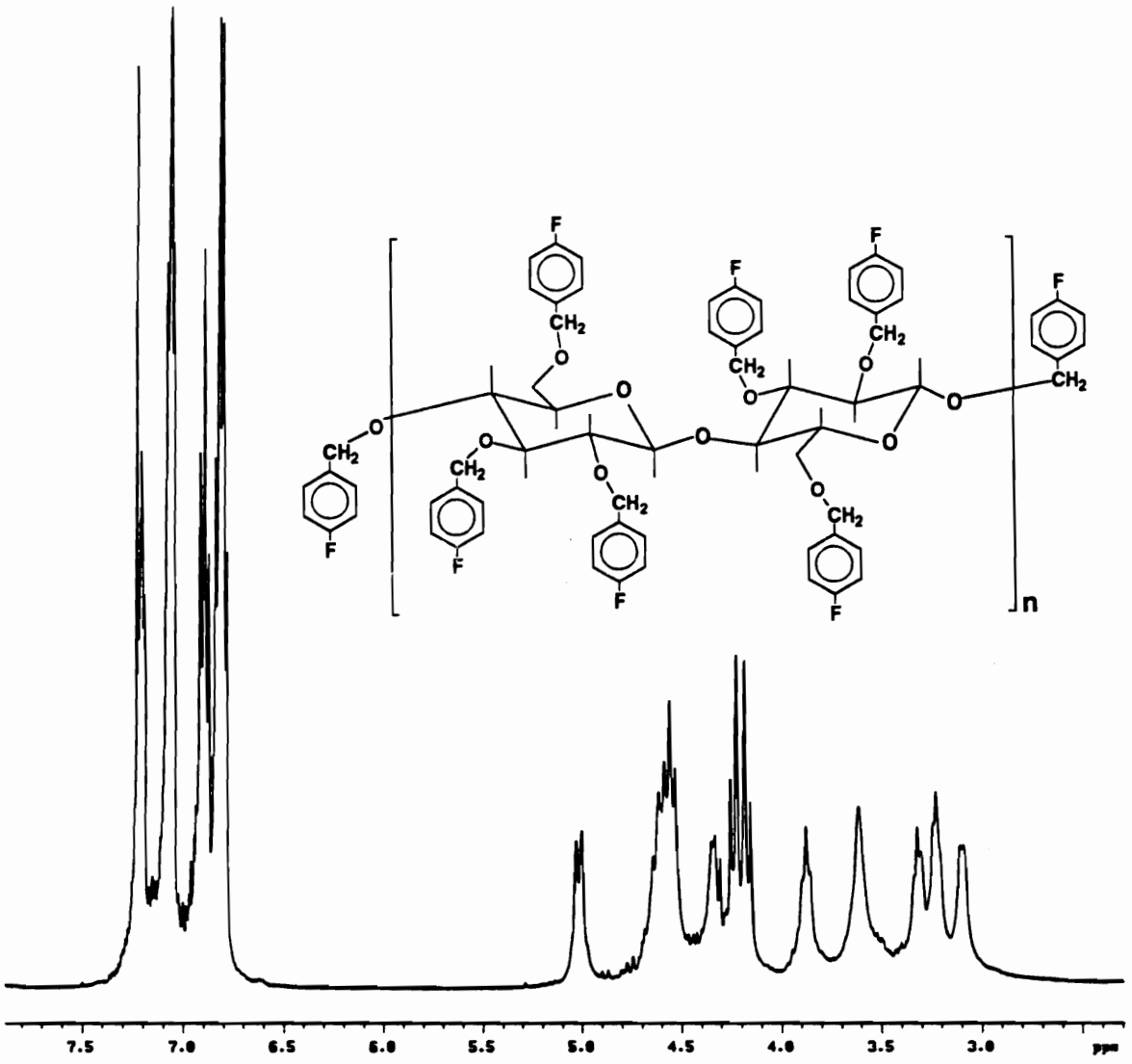

Figure 1. ^1H NMR spectrum of tri-O-p-fluorobenzylcellulose, in $CDCl_3$, at room temperature.

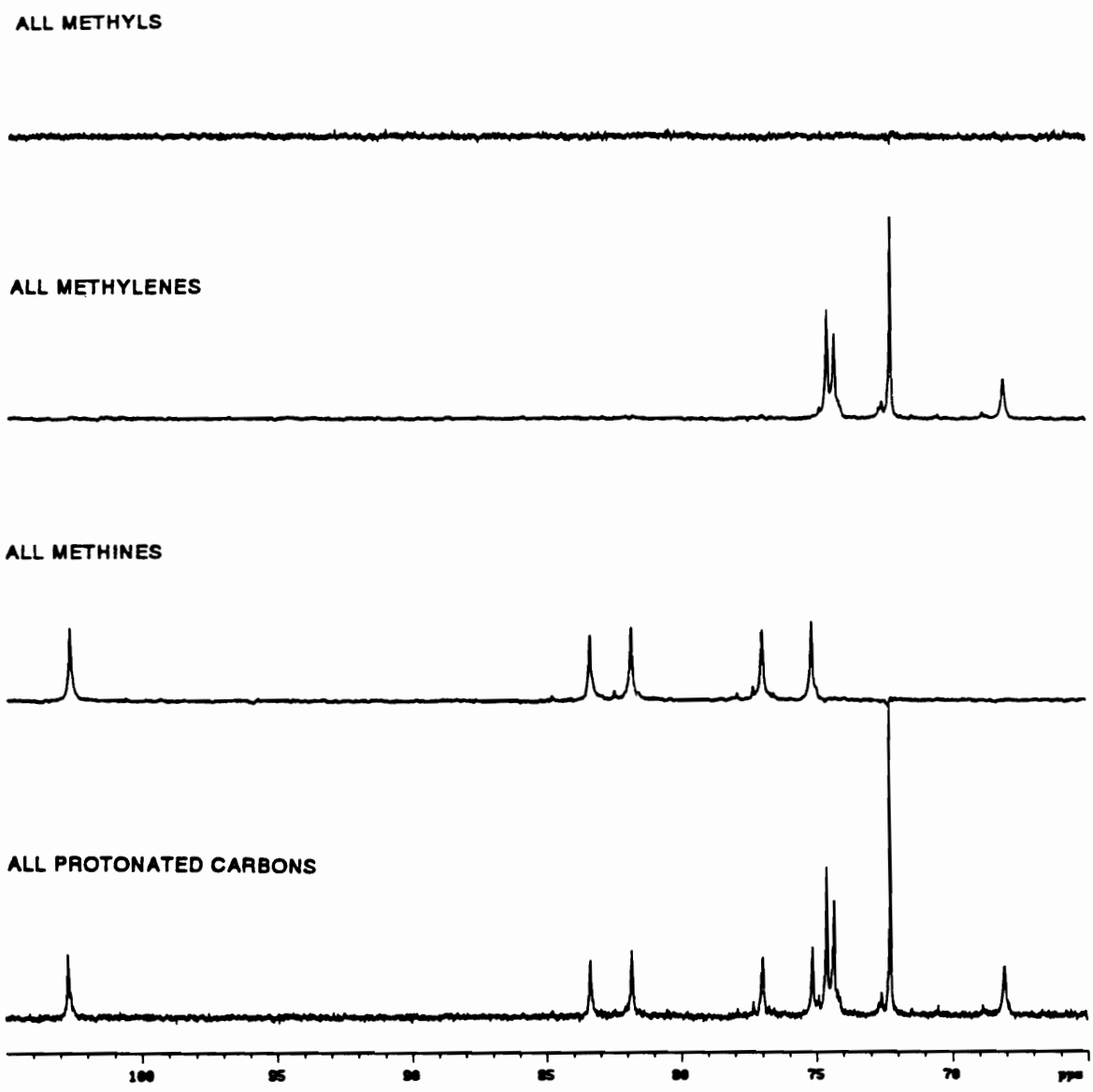

Figure 2. ^{13}C DEPT NMR spectrum of tri-O-p-fluorobenzylcellulose, in $CDCl_3$, at room temperature.

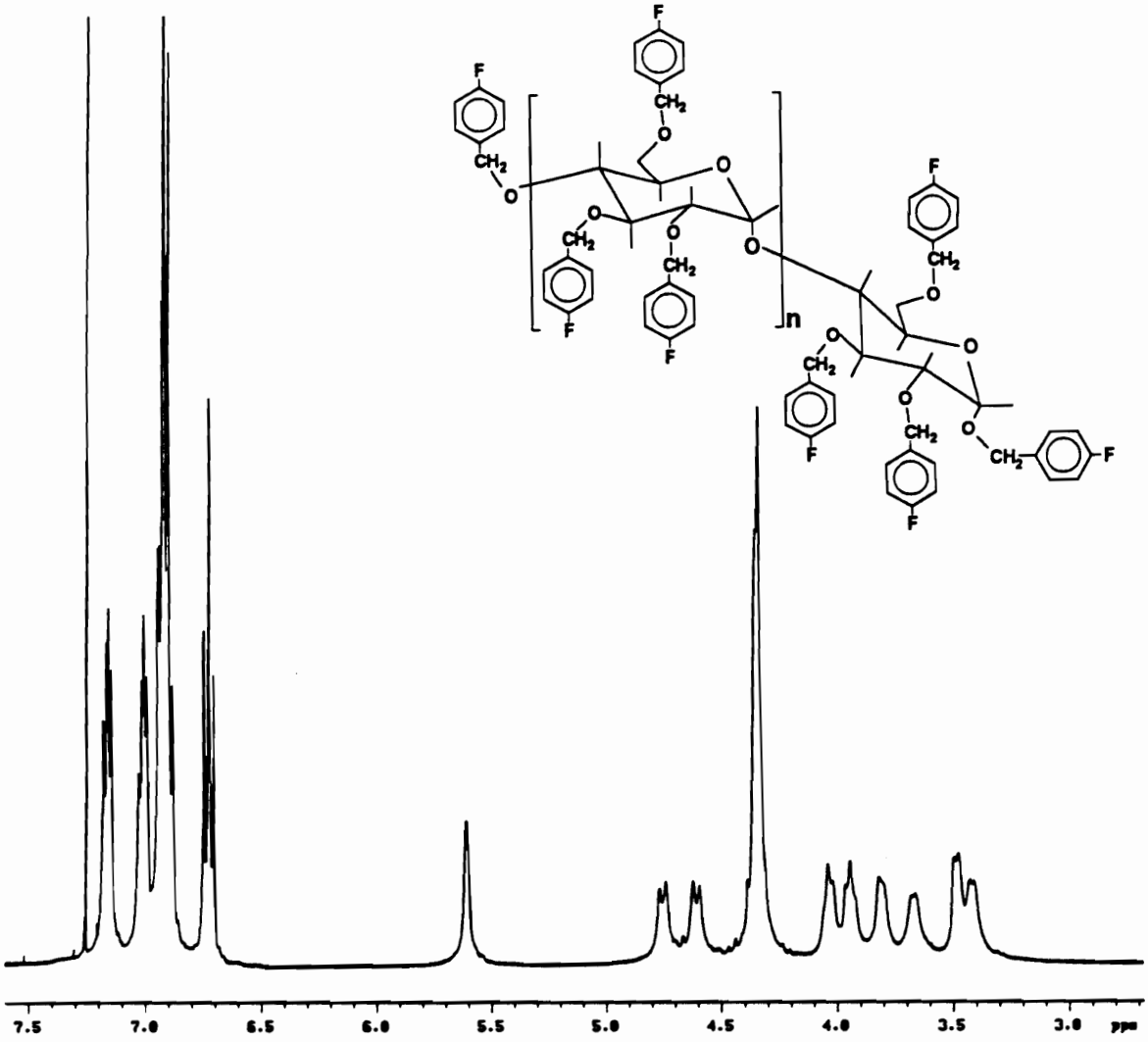

Figure 3. ^1H NMR spectrum of tri-O-p-fluorobenzylamylose, in $CDCl_3$, at room temperature.

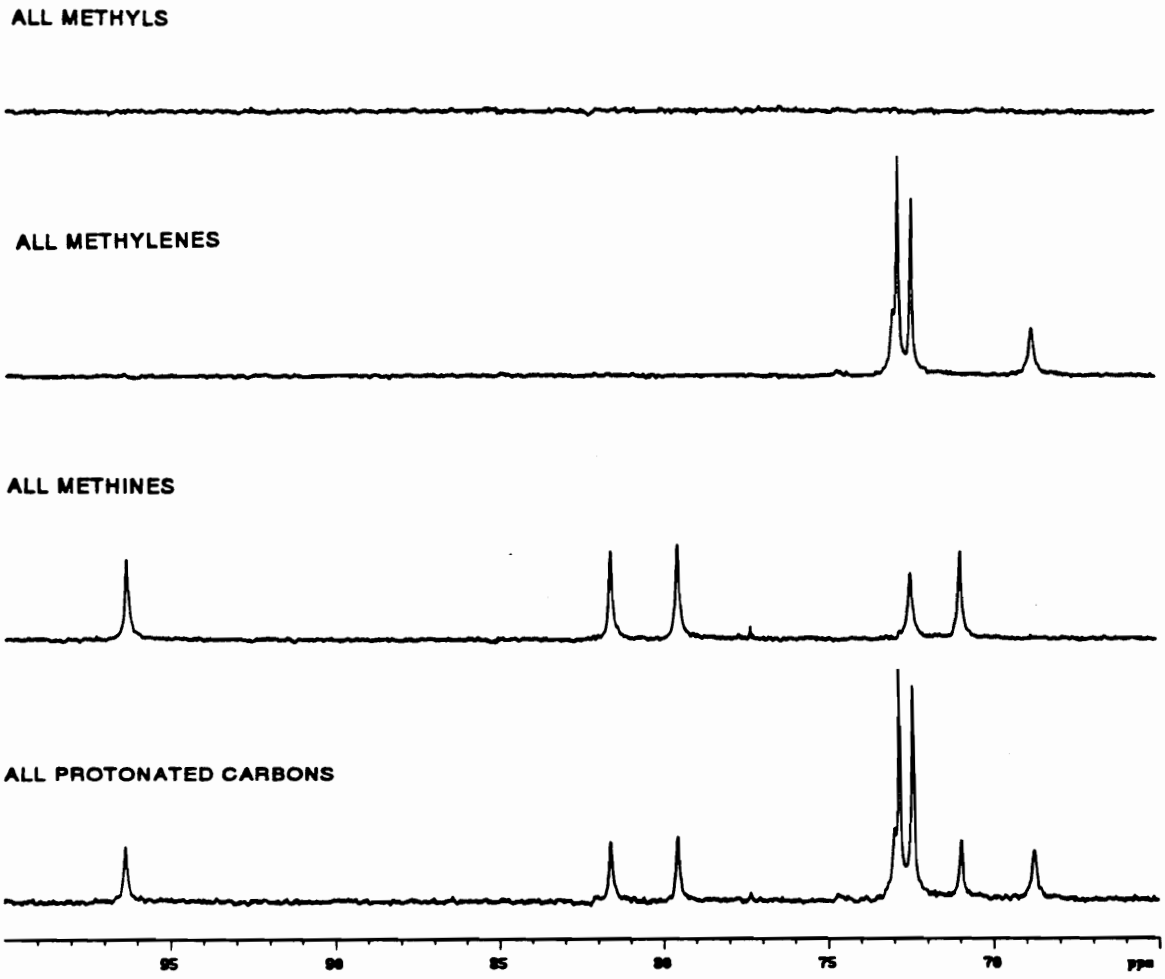

Figure 4. ^{13}C DEPT NMR spectrum of tri-O-p-fluorobenzylamylose, in $CDCl_3$, at room temperature.

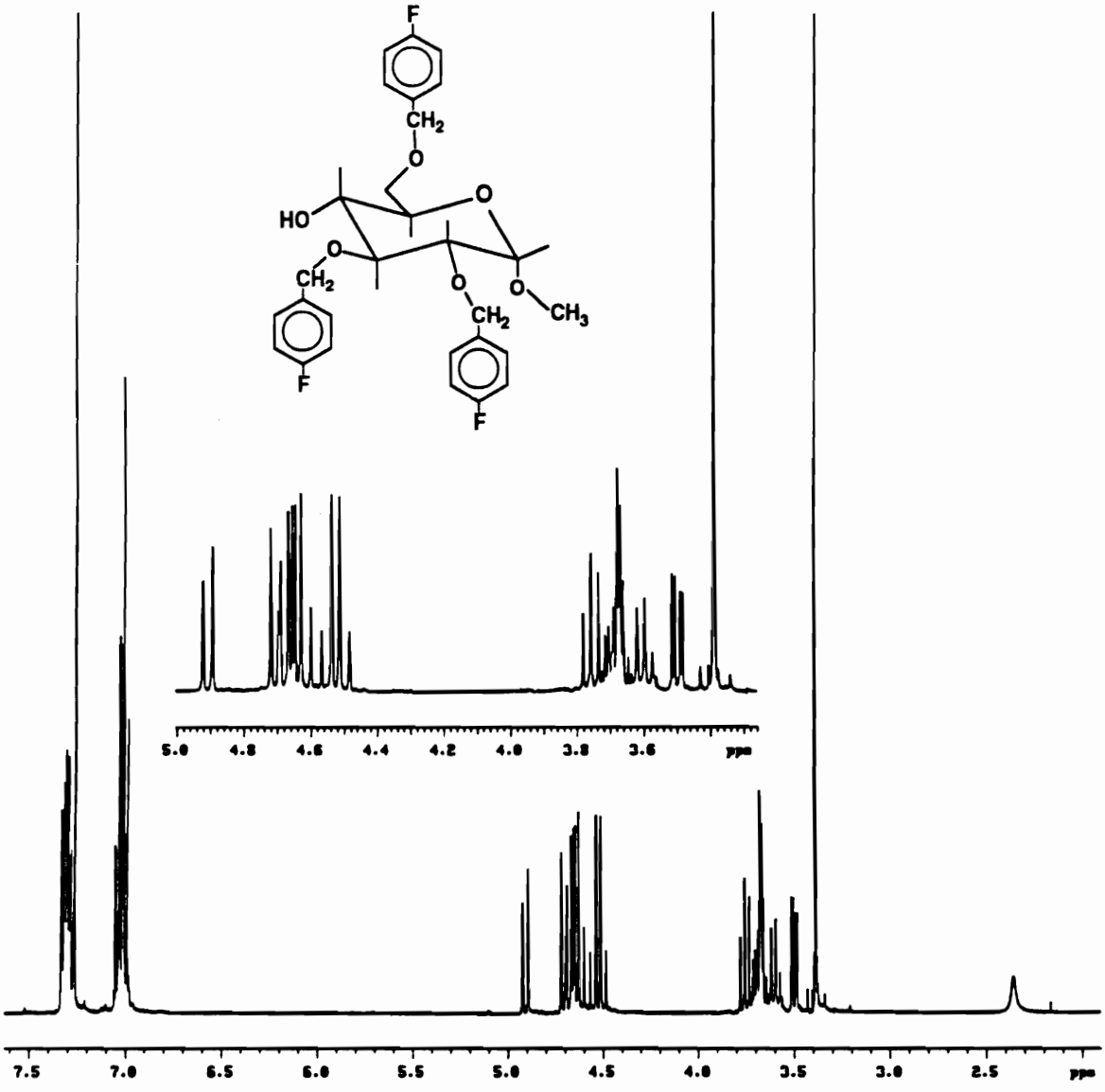

Figure 5. ^1H NMR spectrum of α-2,3,6-tri-O-p-fluorobenzyl methyl glucoside, in $CDCl_3$, at room temperature.

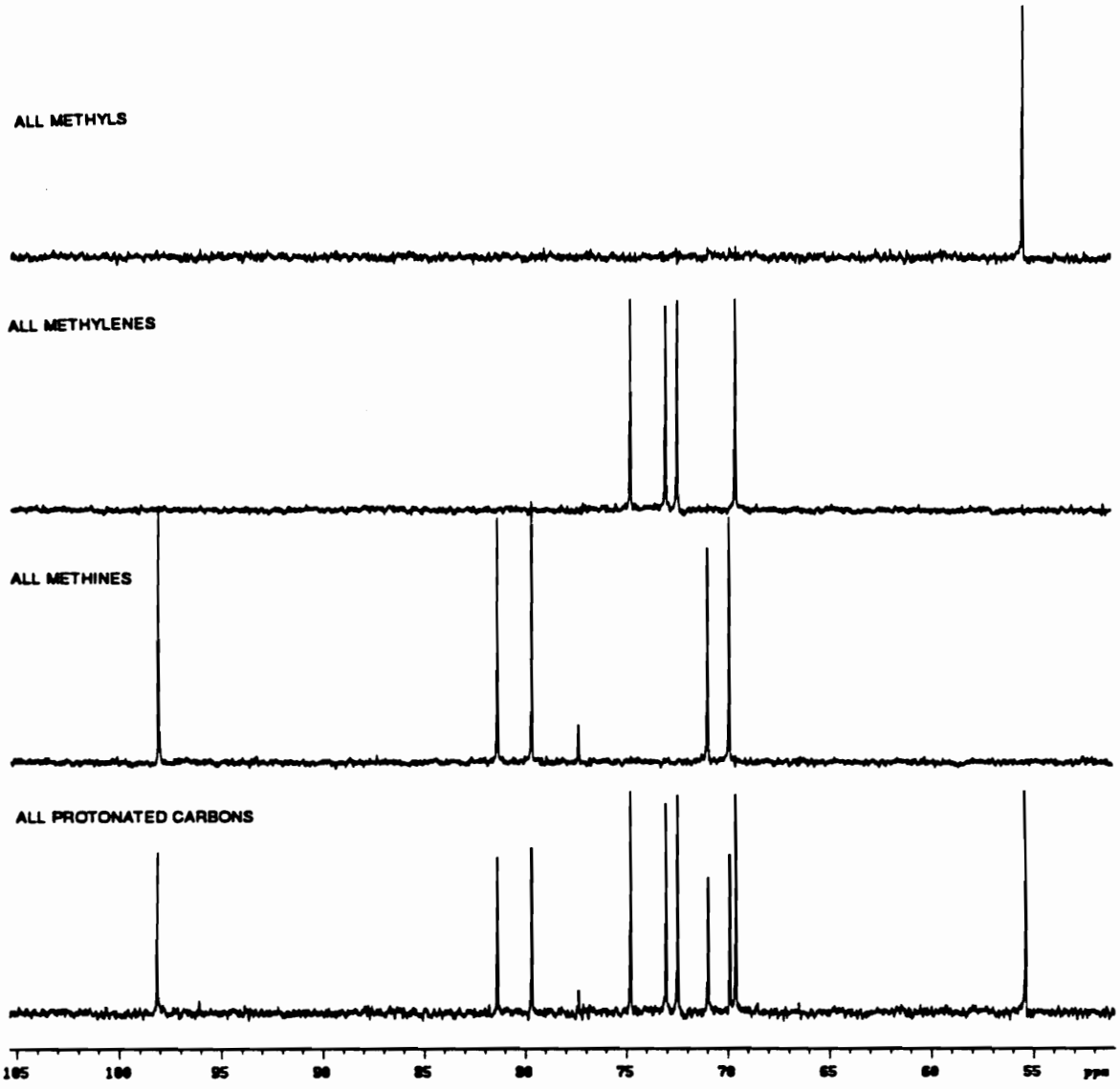

Figure 6. ^{13}C DEPT NMR spectrum of α-2,3,6-tri-O-p-fluorobenzyl methyl glucoside in $CDCl_3$ at room temperature.

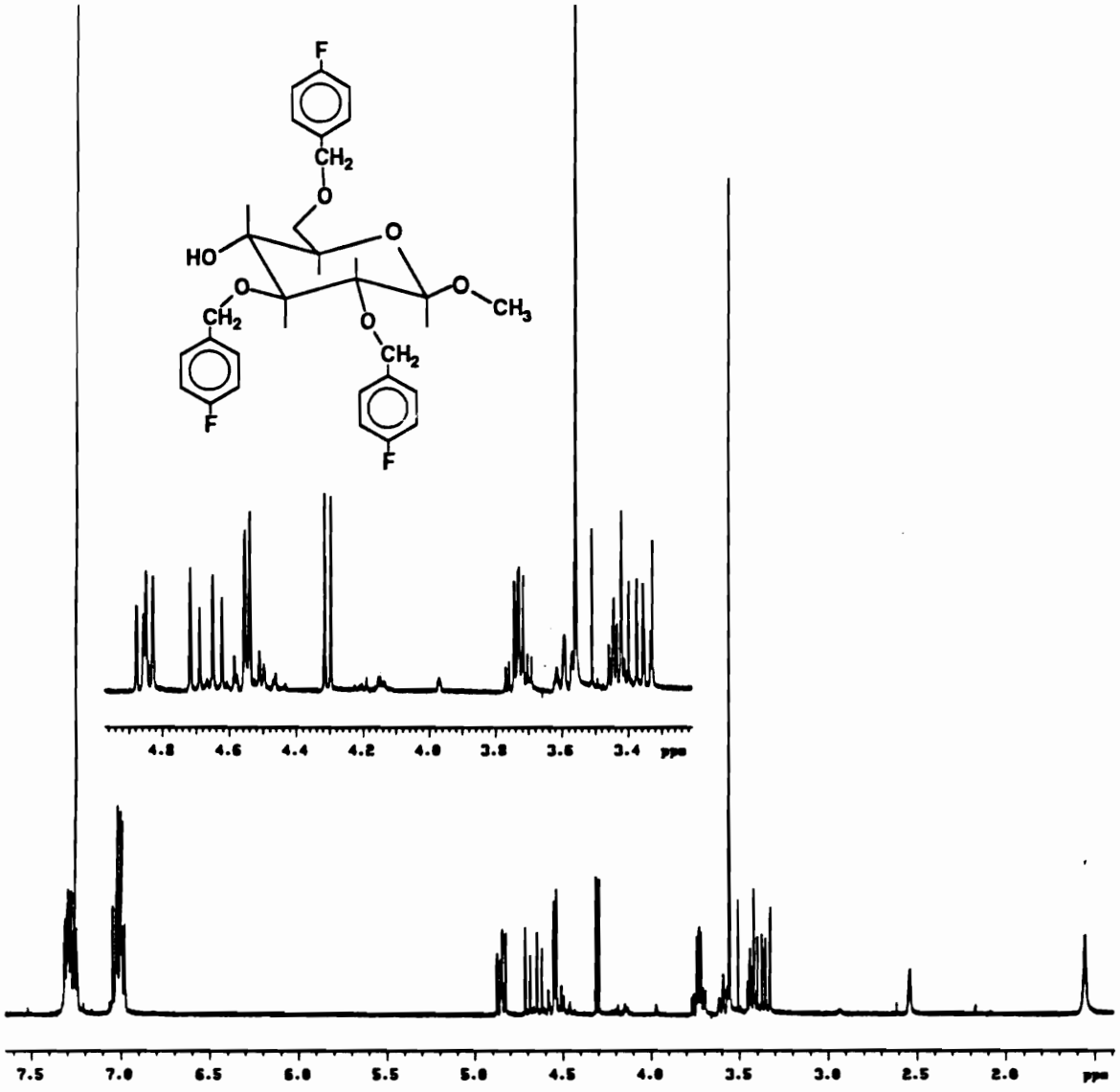

Figure 7. ^{1}H NMR spectrum of β-2,3,6-tri-O-p-fluorobenzyl methyl glucoside in $CDCl_3$ at room temperature.

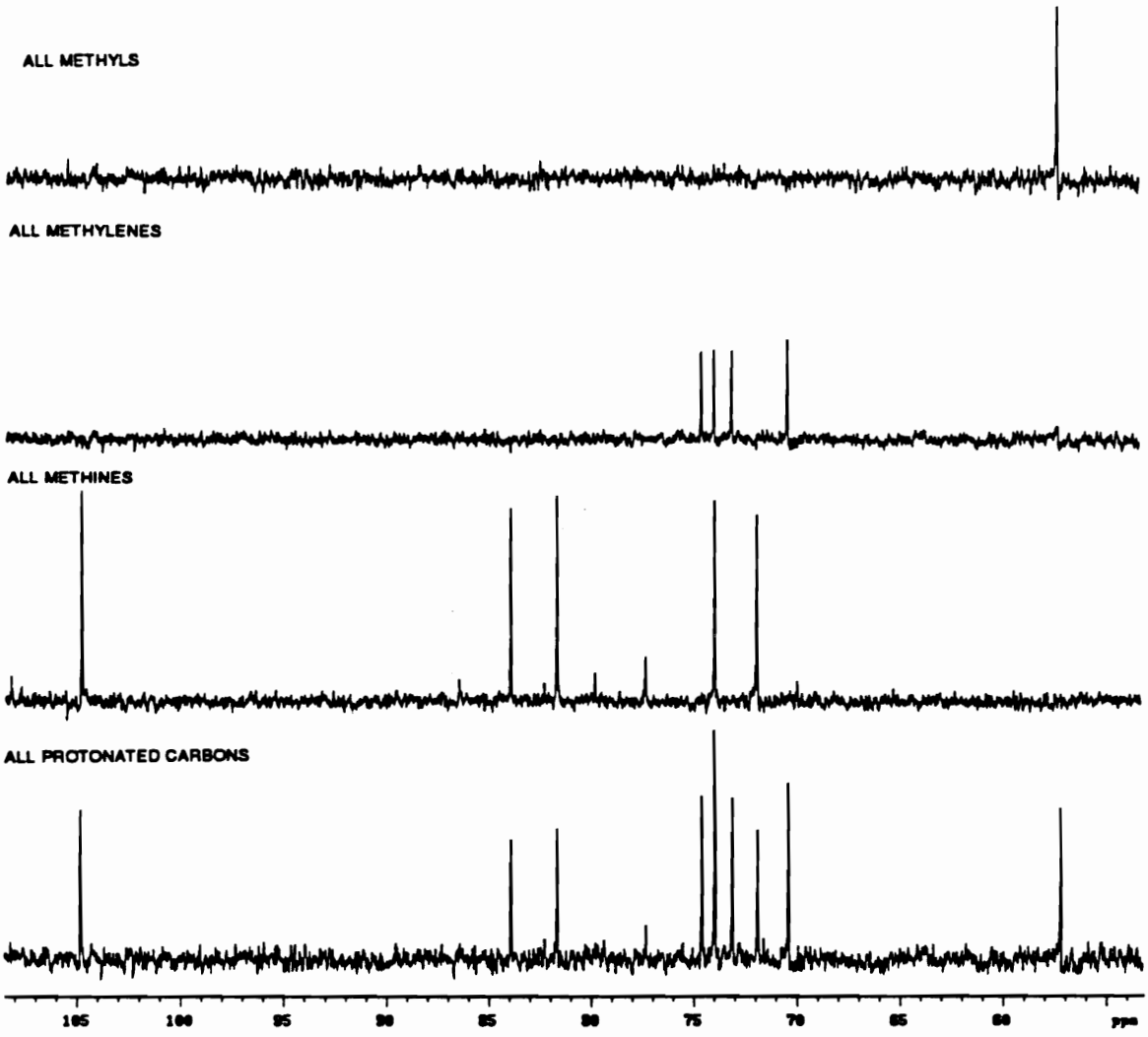

Figure 8. ^{13}C DEPT NMR spectrum of β-2,3,6-tri-O-p-fluorobenzyl methyl glucoside in $CDCl_3$ at room temperature.

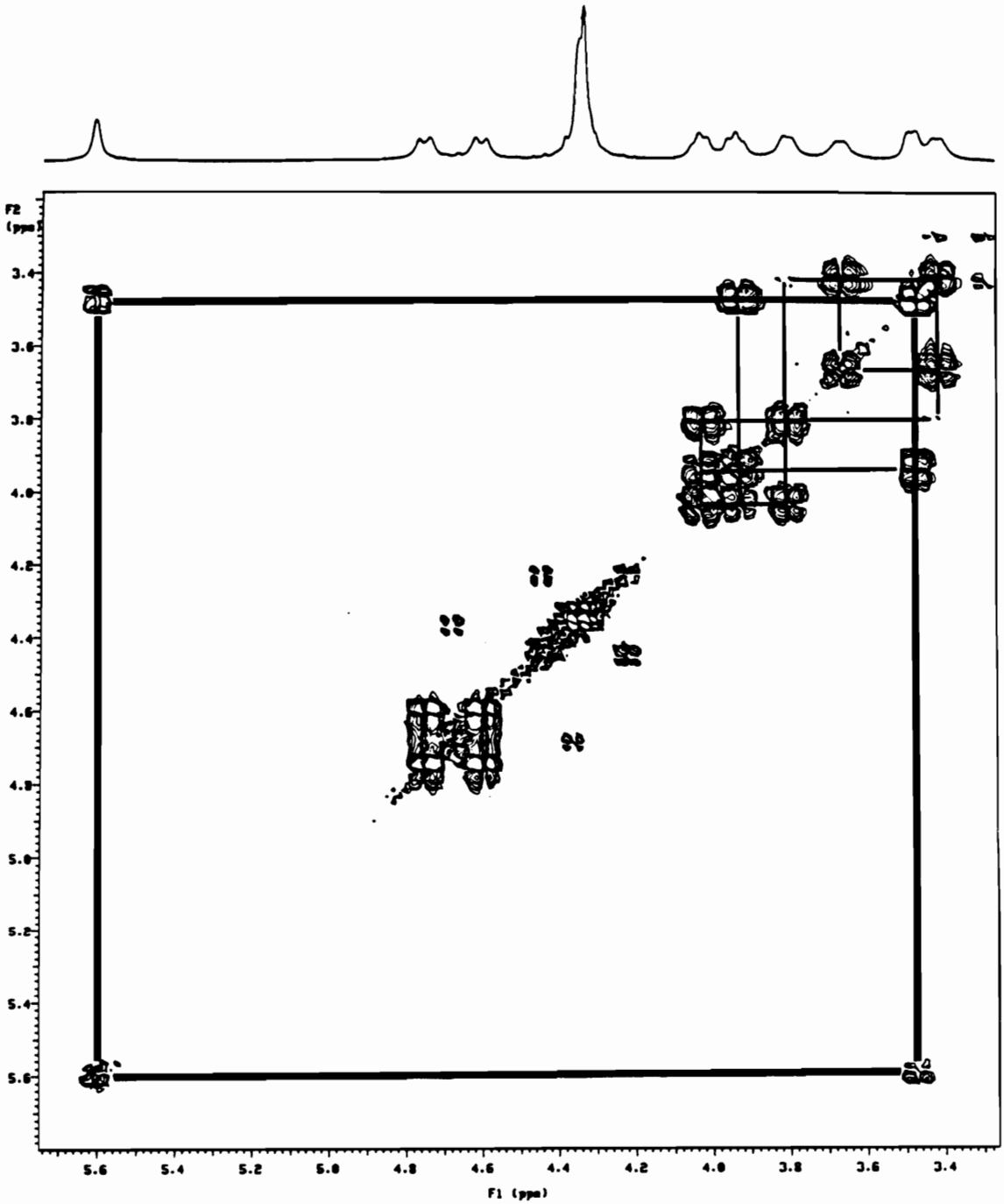

Figure 9. DQCOSY spectrum of tri-O-p-fluorobenzylamylose. This experiment helps to establish the relative proximity of all protons, which aids in the total NMR characterization of the polymer.

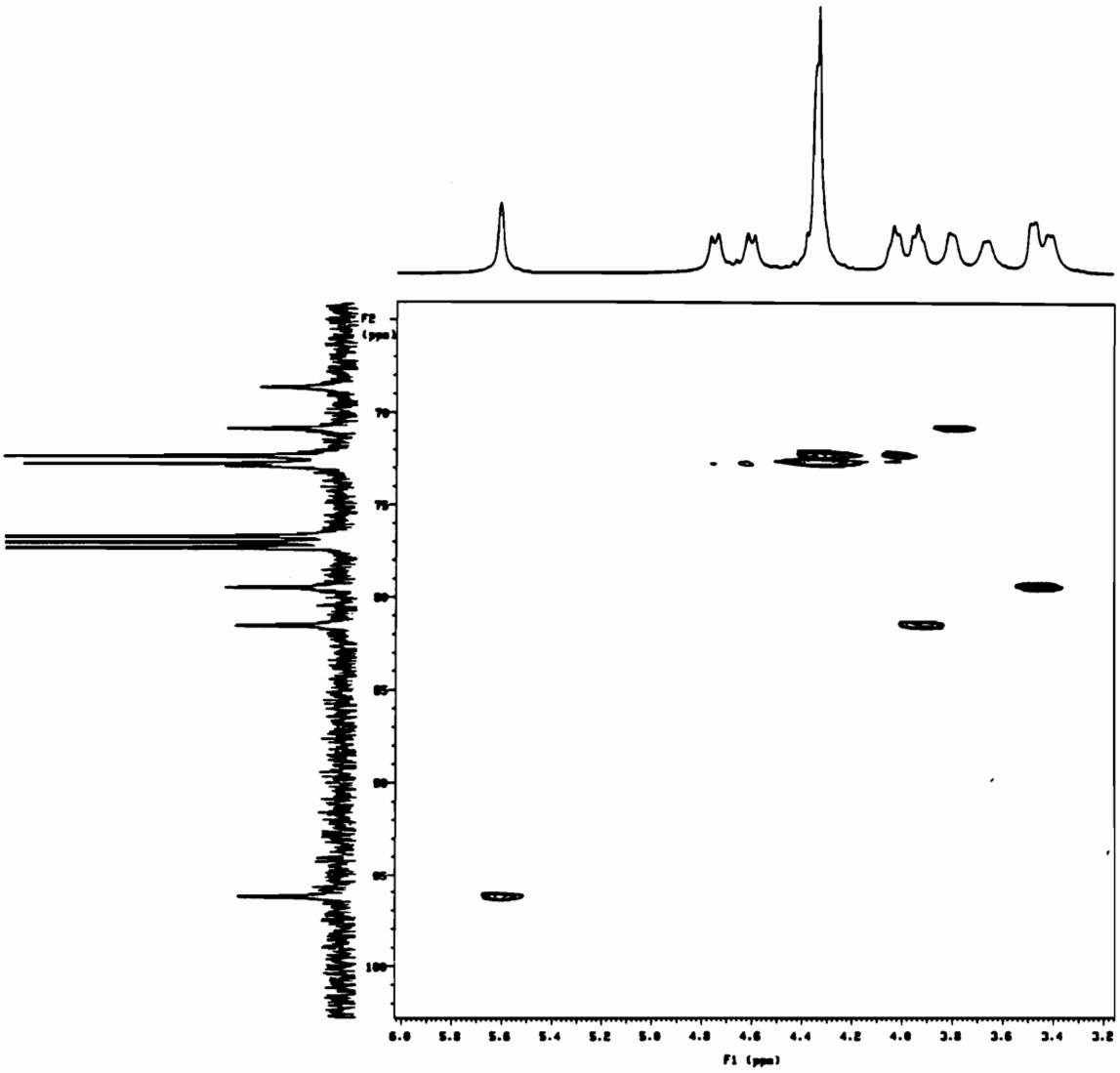

Figure 10. HETCOR spectrum of tri-O-p-fluorobenzylamylose. This experiment helps to establish which protons are connected to which carbon atoms, used in conjunction with the DQCOSY experiment.

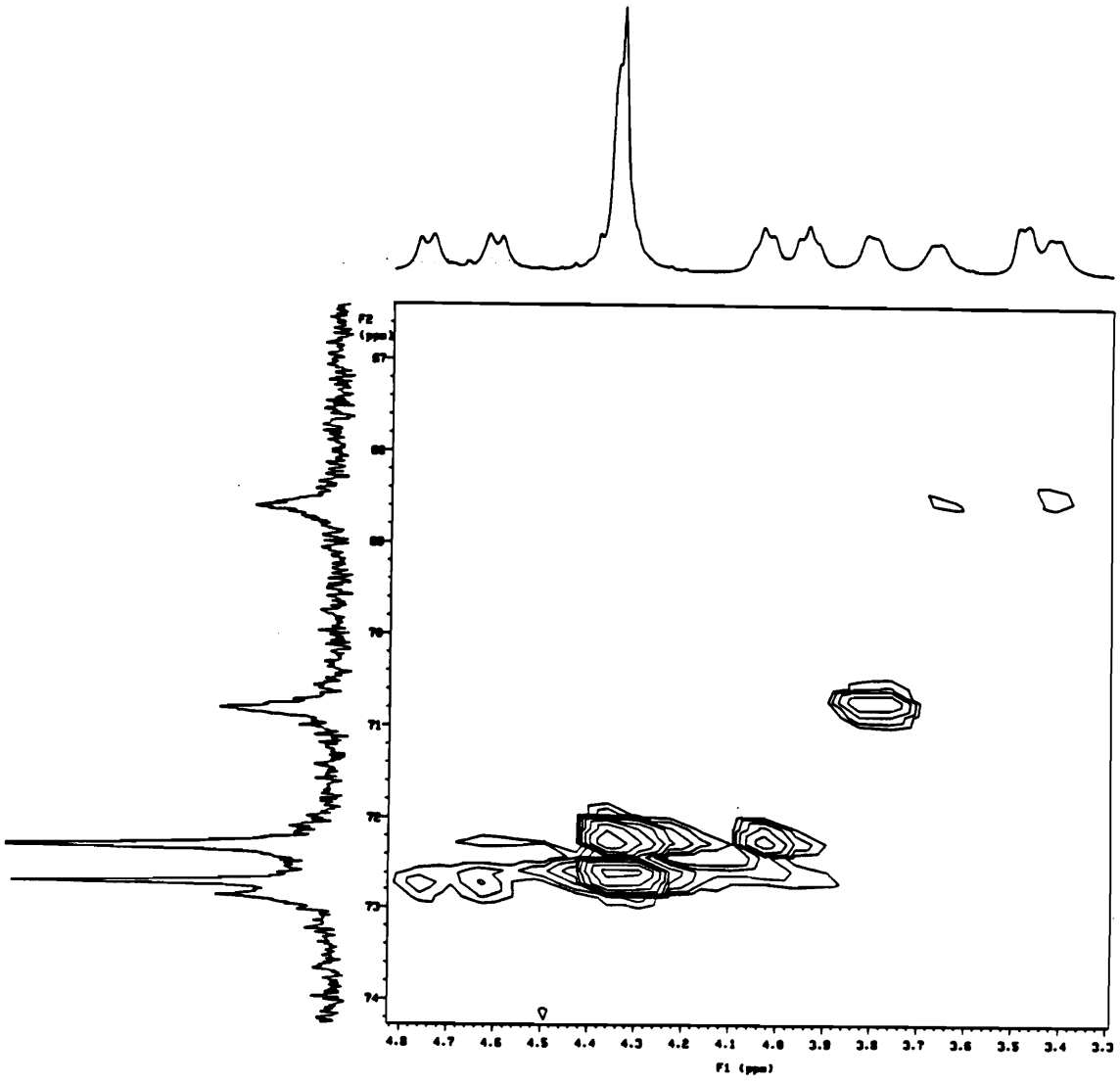

Figure 11. Enhanced portion of HETCOR spectrum of tri-O-p-fluorobenzylamylose, shown in figure 10. This spectra establishes the identity of the C6 carbon, a methylene carbon that should show two correlations.

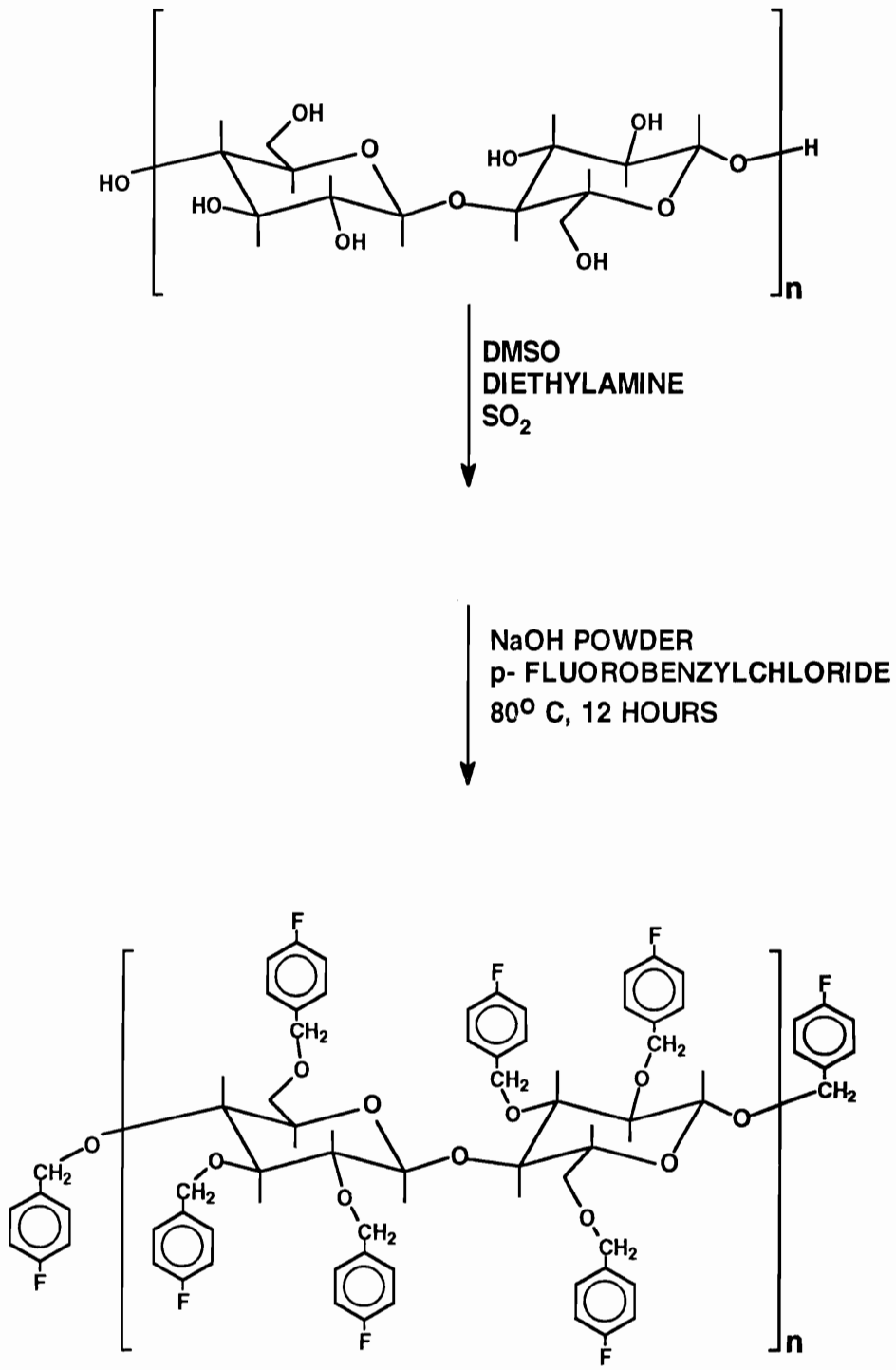

Figure 12. Synthetic scheme showing the dissolution, and subsequent benzylation of cellulose in the DMSO/SO_2/DEA solvent system.

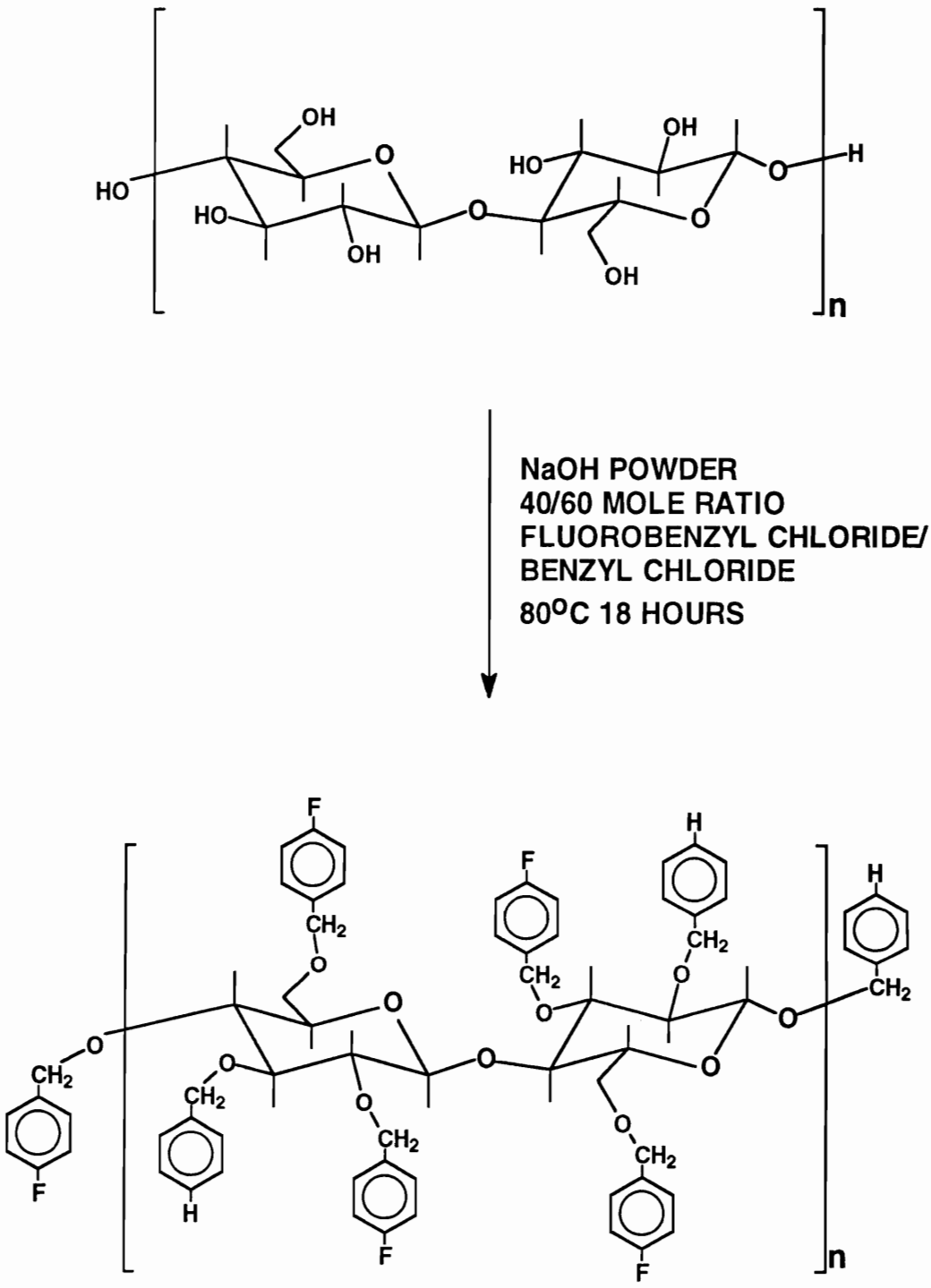

Figure 13. Synthetic scheme showing the synthesis of the mixed fluorobenzyl/benzyl cellulose ether with a DSF of 2.0.

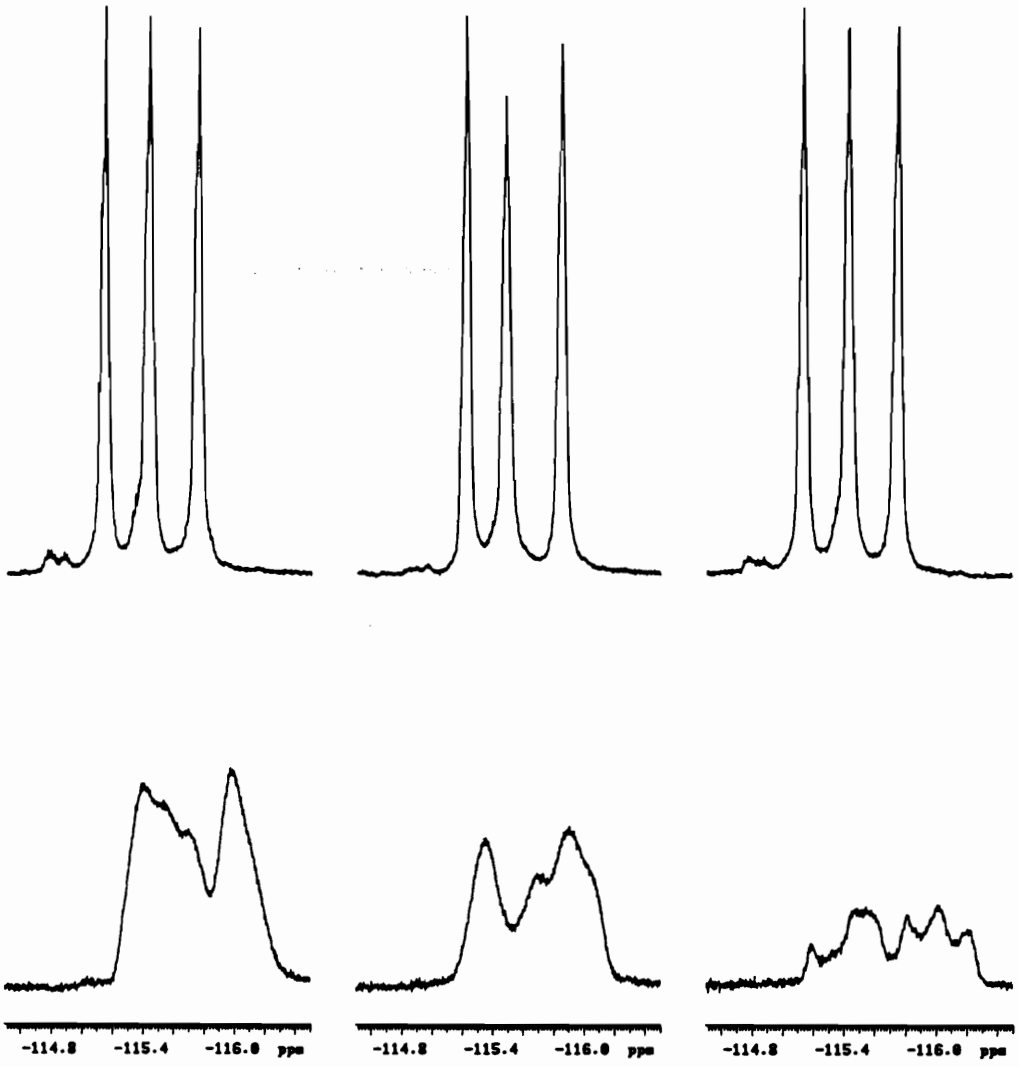

Figure 14. ^{19}F NMR spectra of fluorobenzyl cellulose, DSF 3.0 (TOP LEFT) and the mixed benzyl/fluorobenzyl ethers (FROM TOP MIDDLE TO RIGHT) with DSF 2.9, 2.8, 2.0, 1.3, and 0.65.

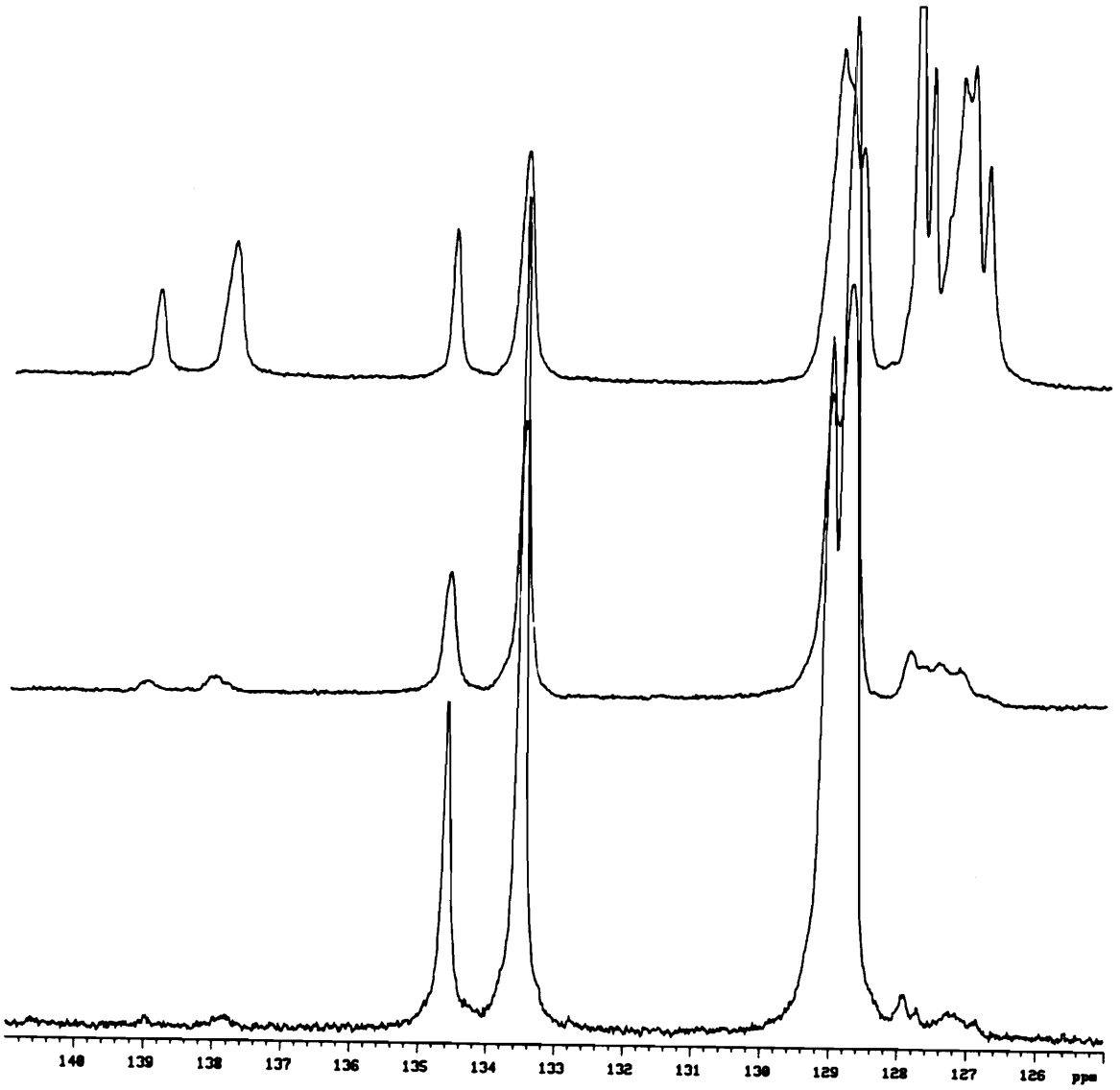

Figure 15. ^{13}C NMR spectra of DSF 2.0 (TOP) DSF 2.8, and DSF 2.9 (BOTTOM). Decreasing signals from top to bottom at 138.5 and 127.5 ppm, prove the samples are mixed benzyl ethers with different degrees of fluorination.

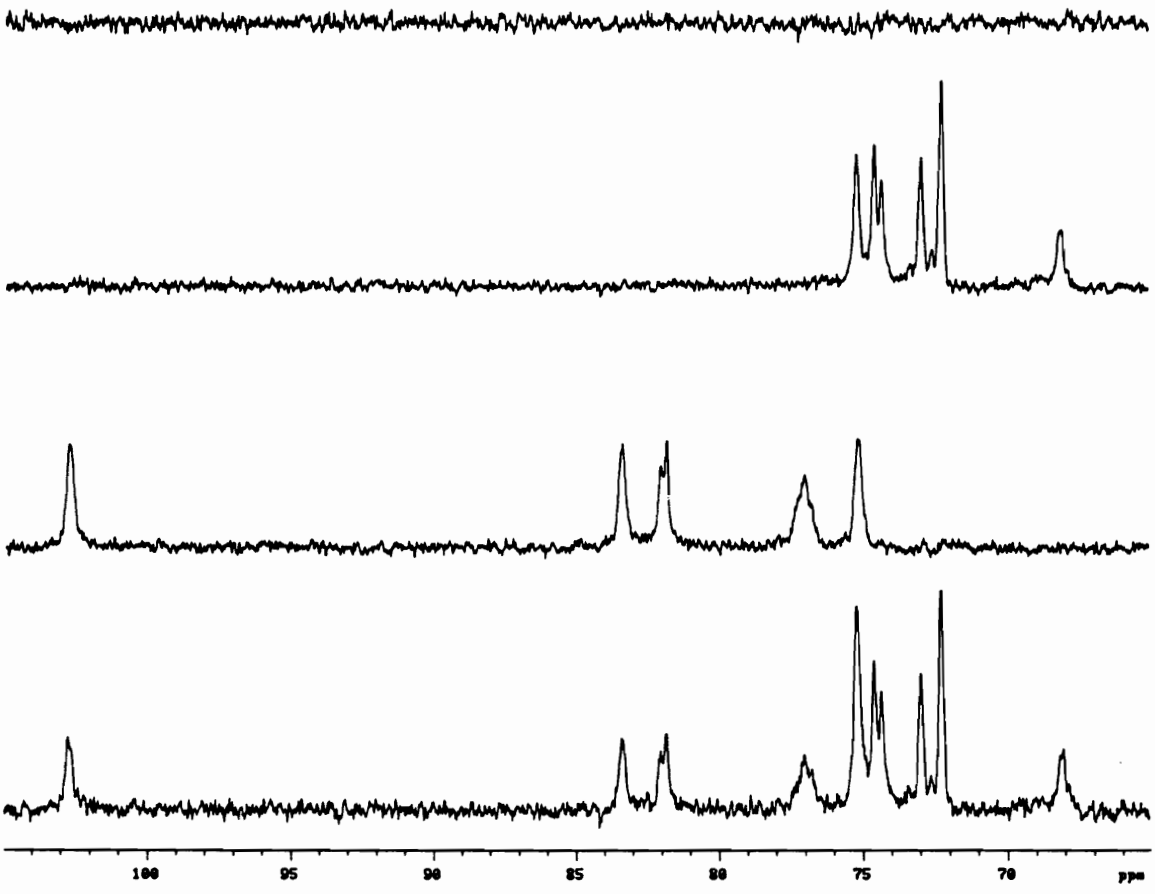

Figure 16. DEPT ^{13}C NMR spectrum of DSF 2.0. Multiple methylene signals between 74 and 76 ppm indicate the copolymeric nature of this polymer.

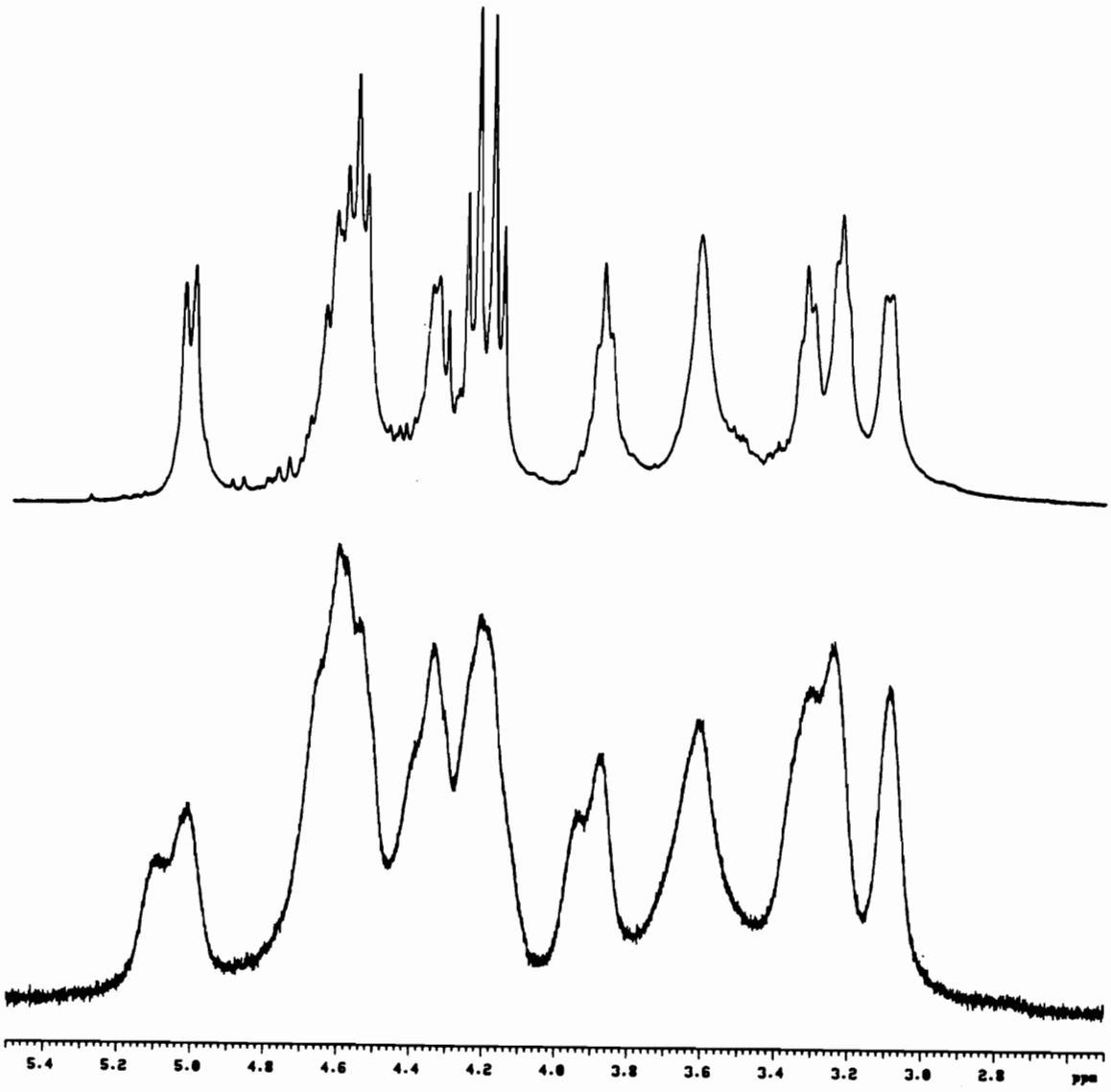

Figure 17 ^{1}H NMR spectra of DSF 3.0, (TOP), compared to that of DSF 2.0. These spectra indicate that the chemical shifts of the mixed ethers remain about the same. The broadening of the signals is another indication of the copolymeric nature of the polymer.

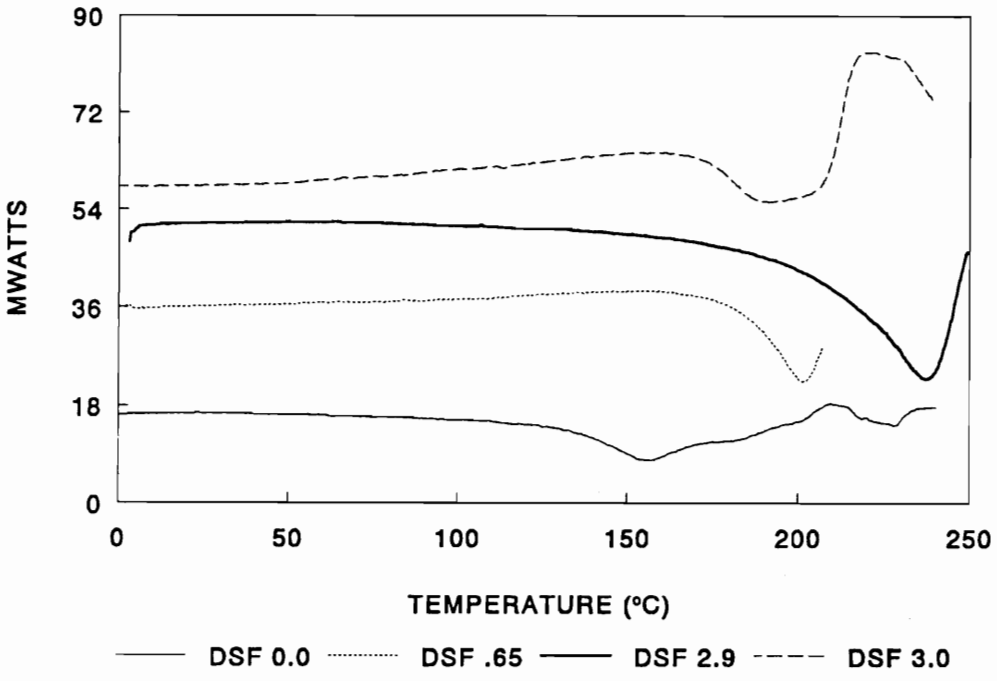

Figure 18. DSC traces of mixed benzyl ethers showing a strong exotherm before melting, followed by degradation. Heating rates were 10° C/min.

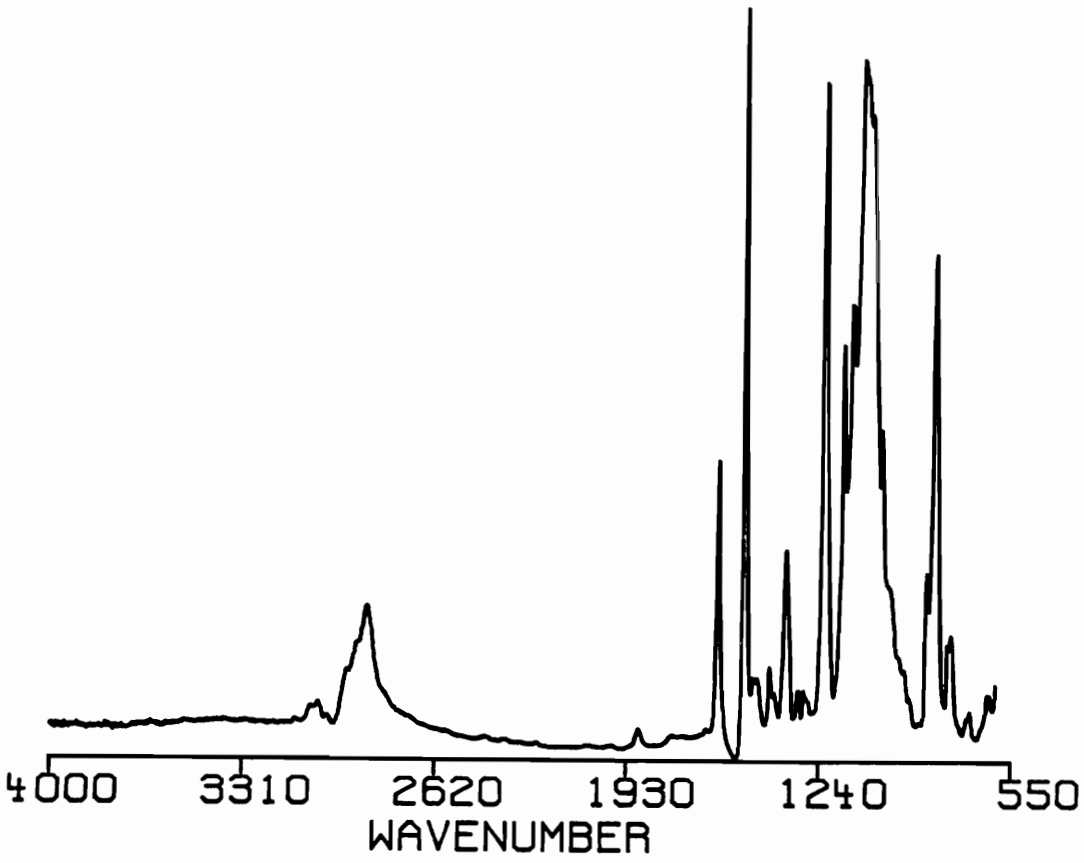

Figure 19. FT infrared spectrum of film of cellulose mixed benzyl ether with a DSF=2.9. The flat region from 4000 to 3300 cm^{-1} indicates that this derivative is completely substituted.

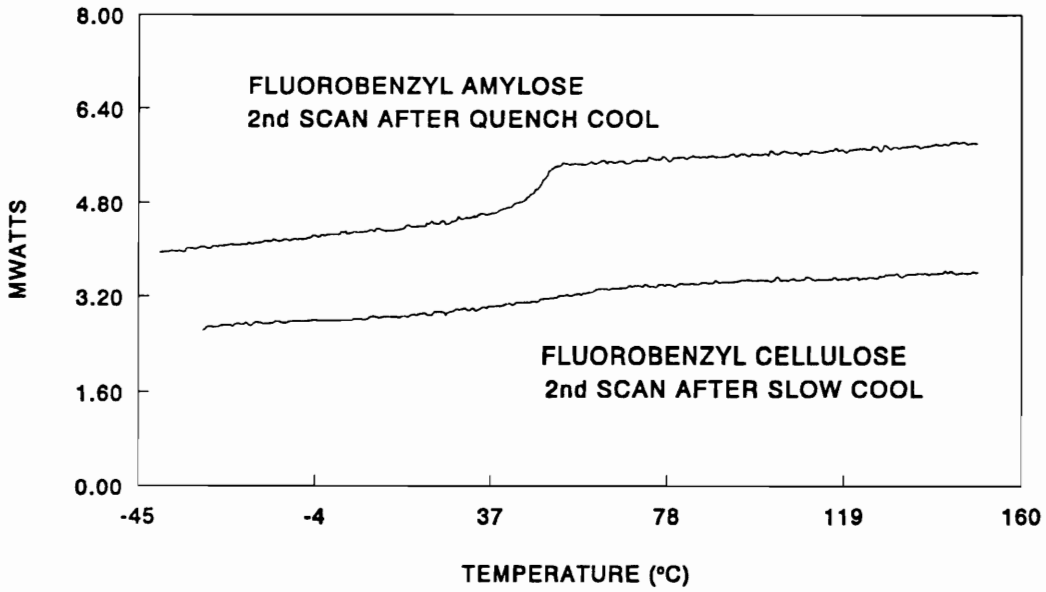

Figure 20. DSC thermograms of tri-O-p-fluorobenzyl cellulose, and tri-O-p-fluorobenzyl amylose, with heating rates of 20 and 10 ° C/min respectively.

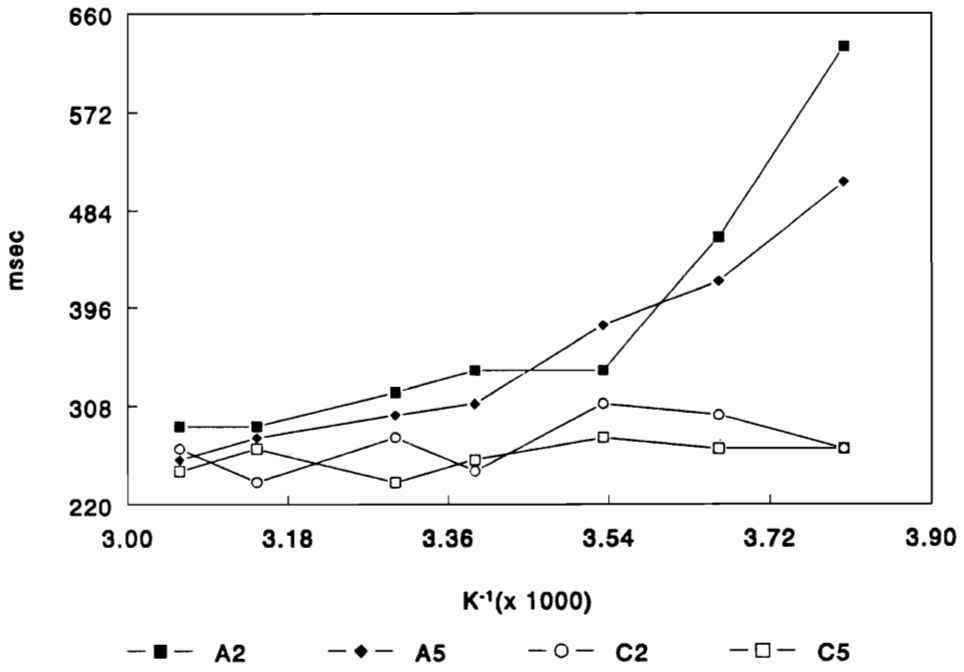

Figure 21. Comparison of the spin-lattice relaxation times of carbons 2 and 5, for tri-O-p-fluorobenzyl cellulose, and tri-O-p-fluorobenzyl amylose. A-amylose, C-cellulose.

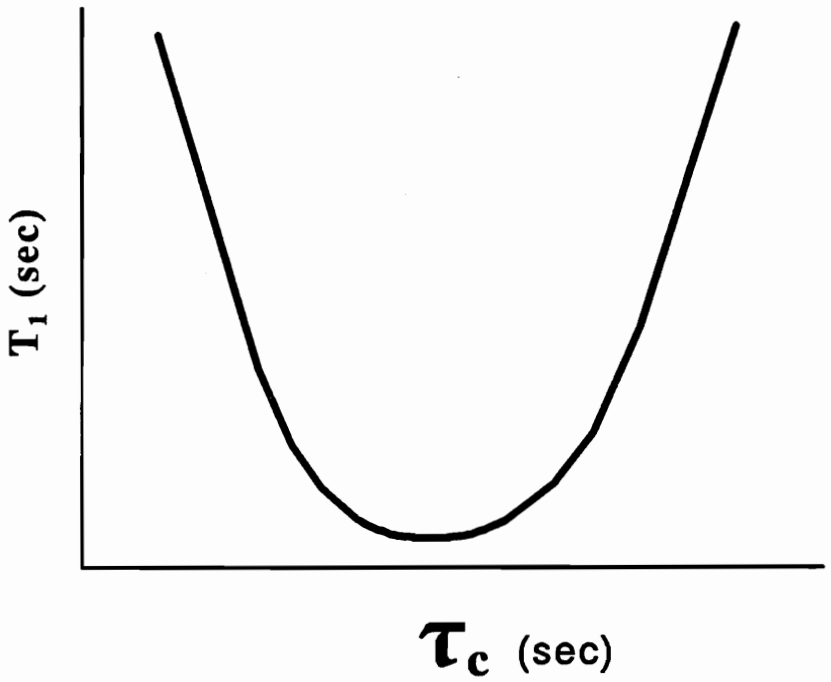

Figure 22. Generalized diagram of the ^{13}C spin-lattice relaxation correlation function.

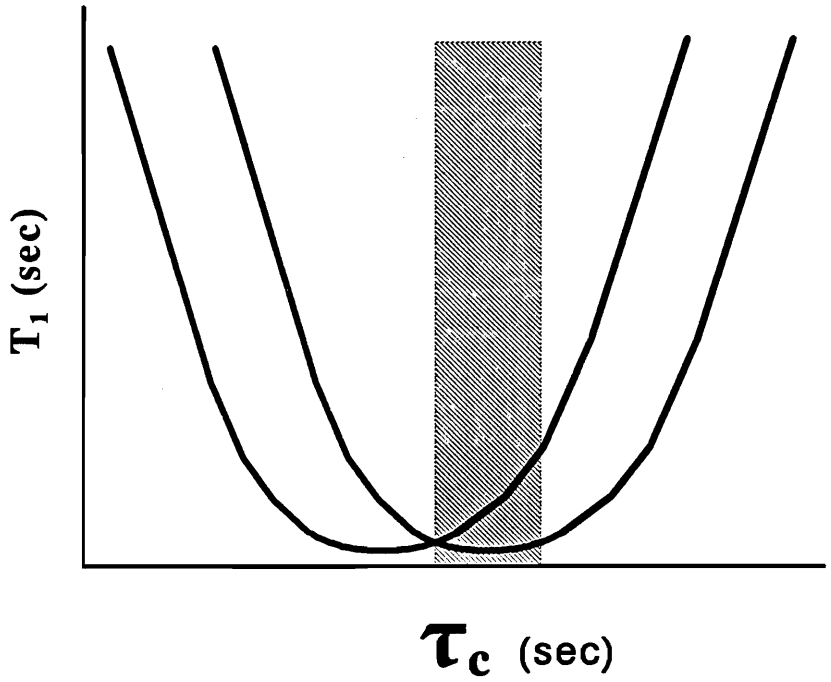

Figure 23. Hypothetical comparison of ^{13}C spin-lattice relaxation correlation functions for tri-O-p-fluorobenzyl cellulose, and tri-O-p-fluorobenzyl amylose.

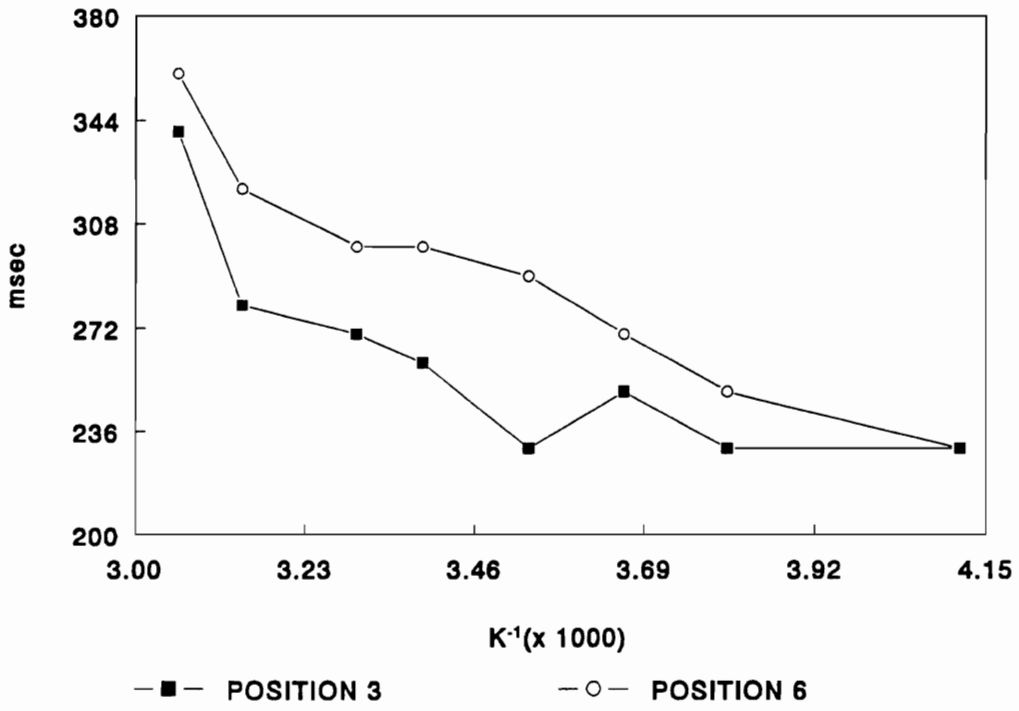

Figure 24. ^{13}C spin-lattice relaxation times of benzyl carbons, of tri-O-p-fluorobenzyl amylose, positions 3 and 6.

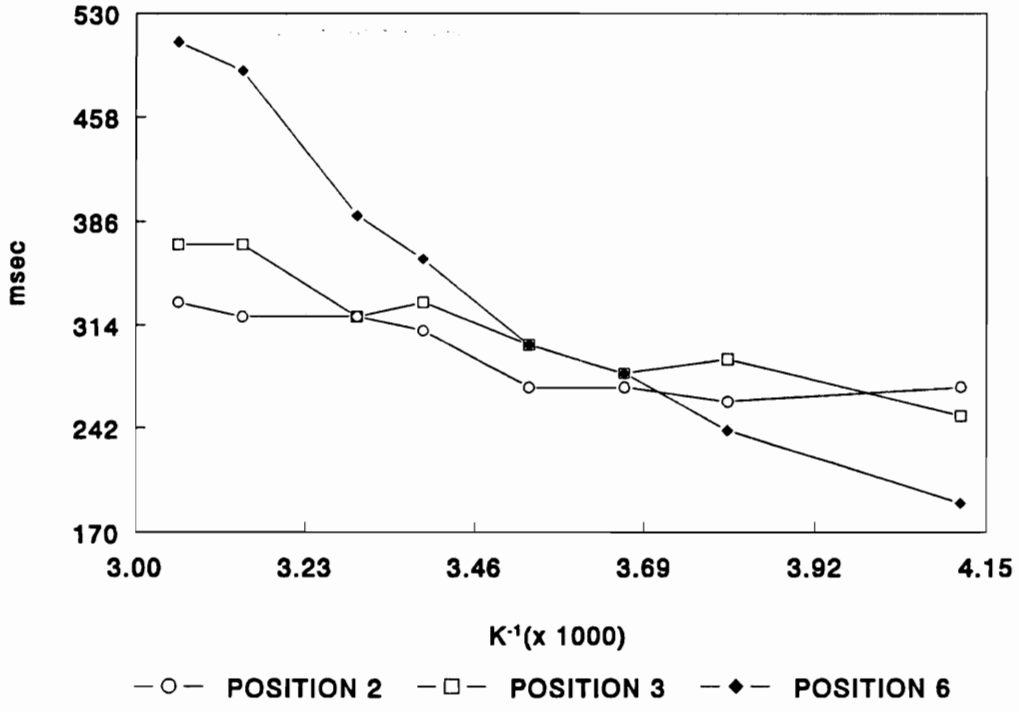

Figure 25. ^{13}C spin-lattice relaxation times of benzyl carbons, of tri-O-p-fluorobenzyl cellulose.

PART TWO

THE EFFECT OF FLUORINE CONTENT ON THE BLENDING PROPERTIES OF BENZYLATED CELLULOSE

INTRODUCTION

The reason for the synthesis of fluorinated cellulose derivatives has been to study the effects of fluorine on polymer-polymer interactions in blended materials. Carbon-fluorine bonds posses a very large dipole, because of the extreme electronegativity of fluorine. When two such dipolar, but different, materials are mixed together, an opportunity exists for nonbonded, or secondary, interactions to occur. These types of interactions serve as attractive forces between dissimilar materials. Attractive forces, such as dipole-dipole interactions, or hydrogen bonding, make the enthalpy of molecular mixing, ΔH, more negative. And this helps to promote molecular mixing, with respect to the Gibbs equation. Where the Gibbs free energy, ΔG, is defined as:

$$\Delta G = \Delta H - T\Delta S \tag{1}$$

In the second term of the Gibbs equation, ΔS, the entropy of molecular mixing, describes the spatial component of the Gibbs free energy. ΔS deals with the randomization that occurs when two groups of dissimilar objects are brought together, and made to occupy the same space. Randomization insures that an individual has an equal chance of encountering a similar or dissimilar object, as a nearest neighbor. Mixing is favored when the number of completely random states, or combinations, is maximized. As such, this component of the Gibbs equation is called the combinatorial entropy.

The balance between energetic and spatial effects determines the likelihood of the mixing of dissimilar molecules. The first requirement for successful molecular mixing is that the balance of enthalpy and entropy result in a negative value of free energy, ΔG. Macromolecules experience a significant spatial barrier to molecular mixing, because randomization is inhibited by entanglements between dissimilar chains. This characteristic of macromolecules has required a specific formalism of the Gibbs equation, that was developed by Flory and Huggins[1,2,3,4]. It appears here in a simplified form.

$$\Delta G = C' \left\{ \frac{\phi_1}{m_1} \ln \phi_1 + \frac{\phi_2}{m_2} \ln \phi_2 + \chi_{12} \phi_1 \phi_2 \right\} \tag{2}$$

C' is a collective term which contains temperature. Φ_1 and Φ_2 refer to the volume fractions of components 1 and 2, of the mixture. The term which contains χ_{12} accounts for the energetics of interaction between components 1 and 2. As with ΔH, negative values of χ_{12} promote molecular mixing. The remaining two terms describe the combinatorial entropy of mixing. They contain values for the size of the molecules, or the degree of polymerization, represented by m_1 or m_2, for the respective polymers. Equation 2 shows that as the degree of polymerization rises, the entropic contribution to ΔG declines. In most cases, the entropy of polymer mixing is negligible because the degrees of polymerization are so great. In fact, most polymers derive their utility from the fact that they are so large.

Consequently, it is often necessary to manipulate the energetic term in order to promote the mixing of polymers. For example, the complete miscibility of polymethylmethacrylate, PMMA, with poly(vinylidene fluoride), PVF_2, is thought to arise from a strongly negative enthalpy of mixing that arises from dipole-dipole

interactions between these polymers[5]. This polymeric mixture satisfies the first requirement of molecular mixing, or miscibility; the Gibbs free energy of mixing is negative. The second requirement for complete miscibility is that there is no inflection in the Gibbs free energy as a function of blend composition. In other words:

$$\left[\frac{\partial^2 \Delta G_M}{\partial \phi^2_2}\right]_{T,P} > 0 \qquad (3)$$

Notice that equation 3 stipulates constant temperature. Because, even when the requirements for miscibility are met, significant variations in temperature can cause polymer demixing. For example, when the enthalpy of mixing has a small positive value, a reduction in temperature can negate the combinatorial entropy and cause demixing. On the other hand, when strong attractions occur between polymers, ΔH has a large negative value, and demixing can occur as a result of increasing the temperature. The increased molecular motions from rising thermal energy are thought to separate interactive groups to the point where the ΔH of mixing becomes more positive[1,2,3,4]. These temperature effects are accompanied by a number of variables that complicate these two examples. Molecular weight has an obvious effect. However, less obvious are the effects of: molecular weight distribution, the change in the interaction parameter as a function of composition, the presence of crystallinity in one or both components, and the forces of extrusion. These variables, alone, and in combination, all have subtle effects that provide a myriad of experimental observations.

Up to this point, we have only considered cases of complete miscibility. From the above discussion, it becomes obvious that many states of intermediate molecular mixing

can occur. These states are sometimes referred to as being partially miscible, partially compatible, or even compatible. The discrepancies associated with these terms require caution on behalf of the reader. Indeed, they also necessitate the author to clearly, and reasonably, define his or her own terms, and strictly adhere to them in subsequent discussions. Within this context, miscibility will be used to describe the unequivocal presence of a single phase, at all compositions, at a given temperature. Partial miscibility refers to blends that exhibit a single phase, at a given temperature, but only at specific blend compositions.

Partially miscible blends may exhibit compatibility at those compositions where the definitions of miscibility are not met. For example, a demixed polymer blend will exhibit various levels of phase separation. The degree of phase separation is judged by the relative size, and pattern, of the domains of pure polymer that result. Sometimes the domains are small enough, that a significant degree of interfacial interaction may occur. If this interfacial interaction positively affects the macroscopic properties, the blend exhibits compatibility. For example, the mixture of an immiscible, but compatible polymer pair, may give rise to a blend with enhanced physical properties. This type of behavior has been referred to as mechanical compatibility[6]. On the other hand, when phase separation is extensive, very little polymer-polymer interaction occurs across the interface. These blends often have poor physical properties, such as brittleness.

Methods for the detection of miscibility generally begin with observation of the glass transition temperature, T_g, as a function of blend composition. This necessarily requires that the T_g's of the respective, pure, polymers are sufficiently distinct to allow resolution in measurement. Miscibility of the polymer mixture is indicated by a single, sharp, glass transition, that varies smoothly between the T_g's of the pure polymers, as a function of composition. If the mixture exhibits two distinct T_g's that are the same as the pure components, no mixing is evident. This is characteristic of an incompatible

blend. Of course, some blends may exhibit intermediate behavior, as a result of interactions across a phase boundary. In any event, the degree of mixing, or demixing, is further investigated by alternative techniques.

One alternative is to observe the blend microscopically. Scanning electron microscopy, SEM, or transmission electron microscopy, TEM, can directly detect phase separation of blended materials. If the blend components do not have a strong contrast in electron density, these techniques may fail. In some cases, this deficiency is overcome by preferential staining of one of the polymers.

If one or both of the blend components is crystalline, calorimetry is useful for observing the effects of blend composition on the melting, and crystallization transitions. If specific interactions occur between an amorphous and semi-crystalline polymer, this interaction can be quantified with accurate measurements of melting point depression[7,8]. However, these studies should be approached with care. Misleading conclusions may result from circumstances that mask equilibrium melting points[9,10].

If specific interactions cause a significant melting point depression, the effect may often be observed using infrared spectroscopy[11,12]. Carbonyl functional polymers lend themselves nicely to this technique, due to the strength and resolution of the carbonyl signal. Specific interactions often cause a signal shift to lower frequencies. For example, carbonyl groups assume greater single bond character due to specific interactions. This can cause a 2-5 wavenumber drop in vibrational frequency.

Even in the absence of specific interactions, simple physical testing is capable of detecting various levels of polymer mixing. In miscible blends, physical properties are often a weight average of the component properties. Sometimes, a synergetic effect is observed, where the blend displays properties in excess of the additive properties of the

components. Otherwise, if phase separation is too great, stresses are not transferred across domain interfaces, and ultimately cracks are initiated, and propagated, during brittle failure.

Many of the above theoretical considerations, and experimental procedures, were used to study blends of benzyl and fluorobenzyl cellulose with polycaprolactone, PCL. PCL is a simple aliphatic polyester which is known to be miscible, or in other cases compatible, with an unusually wide range of polymers[6]. This was one reason for selecting PCL for this study. Additionally, PCL is a low T_g, low modulus polymer therefore, interactions between a high T_g, high modulus cellulose derivative should be easily detected, should they exist.

The goal of this work was to observe the degree of mixing, or demixing, between PCL and benzyl cellulose, and between PCL and p-fluorobenzyl cellulose. Subsequently, the aim was to observe the effect of fluorine content on PCL/benzyl cellulose blends by evaluating mixtures of PCL with mixed benzyl/p-fluorobenzyl cellulose mixed ethers. A series of mixed ethers were synthesized that contained fluorine contents across the spectrum, between the extremes of benzyl cellulose and p-fluorobenzyl cellulose. With this systematic change in fluorine content, the purpose was to determine where an optimum may exist in blend properties.

EXPERIMENTAL

MATERIALS:

The PCL used in this work was Tone 700, supplied by Union Carbide. This sample had a number average molecular weight of 30,000, and a polydispersity of 1.7. The cellulose derivatives used in this study have been described above, section V.

METHODS:

Blend Preparation:

Blends were prepared by dissolving both polymers in tetrahydrofuran, THF. A total of 4 g was dissolved in 25 ml of THF, with magnetic stirring. Stirring was continued until all polymer had dissolved, and the solution appeared homogeneous. At this time, the solution was filtered through Whatman, type-1, filter paper, and 5 additional ml of THF was poured through the filter. So the final solution was approximately 4 g of solids dissolved in 30 ml of THF. This homogeneous solution was poured into a teflon mold, which was placed in a desiccator with the lid, very slightly, cracked open. These conditions were purposely selected to provide slow and even evaporation of solvent. All blends were soft to the touch after four days in the desiccator. The samples were taken from the mold and then vacuum dried at 55°C for 48 hours. After drying, the white films, with average thickness and diameter of 2mm and 10 cm, were packaged in air tight plastic storage bags. All films were stored in a -70°C freezer until analyzed. During transport from the freezer to analysis the samples were kept over dry ice.

Tensile Testing:

Samples were warmed to room temperature before exposure to atmosphere. Small dogbones were punched from the films and analyzed at room temperature in tension using a Polymer Laboratories Miniature Materials-Minimat tester. All samples were deformed at a rate of 0.25 mm per minute. Each data point was an average of 6-9 separate tests.

Differential Scanning Calorimetry:

Thermal transitions of blends were observed using a differential scanning calorimeter, DSC. A Perkin Elmer DSC-4 equipped with the Thermal Analysis Data System, TADS was used with the Perkin Elmer Intracooler. This cooling system allows

scanning from as low as -55°C. The DSC was calibrated in the usual fashion with high purity indium. Thin films of 6mg or less were sealed in the usual sample holder. Melting transitions were measured at the pont where the last trace of crystallinity disappeared, at the end of the transition.

Dynamic Mechanical Thermal Analysis:

Dynamic mechanical thermal analysis, DMTA, was performed using a Polymer Laboratories DMTA. Samples in the shape of small rectangular bars were cut from the films. Analysis was in single cantilever bending, at a frequency of 3 Hz, and displacement setting of 4x. Samples were scanned from -100°C to about 55°C.

Transmission Electron Microscopy:

Transmission electron microscopy, TEM, was performed on microtomed samples using a JEOL TE microscope, model number JEM-100CX-II, with an accelerating voltage of 80.

Infrared Analysis:

Infrared spectra were collected on a Nicolet 5SXC Fourier Transform InfraRed spectrometer, FTIR. Samples were prepared as 1%, wt/wt, solutions of blends in THF. Thin films were deposited directly upon KBr pellets, and dried with a stream of dry nitrogen. Melt studies were carried out when the thin films appeared dry. A Beckman, open thermal cell, with temperature controller was used to observe the samples at 80°C. Samples were allowed to equilibrate for 15 minutes, at 80°C, before scanning. Samples made for room temperature analysis were prepared as above, and then placed under vacuum, in a desiccator, with anhydrous sodium sulphate. These samples were stored in this fashion at room temperature, for 5 months, before scanning. Samples were scanned at a resolution of two cm^{-1}, with at least 32 repetitions.

RESULTS AND DISCUSSION

A. ELECTRON MICROSCOPY

Transmission electron microscopy, TEM, of a blend of 90% PCL, 10% benzyl cellulose shows a dark colored matrix, with interspersed, lightly colored spherical domains(Figure 1). TEM relies upon differential electron density for contrast; therefore the higher electron density of benzyl cellulose, relative to PCL, must give rise to the dark zones in this micrograph. In fact, staining with ruthenium tetroxide does not alter the appearance of this sample. Therefore we may be sure that light and dark zones are from PCL, and benzyl cellulose respectively. Benzyl cellulose makes up only 10% of this blend, so it is unlikely that the continuous phase is entirely cellulosic. Judging from the differential darkness of the continuous phase, it is reasonable to conclude that this is a mixture of benzyl cellulose, and the amorphous component of PCL. Therefore, the spherical globules are probably crystalline PCL domains. Within the continuous phase, there appears to be a differential in darkness that has diffuse boundaries. This could be an indication of phase separation on approximately the 100 to 500 nanometer level. There is certainly no macrophase separation in the continuous phase, which indicates some degree of molecular mixing.

TEM of the blend of 10% fluorobenzyl cellulose with 90% PCL similarly shows a dark continuous phase, with globular PCL crystalline domains(Figure 2). Keep in mind that this is tri-O-p-fluorobenzyl cellulose with a DSF of 3.0. As with the benzyl cellulose/PCL blend, the fluorobenzyl cellulose/PCL blend does not show a clear indication of phase separation in the continuous phase. However, at higher magnification, the continuous phase of a stained sample has a very grainy, or speckled appearance (Figure 3). This could be an indication of phase separation on the level of approximately tens of nanometers.

PCL appears to be phase separated from both celulose benzyl ethers. Therefore

we may tentatively conclude that PCL is not miscible with either of these cellulose derivatives. However, neither blend is macrophase separated. It is difficult to tell from these micrographs, but fluorobenzyl cellulose may be more finely dispersed within the amorphous PCL phase. The fine dispersion of both cellulose benzyl ethers suggests that there may be some degree of compatibility in both blends.

B. TENSILE TESTING

Mechanical tests showed that fluorobenzyl cellulose enhances the tensile properties of PCL(Figures 4 and 5). On average, the addition of 10% benzyl cellulose has little or no effect upon the ultimate strength and ultimate elongation of PCL. On the other hand, the addition of 10% fluorobenzyl cellulose causes a 42% increase in ultimate elongation, and a 64% increase in the ultimate strength of PCL. With greater than 95% confidence, tensile tests prove that both cellulose derivatives enhance the modulus of PCL. But the fluorinated derivative gives a 55% increase in modulus, compared to a 17% increase for the non-fluorinated derivative. As with TEM, tensile tests indicate that both cellulose benzyl ethers may have some degree of compatibiltiy with PCL. However, PCL blends with fluorobenzyl cellulose are clearly superior. This is the first clear indication of the beneficial effect of fluorine in PCL benzyl cellulose blends.

With the benefits of fluorine established, tensile tests were performed on blends of PCL with fluorobenzyl/benzyl cellulose mixed ethers. In PCL blends containing 10% mixed benzyl ether, tensile data is reported against the weight percentage of fluorine in each cellulose derivative(Figures 6, 7, and 8). The modulus of the PCL/benzyl cellulose blend is enhanced by the presence of only 3% fluorine, (DSF=0.65), where the difference is significant at better than 95% confidence. The most striking modulus increase, 112% over that of pure PCL, occurs at a fluorine percentage of 5%, or DSF of 1.3. However, the most curious effects occur at high degrees of fluorination. PCL blends with samples of DSF 2.8, and 3.0 exhibit statistically significant, (90%

confidence) modulus differences over a range of less than 1% fluorine.

The ultimate strain of these same blends is not significantly altered by low fluorine contents(Figure 7). However, as before, PCL blends with fluorine contents slightly below the maximum exhibit the best performance. Interestingly, the ultimate strength of these blends shows the same behavior(Figure 8). These tests suggests that the mechanical compatibilty of PCL/benzyl cellulose blends generally increases with incremental increases in fluorine content, until very high degrees of fluorination are achieved, where it appears that optimum tensile properties are achieved at fluorine contents slightly below the maximum.

C. DYNAMIC MECHANICAL THERMAL ANALYSIS

The above tensile tests indicated that some degree of molecular mixing, or interaction occurs between PCL and fluorobenzylated cellulose ethers. However, dynamic mechanical thermal analysis, DMTA, demonstrated that PCL/DSF 3.0 blends experienced only minor changes in the glass transition temperature, T_g, of PCL, as a function of blend composition(Figure 9). DMTA analysis of these blends was complicated by clamp slippage as the films passed through the damping maxima. This often made plots of tan δ very noisy. The signal integrity was superior in the loss modulus(Figure 10). Given the difficulty with the tan δ curves, glass transition temperatures were measured from both the tan δ, and loss modulus curves, where the T_g has been defined as the point of inflection of the rising tan δ, and loss modulus curves (Figure 10). T_g's determined from the loss modulus show a greater sensitivity to blend composition than T_g's from the tan δ. However, neither follow the Fox equation (Figure 9). The T_g for pure fluorobenzyl cellulose was obtained from DSC measurements. While the T_g of pure semicrystalline PCL was measured directly from the tan δ. These minor shifts in T_g confirm that PCL is not miscible with fluorobenzyl cellulose.

The T_g of PCL/DSF 3.0 blends was not greatly affected by composition; however, the maxima of the tan δ and loss modulus were significantly shifted(Figure 11). The largest deviations occurred for the maxima of the tan δ. While these blends appear to be immiscible, the marked effect upon the damping maxima suggests that some degree of interaction is occurring between phases.

For the above PCL/DSF 3.0 blends, the most significant effects were observed at compositions with 60% PCL. So the effect of fluorine content was studied in PCL/mixed ether blends at the same composition(Figure 12). Curiously, the greatest T_g shift occurred in PCL/DSF 0.0 blends, blends with no fluorine. Among the fluorinated blends, T_g shifts increased slightly as fluorine content increased. It is not clear why the nonfluorinated blend shows the greatest T_g shift. Up to this point, all results have been counter to this observation. That is to say, until now, high fluorine contents have provoked the greatest deviation in PCL properties. The glass transition temperature of PCL is known to have a strong dependence on crystallinity[13]. It may be that the crystallinity of the PCL/DSF 0.0 blend was much higher than for the fluorinated blends. This would explain the higher T_g for the nonfluorinated blend; however, there is no proof for this asseration, as the degree of crystallinity was not measured for these samples.

As before the most significant dynamic effects were not in the change of the T_g, but rather in the maxima of the loss modulus(Figure 13). The maxima of the tan δ curves were too noisy to pinpoint, and are therefore not shown here. Again, inexplicably, the most significant shift in the loss modulus maxima occurs for the nonfluorinated blend, PCL/DSF 0.0. Among the fluorinated blends, higher fluorine contents cause greater shifts in the loss maxima, But again we observe a discontinuity over a 1% fluorine change for blends with DSF 2.8, 2.9, and 3.0.

D. INFRARED ANALYSIS

The tensile, and dynamic experiments demonstrate that PCL/benzyl cellulose blends are affected by the fluorine content of the cellulosic component. In fact the premise of this investigation was that fluorine would create specific interactions with PCL. Such interactions would probably involve the carbonyl group of PCL, and would thus be detectable by infrared analysis. FTIR analysis was conducted at room temperature, using thin films which were annealled at room temperature for 5 months. There were noticeable changes in the vibrational frequency of the amorphous PCL component. However, these changes were not reproducible, and were not a function of blend composition, or of the fluorine content of the cellulose ether. The vibrational maximum of the crystalline PCL component was constant to the nearest hundredth of a wavenumber. In all, there was no indication of specific interaction at room temperature. If interactions were localized at the domain interface, the effects may have be hidden from infrared analysis because of a concentration effect.

Therefore, infrared analyses of melt blends were performed, in hopes of possibly increasing the concentration of interacting species. However, once again, there was no indication of PCL carbonyl interaction. Unlike the room temperature studies, FTIR analysis of the melt showed no variability in the vibrational maxima of the amorphous polymer. It is most probable, that any specific interactions with PCL would involve the carbonyl. Judging from FTIR analysis, there appears to be no such interaction in these blends. It seems less probable that aromatic fluorine would participate in intermolecular associations with carbonyl groups as well as aliphatic fluorine would. A fluorinated phenyl ring would have a dipolar nature, however the electron density would be delocalized around the ring. Consequently, the interactive potential would be reduced accordingly. Aliphatic fluorine dipoles are of course highly localized and readily available for dipole-dipole interactions as in the case of PVF_2 and PMMA. Tentatively then, the compatibility that PCL demonstrates with fluorinated benzyl cellulose must not

arise from specific interactions.

E. DIFFERENTIAL SCANNING CALORIMETRY

Given the results from infrared analysis, observations were directed towards the melt transitions of PCL as a second method for detecting specific interactions. It is well known that interactions between polymers can be detected if one or both polymers is semicrystalline. Given the accurate measurement of equilibrium melting points, these interactions may be quantified by observation of a depression in the melt transition. However, this requires diligence in the accurate measurement of equilibrium melting points[9,10,14,15]. PCL is particularly notorious for complex melting transitions that result from recrystallization during melting[9,14]. This causes a characteristic double endotherm at low heating rates. As the heating rate is increased, the double endotherm disappears. This was found to be exactly the case for the PCL used in this study(Figure 14). As per the literature, the PCL double endotherm vanishes, or is not discernable, at fast heating rates. The double endotherm was also present in PCL/cellulose ether blends. However, the nature of the transition appeared to be affected by the fluorine content of the cellulose component(Figures 15, 16, and 17). The PCL/DSF 3.0 blend stands out, as is failed to display the characteristic double endotherm(Figure 16). In the other 2 cases, recrystallization appears to be inhibited, as the lower temperature endotherm is more prominent(Figures 15, and 17).

The heating rate study mentioned above indicated that the melting transition of PCL is affected by benzylated cellulose, and by the degree of fluorination. Therefore, an attempt was made at measuring T_m depressions using a Hoffman-Weeks analysis of equilibrium melting points[16]. Samples of pure PCL were treated with a thermal regime as shown in Figure 18. Samples were held at 100°C for 15 min, and then cooled to the crystallization temperature at 10°C/min. Annealing times varied between 30 min and 10.5 hours. Crystallization temperatures of 55, 50 ,and 45°C were employed. Melting points

were measured as the point were crystallinity disappears, at the tail end of the transition. In this brief experiment, it was found that reliable equilibrium melting points could not be obtained, at T_c = 50, and 45°C, as T_m's and heats of fusion steadily increased with longer annealing times(Figures 19, and 20). Also notice that the measured T_m's rise as T_c falls. Although, there was no double endotherm, this is an indication of lamellar reorganization during the heating scan, or isothermal thickening. In any case, this complicates an an equilibrium analysis. Given these results, and the well documented propensity PCL has for recrystallization, a Hoffman-Weeks analysis was abandoned. Luckily however, it was discovered that annealing PCL at 55°C gave relatively constant T_m's and heats of fusion, after a 1 hour annealing time(Figures 19, and 20). T_m's and heats of fusion did not significantly change after 10.5 hours of annealing at 55°C. Therefore, recrystallization, and/or isothermal thickening was not a problem when annealing at 55°C. This demonstrated that some useful could be obtained by annealing the blends at 55°C.

Consequently, 60/40 PCL/cellulose ether blends were treated with the above heating regime, and annealed at 55°C for 1 hour. T_m's, and heats of fusion, of these blends were then compared for a qualitative inspection of equilibrium melting. Indeed, there was no indication of interaction in these blends, as there was no melting point depression(Figure 21). In fact, there appeared to be a slight elevation in T_m for these blends. The most significant T_m elevation occurs for the PCL/DSF 2.9 blend. It just so happens that the DSF 2.9 polymer has a number and weight average molecular weight, nearly double that of the other cellulose derivatives(Table 4, section V). The exception is the DSF 0.0 derivative, which has a M_w comparable to DSF 2.9. Interestingly, the PCL/DSF 0.0 blend also shows a slightly higher than average T_m elevation. These two data points suggest that the melting behavior of these blends may have a significant entropic contribution. In order to ascribe an equlibrium melting argument to this data, one has to assume that isothermal thickening of crystall lamellae is the same in the blends

as in the pure PCL. This may, or may not be a valid assumption[9]. The heats of fusion decline as the fluorine content of the blends rise(Figure 22). Recall, that for pure PCL annealed at 50 and 45°C, heats of fusion rose with time. This may demonstrate that there is no isothermal lamellar thickening in the blends at T_c = 55°C. All combined, these observations indicate that there is no negative enthalpy of mixing in this series of polymer blends. In fact, the apparent T_m elevation has been theroretically predicted when the interaction parameter is positive in blends[7]. However, this phenomena has not been observed as phase separation results from the normally low entropy of mixing[9]. Curiously, there is an indication that the entropy of mixing may have a significant contribution in these blends.

The apparent discontinuity in thermal behavior at high fluorine contents prompted another series of DSC measurements. 60% PCL blends were quick cooled from the melt, and then rescaned in order to observe the heats of fusion. The crystallinity, or heat of fusion, declines as the fluorine content of the cellulosic component increases(Figure 23). The degree of crystallinity is unaltered in the nonfluorinated blend, DSF 0.0. Once again, there is a significant discontinuity at the 3 data points with the greatest degree of fluorination. Cellulose derivatives DSF 2.8, DSF 2.9, and DSF 3.0 caused a significant decrease in PCL crystallinity. Notice that these nonequlibrium measurements closely correlate with the above isothermally crystallized samples(Figure 22). The same trend is observed when the heats of crystaillization are measured(Figure 24). The most significant observation is that this general trend is present in the thermal, dynamic, and the tensile experiments. Furthermore, the blend containing DSF 2.9 consistently stands out in the thermal analysis, while also displaying the greatest degree of mechanical compatibility(Figure 8).

Clearly, the sum total of these experiments indicate that: 1) PCL is immiscible with benzyl cellulose, fluorobenzyl cellulose, and all mixed benzyl ethers of intermediate

fluorination, 2) arguably PCL displays some degree of compatibility with all of the above cellulose benzyl ethers, 3) this compatibility may occur from the relatively low molecular weights of PCL, and the cellulose derivatives, 4) compatibility is enhanced at high degrees of fluorination, and is most significant at fluorinations just below the maximum, and finally 5) compatibility at high degrees of fluorination is not due to specific interactions, or the entropic contribution to mixing.

The elimination of these possibile contributions to compatibility leads us to the copolymeric nature of the mixed fluorobenzyl/benzyl cellulose ethers. Imagine a hypothetical compatibility index which is plotted as a function of fluorine content in the cellulose component(Figure 25). Based upon the combined data from these experiments, one may argue that such a plot would be curved upward, with a high degree of asymmetry. Such a plot is reminiscent of the miscibility window that occurs when intramolecular interactions of an A-B copolymer promote mixing with a third homopolymer, with repeat unit C[2,17,18]. This occurs when neither homopolymer A, nor homopolymer B are miscible with hompolymer C. Notice, in this hypothetical plot, that miscibility is not achieved in any case. Instead, this intrachain effect may be may be responsible for differential compatibility, (not miscibility), that PCL is displaying, as the fluorine content of the cellulose ether is changed. For instance, it is probable that no specific interactions would exist between a blend of tri-O-benzyl cellulose, and tri-O-p-fluorobenzyl cellulose. As such, the disparity in solubility parameters all but guarantees the immiscibility of benzyl cellulose with fluorobenzyl cellulose as molecular weight increases. In terms of interaction parameters, B:

$$B_{12} \neq B_{13} \neq B_{23} \tag{4}$$

where, fluorobenzyl cellulose, benzyl cellulose, and PCL, are polymers 1, 2, and 3,

respectively. If a benzyl/fluorobenzyl cellulose copolymer were synthesized, it may have a character very similar to the mixed benzyl ethers in this study. If such a copolymer were blended with PCL, the total interaction parameter of the blend could be written as follows[17].

$$B_{MIX} = B_{13}\phi_1' + B_{23}\phi_2' - B_{12}\phi_1'\phi_2' \quad (6)$$

Φ_i' refers to the copolymer composition, and $\Phi_1' + \Phi_2' = 1$. From the results given here, we may assume that B_{13} and B_{23} are both positive, and that B_{23} is greater than B_{13}. In the event that B_{12} has a large enough positive value, the overall interaction parameter would be negative, and miscibility would result. But we have seen that PCL does not form a miscible mixture with any of these cellulose ethers. Instead, it may be that B_{12} is a large enough positive value to merely make B_{MIX} less positive, but never negative. In this case, intramolecular interactions between benzyl cellulose and fluorobenzyl cellulose segments, could reduce the unfavorability of mixing with PCL. The copolymeric nature of the mixed benzyl ethers is undeniable, as discussed previously. And the nature of their synthesis could give rise to very complex microstructures. For example, there are 8 unique monomer residues that could result from the possible substitution patterns of positions 2, 3, and 6. This level of complexity may possibility contribute to the effects of intrachain repulsions.

CONCLUSIONS

1. Polycaprolactone is immiscible with tri-O-benzyl cellulose, tri-O-p-fluorobenzyl cellulose, and variously fluorinated mixed benzyl/p-fluorobenzyl cellulose ethers.
2. PCL does, however, exhibit some degree of compatibility with each of these polymers. This is based upon observations made with TEM, tensile testing, dynamic thermal analysis, and calorimetry.

3. PCL compatibility is enhanced for benzylated cellulose ethers as fluorine content rises. The best compatibility occurs at fluorine contents just below the maximum.
4. The possible contribution of specific interactions to compatibility has been discounted. No evidence of specific interaction was found from infrared spectroscopy, or from PCL melting point depression.
5. There is an indication that the entropy of mixing may contribute to the compatibility seen here, due to the low molecular weights of the polymers studied. However, at high fluorine contents, the possible entropic contribution to compatibility may not be the most inportant contributing factor. Because, the highest compatibility was with the cellulose sample with the highest molecular weight.
6. Enhanced compatibility of PCL with mixed benzyl/fluorobenzyl cellulose ethers has been postulated to result from intrachain repulsions. Where, the total interaction parameter, B_{MIX}, is made less positive by intramolecular interactions arising from the copolymeric nature of the cellulose mixed benzyl ethers.

LITERATURE CITATIONS

1. Cowie, J.M.G, *The Encyclopedia of Polym. Sci. Eng.*, Supplementary vol., Wiley & Sons, New York, 455, 1989.

2. Paul, D.R., J.W. Barlow, and H. Keskkula, *The Encyclopedia of Polym. Sci. Eng.*, Wiley & Sons, New York, Vol.12, 399, 1988.

3. Bates, F.S., Science, 251, 22 Feb., 898, 1991.

4. Fernandez, M.L., Sci. Progress Oxford, 74, 257, 1990.

5. Paul, D.R., W. Barlow, R.E. Bernstein, and D.C. Wahrmund, Poly. Eng Sci., 18, 16, 1225, 1978.

6. Koleske, J.V., Polmer Blends, editors: D.R. Paul, and S. Newman, Academic Press, New York, Vol. 2, 369, 1978.

7. Nishi, T., and T.T. Wang, Macromolecules, 8, 6, 909, 1975.

8. Morra, B.S., and R.S. Stein, J. Poly. Sci., 20, 2243, 1982.

9. Rim, P.B., and J.P. Runt, Macromolecules, 17, 1520, 1984.

10. Runt, J., and K.P. Gallagher, Polymer Comm., 32, 6, 180, 1991.

11. Coleman, M.M., and J. Zarian, J. Poly. Sci.: Poly. Phys., 17, 837, 1979.

12. Varnell, D.F. J.P. Runt, and M.M. Coleman, Macromolecules, 14, 1350, 1981.

13. Koleske, J.V., and R.D. Lundberg, J. Poly. Sci.: A-2, 7, 795, 1969.

14. Rim, P.B., and J.P. Runt, Macromolecules, 16, 762, 1983.

15. Harrison, I.R., and J. Runt, J. Poly. Sci.: Poly. Phys., 18, 2257, 1980.

16. J.D. Hoffman, and J.J. Weeks, J. Res. Nat. Bureau Stand.: Phys. Chem., 66A, 1, 13, 1962.

17. Paul, D.R., and J.W. Barlow, Polymer, 25, 487, 1984.

18. Alexandrovich, P., F.E. Karasz, and W.J. MacKnight, Polymer, 18, 1022, 1977.

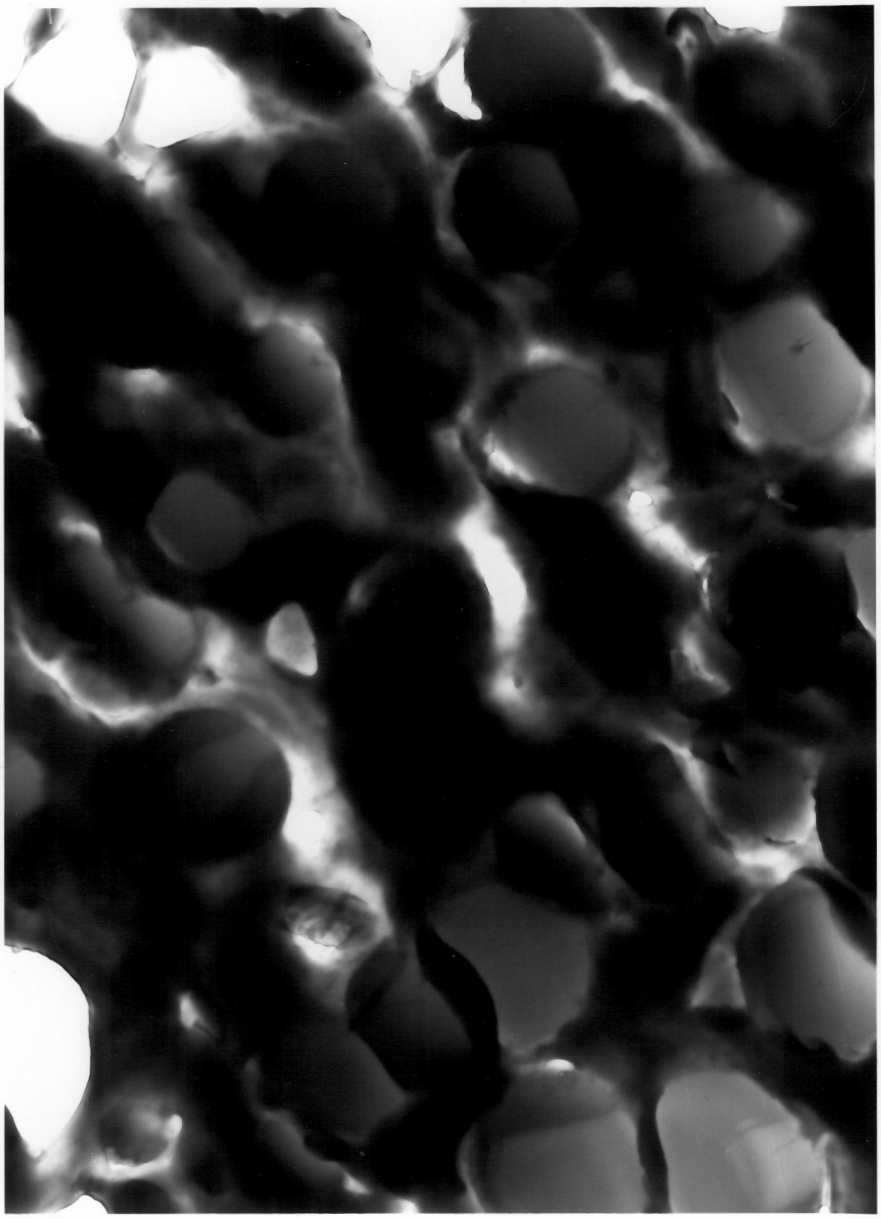

Figure 1. Transmission electron micrograph of a 90% PCL/10% DSF 0.0 blend. The bar equals 1.5 microns.

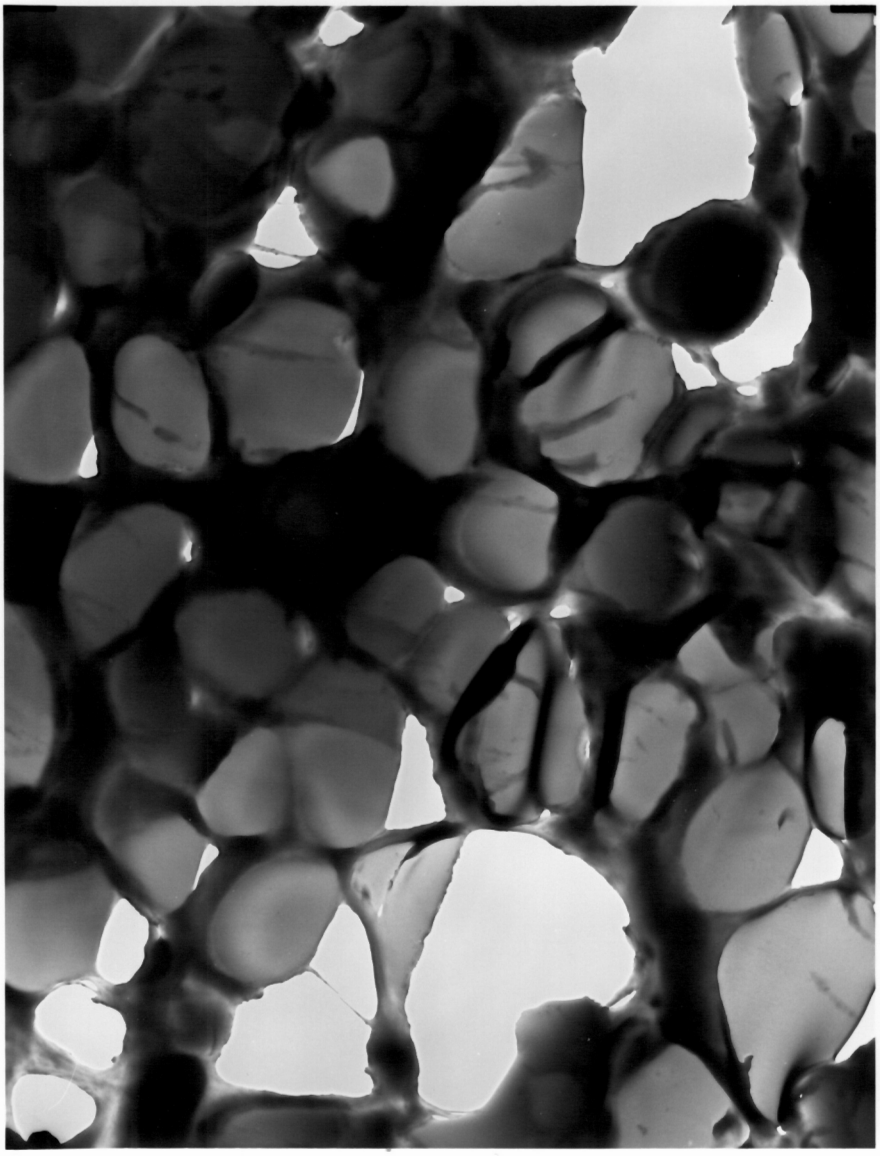

Figure 2. Transmission electron micrograph of a 90% PCL, 10% DSF 3.0, fluorobenzyl cellulose blend. The bar equals 2 microns.

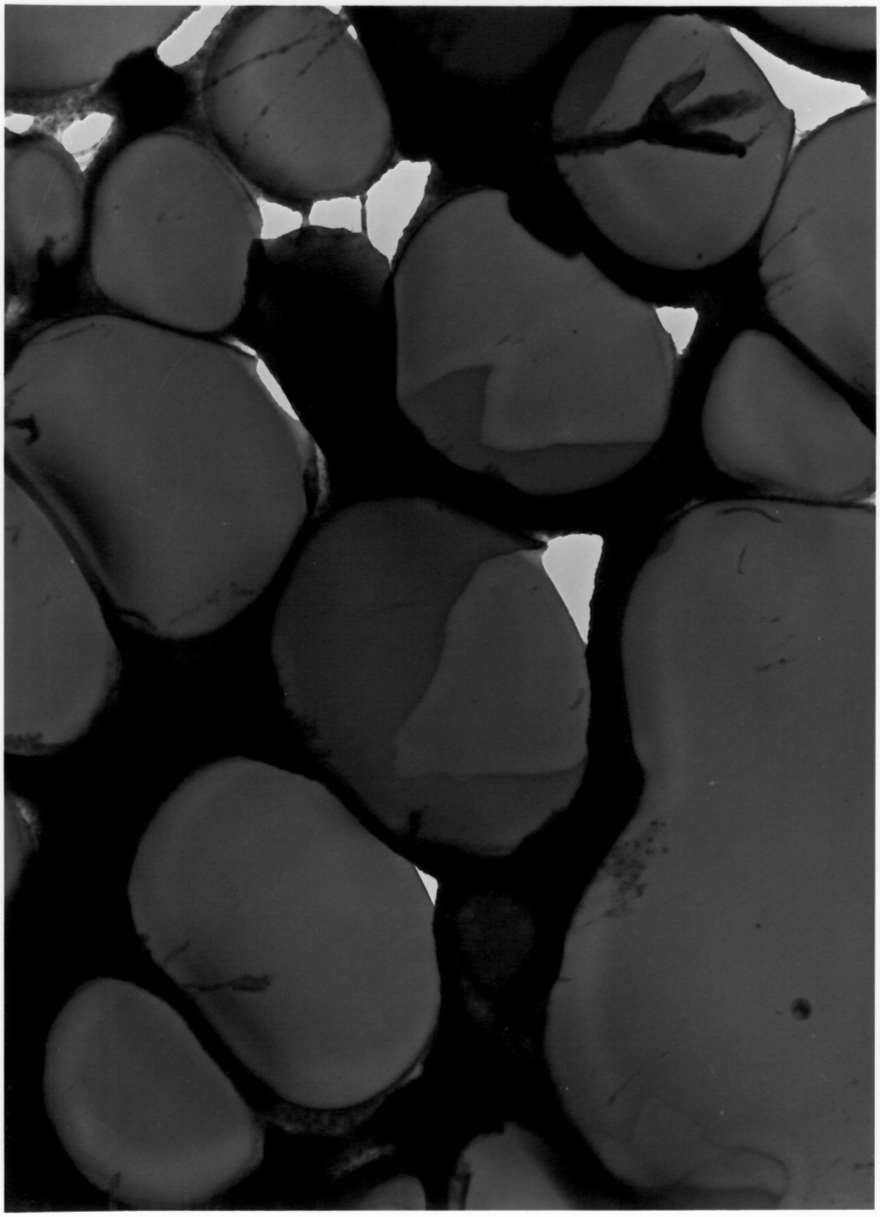

Figure 3. Transmission electron micrograph of a 90% PCL, 10% DSF 3.0, fluorobenzyl cellulose blend, stained with ruthenium tetroxide. The bar equals 1 micron.

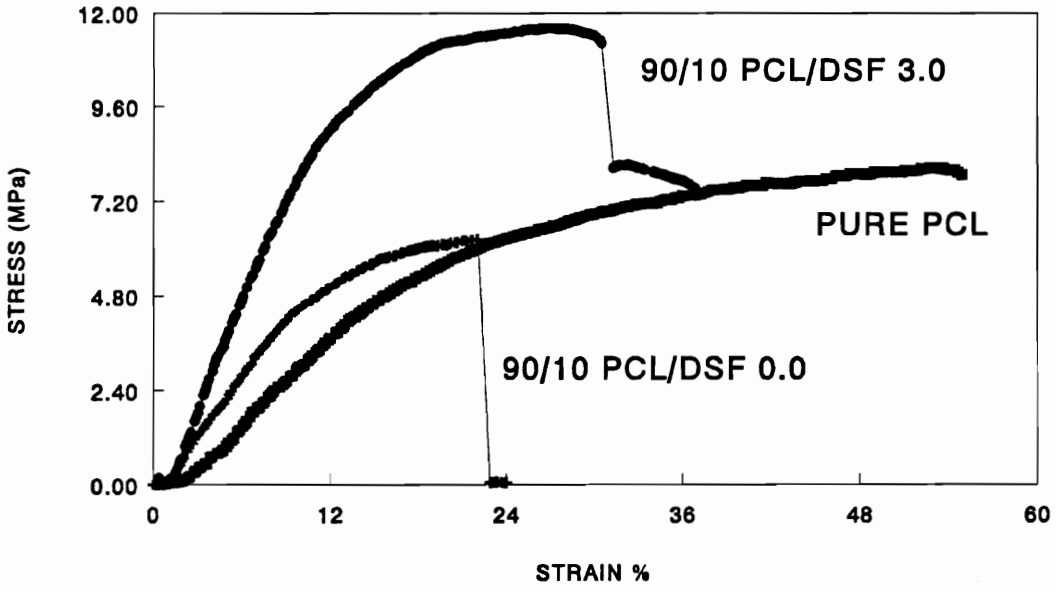

Figure 4. Typical tensile response of pure PCL, and blends of 90% PCL with 10% DSF 0.0, and 10% DSF 3.0.

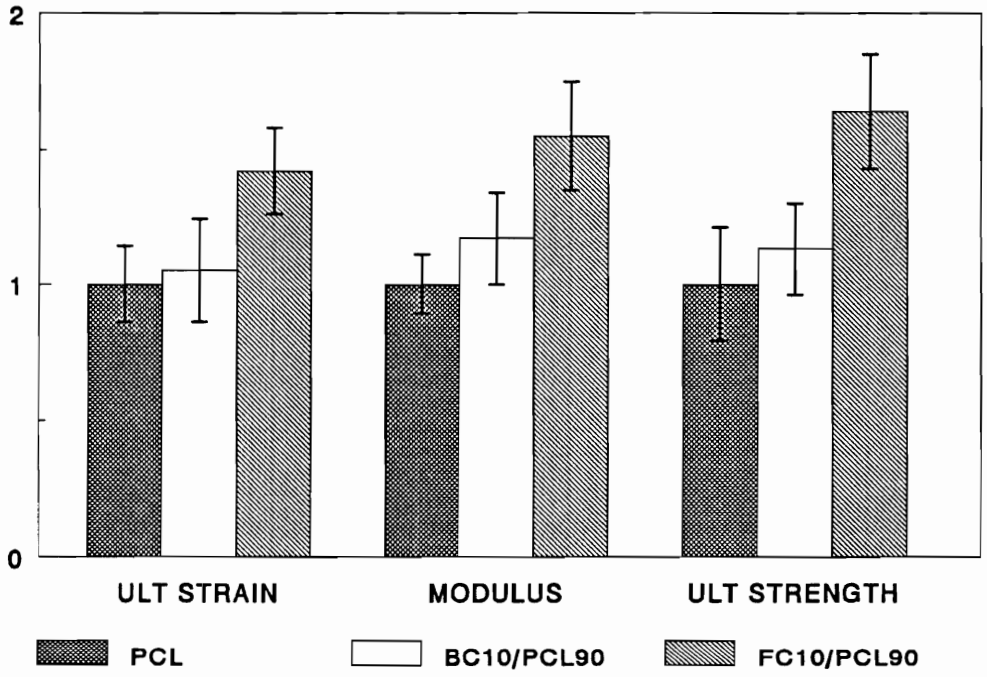

Figure 5. Average tensile test results for pure PCL and blends of 90% PCL with 10% DSF 0.0, and 10% DSF 3.0. FC stands for fluorobenzyl cellulose, BC for benzyl cellulose.

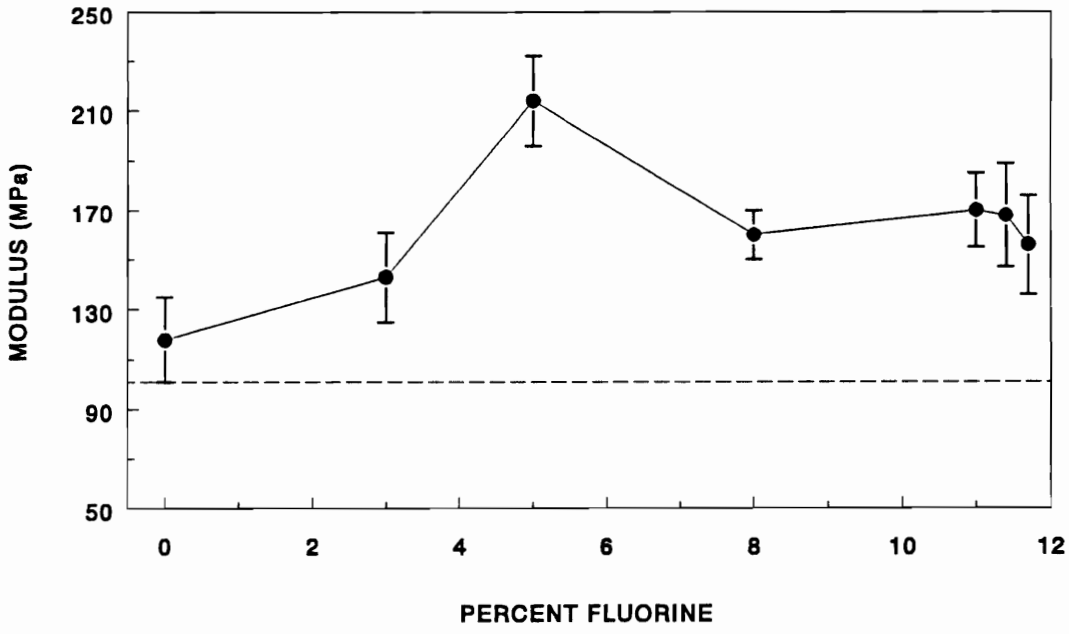

Figure 6. Average modulus of blends containing 90% PCL, and 10% benzylated cellulose of different DSF. The dotted line represents the average modulus of pure PCL. Each point is an average of at least 6-9 tests.

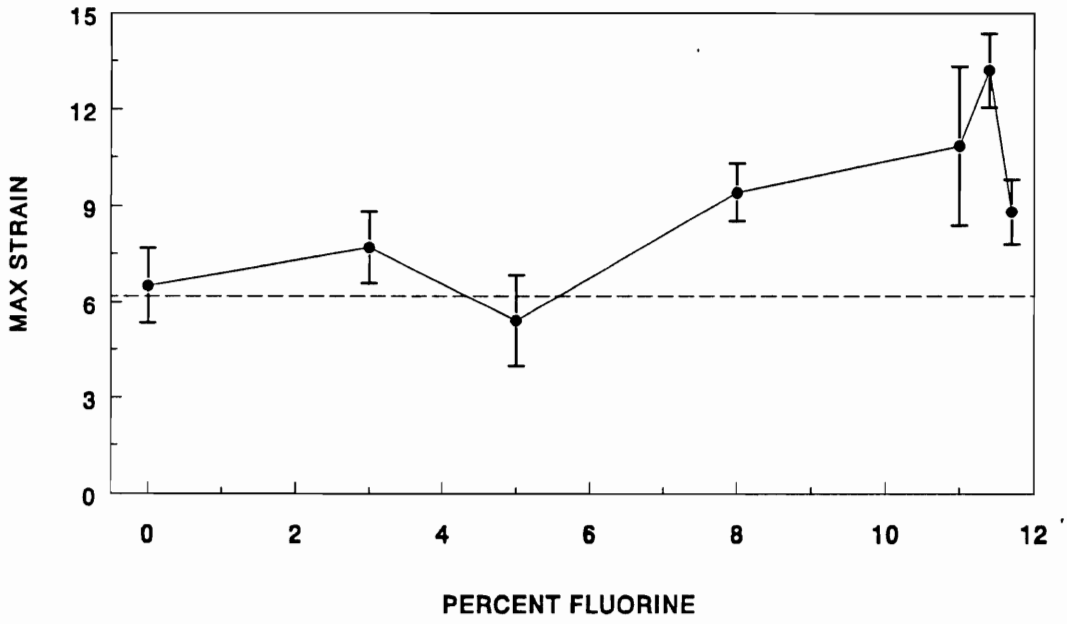

Figure 7. Average ultimate elongation of blends containing 90% PCL, and 10% benzylated cellulose of different DSF. The dotted line represents the average ultimate elongation of pure PCL.

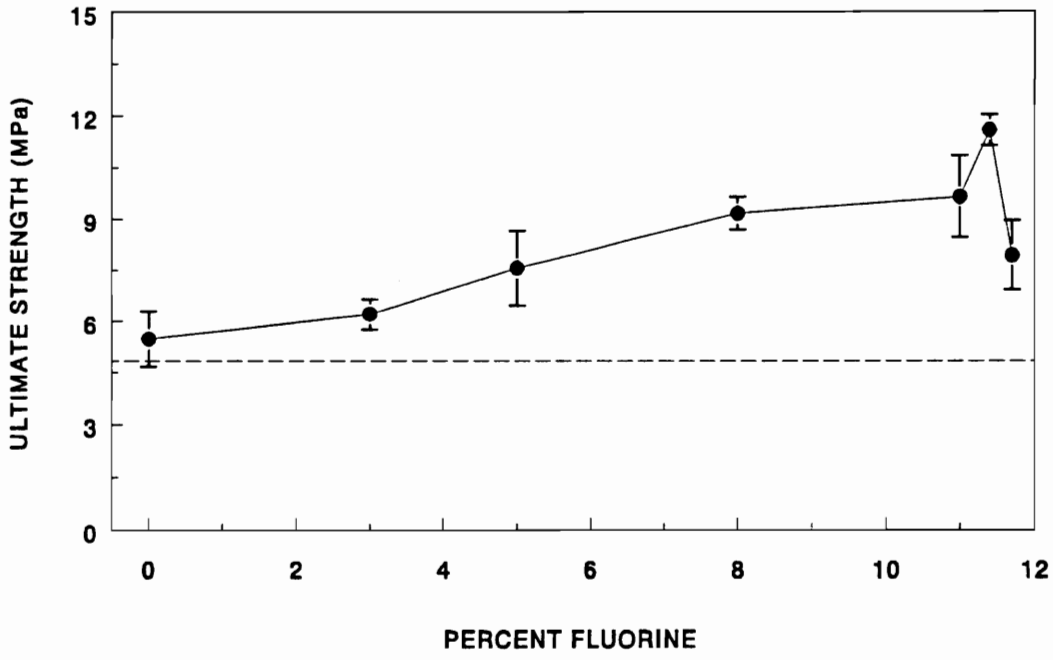

Figure 8. Average ultimate strength of blends containing 90% PCL, and 10% benzylated cellulose of different DSF. The dotted line represents the average ultimate strength of pure PCL.

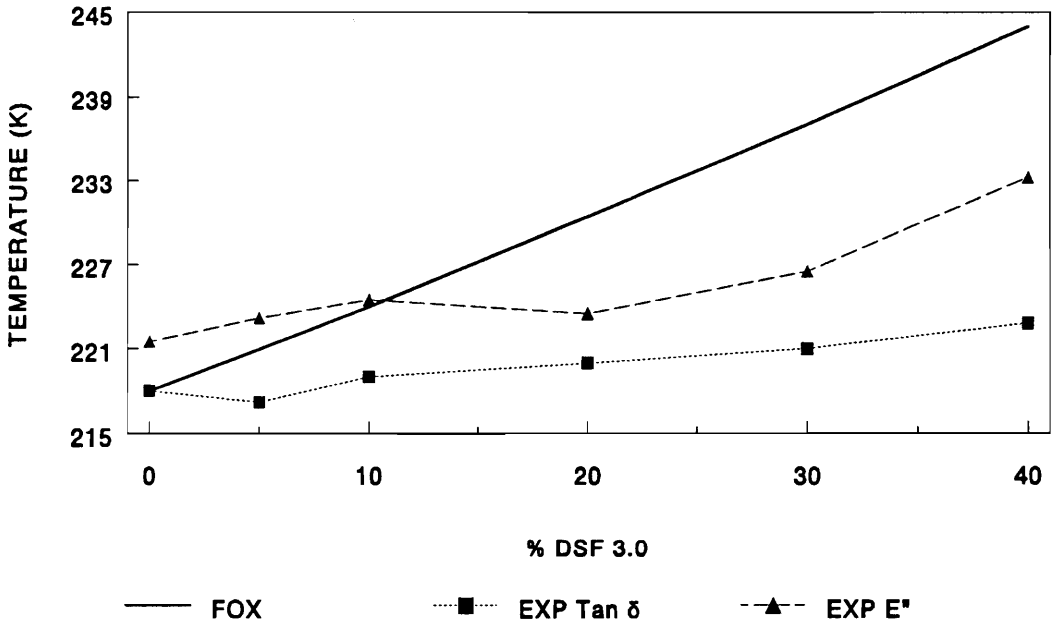

Figure 9. Dynamic T_g as a function of blend composition, for PCL/DSF 3.0 blends. T_g's are shown as calculated from Tan δ, and loss modulus curves.

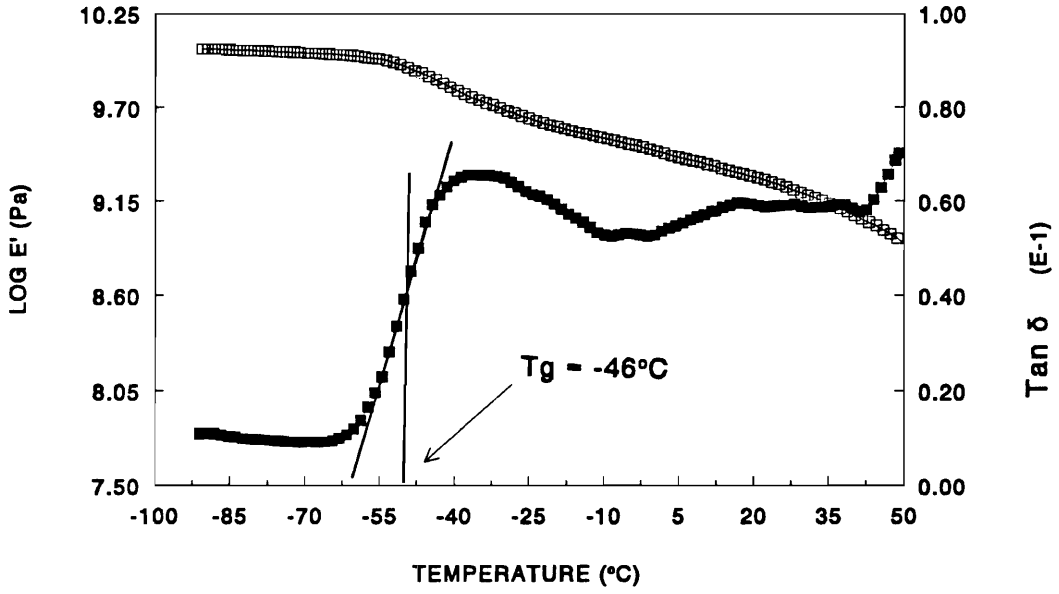

Figure 10. Typical tan δ, and modulus curves of pure, THF cast PCL, from dynamic mechanical thermal analysis. The figure shows the method for calculation of Tg.

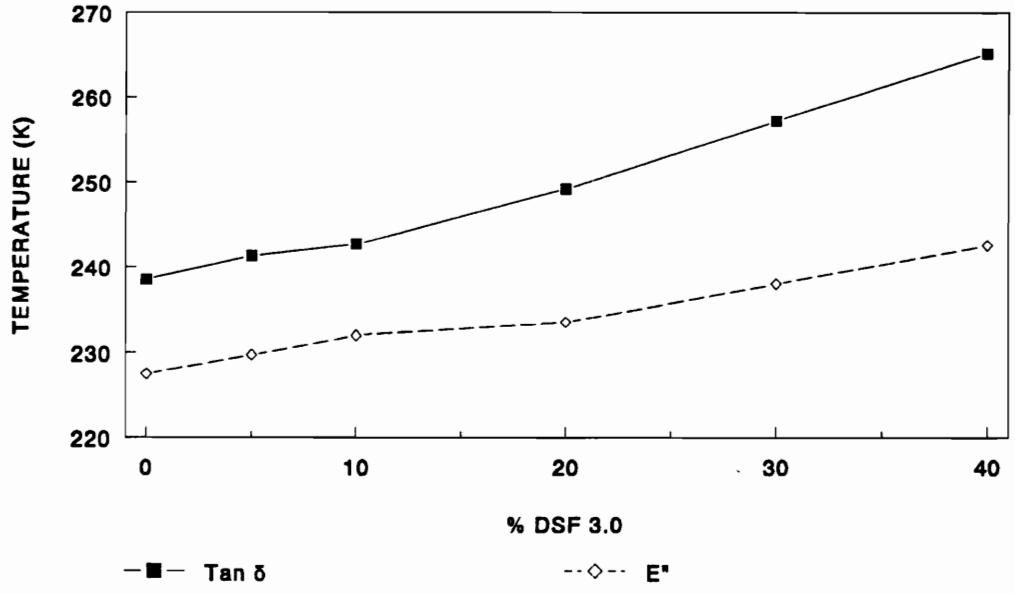

Figure 11. Maxima of the tan δ, and loss modulus curves as a function of blend composition for PCL/DSF 3.0 blends.

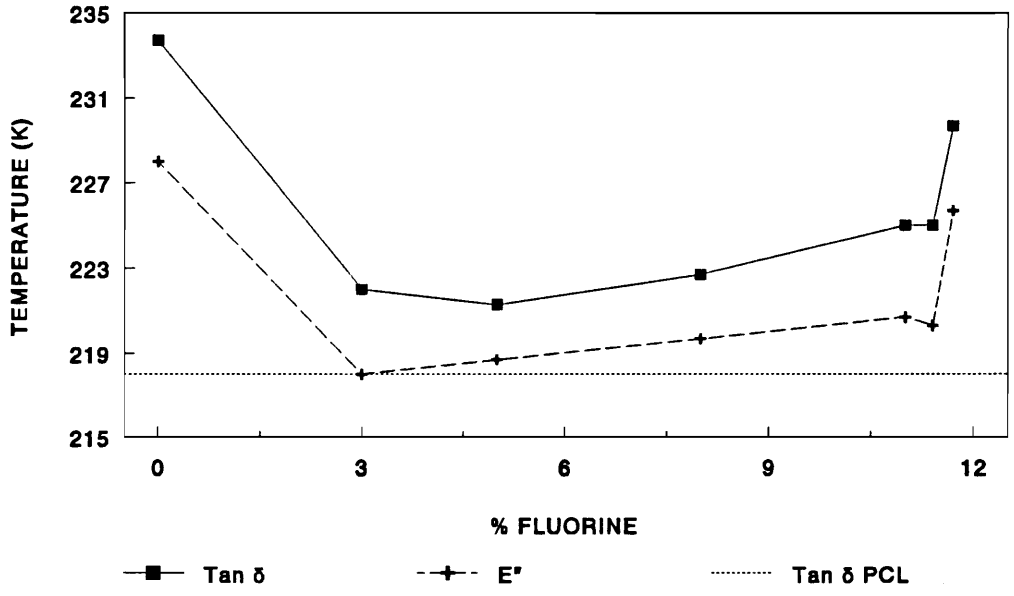

Figure 12. T_g's of 60% PCL, and 40% benzylated cellulose of different DSF. T_g's are shown as caluclated for the tan δ, and loss modulus curves.

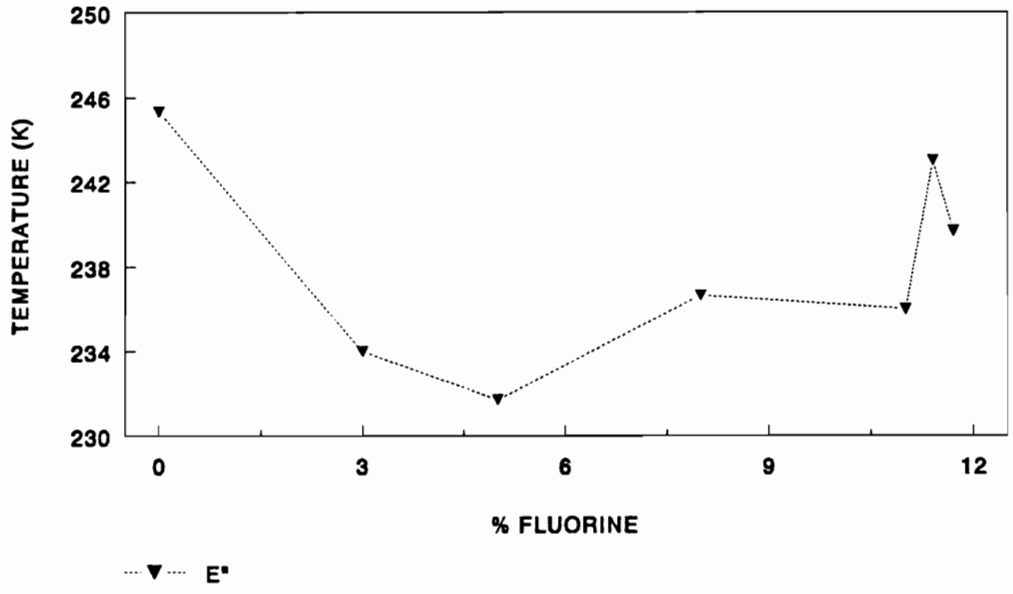

Figure 13. Maxima of the loss modulus curve for 60% PCL, and 40% benzylated cellulose of different DSF.

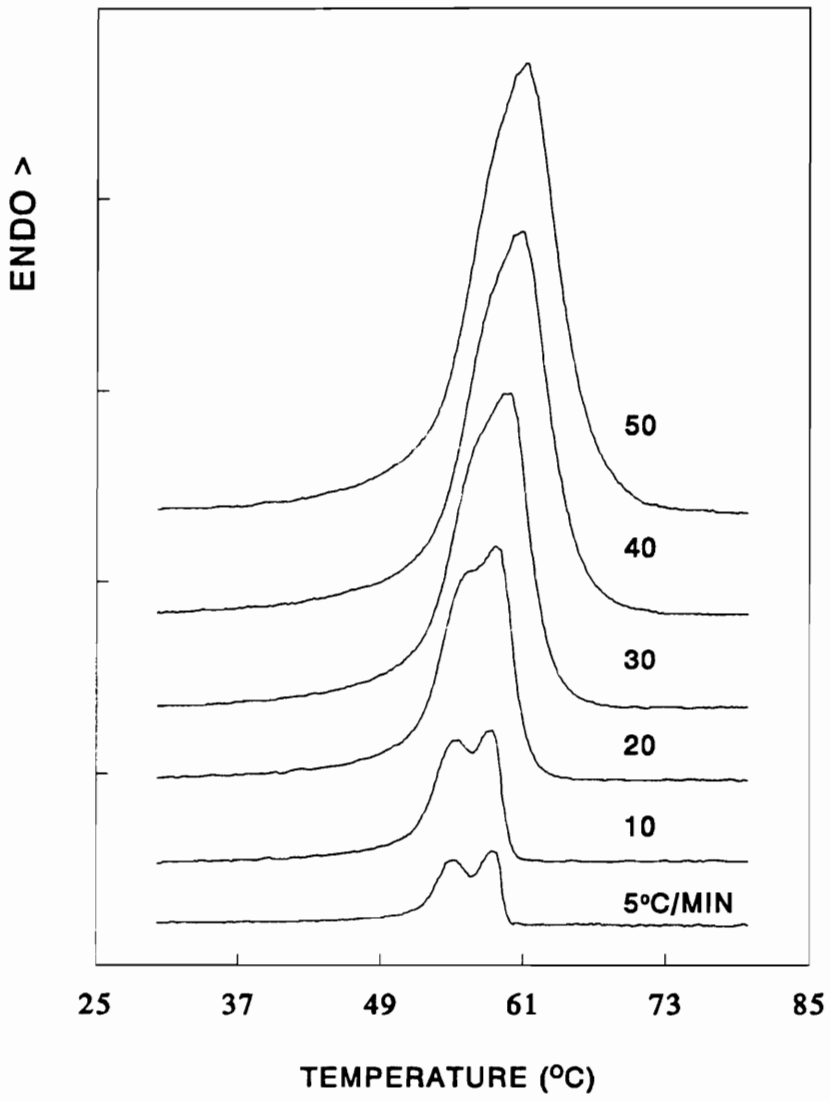

Figure 14. Melting endotherms of pure PCL as a function of heating rate. Loss of the double endotherm with rising heating rate indicates recrystallization during melting.

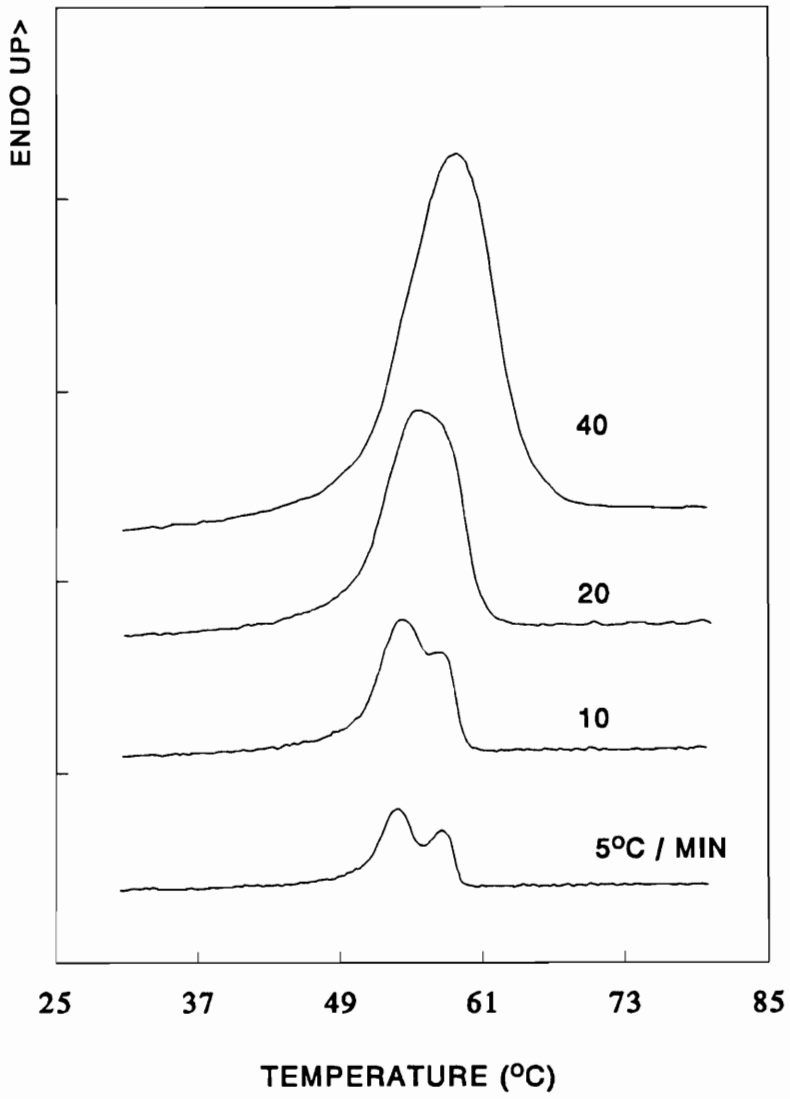

Figure 15. Melting endotherm of 60% PCL/40% DSF 0.0 blend, as a function of heating rate.

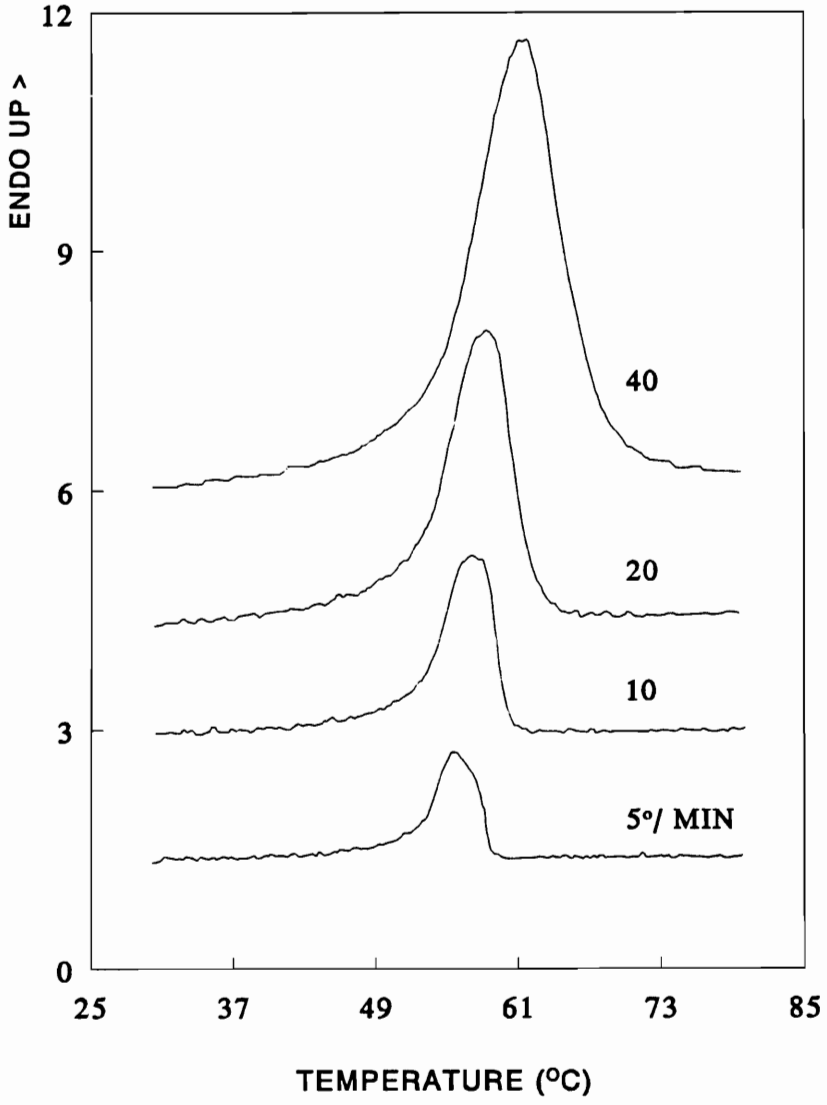

Figure 16. Melting endotherm of 60% PCL/40 % DSF 3.0 blend as a function of heating rate.

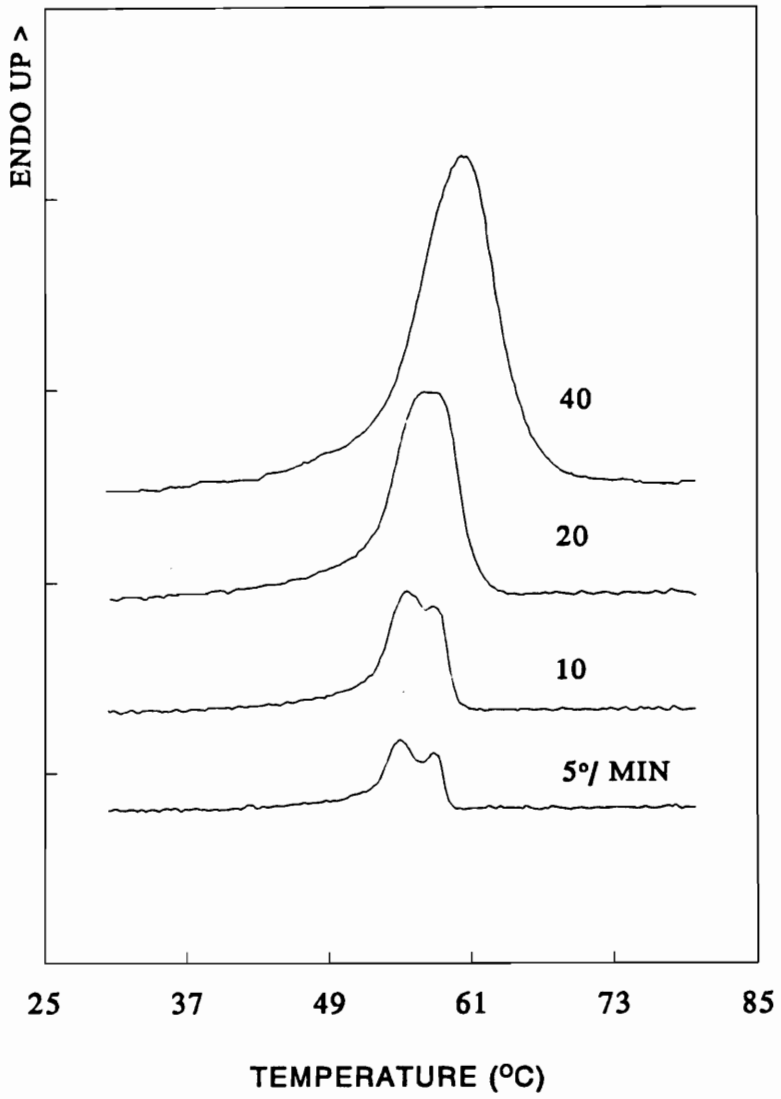

Figure 17. Melting endotherm of 60% PCL/40% DSF 2.9 blend, as a function of heating rate.

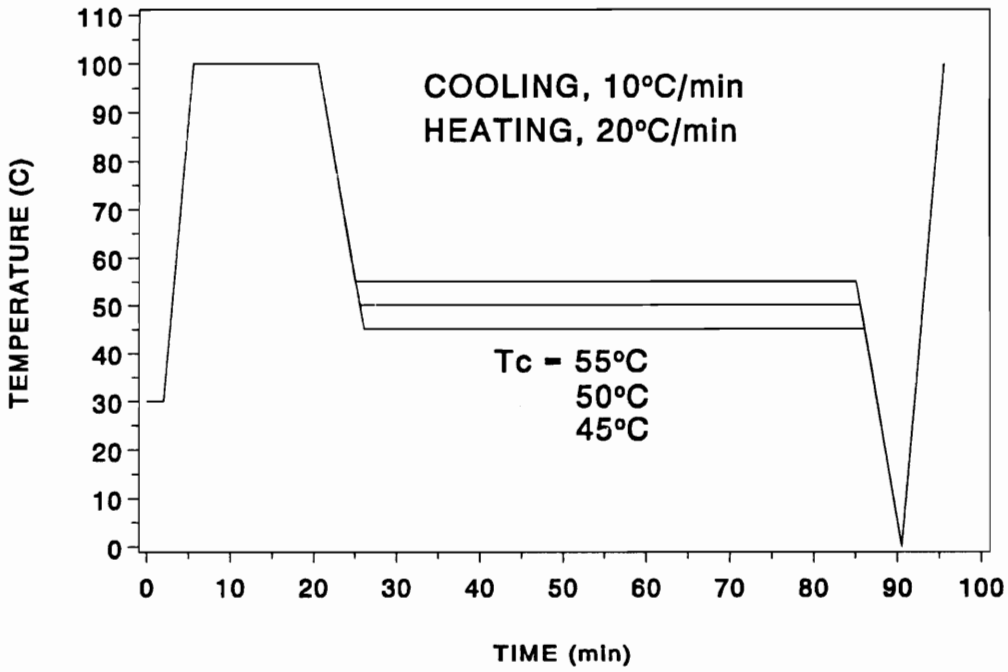

Figure 18. Thermal regime use for isothermal crystallization of pure PCL samples. Annealling times of 0.5, 1, 2, 3, and 10.5 hours were used, a 1 hour annealing time is shown here.

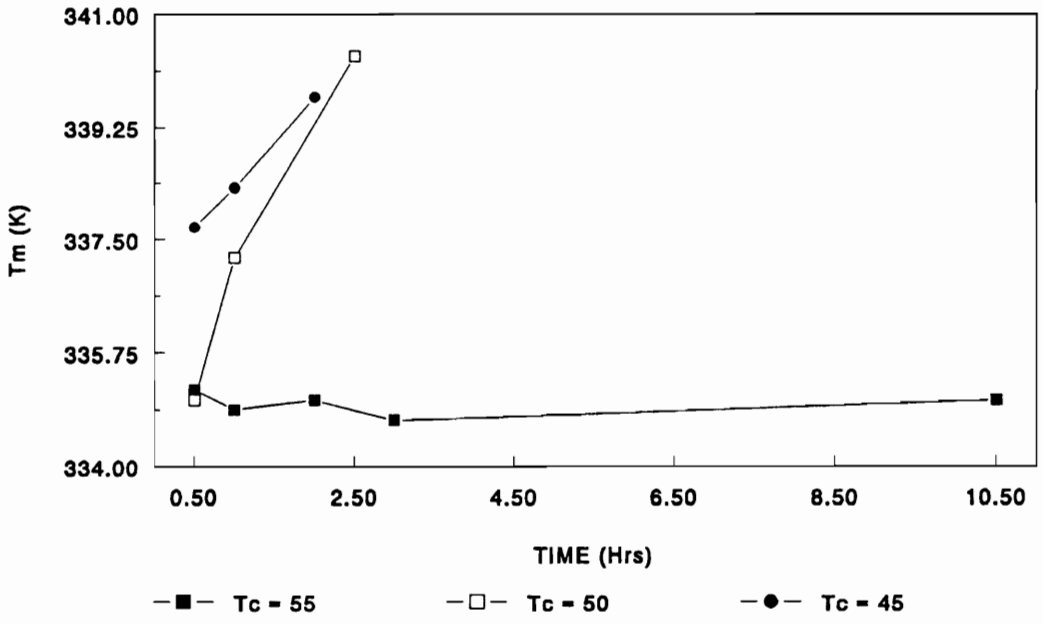

Figure 19. Melting points that resulted from isothermal crystallization of pure PCL. Data at Tc = 50, and 45°C indicate isothermal thickening of crystals.

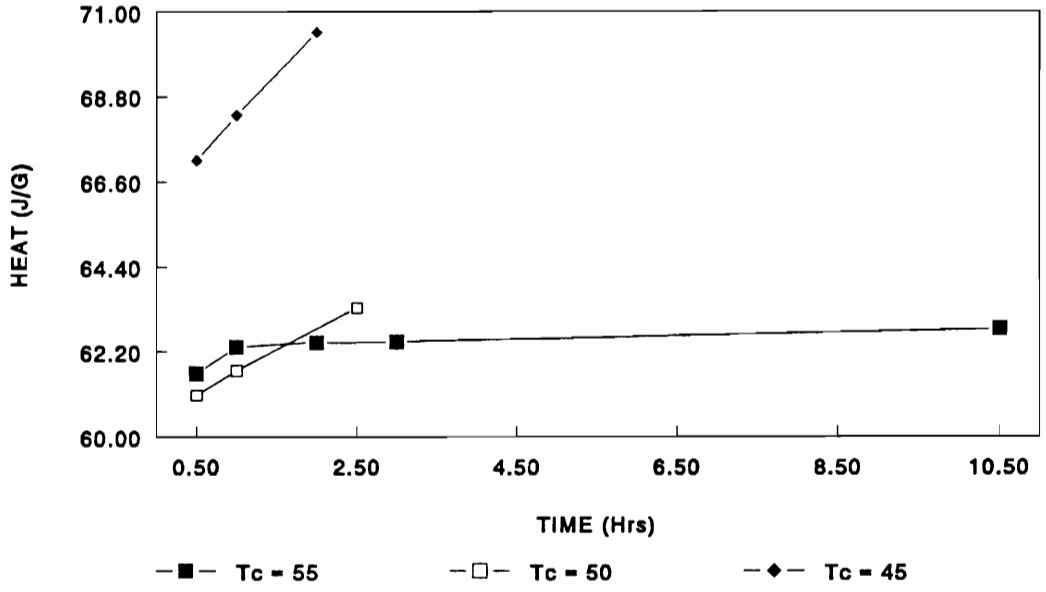

Figure 20. Heats of fusion from isothermal crystallization of pure PCL.

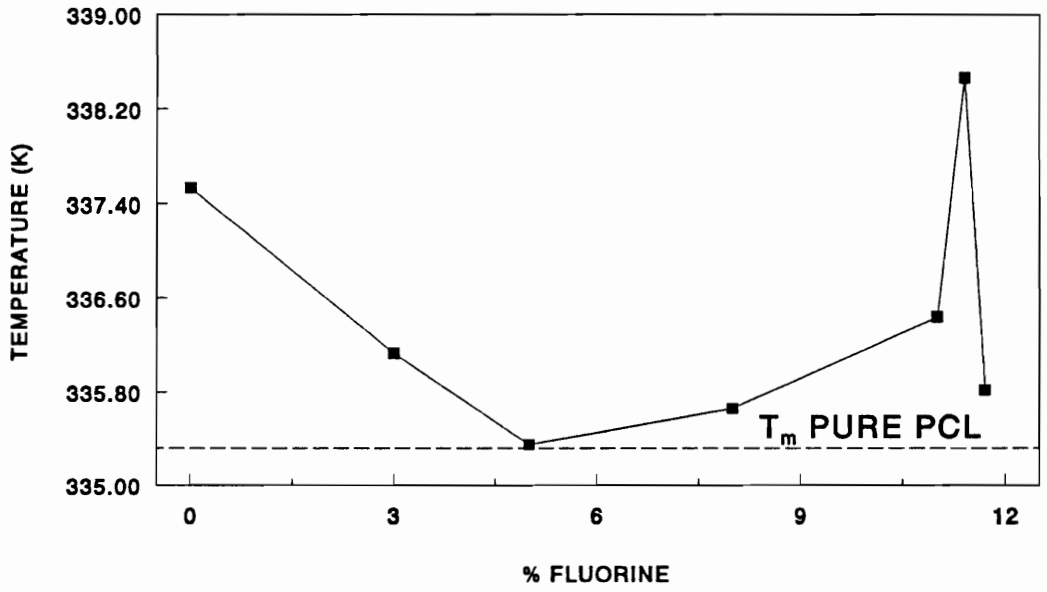

Figure 21. Melting points of isothermally crystallized PCL/cellulose ether blends.

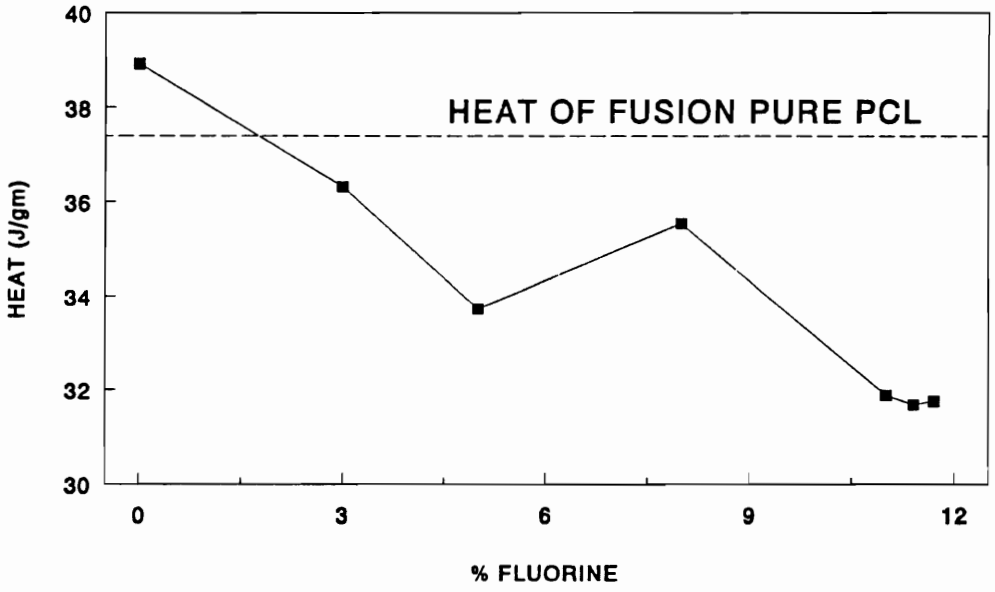

Figure 22. Heats of fusion of isothermally crystallized PCL/cellulose ether blends.

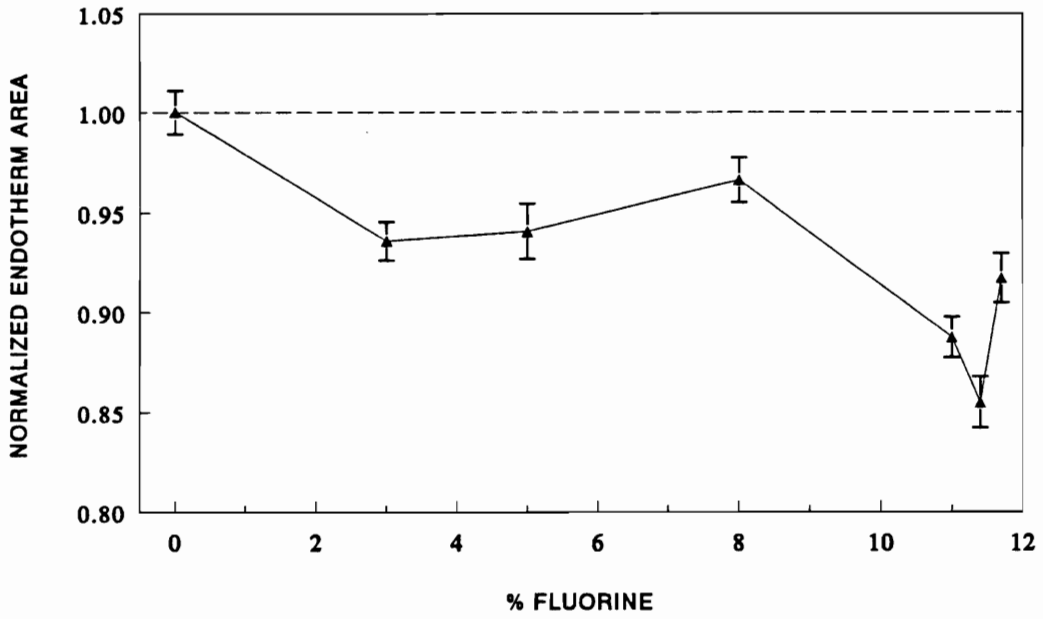

Figure 23. Normalized heats of fusion for 60/40, PCL/DSF X blends, 2nd scan, from 0 to 100°C at 10°/min. Dotted line represents heat of fusion of pure PCL.

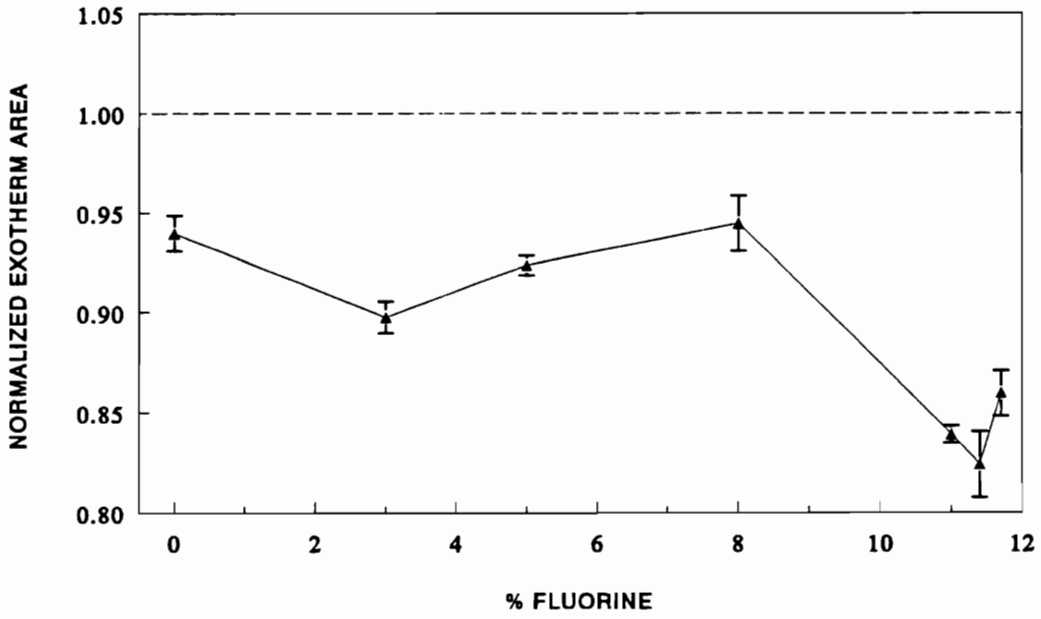

Figure 24. Normalized heats of crystallization for PCL/ cellulose mixed ether blends.

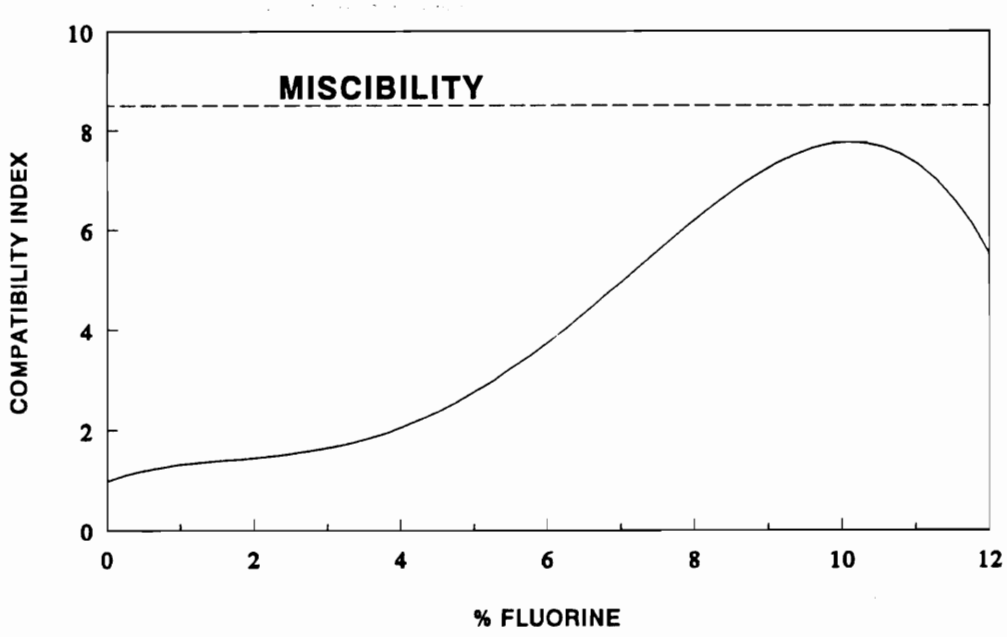

Figure 25. Hypothetical plot of compatibility index between PCL and cellulose mixed benzyl ethers of differing fluorine content.

VITA

Charles Edward Frazier was born the youngest of four boys on May 1, 1963 in Warrenton Virginia. His parents, F. Glenn Frazier and Linda B. Frazier raised him in Warrenton until he left for his college education at Virginia Tech in 1981. He graduated from Virginia Tech in 1985 when he left for Seattle Washington to pursue his masters degree at the University of Washington. After 2 years in Seattle, he returned to Blacksburg Virginia, and Virginia Tech to receive his PhD in the science of Wood and Polymers.